eman ta zabal zazu

Universidad del País Vasco

Euskal Herriko Unibertsitatea

GLIOGENESIS FROM THE SUBVENTRICULAR ZONE AFTER BRAIN ISCHEMIA

DOCTORAL THESIS

MARÍA ISABEL ARDAYA FRANCO

2022

eman ta zabal zazu

Universidad del País Vasco

Euskal Herriko Unibertsitatea

GLIOGENESIS FROM THE SUBVENTRICULAR ZONE AFTER BRAIN ISCHEMIA

DOCTORAL THESIS

MARÍA ISABEL ARDAYA FRANCO

2022

Thesis supervisors:

Fernando Pérez Cerdá

Fabio Cavaliere

Department of Neuroscience

ehugroup

Achucarro

BASQUE CENTER FOR NEUROSCIENCE

This work was supported by:

- Basque Government. Ayudas para el Programa Predoctoral de Formación de Personal Investigador no Doctor 2018.
- Basque Government (IT702-13).
- Ministry of Education and Science, Government of Spain (SAF2013-45084-R and SAF2016-75292-R).
- Centro de Investigación en Red de Enfermedades Neurodegenerativas (CIBERNED)

Index

Index of figures

INTRODUCTION

MATERIALS AND METHODS

RESULTS

Index of figures

DISCUSSION

ANNEXES

ABBREVIATIONS

AG	Astrogliogenesis
ALRs	AIM2-like receptors
AMPA	α-amino-3-hydroxy-5-methyl-4-isoxazolepropionic acid
ANOVA	ANalysis Of VAriance
aNSC	Active NSC
Atf6a	Activating transcription factor 6a
ATP	Adenosine triphosphate
BBB	Brain blood barrier
BM	Bone Marrow
BMP11	Bone morphogenetic protein 11
BrdU	5-bromo-2'-deoxyuridine
BTC	Betacellulin
BV	Blood Vessels
CAG	Glycosaminoglycans
CC	Corpus callosum
CCA	Common Carotid Artery
CLRs	C-type lectin receptors
CNS	Central Nervous System
CNTF	Leukemia inhibitory factor (LIF), ciliary neurotrophic factor
COX-2	Cyclooxygenase 2
CP	Choroid Plexus
CSF	Cerebrospinal fluid
CSPGs	Chondroitin Sulphate Proteoglycans
Ctx	Cortex
DAMPS	Damage-associated molecular patters
DAPI	4′,6-diamidino-2-phenylindole

Abbreviations

DCX	Doublecortin
EAA	Excitatory amino acids
ECA	External Carotid Artery
ECM	Extracelular Matrix
EPO	Erythropoietin
FACS	Fluorescence-Activated Cell Sorting
FGF-2	Fibroblast growth factor-2
GDF11	Growth differentiation factor 11
GFAP	Glial fibrillary acidic protein
GFP	Green Fluorescent Protein
GL	Glomerular layer
GrL	Granular layer
HA	Hyaluronic Acid
HABP	Hyaluronic Acid Binding Protein
HAS2	Hyaluronic Acid Synthase 2
HIF1α	Hypoxia inducible factor-1 alpha
HMW-HA	High Molecular Weight Hyaluronic Acid
HSPGs	Heparan Sulphate Proteoglycans
ICA	Internal Carotid Artery
IdU	5-Iodo-2′-deoxyuridine
IFN-1	Type 1 interferon
IFNγ	Interferon-γ
IGF1	Insulin-like growth factor 1
IGF2	Insulin-like growth factor 2
IL1β	Interleukin-β
IL4	Interleukin-4

IL6	Interleukin-6
iNOS	Nitric oxide synthase
iPSC	Induced pluripotent stem cell
LGE	Lateral ganglionic eminences
LMW-HA	Low Molecular Weight Hyaluronic Acid
MAPK	Mitogen-activated protein kinase
MCA	Middle Cerebral Artery
MCAO	Middle Cerebral Artery Occlusion
MGE	Medial ganglionic eminence
MGV	Mean Gray Value
Mll1	Mixed-lineage leukemia 1
MMPs	Matrix metalloproteinases
MPO	Myeloperoxidases
NA	Numerical Aperture
NFIA	Nuclear factor I subtype A
NF-Kb	Nuclear factor kappa-light-chain-enhancer
NG	Neurogenesis
NG1	Neurogenesin-1
NLRs	NOD-like receptors
NMDA	N-methyl-D-aspartate
NO	Nitric Oxide
NSC	Neural Stem Cells
NSPH1	NSC from neurospheres with 1 passage
NSPH2	NSC from secondary neurospheres
NT3	Neurotrophin 3
OB	Olfactory bulb

Abbreviations

OFR	Oxygen Free Radicals
OGD	Oxygen and Glucose Deprivation
OPC	Oligodendrocytes Precursor Cells
OXPHOS	Oxidative phosphorylation process
PEDF	Pigment epithelium-derived factor
PGD2	Prostaglandin D2
PNN	Perineuronal nets
PTX-3	Pentraxin-3
qNSC	Quiescent NSC
RGC	Radial glial cells
RHAMM	Receptor for hyaluronan mediated motility
RLRs	RIG-1 like receptors
RMS	Rostral migratory stream
RNA	Ribonucleic acid
RNS	Reactive nitrogen species
ROI	Region of Interest
ROS	Reactive oxygen species
r-tPA	Recombinant tissue plasminogen activator
S1P	Sphingosine-1-phosphate
SDF1	Stromal cell-derived factor 1
SHH	Sonic Hedgehog
STAT3	Signal Transducer and Activator of Transcription 3
Str	Striatum
TAC	Transient amplifying cells
TdTOM	tdTomato
TGFα and β	Transforming growth factor alpha and beta

Thbs1	Thrombospondin-1
Thbs2	Thrombospondin-2
Thbs4	Thrombospondin 4
TLRs	Toll-like receptors
TNFα	Tumor necrosis factor-α
TR-qPCR	Real Time-Polymerase Chain Reaction
TTC	2,3,5-triphenyltetrazolium chloride
VEGF	Vascular endothelial growth factor
Wnt	Wingless

ABSTRACT

Brain stroke is the second cause of death worldwide. Among the cerebrovascular accidents, ischemic stroke is the most common. It is caused by an interruption of blood flow, and it is characterized by sudden neuronal death (necrosis in the core) and apoptotic neuronal loss in the penumbra. After the generation of the glial scar surrounding the penumbra, ischemia in animal model can activate the neurogenic machinery in the subventricular zone (SVZ). However, the rapid formation of the glial scar after brain ischemia represents a double edged sword for brain survival. On one side, the ischemic scar isolates the healthy tissues from deadly factors released in the ischemic core but on the other hand, it impedes the neuronal regeneration from the SVZ. Previous results in our laboratory demonstrated that high levels of extracellular adenosine, one of the factors released after brain ischemia, could activate the SVZ and generate new astrocytes. In this PhD project, we used a mice model of transient brain ischemia by middle cerebral artery occlusion (MCAO) to accomplish the following objectives:

1) To characterize the SVZ activation and astrogliogenesis following brain ischemia;

2) To investigate the role of newborn astrocytes generated from the SVZ.

By combining immunofluorescence with genetic cellular tracing (*in vivo* electroporation of neural progenitor cells) we demonstrated that brain ischemia induced the generation of newborn astrocytes from the SVZ. Newborn astrocytes expressed the specific marker Thbs4 and were derived from the activated Type B cells at the dorsal SVZ. The neural stem cells and the Thbs4 astrocytes generated from the SVZ, deviated their physiological route to the olfactory bulb and reached the ischemic scar. Here, astrocytes generated after brain ischemia could degrade and synthetize the hyaluronic acid of the extracellular matrix suggesting a dual role in the modulation of the ischemic glial scar. We demonstrated for the first time that astrocytes derived from SVZ can produce, uptake and degrade the hyaluronic acid of the extracellular matrix. Our results can open a new pharmacological strategy to modulate the formation and the remodeling of the glial scar, facilitate the tissue regeneration after brain ischemia, and propose astroglia as a possible pharmacological target.

INTRODUCTION

1. ISCHEMIC STROKE

1.1. Description

Stroke is a devastating disease of which sudden onset produces neurologic deficits due to a focal disruption of the cerebral blood circulation. Stroke occurs as an acute event, mainly unilateral that trigger a pathological cascade at macro and micro levels. Based on the place where disruption occurs, neurological deficits are translated into motor, sensory and social disabilities that can produce the person disablement to execute daily activities.

The vascular pathology occurs in the setting of either brain ischaemia or cerebral haemorrhage even though ischemic stroke is the most common type in humans (88% of all cases) (Mozaffarian et al., 2016). While hemorrhagic stroke is the result of bleeding inside the brain or in the subarachnoid space by the rupture of a vessel, ischemic stroke is caused by an obstruction of blood supply to the brain caused by a thrombosis or an embolus (Fig. 1) (Alia et al., 2017). Within ischemic stroke, brain damage results from a transient or permanent vessel occlusion, most often (71%) of the middle cerebral artery (MCA) (Fluri et al., 2015). While hemorrhagic stroke produced the death of most people who suffer it, more than 70% of people survived to the ischemic stroke, most of them with serious disabilities lifelong (Wieloch & Nikolich, 2006; Campbell et al., 2019).

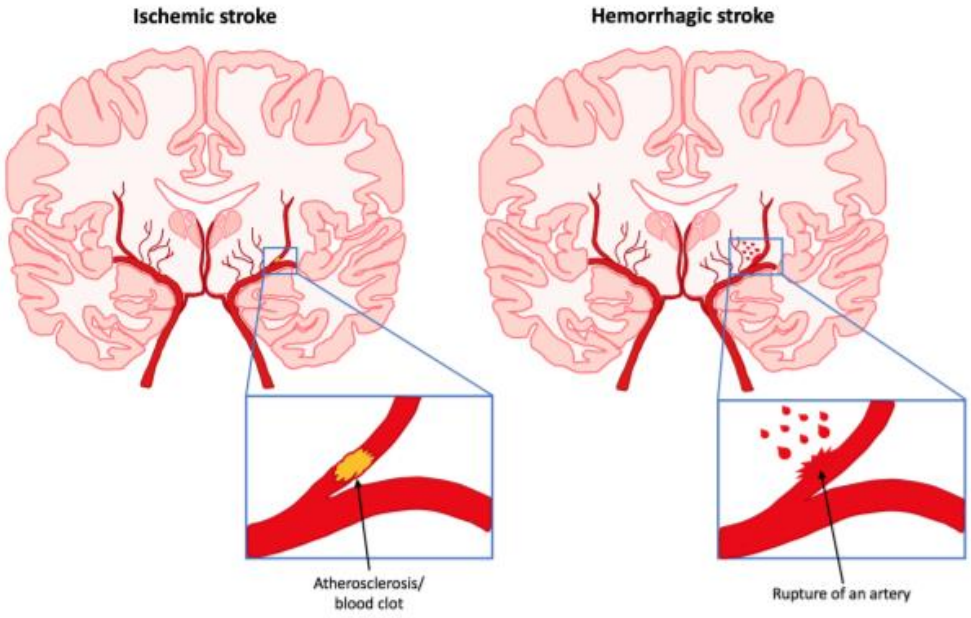

¡Error! No se encuentra el origen de la referencia.**. Ischemic stroke and cerebral haemorrhage are the main brain stroke subtypes.** Ischemic stroke is caused by the occlusion of a brain artery by a thrombus or an embolism, leading to reduced blood supply to the brain. Hemorrhagic stroke arises when an artery in the

brain ruptures and causes bleeding into the tissue or in the subarachnoid space. Taken from Augestad (2017).

Despite that, available therapeutic tools mainly focused in palliating brain damage. For this reason, in this study we focus on brain ischemia, the current major brain vascular disease. Even it is a complex illness, understanding what happens in the ischemic brain is instrumental to develop proper treatments that revert the damage caused by the occlusion.

1.2. Etiology and risk factors

The **etiology** of ischemic stroke includes a heterogeneous vascular and, less common, by non-vascular causes. Arterial occlusion is most often caused by a thrombus that has travelled to the brain (embolized) from a more proximal location in the body, such as the heart or from an atherosclerotic plaque in the wall of large artery. There are several sources to develop brain ischemia that can be classify in five groups: large vessel disease, small vessel disease, cardiogenic embolism, cryptogenic stroke and because other determined etiology (Fig. 2).

a. *Large vessel atherosclerosis disease* represents 30-40% of all ischemic strokes. Main causes are atherosclerotic disease in the aorta and major extra/intracranial arteries (flow limiting stenosis). Thrombosis can develop locally in a brain artery (less common) or in a body artery (aorta or internal carotid artery) where can be a source of embolism to a more distal segment such as of the middle cerebral artery.
b. *Small vessel disease or arteriolosclerosis* represents 20% of ischemic strokes. Arteriolosclerosis is caused by the occlusion of small penetrating cerebral end-arteries and produce small infarct areas between 3 and 15 mm size in the brain. This source of ischemic stroke is also known as "*lacunar infarcts*".
c. *Cardiogenic embolism* represents 25% of all ischemic strokes. In this case, the occlusion of the brain artery is caused by an emboli derived from the heart atherosclerotic plaque. Other cardioembolic stroke causes including atrial fibrillation or cardiac valve disease.
d. *Cryptogenic strokes* represent more than 30% of all cases. Even after exhaustive diagnosis studies, some cases remain without a determined cause. Also in this category are included patients with more than one possible etiology.
e. *Other determined etiology* refers to uncommon causes of ischemic stroke such as non-arterial causes, arterial dissection, hypercoagulate states or vasospasm. Most common causes of ischemic stroke in this group are watershed and

multifocal strokes together with degenerative vasculopathies and secondary consequences of different primary disease.

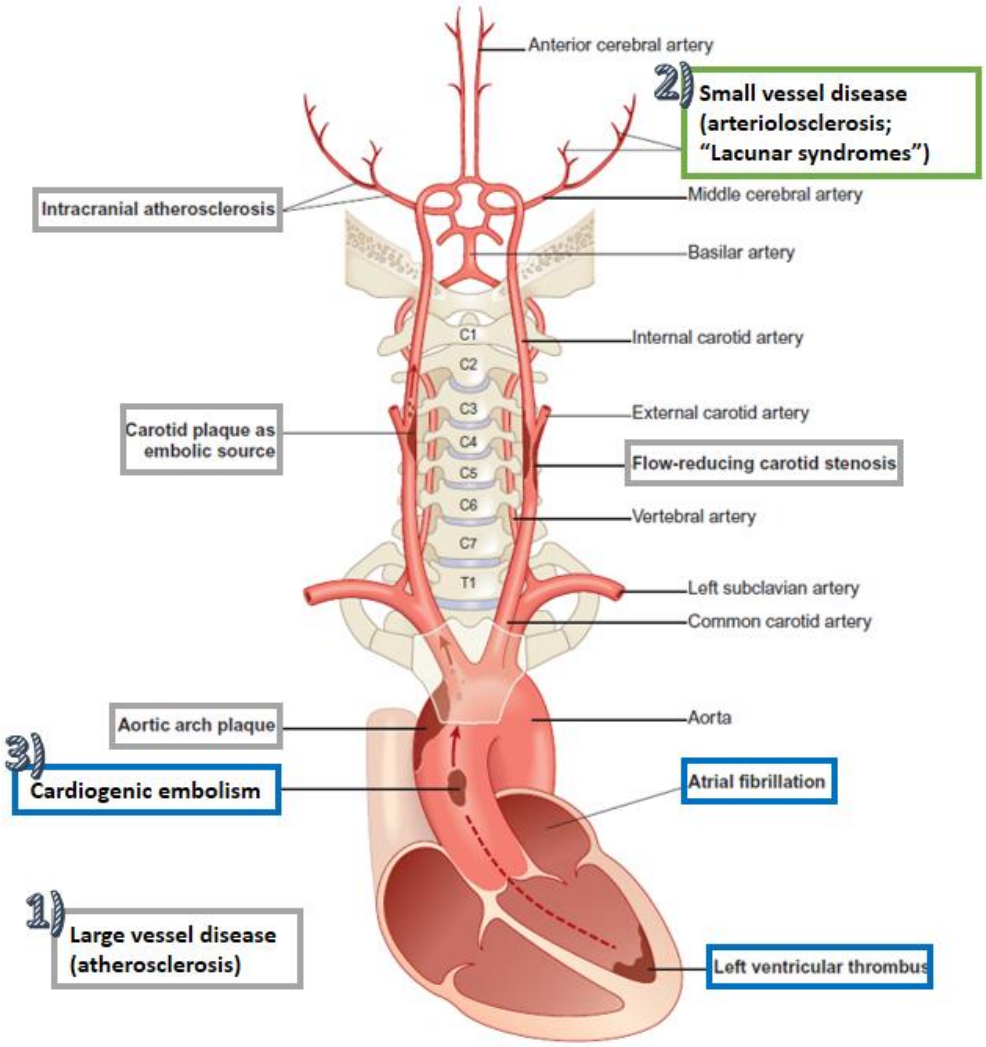

Figure 2. **Main causes of ischemic stroke.** 1) Large vessel disease (atherosclerosis) include flow-reducing carotid stenosis or intracranial atherosclerosis (in gray). 2) Small vessel disease (arteriolosclerosis or "Lacunar syndromes") in green. 3) Cardiogenic embolism (in blue) include atrial fibrillation or left ventricular thrombus as embolic source in the internal carotid artery. Modified from Silverman & Rymer (2009).

The **risk factors** are divided in modifiable and non-modifiable factors. Genetic and environmental factors depend on if factors can be changed, treated or medically managed (modifiable factors) or can not be changed (non-modifiable):

- *Modifiable factors:* drug abuse (for instance, cocaine-induced vasospasm), smoking, sedentary lifestyle, unhealthful diet, obesity, high blood pressure, vascular and heart disease (particularly atrial fibrillation), diabetes, body temperature, oral contraceptives, history of transient ischemic attacks, high red blood cell count, abnormal heart rhythm, cardiac structural abnormalities, high

blood cholesterol and lipids levels, hemiglobinopathy, hypercoagulate states, homocystinemia, among other.

- *Non-modifiable factors:* age (more than 65 years), gender (more frequent in women), race/ethnicity and heredity/genetics.

Although risk factors correlate with the presence of brain stroke, this vascular illness can be suffered by people without them.

1.3. Stroke incidence, symptoms and outcome

In the world, stroke affects more than 13.7 million people causing about 5.5 million deaths every year (Campbell et al., 2019). Stroke is the second most frequent cause of death and a leading cause of adult serious, long-term disability in many countries (Silverman, & Rymer, 2009). The annual incidence of the brain stroke in Spain is 71780 new cases every year (SEN, 2019), that is, one person every 7 minutes suffers brain stroke. Overall, more than 650000 people in Spain are affected by brain stroke. The number of death caused by brain vascular failure rise to more than 27000 people every year (SEN, 2019). In the Basque Country, we have around 3379 new cases of brain stroke within a year (SEN, 2019). Approximately 1363 people die because vascular pathologies in the Basque Country in a year-around (SEN, 2019) being the second cause of death in our region.

Despite an overall decrease in mortality over the last years, the number of stroke incidents is expected to increase due to the steadily growing population of elderly people. For this reason, it is urgent to develop therapeutic strategies to prevent (acting in the modifiable risk factors) and treat properly brain stroke when already occurs. As mentioned before, most people who suffer ischemic stroke survive and develop serious lifelong motor, sensory and cognitive disabilities. Ischemic stroke symptoms will vary depending on the cerebral location and size of the damaged tissue by the reduced blood flow. Most common symptoms include paraplegia, weakness of the limbs or face, aphasia, sensory disturbances, headache, dizziness and personality/emotional changes (Musuka et al., 2015; Schaapsmeerders et al., 2013). In addition, more than 80% of the stroke survivor develop long-term deficits that involve cognitive dysfunctions such as impairing memory and executive functions (Brainin et al., 2015; Jokinen et al., 2015). In fact, one of the main causes of dependency is the development of post stroke dementia in about 30% of stroke survivors, which is related to the brain atrophy caused by the vascular insult (Leys et al., 2005; Pohjasvaara et al., 1998). In addition to the personal deficits, ischemic stroke also entail social, economic and family burden. Most of people

who survive to ischemic stroke develops serious life disabilities and dependency (daily assistance, home attendant or admission to nursing home) of which force the family to adapt to the new situation. In addition to the family restructuration, patients need a constant health care from the ischemia onset to years or forever. Motor rehabilitation and early assistance have proven to be essential for the outcome of the disease.

1.4. Current treatment and therapeutic strategies

Diagnosis is needed to start the treatment in accordance with the etiology of the brain vascular occlusion. The goal of therapy in the ischemic stroke is to preserve tissue in cerebral areas where blood flow is reduced. Specifically, ischemic stroke treatment in the onset of the disease focuses in the clot removal. Thrombolysis is the standard clinical treatment for ischemic stroke, aimed to restore blood flow by dissolving the blood clot. Endovascular procedure or mechanical thrombectomy are strongly recommended to remove blood clot in patients with large vessel disease at sub-acute stages. However, around 15% patients are suitable for these treatments (Chia et al., 2016).

The gold treatment in ischemic stroke is the administration of recombinant tissue plasminogen activator (r-tPA). This thrombolytic drug breaks up the clot and improves blood flow to the part of the brain being deprived. Despite its beneficial results, r-tPA is rarely administrated and only 5% of patients benefit from this therapy because clot buster must be used within 4 hours from the stroke onset to be successfully applied (Vidale & Agostoni, 2014; Wardlaw et al., 2014). Many people do not arrive to the hospital in time to receive the medication and once this temporal window past, cerebral damaged is irreversible.

Besides technologic and scientific develop in the last years, current therapeutic strategies for ischemic stroke present limited benefits for patients and long-term disabilities appear in most of the cases. In fact, pathophysiological events, such as Wallerian Degeneration, happening in the later stages of the disease do not receive a proper treatment because are poorly understand (Dirnagl, Iadecola & Moskowitz, 1999). New clinical therapeutic approaches including melatonin, anti-apoptotic and anti-inflammatory drugs and hypothermia are in human clinical trials although with limited results (Dirnagl, Simon and Hallenbeck, 2003; Campbell et al., 2019). A better knowledge about the progression of ischemic stroke together with a detailed understanding of the brain endogenous mechanisms for neuroprotection, repair and neuroanatomical rewiring are needed to develop new strategies and improve stroke care.

More studies are needed to find suitable strategies considering that prevention is the most efficient therapeutic strategy available at the moment.

1.5. Brain vascular architecture

Brain vascular system consists in an intricate network of arteries and veins which supply cell support elements and remove the cellular waste. Blood is supplied to the brain by two carotid arteries and the basilar artery, formed by the two vertebral ones which arrive to the Willis polygon and once there, are distributed in three main brain regions by the anterior, middle and posterior cerebral arteries (Fig. 3). Each one irrigates a specific brain region and although some collateral arteries can minimize the reduction of the blood flow by the occlusion, ischemic damage can still occur due to not all brain regions are covered by collateral arteries (Rusanen, Saarinen & Sillanpää 2015). Ischemic stroke is mainly produced in the main cerebral artery, the MCA (Fluri et al., 2015). Occlusion of the MCA produces serious brain damage because this artery irrigate large regions.

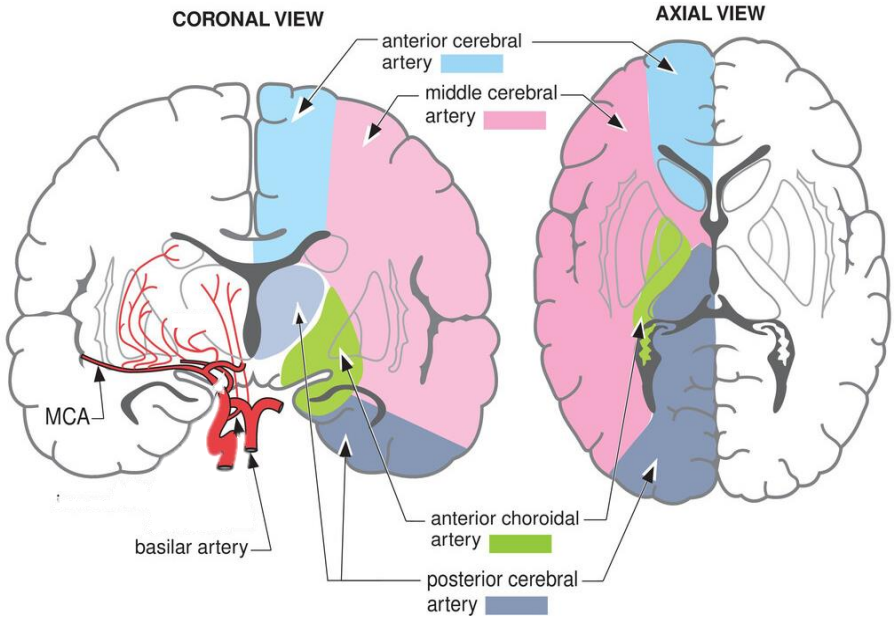

***Figure 3*. Brain arteries territory.** Anterior cerebral artery (in pale blue), middle cerebral artery (in pink) and posterior cerebral artery (in dark blue) and their irrigated regions in the brain. Modified from Greenberg (2016).

1.6. Pathophysiology: ischemic cascade at macro levels

Brain is the most energy demanding body organ. More than 20% of energy consumption in the body occurs in the brain and most of this energy relies on oxidative phosphorylation process (OXPHOS) (Hossmann, 1994). When a cerebral artery is

occluded and blood supply is interrupted, surrounding tissue undergoes oxygen and nutrients deprivation (Kalogeris et al., 2012). The brain tissue affected by the occlusion suffers an irreversible damage that constitutes the infarct **core**, while the surrounding area where cells suffer a partial blood flow deprivation is known as **penumbra area** (Paciaroni et al., 2009). Cells in the penumbra area do not die because collateral arteries diminish the oxygen and nutrients deprivation but display dysfunctional activities (Rusanen et al., 2015). Since ischemic stroke onset to chronic phases of the disease, brain tissue inside and outside the infarct tissue undergoes considerable changes over time. One of the most relevant relies in the growth of the necrotic core tissue overtime if nothing is done to avoid it (Fig. 4). Because cells surrounding necrotic tissue do not suffer of a total deprivation and, though dysfunctional, maintain the cellular activity, it is considered the penumbra area as the major therapeutic target to treat ischemic stroke.

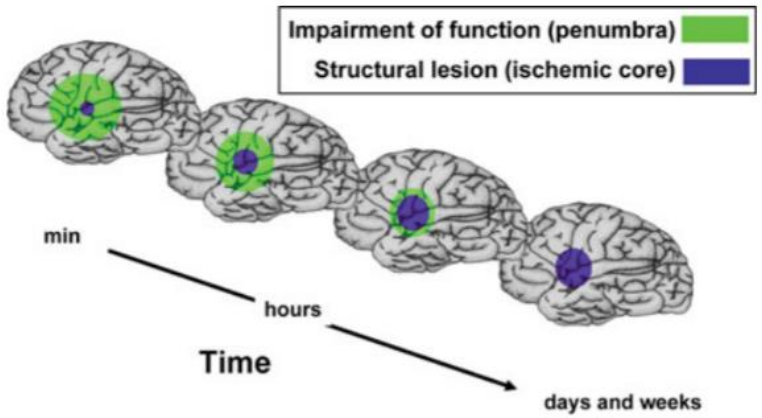

Figure 4. Progression of ischemic brain damage. Taken from Dirnagl, Iadecola & Moskowitz, 1999.

1.7. Pathophysiology: ischemic cascade at micro levels

Time course of ischemic stroke can be generally divided into three clinical phases: acute, sub-acute and chronic (Fig. 5; Zhao and Willing, 2018). The first phase, the acute one is mainly characterized by the primary damage that is produced by the occlusion *per se*. The second phase, the sub-acute one is characterized by the secondary damage caused by neuroinflammation and apoptotic processes in the surrounding penumbra area. The last phase, the chronic one, is characterized by the presence and resolution of primary and secondary damage in addition with the beginning of neuroprotective responses that brain performs against ischemic stroke. Brain protective response including neurogenesis, angiogenesis, scar tissue formation, oligodendrogliogeneses, axonal sprouting and synaptogenesis (Dirnagl, Simon and Hallenbeck, 2003; Zhang & Chopp, 2009; Deb, Sharma & Hassan, 2010).

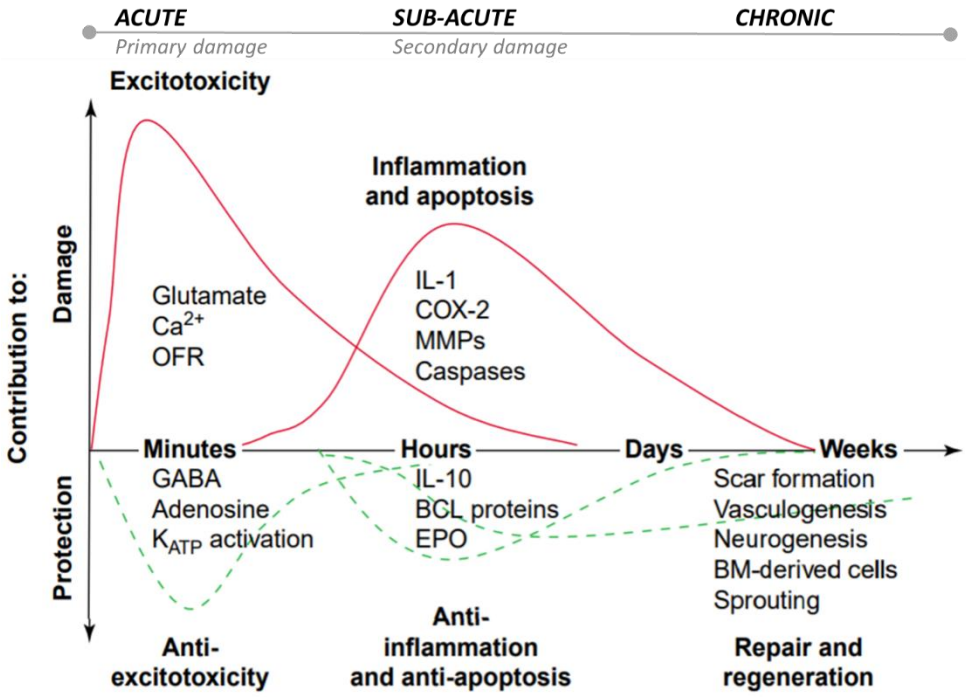

Figure 5. **Ischemic stroke clinical phases from the onset to chronic stages**. Acute phase also known as primary damage is characterized by occlusion consequences. Sub-acute phase or secondary damage is characterized by secondary damage derived from the occlusion process that comprise neuroinflammation and apoptotic processes. Chronic phase occurs weeks and months after occlusion and is characterized by continuing primary and secondary damage together with brain protective and regeneration responses. Abbreviations: OFR, Oxygen Free Radicals; COX-2, Cyclooxygenase 2; EPO, Erythropoietin; BM, Bone Marrow. Adapted from Dirnag, Simon & Hallenbeck, 2003.

Pathophysiology of cerebral ischemia is complex; a wide variety of cellular processes, initiated by ischemia, have been shown to be integral for neuronal injury. At micro levels, each clinical phase implies different cell responses (Fig. 6). Initial ischemic consequences in the cell trigger accumulation of cytosolic calcium, excitatory amino acids (EAA) release, oxidative stress signals, reactive nitrogen species (RNS) signals and activation of inflammatory mediators. Reduction of oxygen and glucose at early stages produce an imbalance in the energy requirements and availability (neurons and glia). Immediately after complete oxygen and glucose deprivation, cells begin anaerobic metabolism which increase the metabolic acidosis because of lactate production (Yenari & Han, 2012). Due to ATP depletion, this process peaks in necrotic cell death by excitotoxicity. Cell death also happens when neurons and glia are non-capable to uptake synaptic glutamate (or other EAA) because energy failure. Accumulation of glutamate activates N-methyl-D-aspartate (NMDA) and α-amino-3-hydroxy-5-methyl-4-isoxazolepropionic acid (AMPA) post-synaptic receptors causing the depolarisation of

cellular membrane which facilitates the intracellular entry of sodium, potassium and calcium, promoting the biochemical cascade leading to ultimate neuronal death.

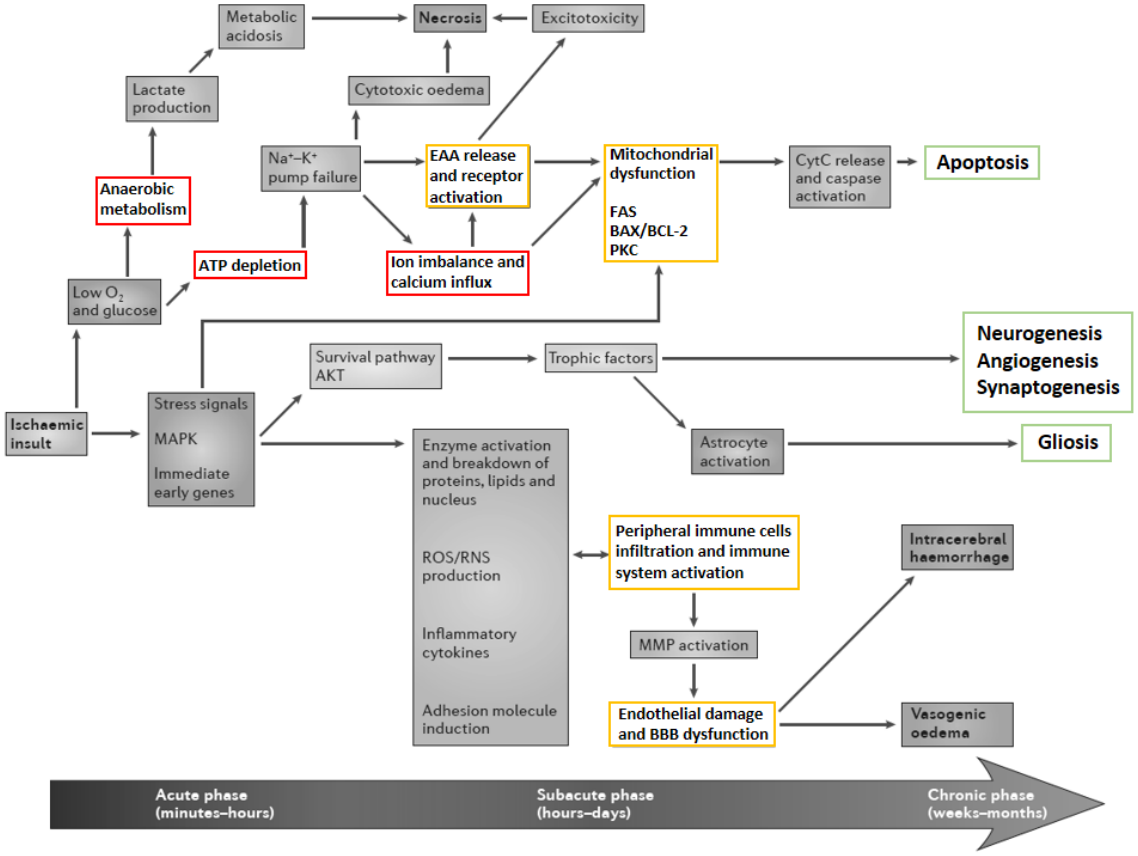

Figure 6. **Cellular processes derived from ischemic stroke in every clinical phase.** Artery occlusion produces in the acute phase deprivation of oxygen and glucose in the cells which trigger several cell signals (anaerobic metabolism, stress signals, ion pump failure or ATP depletion among others). At sub-acute phase, cell alterations in the penumbra area comprise mitochondrial dysfunction, excitatory amino acid (EAA) release such as glutamate, infiltrating immune cell and brain blood barrier breakdown, among others. Chronic phase is characterized by damage consequences (apoptosis or gliosis in the penumbra) and neuroprotective processes such as neurogenesis, angiogenesis and synaptogenesis (modified from Yenari & Han, 2012).

Accumulation of cytosolic calcium induce the activation of numerous enzymes as lipases, proteases, phospholipase C, endonucleases which affect the structural integrity of the cell. It also causes uncoupling of oxidative phosphorylation in mitochondria which leads the formation of reactive oxygen species (ROS). ROS damage the cells by peroxidation of lipid membrane, alteration of membrane potential, activation of pro-apoptotic mediators and direct DNA and protein damage. Regarding the RNS, Nitric Oxide (NO) pathway is surely the most important ischemic event. NO is activated by increased intracellular calcium and its interaction with oxygen free radical superoxide (O^{2-}) produce highly reactive and toxic peroxynitrite ($ONOO^{-}$) which activates lipid

peroxidation. NO also enhances glutamate release. Finally, inflammatory mediators, such as pro-inflammatory cytokines release by immune cells, induce protein misfolding, cytoskeletal breakdown or release of reactive ROS in neurons (Campbell et al., 2019).

Once initiate these events, pathological cell signals feed each other being almost impossible to stop the ischemic cell cascade. The final consequence is the cell death by necrosis or apoptosis although apoptosis is most often in the penumbra area where brain tissue suffer a partial deprivation of oxygen and nutrient (Yao et al., 2001; Onténiente et al., 2003; Broughton, Reutens & Sobey, 2009; Puyal, Ginet & Clarke, 2013). How the pathological events and brain responses are managed is fundamental for the outcome of the disease.

1.8. Neuroinflammation

Neuroinflammation, along with apoptosis, is the main secondary damage located in the sub-acute phase and could continue to chronic phases of the disease. After resolution of the damage cause by the arterial occlusion *per se*, neuroinflammation is the second cerebral therapeutic target. Indeed, neuroinflammation induces more brain damage compared with the primary lesion due to inflammation resolution require an extensive brain demand and time. Ischemia induces first the innate immune activation by neural immune cells, microglia, and by peripheral immune cells as perivascular macrophages and neutrophils. Because brain blood barrier (BBB) disruption and infiltration of peripheral immune cells hours and days after the occlusion, adaptive secondary immune response also occurs. Although inflammation facilitates the elimination of cellular debris and pathogens, it is also known that contribute to cell death and infarct growth (Dirnagl, Iadecola & Moskowitz, 1999).

Due to oxygen and nutrients deprivation, BBB elements like endothelial cells, pericytes and astrocytes suffer ion pumps imbalance which affect to the membrane stability and finally produce the death of the cells (Peruzzoti-Jametti et al., 2014). Necrotic cells release damage-associated molecular patters (DAMPS) that initiate the activation of pattern recognition receptors such as Toll-like receptors (TLRs), RIG-1 like receptors (RLRs), NOD-like receptors (NLRs), AIM2-like receptors (ALRs) and C-type lectin receptors (CLRs) (Hanke & Kielian, 2011; Chamorro et al., 2012). Activation of pattern recognition receptors in **microglia** induces a downstream signalling pathways including the nuclear factor kappa-light-chain-enhancer (NF-κB), the mitogen-activated protein kinase (MAPK) and type 1 interferon (IFN-1) which in turn upregulate proinflammatory cytokines, chemokines and ROS that culminate in the cell death (Takeuchi & Akira, 2010; Kim et al., 2016). Even microglia seem to play a negative role

by default, its role in debris clearance and promoting axonal sprouting and regrowth is fundamental for the damage resolution (Ma et al., 2017).

Peripheral immune cells also play a role in the neuroinflammation cascade initiate by the vascular occlusion. Infiltrating **neutrophils** arrive to the lesion around 4 hours after the occlusion and once there, these peripheral immune cells begin to produce proteases, cytokines, elastase, free oxygen radicals, inducible nitric oxide synthase (iNOS), matrix metalloproteinases (MMPs) and myeloperoxidases (MPO) (Justicia et al., 2003; Amulic et al., 2012). The release of these elements induce excitotocixity by NO production and the degradation of the extracellular space that facilitate the infiltration of other peripheral immune cells and blood-related elements (Asahi et al., 2001; Elali et al., 2011).

The second immune peripheral cells which take part in the neuroinflammation cascade are **macrophages**. Macrophages play a dual role in the ischemic area due to it is known these cells contribute to the regeneration of the damage tissue through removing necrotic cell and myelin debris that is necessary for the proper inflammation resolution, promotion of angiogenesis, scar formation and secretion of growth factor like oncomodulin or neurotrophins that enhance axonal sprouting and regrowth (Dougherty et al., 2000; Hashimoto et al., 2005; Yin et al., 2006; Shi & Pamer, 2011; Brancato & Albina, 2011; Koh & DiPietro, 2011; Ma et al., 2017). However, macrophages are also known for releasing pro-inflammatory cytokines and toxic molecules such as tumour necrosis factor alpha (TNF-α) and NO that promote leukocytes recruitment and by producing glutamate that further induced cell death (Lewén et al., 2000; Leonoudakis et al., 2008; Olmos & Lladó, 2014; Roth et al., 2014).

Later infiltration of peripheral immune cells as **eosinophils, lymphocytes and mast cells** also participate in the inflammatory response to stroke. Indeed, peripheral cells release adhesion molecules such as selectins which induce accumulation of platelets and fibrin in the ischemic territories (Marquardt et al., 2009). Because this accumulation, vessels persist occluded, BBB disrupted and perfusion reduced, enhancing infarct expansion (Ritter et al., 2009). Astrocytes become activated due to the immune-released cytokines and its reactivity limits accumulation and facilitate the removal of peripheral immune cells through the scar tissue formation (Bush et al., 1999; Sofroniew, 2009). With the resolution of the inflammation, glial activation like reactive astrocytes are allowed to restore the BBB through angiogenesis and vasculogenesis (Álvarez et al., 2013), initiating neurorepair and neuroprotective processes in the infarcted tissue.

2. GLIAL CELLS IN THE HOMEOSTATIC AND ISCHEMIC BRAIN

Glial cells and neurons are found in a ratio of 1:1 in the brain although there are differences based on the neural development step and the brain region (Herculano-Houzel, 2014). The most studied types are: microglia, oligodendrocytes and astrocytes. Glial cells in the central nervous system (CNS) develop heterogeneous functions under physiological and pathological brain conditions. In brain ischemia, glia participates in neuroprotective responses implemented to control and regenerate the damaged tissue.

2.1. Glial role under physiological conditions

In the non-pathological brain, glial cells are crucial for proper synapses formation at embryonic stages and neuronal homeostasis at adult stages including axonal conductance, ionic balance in the extracellular space, synapses participation, protection against external pathogens and metabolic support. Microglia is known for its role in the phagocytosis of apoptotic cells and synapses pruning during development that favour correct conformation of neuronal network (Tremblay et al., 2011; Kettenmann, Kirchhoff & Verkhratsky, 2013). In addition, microglia also play a relevant role at postnatal stages including its participation in the synapsis and its role as a resident immune cells of the brain (Wake et al., 2009; Kettenmann, Kirchhoff & Verkhratsky, 2013; Parkhurst et al., 2013). Oligodendrocytes, in contrast, play a key role in the axonal myelination which facilitate neuronal inputs and thus the neuronal network (Fields, 2008; Zatorre, Fields & Johansen-Berg, 2012). Likewise, oligodendrocytes participate actively in the periaxonal ion and neurotransmitter homeostasis, as well as, provide axonal metabolic support (Du & Dreyfus, 2002; Yamazaki et al., 2010). Thus, oligodendrocytes can modulate action potential propagation in the neuronal axons (Fields, 2008). Finally, astrocytes are mainly characterized by its role as neuronal-supporting cells including processes involved in synapses, metabolic support and control of the amount of extracellular molecules to avoid excitotocicity. Astrocytes contact the blood vessels (BV) with their end-feet, being part of the BBB structure and thus obtain oxygen and nutrients that metabolize and supply to the neurons for the proper neuronal function (Abbott et al., 2010; Mathiisen et al., 2010). In addition, astrocytes play a key role in synapses by rescuing released neurotransmitter which can be toxic if accumulates in the extracellular space (Eulenburg & Gomeza, 2010; Boison, Chen & Fredholm, 2010; Zhou & Danbolt, 2013). Thus, astrocytes and other glial cells develop a crucial role in the physiological brain through supporting and modulating vital neuronal activities.

2.2. Glial role under ischemic conditions

Under pathological conditions, such as ischemic stroke, glial cells become reactive and respond to the injury (for a review, see Verkhratsky et al., 2014). In the ischemic stroke, even glial activation occurs early after occlusion, their main action become relevant at chronic stages of the disease (Dirnagl, Simon and Hallenbeck, 2003; Zhang & Chopp, 2009; Deb, Sharma & Hassan, 2010). Astrocytes and oligodendrocytes play a crucial role in the recovery of the ischemic tissue (Giaume et al., 2007; Burda & Sofroniew, 2014) whereas microglia play a relevant role in the neuroinflammation cascade at sub-acute phases and its function at later stages is mainly focused to the proper resolution of the neuroinflammation as described above (Ma et al., 2017; Qin et al., 2019). At later stages, glial response is context-dependant since injury state determines the phenotype of reactive glial cells. In this part, we discuss the glial role from onset to chronic phases of the vascular disease.

2.2.1. Microglia role in the ischemic lesion

Even the dual role of microglial cells in the onset of the disease described above in the *1.8 section*, microglia play an essential role at later stages when neuroprotective and neurorepair processes occur. In addition to the role in the inflammation resolution, microglia promote synapses formation and neuronal viability in the penumbra area through complement system activation (Ahmad et al., 2019). Depletion of microglia has found to be detrimental for the proper damage resolution causing exacerbated infarct volume, brain swelling, and neurological deficit (Lalancette-Hébert et al., 2007; Jin et al., 2017). Understanding how microglia swift from toxic to protective phenotype in the ischemic stroke is one of the most current trending topics in the field.

2.2.2. Oligodendrocytes role in the ischemic lesion

Regarding oligodendrocytes, lesion size and how resolution has been managed is instrumental to determine what kind of role oligodendrocytes will develop. In the lesion area, oligodendrocytes die contributing to the excitotoxicity and remyelinization of living neuronal axons is inhibited (Dewar, Underhill & Goldberg, 2003; Arai & Lo, 2009; Bakiri et al., 2009). Although oligodendrocytes is reported to contribute to neuroprotective processes (Mandai et al., 1997; Tanaka et al., 2003), their role in enhancing neuronal survival in the penumbra area through promoting axonal conductance fail by high toxic molecules released in the extracellular space (Franklin & Ffrench-Constant, 2008;

McTigue & Tripathi, 2008; Zhang et al., 2013). It is not until total elimination of excitotoxic molecules by removing myelin debris and necrotic cells when oligodendrocytes precursor cells (OPC) arrive to the lesion, proliferate and differentiate into immature oligodendrocytes in order to replace dead oligodendrocytes in the lesion and in an effort to restore the conductance of living neuron axons (Nait-Oumesmar et al., 2008; Tepavčević et al., 2011). However, neurons in the ischemic area at later stages usually die by the adverse environment and oligodendrocytes are not able to restore axonal viability in a greater extend, producing neurodegenerative diseases like Wallerian degeneration (Dirnagl, Iadecola & Moskowitz, 1999).

2.2.3. Astrocytes role in the ischemic lesion

Astrocytes play a pivotal role in the physiological CNS and become reactive in response to injury. The activation state of reactive astrocyte changes according to the nature and severity of the insult, showing from alterations in molecular expression or progressive cellular hypertrophy to, in severe cases, proliferation and scar formation (Sofroniew, 2009). Astrocytes sense released toxic molecules and begin to express a wide range of genes involve in the activation state such as glial fibrillary acidic protein (GFAP), vimentin and nestin (Pekny & Nilsson, 2005; Burda & Sofroniew, 2014), which result in the appearance of multiple reactive phenotypes. In the ischemic stroke, as severe injury, astrocytes acquire an extremely reactive phenotype in the lesion core that contribute to beneficial and detrimental actions in the development of the disease. In the penumbra area, astrocytes adopt a hypertrophy morphology that help them to sense toxic molecules.

Based on lesion size and location of astrocytes, they develop a biphasic function in the ischemic brain. As a response to ischemic stroke, astrocytes adopt an extremely hypertrophic morphology and proliferation (Sofroniew, 2009). In the core of the lesion and early stages of the disease, astrocytes promote BBB and Extracellular matrix (ECM) disruption by releasing molecules such as MMPs (Zhao et al., 2006; Candelario-Jalil, Yang & Rosenberg, 2009), lactate (Yenari & Han, 2012) and by retracting end-feet from BV (Dodson et al., 1977; Swanson, Ying & Kauppinen, 2004). This BBB disruption induce a delay in restoration of the vascular system and contribute to vascular extravasation of blood-related elements like peripheral immune cells and exacerbation of the inflammation cascade (Buffo, Rolando & Ceruti, 2010; Burda & Sofroniew, 2014). Even though, the most reliable pathological event by reactive astrocytes is the formation of the glial scar in the perilesional area that inhibit axonal sprouting and regrowth, inhibiting the repair of the damage tissue (Schwab, Kapfhammer & Bandtlow, 1993; Frisén, 1997).

Negative role of astrocytes seem to be restricted to the high toxic core area and early stages of the disease. Likewise, astrocytes hypertrophy, the increase in proliferation and up-regulation of different genes must be directed to promote brain repair (Sofroniew, 2014).

In the penumbra area or later stages of the disease, astrocytes display a positive role when astrogliogenesis is moderated or well-resolved. In this case, astrocytes help in removing extracellular toxic molecules such as calcium or glutamate (Ottersen et al., 1996; Danbolt, 2001; Phillis & O´Regan, 2004), support neurons of energy through glycolytic metabolism (Brown, 2004), restore BBB by vascular endothelial growth factor (VEGF) release (Argaw et al., 2009; Williamson et al., 2021), promote OPC recruitment, proliferation and differentiation (Williams, Piaton & Lubetzki, 2007), modulate microglia function (Hauwel et al., 2005), promote glial scar formation to limit injury from healthy tissue (Pekny et al., 1999; Bush et al., 1999; Faulkner et al., 2004), ECM remodelling at later stages (Buffo, Rolando & Ceruti, 2010) and overall, improve the outcome of the disease. Indeed, deletion of reactive astrocytes in the damaged area after ischemic stroke induced a huge increase of cell death and demyelination promoting a worse recovery of the tissue damage (Pekny et al., 1999; Bush et al., 1999; Faulkner et al., 2004; Li et al., 2008; Wanner et al., 2013). Using a transgenic mice approach to reduce the nestin and vimentin expression which are necessary for astrocytes activation, Pekny et al. (1999) shown reactive astrocytes ablation induced an increase of the damage tissue. Moreover, ablation of proliferation in reactive local astrocytes induces a worse performance of behavioural function and limits restoration of blood flow after cortical infarct (Willianson et al., 2021). Therefore, reactive astrocyte phenotypes, according to the ischemic phase and their location respect to the injury, may be a potential therapeutic target to prevent neural detrimental responses against to the ischemic insult.

As mentioned before, astrocytes are responsible of the **glial scar** formation in an ultimate state (Fig. 7). Scar tissue is composed by platelet, fibrins and peripheral immune cells in the core of the lesion, and by reactive astrocytes in the penumbra area that become fibrotic and create a physical wall to divide damaged and healthy tissue (Sofroniew, 2009). Besides glial scarring and tissue remodelling are necessary for diminishing brain damage sealing off the damaged area, preventing microbial infections and limiting infiltration of peripheral immune cells and blood-related elements (Bush et al., 1999; Faulkner et al., 2004; Anderson et al., 2016), glial scar becomes detrimental at later stages because inhibit the regrowth of axons in the ischemic region (Yi & He, 2006; Lo, 2008). This incident can explain why patient develop delayed cognitive impairment after stroke (Brainin et al., 2015). However, ablation of glial scar at early

stages induced a huge increase of the ischemic damage. Genetic silence of pentraxin-3 (PTX-3), a key element in the glial scar formation, shown BBB damage and an increase edema due to the impairment of astrogliosis response (Rodríguez-Grande et al., 2014). Likewise, Benner et al. (2013), who deleted the expression of a key regulator of glial scarring, observed an increase of the edema volume in their transgenic mice. In spinal cord injury, ablation of STAT3 signals induced a glial scar malformation that drive to worse outcome of the disease (Barnabé-Heider et al., 2010; Anderson et al., 2016). Understanding why glial scar is not proper degraded after core resolution like in the spinal cord injury (Frisén, 2016; Anderson et al., 2016) is instrumental to improve repair and regenerative brain actions.

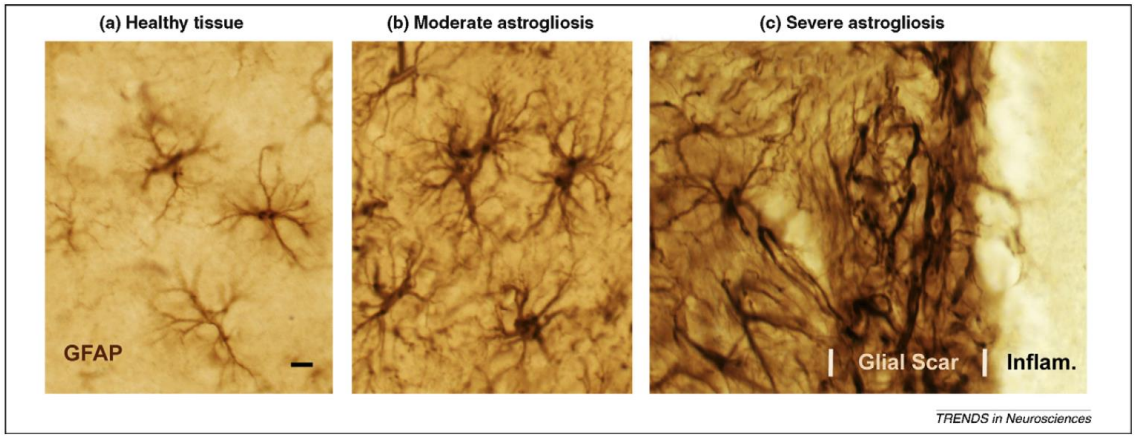

***Figure 7*. Astrocytes activation and glial scar formation following brain injury.** GFAP staining in the healthy tissue (a), moderate astrogliosis (b) or severe astrogliosis (c). Taken from Sofroniew (2009).

3. ADULT NEUROGENIC NICHE: THE SUBVENTRICULAR ZONE

Another neuroprotective response against ischemic stroke involves adult Neural Stem Cells (NSC) which participate in the progression of the disease. Here, we focus in the Subventricular Zone (SVZ), one of the main neurogenic niche in the adult mice brain.

Stem cells are commonly found in the body tissue although their existence in the brain remained far unknown until the mid-60s decade (Altman, 1962; Altman & Gas, 1965). In the developing of CNS, neuroepithelial cells located in the neural tube begin to proliferate and expand, later producing the embryonic neural progenitor cells known as radial glial cells (RGC) (Taverna et al., 2014). RGC also proliferate and produce new-born neurons that migrate toward the pial surface. Therefore, neurogenesis occurs mainly at embryonic stages where RGC are highly found and create most adult neurons, acting as a guiding scaffolds to help new-born neurons to arrive at their final location (for review, see Borrell & Götz, 2014). Later on, at postnatal stages, RGC derive into NSC

that persist in discrete areas of the adult brain and retain neurogenic capacity throughout life (Tramontin et al., 2003; Merkle et al., 2004; Ming & Song, 2011). Among these remaining neurogenic niches, SVZ is the largest germinal area in the adult mice brain (Mirzadeh et al., 2008) which is located along the walls of the lateral ventricle. Another main neurogenic niche is the dentate gyrus of the hippocampus (Álvarez-Buylla & García-Verdugo., 2002). Adult NSC from SVZ are undifferentiated precursor cells derived from the embryonic RGC which retain the stemness capacity through self-renewal, proliferation and differentiation processes, described the last as the capacity to give rise to both neuronal and glial lineages (Shi et al., 2008).

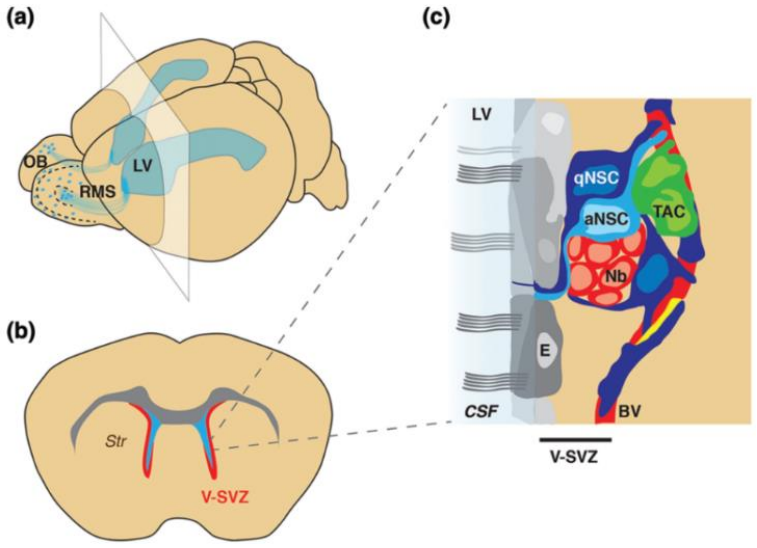

Figure 8. **Subventricular zone location and architecture.** SVZ niche in the whole brain (a). Coronal view of SVZ lining lateral ventricles (b). NSC types in the SVZ: ependymal cells in gray, quiescent NSC (qNSC) in dark blue, active NSC (aNSC) in pale blue, transient amplifying cells in green and neuroblast in red (c). Taken from Chaker, Codega & Doetsch (2016).

Unlike dentate gyrus, NSC in the SVZ harbour a potential capacity to migrate long distance via the rostral migratory stream (RMS) toward the olfactory bulb (OB) where neurogenesis occurs (Fig. 8; Johansson et al., 1999). Gliogenesis and oligodendrogenesis from SVZ stem cells also happen at adult stages (Luskin & McDermott, 1994; Menn et al., 2006; Ortega et al., 2013; Sohn et al., 2015). NSC comprise several population or phases that are generally classified into quiescent NSC or type B1 cells, transient amplifying cells (TAC) or type C and neuroblast or type A cells (Fig. 8; Doetsch, García-Verdugo & Álvarez-Buylla, 1997; Ihrie et al., 2011). Quiescent NSC or Type B1 cells become activated and give rise to neuroblasts (type A cells) through quickly proliferating TAC or type C cells. Neuroblasts migrate attached to glial chains and constitute the RMS. After arriving to the OB, neuroblasts differentiate into different types of OB interneurons base on their SVZ location and NSC population (Merkle et al., 2014; Fiorelli et al., 2015). Once in the OB, neuroblasts change their tangentially migration and begin to migrate radially until their final location in the OB layer, integrating in the pre-existing neuronal network (Luskin, 1998; Petreanu & Álvarez-

Buylla, 2002; Imayoshi et al., 2008). NSC express different markers according to their undifferentiated or differentiated stage (Fig. 9) what make a challenge to track NSC in their travel since the SVZ to the OB.

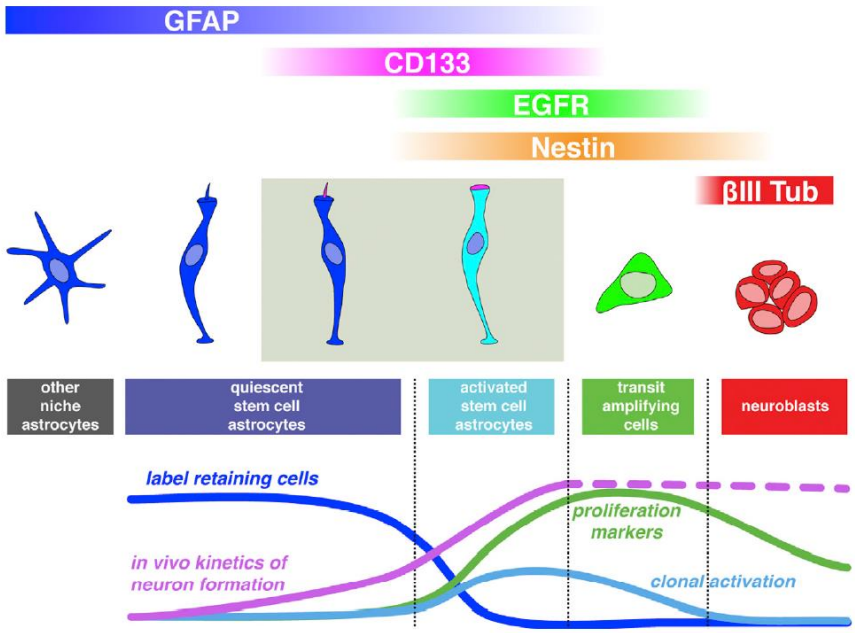

***Figure 9*. NSC markers from undifferentiated to differentiated stages.** Taken from Codega et al. (2014).

Quiescent NSC produce more than 10.000 immature interneurons from TAC (Doetsch et al., 1999). TAC can divide three or four time before differentiating into neuroblasts, thus, TAC expand the number of young neurons that travel to the OB (Ponti et al., 2013). However, even neurogenesis occurs in the adult brain every day, NSC pool remain at adult stages because of self-renewal capacity. Self-renewal, the gold features of NSC, can be described as the process to produce more undifferentiated NSC and retain the stemness feature through asymmetric division. When a stem cell enter in the cell cycle originate two daughter cells. In the symmetric division, both daughter cells receive the same factors whereas in the asymmetric division, one daughter cell receive RNAs, proteins and other molecules that maintain the undifferentiated program and the other cell receive lineage commitment factors (Obernier et al., 2018). Thus, NSC remain in the SVZ and avoid the exhaustion of the neurogenic pool.

3.1. Local and long distance niche signals are key regulators of NSC behaviour

Several elements in the SVZ niche are involved in NSC maintenance, proliferation and differentiation. Quiescent NSC display a particular morphology and localization in the SVZ, touching on one hand BV and on the other the lateral ventricle

through a small apical cilium that conform together with ependymal cells the pinwheel structure (Mirzadeh et al., 2008; Ihrie et al., 2011). In addition to the special cell shape, quiescent NSC display features like low levels of oxygen, between 2-5%, that drive to a glycolytic metabolism (Zheng et al., 2016) and subsequently, to the accumulation of molecules such as ROS, hypoxia inducible factor-1 alpha (HIF1α) and Transforming growth factor alpha and beta (TGFα and β) at physiological conditions (Tropepe et al., 1997; Guerra-Crespo et al., 2009; Pavlica et al., 2012; Dias et al., 2014; Li et al., 2014; Zheng et al., 2016). Indeed, hypoxic stimuli promotes NSC self-renewal through VEGF and erythropoietin (EPO) production induced by HIF1α pathway (Pavlica et al., 2012; Li et al., 2014). Also ROS accumulation is observed to trigger self-renewal and neurogenesis (Le Belle et al., 2011). In addition to their own homeostasis, quiescent NSC maintenance is regulated by local and long-distance stimuli (Fig. 10). Among local regulators, signals from neighbouring cells (NSC, ependymal cells, microglia and astrocytes), from BV and endothelial cells, and finally, from cerebrospinal fluid (CSF) and Choroid Plexus (CP), influence NSC behaviour. Regarding long distance regulators, SVZ NSC sense neurotransmitter from multiple neuronal types from distance brain regions.

Local regulators control the quiescence of NSC by releasing neurotransmitters, trophic factors, calcium waves, and other mechanisms. Local cells and NSC themselves stimulate each other because their close anatomical location in the SVZ. Because SVZ niche displays a unique extracellular space, the cell-cell contact and signalling is easy to perform. All efforts in the physiological SVZ point to preserve stemness capacity avoiding exhaustion of quiescent NSC. Autocrine regulators of NSC comprise TGF α and β (Guerra-Crespo et al., 2009; Dias et al., 2014), amphyregulin, fibroblast growth factor-2 (FGF-2), endothelin-1 (Adams et al., 2020), insulin-like growth factor 2 (IGF2), leukemia inhibitory factor (LIF), ciliary neurotrophic factor (CNTF) and transglutaminase 2 promote proliferation (Mercier & Douet, 2014; Marques et al., 2011; Emsley & Hagg, 2003; Lee et al., 2013; Kjell et al., 2020) whereas sphingosine-1-phosphate (S1P) or prostaglandin D2 (PGD2) maintain quiescence (Codega et al., 2014; Chaker, Codega & Doetsch, 2016).

Neuroblasts in the SVZ inhibit NSC proliferation and differentiation via GABA inhibition and maintain NSC in a dormant state (Liu et al., 2005; Fernando et al., 2011). Also, other local SVZ cells such as microglia and astrocytes also play a role in NSC maintenance. Microglia display a different shape in the SVZ neurogenic niche and its processes can contact CSF (Sirerol-Piquer et al., 2019). One of its main function is to maintain niche homeostasis through removing apoptotic cells derived from dividing cells (Sierra et al., 2010). Activated microglia inhibit neurogenesis (Sierra et al., 2014) and

favour gliogenesis via tumor necrosis factor-α (TNFα) (Carpentier & Palmer, 2009). However, when exposed to interleukin-4 (IL4) and interferon-γ (IFNγ), microglia secrete insulin-like growth factor 1 (IGF1) and promote neural differentiation of NSC (Butovsky et al., 2006). SVZ astrocytes also modulate NSC proliferation through ATP release (Cao et al., 2013) whereas Wnt3, neurogenesin-1 (NG1), thrombospondin-1 (Thbs1), interleukin-β (IL1β) and interleukin-6 (IL6) promote neuronal differentiation (Ueki et al., 2003; Lie et al., 2005; Barkho et al., 2006; Lu & Kipnis, 2010). Moreover, local acetylcholinergic neurons avoid activation of quiescent NSC (Paez-Gonzalez et al., 2014).

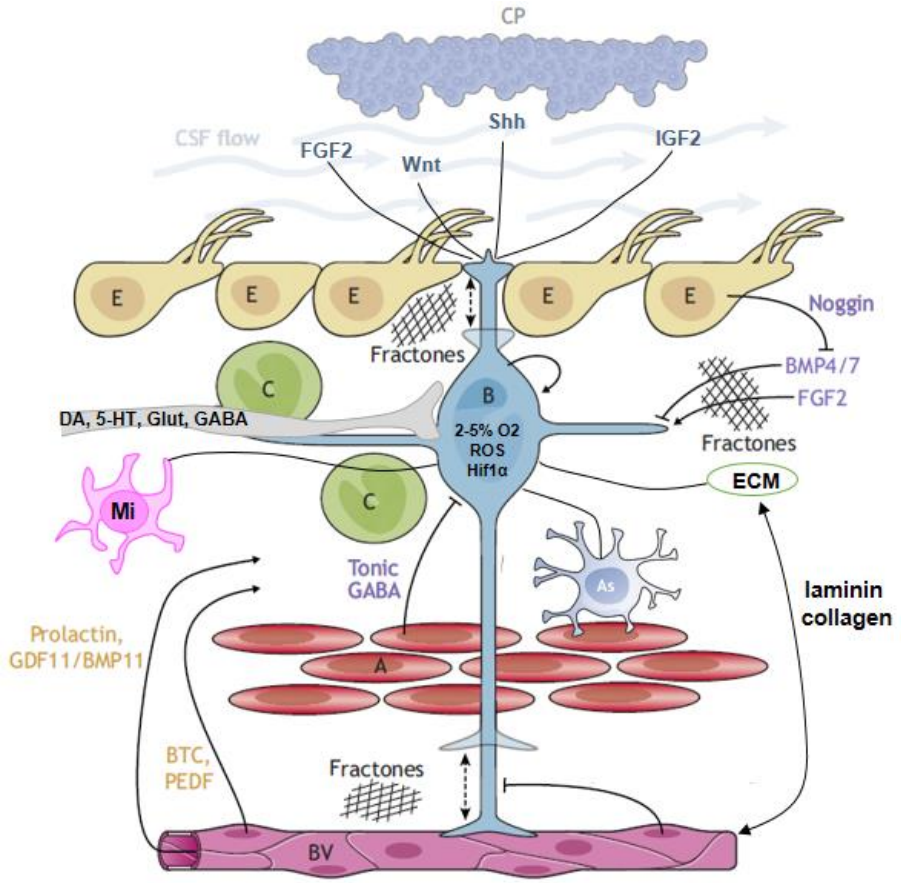

***Figure 10*. Local and long distance signals modulate SVZ neurogenic niche homeostasis.** NSC regulators are cell-cell contacts themselves, microglia, astrocytes, ependymal and endothelial cells, vascular niche, ECM elements such as fractones, cerebrospinal fluid (CSF) and Choroid Plexus (CP) signals and local and long-range neuronal innervation (DA: Dopamine; 5-HT: Serotonine; Glut: Glutamine; GABA: gamma-Aminobutyric acid). Quiescent NSC (type B1 cells), TAC (type C cells) and neuroblasts (type A cells). Modified from Obernier & Álvarez-Buylla (2019).

In addition to local cells, quiescent NSC are in close contact with the vascular SVZ structures (vascular niche) and receive blood and endothelial cell-released molecules such as prolactin (Shingo et al., 2003), growth differentiation factor 11

(GDF11), bone morphogenetic protein 11 (BMP11) (Katsimpardi et al., 2014), betacellulin (BTC), neurotrophin 3 (NT3), pigment epithelium-derived factor (PEDF) (Gómez-Gaviro et al., 2012; Andreu-Agulló et al., 2009; Delgado et al., 2014) and Notch ligand Jagged 1, Jagged 2 and Delta-like 4 (Gaiano & Fishell, 2002; Shen et al., 2004; Androutsellis-Theotokis et al., 2010; Butti et al., 2014) that preserve self-renewal and neurogenesis homeostasis. However, other blood-derived molecules such as VEGF promote angiogenesis and neurogenesis (Jin et al., 2002; Cao et al., 2004; Udo et al., 2008; Ruiz de Almodovar et al., 2009) whereas stromal cell-derived factor 1 (SDF1) stimulate motility of quiescent NSC, TAC and neuroblasts (Kokovay et al., 2010). Blood molecules contact quiescent NSC also through small structures called fractones (Obernier et al., 2018; Mercier et al., 2002). ECM displays a unique SVZ environment composed by fractones which are projections of vascular basement membranes and are mainly composed by laminin, collagen IV, nidogen, heparan sulphates, perlecan and proteoglycans (Gattazo et al., 2014; Ottoboni et al., 2017). These ECM elements are fundamental for neurogenic pool maintenance because play a key role promoting quiescence (Kjell et al., 2020) or enhancing physiological activation by sequestering, concentrating and presenting release molecules (Kerever et al., 2007).

Finally, CSF and CP influence quiescent NSC activity through ependymal cells release molecules (Lim et al., 2000; Siegenthaler et al., 2009; Petrik et al., 2018). Also, quiescent NSC contact directly the CSF and sense morphogens such as FGF2, IGF2, Wnt and Sonic Hedgehog (SHH) (Corbit et al., 2005; Rohatgi et al., 2007; Breunig et al., 2008; Ihrie et al., 2011; Lehtinen and Walsh, 2011). CSF itself can induce changes via mechano-sensing signalling such as calcium waves, promoting proliferation and differentiation (Arulmoli et al., 2015; Jagielska et al., 2017; Petrik et al., 2018). Ependymal cells themselves can modulate NSC quiescence via noggin release (Lim et al., 2000). Noggin is an antagonist of BMP4 of which act in the quiescent NSC and inhibit cell proliferation and favours glial differentiation (Lim et al., 2000; Mercier & Douet, 2014).

Far regulators include innervation of distant neurons. NSC from SVZ receive glutamatergic and GABAergic terminals from striatal neurons that promote survival and proliferation of neuroblasts (Song et al., 2017) and maintenance stemness (Young et al., 2012) respectively. Serotoninergic projection from dorsal raphe nucleus innerve the dense network of supraependymal axons and contact directly with the apical processes of quiescent NSC enhancing proliferation (Brezun and Daszuta, 1999; Tong et al., 2014). Dopaminergic neurons also send terminals to SVZ where dopamine neurotransmitter induce NSC activation (Kippin et al., 2005; Kim et al., 2010) or NSC homeostasis (Höglinger et al., 2004; Baker et al., 2004; Lennington et al., 2011). Finally,

propiomelanocortin signals, a hormone precursor, released by hypothalamic neurons promote NSC proliferation in the antero-ventral SVZ and link neurogenesis with neuroendocrine function (Paul et al., 2017).

External unmodified factors such as aging, gender, genes and diseases influence NSC homeostasis, proliferation and differentiation throughout life (Maslow et al., 2004; Luo et al., 2006; Shook et al., 2012; Capilla-Gonzalez et al., 2014). Indeed, **aging** induces a decrease in the number of NSC, an increase of cell senescence, loss of SVZ niche integrity, defects in cell-cell contacts and signalling and an alteration in NSC metabolism (Oh et al., 2014). Main consequences of aging is NSC exhaustion and subsequently reduction of neuroblasts population (Kerever et al., 2015). Causes included increase of aged-related genes that drive the accumulation of damaged DNA (Bailey et al., 2004); metabolic changes which prevent the swift from glycolytic to mitochondrial respiration, a requisite for NSC activation (Rabie et al., 2011; Chaker et al., 2015); and accumulation of toxic molecules that contribute to a low-grade of inflammation in aging (Franceschi & Campisi, 2014) which reduce neurogenesis, neuroplasticity and cause cognitive decline in aging (Villeda et al., 2011; Kerever et al., 2015; Wyss-Coray, 2016).

3.2. Regional heterogeneity in the SVZ

NSC derive from embryonic RGC, inherit their regional signature (Fuentealba et al., 2015) and formed a heterogeneous population that, based on their rostro-caudal and ventro-dorsal location, generate different type of OB interneurons (Fig. 11; for a review, see Chaker, Codega & Doetsch, 2016). Transcription factors that characterize embryonic RGC are also expressed by inherited adult NSC. Pallial markers such as Emx1 (Young et al., 2007; Llorens-Bobadilla et al., 2015), Pax6 (Kohwi et al., 2005; Hack et al., 2005; López-Juárez et al., 2013; Llorens-Bobadilla et al., 2015), Tbr2 (Brill et al., 2009), Neurog2 (Brill et al., 2009; Winpenny et al., 2011; Llorens-Bobadilla et al., 2015) or Sp8 (López-Juárez et al., 2013) are expressed in the adult dorsal regions whereas in the subpallium, lateral ganglionic eminences (LGE) and medial ganglionic eminence (MGE), transcription factors such as Dlx1/2/5 (Azim et al., 2012), Gsx1/2 (López-Juárez et al., 2013) and Nkx2.1 (Merkle et al., 2014; Delgado & Lim, 2015; Llorens-Bobadilla et al., 2015), Nkx6.2 (Merkle et al., 2014; Llorens-Bobadilla et al., 2015), Gli1 (Merkle et al., 2014) are expressed in lateral and ventral SVZ regions. Finally, zinc is expressed in the septal wall and its expression persists in the adult medial SVZ (Merkle et al., 2014).

Different endogenous regulators in the adult SVZ also differ their presence along rostro-caudal and ventro-dorsal location. For example, wingless (Wnt) is expressed dorsally (Ortega et al., 2013; Azim et al., 2014) while SHH is ventrally expressed (Ihrie et al., 2011) even though recent report suggest mixed-lineage leukemia 1 (Mll1) and not SHH maintains Nkx2.1 expression in the ventral NSC (Delgado et al., 2021). Others transcriptional factors expressed from embryonic stages also determine cell fate of NSC. In addition, CSF flow and ependymal cells regulate cell fate of new-born interneurons. Ependymal cells which are known to modulate BMP signalling (Colak et al., 2008; Falcao et al., 2012) are denser and mature more rapidly in the medial and the dorsal SVZ (Spassky et al., 2005) determining the cell fate of these regions. Limitation of Wnt signals in dorsal SVZ is also restricted by mature oligodendrocytes located in the corpus callosum (Ortega et al., 2013). CSF flow, which is higher in the lateral wall of the ventricles, also defines new-born neurons fate through limiting Wnt signal in the lateral SVZ (Azim et al., 2014). Finally, cell cycle defines cell type production in the OB and their location as well (Ponti et al., 2013).

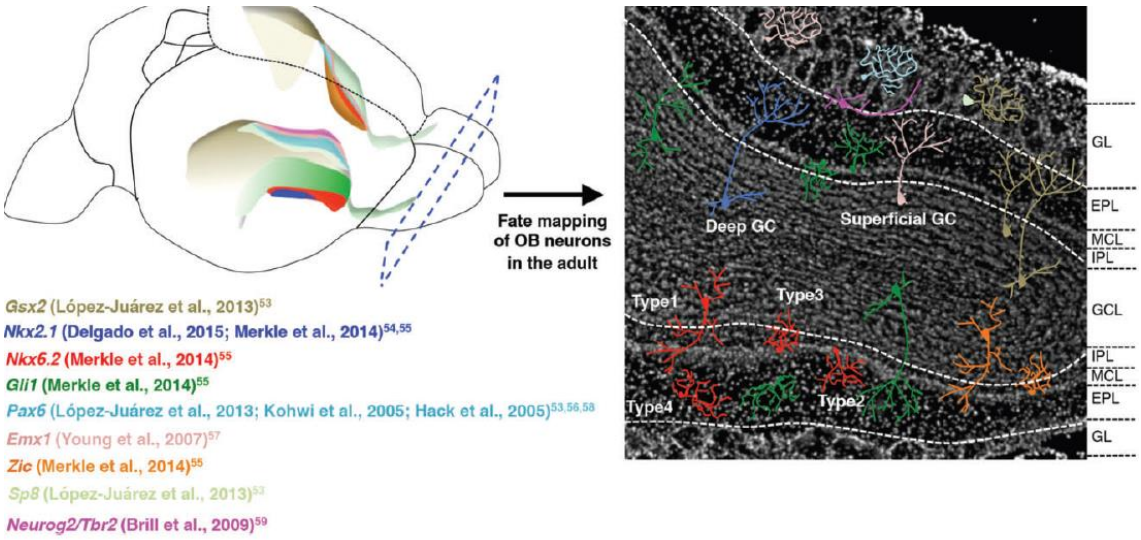

***Figure 11*. Topographic characterization of NSC and their cell fate in the OB layers based on their SVZ location.** Taken from Chaker, Codega & Doetsch (2016).

Topographic characterization of the SVZ shows that specific NSC populations present a pre-establish neural program that control final post-mitotic cell type in the OB (Merkle et al., 2014; Fiorelli et al., 2015; Delgado et al., 2021). Calretinin periglomerular cells, superficial granular cells, tyrosine hydroxylase positive periglomerular cells and a small number of glutamatergic juxtaglomerular cells are preferentially generated in medial and dorsal SVZ (Merkle et al., 2007; Young et al., 2007; Brill et al., 2009; Fernando et al., 2011; de Chevigny et al., 2012) whereas calbindin positive

periglomerular cells and deep granular cells are mainly generated from ventral and lateral SVZ (Merkle et al., 2007; Young et al., 2007). In summary, periglomerular cells and dopamine periglomerular neurons are produced from dorsal regions whereas ventral NSC derive into deep granular interneurons (Cebrián-Silla et al., 2021). Ultra-specialization of SVZ niche suggests a large variety of NSC and a "cellular program" that determines the NSC fate under physiologic.

4. SUBVENTRICULAR ZONE RESPONSE TO ISCHEMIC STROKE

As a part of regenerative processes started after ischemic stroke, NSC become reactive and respond to injury. NSC from SVZ harbour the capacity to migrate long distance and after a sudden vascular occlusion, migrate toward the damaged area. SVZ response to injury take place in three phases: activation, migration of NSC-derived cells and their integration or role in the ischemic zone (Fig. 12). NSC become activated and proliferate in response to brain stroke at early stages of the disease (Jin et al., 2001; Zhang et al., 2001; Li et al., 2001; Parent et al., 2002; Zhang et al., 2004; Tonchev et al., 2005). Next, NSC differentiate and leave the SVZ. NSC-derived cells travel long-distances attracted by chemokines, cytokines and other ischemic-related molecules created by immune cells, fibroblasts, stromal cells and local cells in the lesion core (Jin et al., 2001; Arvidsson et al., 2002; Parent et al., 2002; Zhang et al., 2001, 2004; Yamashita et al., 2006; Benner et al., 2013). Migration step takes some days or weeks after occlusion and it is not until several weeks or months that NSC-derived cells arrived to the injury and perform their role. Once there, NSC-derived cells display different functions including neuron repopulation (Yamashita et al., 2006; Kolb et al., 2007), removal of toxic molecules via glial scar formation or sequestation them to diminish the excitotoxic environment (Pekny et al., 1999; Benner et al., 2013; Faiz et al., 2015).

Once in the lesion, NSC-derived cells are modulated by ischemic-related elements such as excitotoxicity (Yao et al., 2001; Onténiente et al., 2003; Broughton et al., 2009; Puyal et al., 2013), blood-derived elements such as fibrinogen (Pous et al., 2020) or infiltrating immune cells (Imitola et al., 2004; Gordon, McGregor & Connor, 2009). In addition, ischemic-related elements also influence NSC in the SVZ. Ischemic stroke increase SVZ vascular permeability allowing NSC to sense blood-derived molecules that later influence NSC-derived cells behaviour in the ischemic area (Young et al., 2012; Zhang et al., 2014).

Four different SVZ responses are described to take place in the ischemic stroke: neuroblasts change their physiological stream path toward infarcted areas (Zhang et al.,

2001; Ardvisson et al., 2002; Parent et al., 2002; Zhang et al., 2004; Yamashita et al., 2006; Thored et al., 2007; Kolb et al., 2007; Zhang et al., 2014), NSC proliferate and differentiate into astrocytes that migrate to the lesion (Li et al., 2010; Young et al., 2012; Benner et al., 2013; Laug et al., 2019) NSC themselves migrate to the injury and once there differentiate in both neuronal and glial lineage (Liu et al., 2007; Faiz et al., 2015; Pous et al., 2020) and finally, due to the exhaustion of NSC pool, ependymal cells behave like progenitor cells, differentiate into new-born neurons and migrate to the damaged area (Carlen et al., 2009).

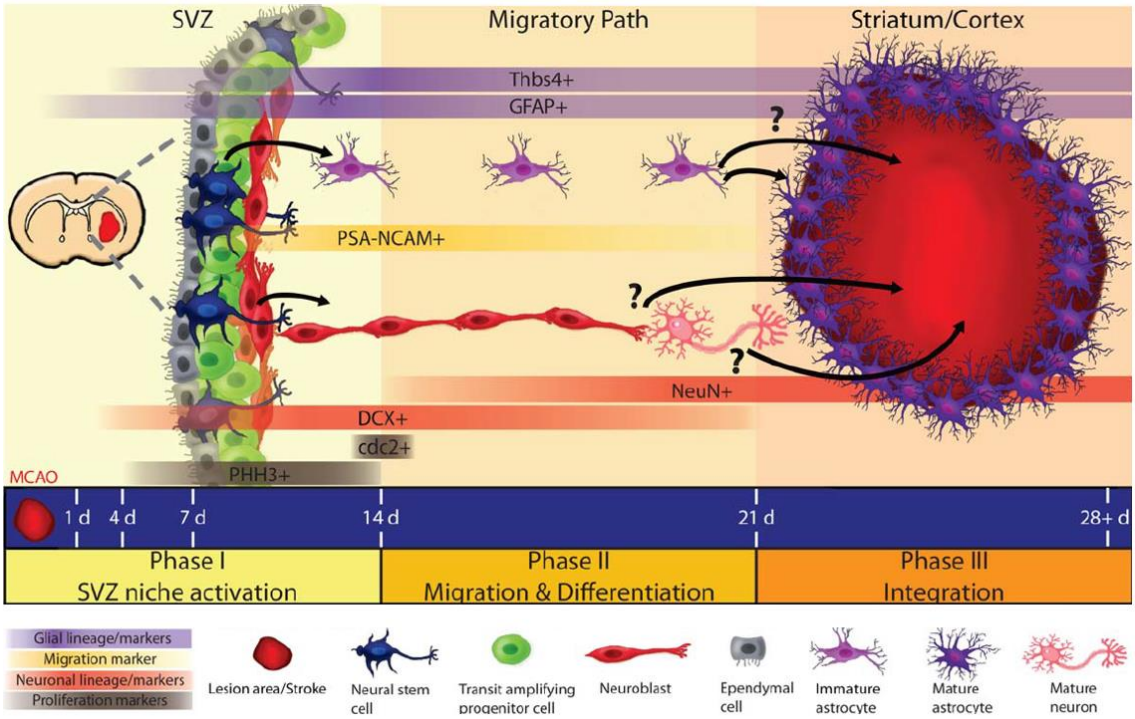

***Figure 12*. SVZ response and NSC activation to the ischemic lesion.** Neurogenesis (in red) and astrogliogenesis (in purple). SVZ response can be classify in three different phases: activation, migration and integration. Modified from Gregoire et al (2015).

Neurogenesis is the most studied SVZ response because migrating neuroblasts can repopulate the lost area and make possible to revert the damage caused by the occlusion. However, even many reports show immature neurons arrive to the injury, they fail in achieving the repopulation of the lost area (Arvidsson et al: 2002; Yamashita et al., 2006; Magnusson et al., 2014). One possible reason is the high toxic environment and other ischemic-related elements not well understood at later stages that could inhibit the neuronal replacement. Relevant publications are summarized in *Annex 1 section*.

Despite this fact, other protective events related with the NSC-generated astrocytes take place in the ischemic area and can determine the survival of these new-

born neurons or can themselves work as a neurogenic source through internal reprogramming from glial to neuronal lineage (Faiz et al., 2015; Chen et al., 2018). Astrocytes production is not only important for supporting new-born neurons but also play another major function, the formation and remodelling of the glial scar.

As mentioned before, local proliferating astrocytes are not the only source of astrocytes in the ischemic region because NSC can also produce astrocytes which take part in the glia response to the ischemic stroke (Li et al., 2010; Young et al., 2012; Benner et al., 2013; Faiz et al., 2015; Laug et al., 2019; Pous et al., 2020). However, astrocytes production by NSC is an event far unknown. Benner et al., (2013) shown astrocytes derived from SVZ cells are essential for the proper formation of the glial scar. Using a transgenic mice approach to knock out astrocytes derived from NSC, Benner et al (2013) found that these animals shown an increase in the edema volume and infarct size causing a worse progression of ischemic lesion and mice deficits. Moreover, in other meticulous transgenic work, authors shown that SVZ mainly produce astrocytes in response to chemical focal lesion in the cortex which are necessary for the proper resolution of the disease (Faiz et al, 2015). Revealing the role of SVZ-derived astrocytes is instrumental for understanding the neuroprotective responses against brain ischemia.

However, one limiting element is how to distinguish between local and SVZ-derived astrocytes due to both populations share almost all their markers. A decade ago, researchers found a specific marker to identify astrocytes derived from NSC in the SVZ, the Thrombospondin 4 (Beckervordersandforth et al., 2010; Benner et al., 2013; Girard et al., 2014; Llorens-Bobadilla et al., 2015; Basak et al., 2018; Mizrak et al., 2019; Kjell et al., 2020; Cebrian-Silla et al., 2021). In this study, we characterize the astrocyte generation from NSC after ischemic stroke via Thrombospondin 4 expression.

5. THROMBOSPONDIN 4: A MATRICELLULAR GLYCOPROTEIN

Thrombospondin 4 (Thbs4) is a matricellular glycoprotein which takes part in the brain ECM (Lawler et al., 1995). Thbs4 is a homo-pentamer from the Thrombospondin family (Fig. 13) and unlike its sibling Thrombospondin 1 and Thrombospondin 2 that play a role in the synapses (Christopherson et al., 2005), Thbs4 is low expressed in the brain and its function remains further unknown. In the peripheral tissue, Thbs4 expression is related to muscle cells of the heart where participate in calcium waves regulation (Lawler et al., 1995; Vanhoutte et al., 2016). Thbs4 domain is cleaved in the endoplasmic reticulum and link with activating transcription factor 6a (Atf6a) in the Golgi organelle,

thus, Thbs4 modulate intracellular calcium reservoir (Lynch et al., 2012; Brody et al., 2016). Thbs4 also seem to play a role in cancer development (Shi et al., 2021; Chou et al., 2021) by TGF-β-induced angiogenesis (Muppala et al., 2017). However, its function in the brain remain poorly understand.

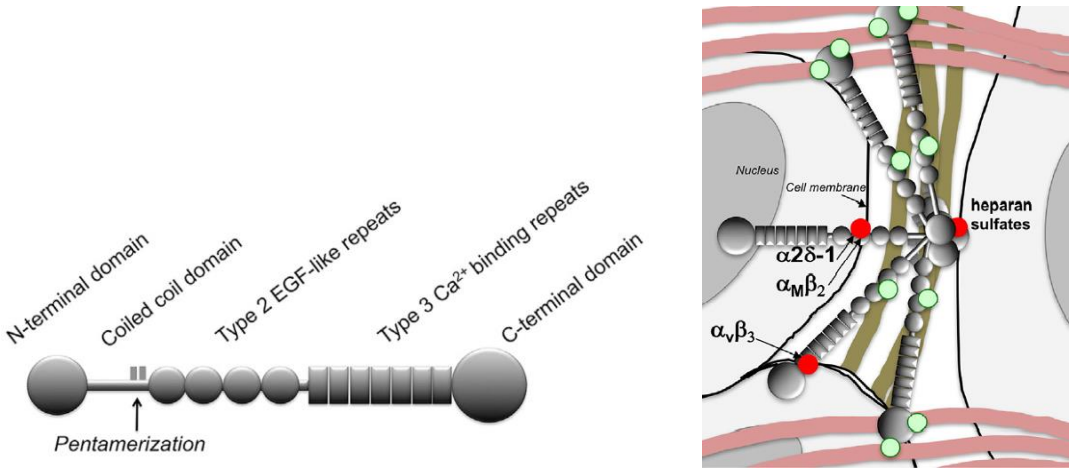

Figure 13. **Thrombospondin 4 domains and extra-intracellular location of the homo-pentamer form.** Hyaluonic acid is representated in pink. Taken from Stenina-Adognravi & Plow (2019).

Recent reports demonstrated that Thbs4 expression is mainly restricted to the SVZ niche including RMS (Girard et al., 2014; Llorens-Bobadilla et al., 2015; Kjell et al., 2020). A decade ago, Thbs4 expression was described in the SVZ and as specific marker for this niche (Beckervordersandforth et al., 2010). Since then, even more studies focused in Thbs4 expression in the SVZ because its role in the NSC maintenance and its rectricted expression in this germinal niche (Codega et al., 2014; Llorens-Bobadilla et al., 2015; Basak et al., 2018; Mizrak et al., 2019; Kjell et al., 2020; Cebrían-Silla et al., 2021). Most reports observed that Thbs4 expression is extremely related to quiescent NSC (Codega et al., 2014; Llorens-Bodadilla et al., 2015; Cebrían-Silla et al., 2021) although its expression is also observed in other NSC (Basak et al., 2018; Mizrak et al., 2019; Nam & Capecchi, 2020). Few publications reported the expression of Thbs4 by active NSC (Mizrak et al., 2019; Nam & Capecchi, 2020). Basak et al (2018) observed that specific SVZ cells expressed Thbs4 and also presented genes related with a primed state of NSC. Primed NSC are understood as NSC with a pre-establish program to respond to external harmful stimulus. Indeed, SVZ-derived astrocytes in the ischemic tissue differ from local reactive astrocytes because express the Thbs4 glycoprotein (Benner et al., 2013; Laug et al., 2019; Zhao et al., 2020; Pou et al., 2020). Several works showed the astrocytes production from SVZ in response to ischemic stroke using Thbs4

marker and result as a specific tag to identify NSC-derived astrocytes (Benner et al., 2013; Laug et al., 2019; Zhao et al., 2020; Pous et al., 2020).

6. EXTRACELLULAR MATRIX UNDER PHYSIOLOGICAL AND ISCHEMIC CONDITIONS

6.1. Extracellular Matrix in the physiological brain

ECM in the brain constitutes around 20% of a unique three-dimensional cell environment that surround neural cells and contribute to the features of the cerebral tissue (van Harreveld, Crowell & Malhotra, 1965; Nicholson & Hrabětová, 2017). Long polysaccharide chains called glycosaminoglycans (CAG), which are the backbone of the extracellular space, form the basis of the brain ECM. Brain presents a special ECM conformation, with a single non-sulphated CAG backbone structure, the hyaluronic acid (HA) (Preston & Shermann, 2011). This sugar is the main component of the brain ECM and its regulation by other ECM-related elements is what define its role in physiological and pathological processes (Fawcett et al., 1999). ECM is formed by different elements which attach to HA chain and are called “matrisome”. The rest of ECM elements are proteins decorated with CAG chains with different disaccharides composition like chondroitin sulphate, dermatan sulphate, heparan sulphate and keratan sulphate. These attach covalently to a core protein forming the proteoglycan, which links to HA and form the matrix network that occupies the extracellular space (Nicholson & Hrabětová, 2017). Among them, chondroitin sulphate proteoglycans (CSPGs) are the major population of proteoglycans in the brain (Margolis & Margolis, 1989; Ruoslahti, 1996) and include neurocan, aggrecan, versican, brevican, syndecan or CD44 among others (Shabani et al., 2021). The second major ECM elements are adhesive glycoproteins known as associated ECM proteins and ECM receptors. Among them, the most abundant in the brain includes fibronectin, laminins, collagens, integrins and nidogen glycoproteins. ECM receptors such as CD44, the receptor for hyaluronan mediated motility (RHAMM) or TMEM2 and ECM enzymes such as HA synthases and hyaluronidases are also key regulators of the ECM (Al’Qteishat et al., 2006; Peters & Sherman, 2020). Altogether, from the diversity of the core proteins and the sugar molecules decorating them, the ECM presents a huge diversity with a wide functional heterogeneity (Herdon & Lander, 1990).

Brain ECM is roughly divided into three compartments (Lau et al., 2013; Bennarroch, 2015): (i) the neural interstitial matrix, (ii) the perineuronal nets and (iii) the basement membrane (Fig. 14). In the brain, ECM structure that bind cells together are called the neural interstitial matrix and are conformed by dispersed ECM molecules in

the parenchyma. However, ECM also conforms dense compartment known as the perineuronal nets (PNN) and the basement membrane. PNN are a dense matrix structure which wrap the neuronal surface and are crucial in controlling synaptic and neuronal plasticity in the developing and injured CNS (Deepa et al., 2006; Carulli et al., 2010; Wang et al., 2012). PNN are mainly formed by HA and CSPGs (Köppe et al., 1997; Carulli et al., 2006; Deepa et al., 2006; Kwok et al., 2011). The second condense ECM structure is the basement membrane that delimit endothelial cells from parenchymal tissue. Basement membrane is formed mainly by collagen type IV, laminin, nidogen and fibronectin (Lau et al., 2013; Bennarroch, 2015).

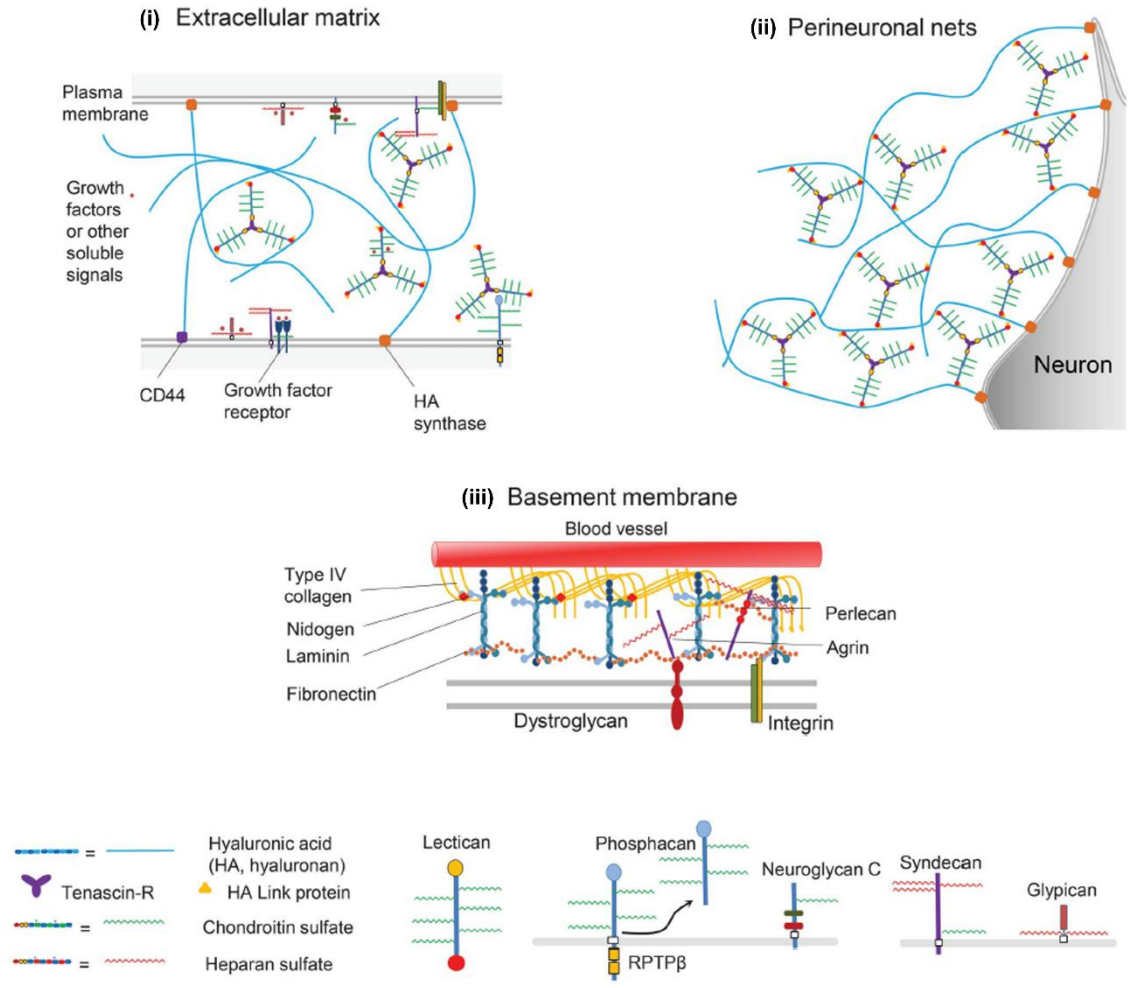

***Figure 14*. Composition of the ECM in the physiological brain.** (i) Extracellular matrix or neural interstitial matrix, (ii) Perineuronal nets and (iii) Basement membrane are the three compartment of the ECM in the brain and are conformed by a diverse range of ECM molecules. Adapted from Bennarroch (2015).

ECM is involved in a wide range of physiological and pathological processes in the brain, including a key role of ECM in development and maintenance of neural cells from embryonic to adult stages and beyond (Peters & Sherman, 2020). Extracellular

environment modulate responses which aim to cell migration, axonal guidance, synaptogenesis and synapsis maintenance and participate in the protective brain responses to injury. Among extracellular elements, HA the most abundant one is a highly versatile molecule which in the brain also develop different functions in addition to the neuronal support. High Molecular Weight (HMW) HA contributes to brain repair and homeostasis under physiological and pathological conditions whereas Low Molecular Weight (LMW) HA promotes neuroinflammation responses by glial cells (Litwiniuk et al., 2016; Chistyakov et al., 2019), a huge relevant role under pathological diseases such as ischemic stroke. Other functions of ECM-related elements include the role of the CSPG in the inhibition of neurite extension and conservation of pre-existing ones (Chiu, Matthew & Patterson, 1986; Challacombe, Snow & Letourneau, 1997) whereas laminins, integrins and fibronectin promote the growth of new neurites (Ichikawa et al., 2009; Tan et al., 2011; Vecino et al., 2015). In addition, heparan sulphate proteoglycans (HSPGs) are located in the membrane of the cells and are involved in different intracellular signalling. Sydecan and glypican are the main HSPGs in the brain and are associated to the basement membrane ECM structures (Bennarroch, 2015). Together with HSPGs, adhesion ECM proteins and ECM receptors like integrins and thrombospondin mediated the mechanotransduction signalling of the cells in response to the extracellular requirements (Hynes, 1987; Morgan et al., 2007).

6.2. Extracellular Matrix in the ischemic brain

During embryonic development, ECM is mainly produced by immature and mature neurons (Luckenbill-Edds & Carrington, 1988; Bignami & Asher, 1992; Peters & Sherman, 2020) whereas at adult stages, astrocytes are the main producer of ECM components in physiological and pathological brain (Fawcett et al., 1999; Faissner et al., 2010). In the ischemic stroke, ECM suffers a thorough restructuration due to the occlusion and must undergo successful remodelling to encourage brain repair. ECM elements involved in the ischemic cascade, such as LMW HA, induce activation of astrocytes and microglia which in turn modulate ECM structure by releasing glycoproteins to the extracellular environment (Fawcett et al., 1999; Bush & Silver, 2007; Faissner et al., 2010). For instance, accumulation of fibrinogen, an adhesive glycoprotein presented in blood cells and fibroblasts, induces a huge reactivity of local glial cells in the ischemic injury and evokes the formation of the glial scar (Pous et al., 2020). However, the main event related to ECM in the ischemic lesion is the formation of the glial scar which is created locally by reactive astrocytes and astrocytes-secreted ECM molecules such as HA and CSPGs (Lau et al., 2013; Bennarroch, 2015). Other ECM-

related elements involved in the development of the ischemic cascade are CSPGs, such as neurocan or NG2, which are highly upregulated in the glial scar territory (Fawcett et al., 1999). Indeed, CSPGs are mainly produced locally by reactive astrocytes in the perilesional areas (Bush & Silver, 2007) and its inhibition through chondroitinase ABC promote axonal sprouting and regrowth (Moon et al., 2001; García-Alias et al., 2009). Further studies are needed to unreveal the potential role of ECM as a therapeutic target for brain ischemia.

6.3. Extracellular Matrix in the Subventricular Zone

SVZ harbours a special ECM structure just like the PNN in the brain parenchyma. ECM-related elements such as adhesive proteins like integrins, fibronectin, collagen, tenascin or nidogen are also found in the SVZ niche (Mercier et al., 2002; Kazanis et al., 2007; Kazanis et al., 2010; Marthiens et al., 2010; Gatazzo et al., 2014) and perform essential functions for NSC homeostasis (Garcion et al., 2004; Kazanis et al., 2007; Shabani et al., 2021). ECM-related elements are involved not only in the physical support of NSC, but also promote cellular responses which regulate kinases and scaffolding proteins to transduce signals (Morgan et al., 2007). Tenascin-C is highly found in the SVZ because is a key regulator of NSC homeostasis and differentiation (Garcion et al., 2004; Kazanis et al., 2007). Likewise, transglutaminase 2, which is also highly found in the SVZ, has been reported to control neurogenesis (Kjell et al., 2020). Similar to the extracellular microenvironment of the brain parenchyma, ECM elements surround NSCs and modulate cell-signalling responses through, for instance, the presence of integrins receptors (Humpries et al., 2006; Kazanis et al., 2010). Ependymal cells, fractones and SVZ vasculature also present ECM-related elements such as N-cadherin, laminins, integrins, nidogen, fibronectin, collagens, heparan sulphate proteoglycans (HSPG) or CSPGs which modulate NSC homeostasis (Gatazzo et al., 2014; Morante-Rodolat & Porlan, 2019).

However, the most important ECM element in the SVZ niche is possibly hyaluronan. HA is enriched in NSC niches (Preston & Sherman, 2011). Increase of HA in the SVZ provide a high condense environment for NSC and is translated in to ECM stiffness. Indeed, Kjell et al (2020) found that this increase in the SVZ stiffness avoids NSC exhaustion. High expression of HA or HMW HA correlate with NSC quiescence (Preston & Sherman, 2011; Kjell et al., 2020) whereas CD44 and TLR signalling activation regulate NSC proliferation and differentiation (Okun et al., 2010; Su et al., 2017). NSC activation from SVZ require HA digestion through hyaluronidases and HA

receptors which allow NSC proliferation, differentiation and response to brain injuries (Preston & Sherman, 2011).

7. NEURAL STEM CELLS AS A POTENTIAL THERAPEUTIC TOOL FOR BRAIN DISEASES

The interest in NSC stand out due to the potential therapeutic response these cells comprise. Multiple preclinical approaches has been performed using NSC as a central therapeutic response in several neurological diseases. Among them, in addition to the stimulation of endogenous NSC, the most outstanding are the *in vivo* reprogramming of local glial into neurons through neurogenic signals to recover the lost tissue and the *in vivo* transplantation of pre-conditioned NSC to differentiate into neurons (Fig. 15; Li & Chen, 2016).

Regarding the conversion of local glia to neurons in order to restore neuronal death, different paradigms have been described although these tools are far distance to be fully understood nowadays. Even the clinical relevance, *in vivo* reprogramming through induced pluripotent cells or transdifferentiation techniques are not well-understood yet and most of this work has been made in *in vitro* experiments (Berninger et al., 2007; Heinrich et al., 2010). Nevertheless, successful reconversion of neurons from astrocytes (Buffo et al., 2005; Torper et al., 2013; Niu et al., 2013; Guo et al., 2014; Mattugini et al., 2019), NG2 glia (Heinrich et al., 2014; Guo et al., 2014) and microglia (Matsuda et al., 2019) has been performed under physiological brain condition (Niu et al., 2013; Guo et al., 2014) or pathological models of acute insult (Buffo et al., 2005; Mattugini et al., 2019) or neurodegenerative diseases (Guo et al., 2014; Rivetti di Val Cervo et al., 2017; Qian et al., 2020). Indeed, glial cells can be reprogramming into specific neurons population (for review, see Lei et al., 2019; Qian et al., 2020). Relevance of this discover must be fully understood in order to further harness it for brain repair.

About transplantation of NSC, controversial results shown its potential as therapeutic tool. Because CNS environment specialization and the particular phenotypes of resident neural cells acquired, transplantation of undifferentiated and differentiated neural cells in the brain might be insufficient for cell replacement after brain injury. In this way, the direct induction of final neuronal phenotype increases transplantation success and maturation of transplanted cells (Victor et al., 2014; Zhang et al., 2015; Sun et al., 2016). Although transplantation of induced NSC have shown beneficial results restoring stroke deficits in mouse (Liu et al., 2014; Yao et al., 2015; Wu et al., 2015; Bacigaluppi

et al., 2016) and clinical trial began to use it for several brain disorders (for review, see Ottoboni, von Wunster & Martino, 2020), the transplantation of induced pluripotent stem cell (iPSC) *per se* entail a high risk of tumorigenesis (Fujimoto et al., 2012; Wu et al., 2015; Yao et al., 2015). New future advances must compensate this fact in order to harness this tool for therapeutic purpose. Because side effects of the transplantation approach, studies over the last two decades has focused in using endogenous NSC not only for cell replacement but also as regulators of post-ischemic responses.

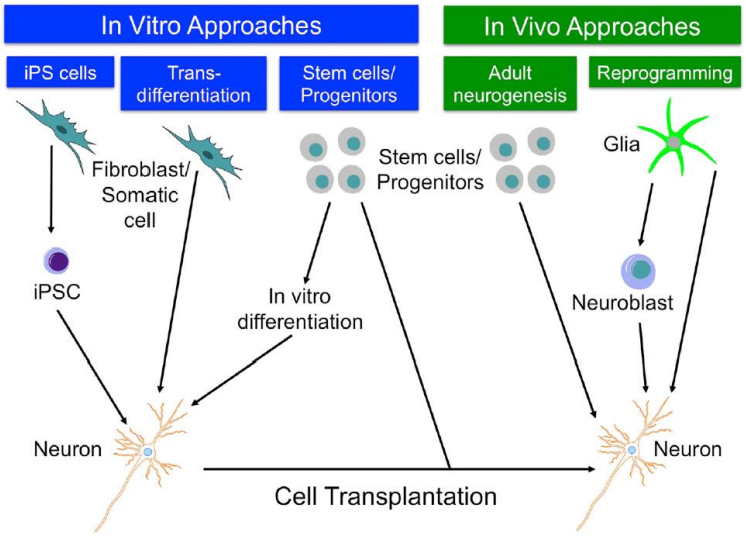

Figure 15. **Cell replacement strategies using NSC as a central component for brain repair.** Stimulation of endogenous NSC, transplantation of induced pluripotent stem cells and *in vivo* reprogramming of glial cells into neurons are the main therapeutic approaches. Taken from Li & Chen (2016).

For this reason, stimulation of endogenous NSC have been widely studied for brain repair. Not only for ischemic stroke (Arvidsson et al., 2002; Parent et al., 2002; Thored et al., 2007; Faiz et al., 2015), also for Traumatic Brain Injury (Thomsen et al., 2014; Zhao et al., 2020) or spinal cord injury (Barnabé-Heider et al., 2010; Anderson et al., 2016; Llorens-Bobadilla et al., 2020) and neurodegenerative diseases such as Parkinson disease (van den Berge et al., 2011; Donega et al., 2019), Multiple Sclerosis (Nait-Oumesmar et al., 2008; Tepavčević et al., 2011; Liu et al., 2016), Huntington disease (Curtis et al., 2003; Jurkowski et al., 2020) and Psychiatric disorders (Wakade et al., 2002). However, NSC multipotency has been associated also with the formation of brain tumours (Quiñones-Hinojosa & Chaichana, 2007; Bardella et al., 2018; Lee et al., 2018). Understanding how NSC swift from beneficial to detrimental phenotypes will help us to harness this tool for brain repair in the future.

8. HOMOLOGOUS ADULT NEUROGENIC NICHE BETWEEN HUMAN AND RODENTS: CURRENT EVIDENCES

Adult neurogenesis in mice and humans are extremely controversial (Martino, Butti & Bacigaluppi, 2014; Kempermann et al., 2018). The most remarkable reason is cytoarchitecture changes of SVZ between both species (Quiñones-Hinojosa et al., 2006). Human adult SVZ display a different conformation characterized by four layers: the ependymal layer; a hypocellular gap, composed by projections of ependymal and glial cells; a dense ribbon of astrocytes where NSC-like astrocytes are located; and a transitional zone to the striatum parenchyma, rich in myelin and oligodendrocytes (Capilla-Gonzalez et al., 2016). These astrocytes showed neurogenic potential when are cultured *in vitro* even the presence of these astrocytes in the human SVZ drop dramatically after birth (Sanai et al., 2011). No evidence about proliferation is found in the astrocytes layer although few DCX^+ neuroblasts are found surrounding this layer and the hypocellular gap (Sanai et al., 2004; Quiñones-Hinojosa et al., 2006). If RMS and neurogenesis in the OB exist in the adult human brain remain unknown and controversial (Sanai et al., 2004; Curtis et al., 2007).

Neurogenesis in the SVZ is widely described in mice throughout life, despite it is not the case of human. The first evidence of human adult neurogenesis was provided though using BrdU-labelled neurons in the hippocampus of cancer patients receiving BrdU for diagnosis purpose (Eriksson et al., 1998). By using ^{14}C dating, Ernst et al. (2014) demonstrated that adult human brain harbour the capacity to produce new neurons through life. However, neurogenesis in humans drops sharply after birth and few neuroblast can be found in the classical neurogenic niche at adult stages (Knoth et al., 2010; Sanai et al., 2011; Wang et al. 2011; Göritz & Frisén, 2012; Spalding et al., 2013; Sorrells et al., 2018). Despite that, some publication has been found adult neurogenesis persists through aging in the dentate gyrus of the hippocampus (Boldrini et al., 2018; Moreno-Jiménez et al., 2019) and the striatum (Ernst et al., 2014) at minimum but stable levels (Fig. 16). Indeed, striatum is known as the neurogenic niche destination in the human brain instead of the olfactory bulb due to neurogenesis in the last area is far vestigial in the human brain (Sanai et al., 2011; Ernst et al., 2014).

Although controversial, adult neurogenesis seems to be evident in most of the current publications in rodents and humans. A minimal turnover is found in the neurogenic niche of the human brain (Ernst et al., 2014; Boldrini et al., 2018). Moreover, when compare new versus old neurons, Kempermann (2012) showed adult

neurogenesis in human and mouse are quite similar and can be comparable (Bergmann et al., 2015).

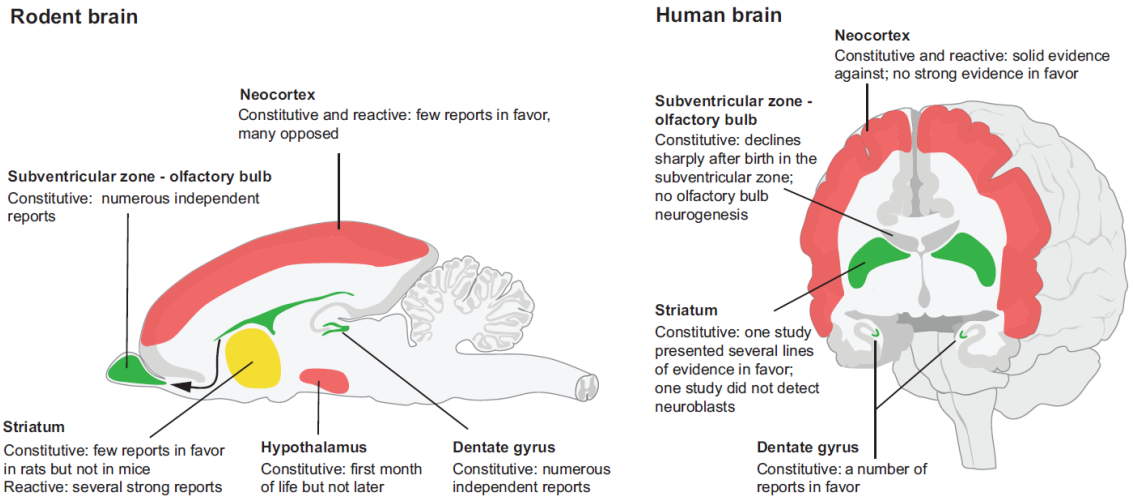

***Figure 16*. Neurogenic niche in the mice and humans brain: differences, pros and cons.** Taken from Magnusson & Frisén (2016).

The key to understand neurogenesis in the adult human brain seem to be the samples analysed in each work. Most publications that did not observe neurogenesis in the human brain have performed the analysis in aging non-pathological human brain samples (Sorrells et al., 2018) whereas neurogenesis is reported in adult human brain samples with neurodegenerative or psychiatric disorders (Ernst et al., 2014; Boldrini et al., 2018) our acute ischemic insult (Martí-Fabregas et al., 2010; Tatebayashi et al., 2017). Further studies are needed to know if SVZ neural stem niche persist in the human brain.

HYPOTHESIS AND OBJECTIVES

Hypothesis

Previous results at the host laboratory, demonstrated that high level of extracellular adenosine, an hallmark of brain ischemia, could activate the adult mice SVZ and sustain the astrogliogenesis by generation of newborn Thbs4^{+} astrocytes (Benito-Muñoz et al., 2016) (also shared by Benner et al., 2013; Llorens-Bobadilla et al., 2015; Pous et al., 2020).

According to this, our main hypothesis is that brain ischemia in mice can activate the adult SVZ and sustain the astrogliogenesis.

Objectives

To demonstrate our principal hypothesis we defined the following objectives:

Objective 1: To characterize the SVZ activation and NSC response following an *in vivo* ischemic model in mice. *Methodology*: middle cerebral artery occlusion (MCAO) model.

Objective 2: To demonstrate that SVZ-derived astrocytes recruitment to the infarcted area. *Methodology*: 5-Bromo-2´-Deoxyuridine incorporation and immune-characterization; cell tracing by *in vivo* electroporation.

Objective 3: To study the role of SVZ-derived astrocytes in modulating the glial scar after brain ischemia. *Methodology*: HA metabolism; matrisome analysis by RT-qPCR; viral injection of adeno-associated virus for uregulating HA synthase 2 expression; ImageJ scripts and image analysis.

MATERIALS AND METHODS

Summary of method used in this project

Experimental paradigm	Model	Techniques
***In vitro* experiments**	Neurosphere cultures	• Oxygen and glucose deprivation
	Organotypic cultures	• *In vitro* immunofluorescence
	Astrogliogenesis	• Fluorimetry assay
	In vitro coculture	• Fluorescence-Activated Cell Sorting
	Hyaluronan and lactate treatment	• Protein extraction and Western blot
***In vivo* experiments**	Middle Cerebral Artery occlusion	• Wholemount assay
	5-bromo-2'-deoxyuridine treatment	• Protein extraction and Western blot
	In vivo postnatal electroporation	• Subcloning protocol
	Adeno-associated viral injection	• RNA extraction and Real Time-Polymerase Chain Reaction
		• Tissue fixation and dissection
		• Immunofluorescence protocol for *in vivo* experiments
Image acquisition and processing		
Statistical processing		

1. *In vitro* experiments

1.1. Models, conditions and protocols

1.1.1. Animals and experimental groups

Male and female Sprague Dawley rat pups from P4 to P7 were used for *in vitro* experiments (CEEA/340/2013/MATUTE ALMAU). All animals for *in vitro* studies were handled in accordance with the European Communities Council Directive (2010/63/EU). All possible efforts were made to minimize animal suffering and number of animals used. Animals were maintained under standard laboratory conditions with food and water ad libitum.

All *in vitro* experiments and conditions were performed using Control (CTRL) and hypoxic group as experimental groups. Drug treatments were performed at the same concentration both in hypoxic and control groups.

1.1.2. Neurosphere culture

Neurospheres were prepared from P5- P7-days old Sprague-Dawley rats as previously described (Cavaliere et al., 2012) (see Fig. 17 for details). Four pups were sacrificed and the brain was collected for lateral SVZ isolation. Approximately 1 mm coronal slice containing the lateral ventricles was cut by hand and collected for further and more precise isolation. Lateral SVZ was isolated taking the lateral ventricles as a reference. Once extracted, SVZ was minced in 200 µm pieces with a Mc Illwain tissue chopper (Campden Instrument, www.campdeninstrument.com), and later digested for 7 minutes in 5 milliliters of trypsin/EDTA at 37°C (Sigma, Madrid, Spain). Enzymatic digestion was blocked adding trypsin inhibitor (Sigma) and 0.01% of DNAse I (Sigma) for 10 minutes at room temperature.

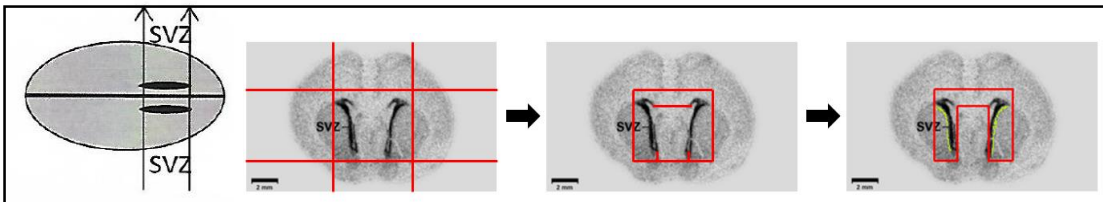

***Figure 17*. SVZ isolation for neurosphere culture.** P4-7 pups were sacrificed and brain removed. Approximately 1mm coronal slice were cut by hand collecting SVZ. Taking lateral ventricles as reference, lateral SVZ was isolated as described in pictures. Tissue was mechanical minced and enzymatically digested. Single cell suspension was cultured with proliferative medium supplemented with EGF and b-FGF. After five-seven days, progenitor cells proliferated and created neurosphere.

Mixture was centrifuged at 800G for 10 minutes and supernatant was discarded. Pellet was triturated in NeuroCult medium (Stem Cell Inc., Grenoble, France), with a glass Pasteur pipette for 25 times and 1000 µl pipette for 20 times. Non-dissociated cells were removed after suspension decant 20 minutes. Single cell suspension in the supernatant was diluted into the proliferation medium [NeuroCult with 10% neural stem cell factors from Stem Cell Inc., 2 mM glutamine, penicillin/streptomycin mix, 20 ng/mL EGF (Promega, Madrid, Spain), 10 ng/mL bFGF (Promega)], seeded at a density of 10^4 cells/cm^2 and cultured in suspension for 7 days at 37°C and 5% CO_2. Single neurospheres were generated after 5-7 days of cell culture.

1.1.3. Astrogliogenesis and oxygen and glucose deprivation (OGD) *in vitro*

After 7 days of proliferation, neurospheres were enzymatically dissociated with Accutase (Sigma) to single cells and seeded in Poly-L-Ornithine-coated (Gibco, Madrid,

Spain) 12Ø and 0.17 mm glass coverslips at 100.000 cells/well. Cells were differentiated to astrocytes in serum-free-medium contained 50% DMEM (Gibco), 50% Neurobasal (Gibco), 5 ng/ml HBEGF, 100 units/ml pen/strep, 1mM sodium pyruvate, 2mM L-Glutamine, 5 µg/ml N-acetylcysteine and 1X SATO (as previously described by Zhang et al., 2015). OGD protocol was performed the day after as previously described (Cavaliere et al., 2012). Differentiation medium was replaced by OGD medium (130 mM NaCl, 5.4 mM KCl, 1.8 mM $CaCl_2$, 26 mM $NaHCO_3$, 0.8 mM $MgCl_2$, 1.18 mM NaH_2PO_4, 10 mM sucrose, ph 7.2) previously saturated with N_2. Cells were subjected to OGD for 60 minutes in 3% O_2, 37°C and with humidity saturation. After OGD cells were returned to previously conserved medium and differentiated for 7-10 days at 37°C and 5% CO_2. OGD condition was evaluated using Image IT green reagent (Thermo Fisher Scientific) for Hypoxic Inducible Factor 1 Subunit Alpha (HIF1α) expression and MitoSox red reagent (Thermo Fisher Scientific) for mitochondrial oxidation. After 7-10 days, cells were fixed with 4% paraformaldehyde (PFA) for 10 minutes and treated for immunofluorescence.

1.1.4. *In vitro* co-culture

In order to analyse if activated microglia could affect NSC differentiation under hypoxic conditions, we performed NSC/microglia co-culture. Rat microglia was isolated as previously described by Montilla et al. (2020). P0 Sprague-Dawley rats were sacrificed, brains collected and cortex carefully isolated. Tissues were first mechanical disrupted 20 times with 29G needle-syringe and 20 times with 27G needle-syringe. The homogenized was also chemically digested with trypsine 0.05% EDTA (Gibco). Trypsine was washed after centrifugation, the pellet dispersed in a medium contained Neurobasal and 10% FBS (both from Gibco) and cell suspension cultured in Poly-D-lysine pre-treated 12.5 cm^2 flasks for one week before performing the experiments. Microglia was collected in the suspension after shaking for one hour the mixed culture at 37°C and 5% CO_2. Microglia was co-cultured with NSC in a ratio of 1:5 in serum-free-medium. NSC/microglia co-cultures were subjected to OGD using the same protocol for astrogliogenesis. Pure microglia cultures were used as a control using the same medium and protocol.

1.1.5. Hyaluronic acid *in vitro*

To understand if NSC internalize or produce Hyaluronic Acid (HA) of the cellular matrix, differentiating astrocytes were cultured in three different coating plates: a) with HA, b) Poly-L-Ornithine and c) the combination of HA with Poly-L-Ornithine. 12Ø 0.17

mm coverslips were pre-treated with 1 mg/ml of high molecular weight HA overnight at room temperature. Dissociated neurospheres were seeded after 3 washes with sterile PBS 1X and differentiated with or without OGD. In some experiments (Fig. 46), hyaluronidase (OmniPur Hyaluronidase Sigma, HX0514-1, #37326-33-3) was added to the coating to remove extracellular hyaluronan spots.

1.1.6. Organotypic culture

Organotypic cultures are an intermediate model between *in vitro* and *in vivo* systems. With this approach we are able to maintain a tridimensional culture *in vitro*, simulating tissue response to external stimuli. Organotypic cultures maintain the cytoarchitecture, preserve cell-cell interactions, molecule transport and ion diffusion systems. In addition, slices can be cultured for weeks or months. Nevertheless, organotypic culture are not provided with the vascular system. As a crucial element in brain ischemia, vascular system exclusion is an important limitation of the model. However, recollecting all slices from the most rostral to the most caudal part of the SVZ allows us to analyse different sub-regions of the SVZ. It is well described SVZ harbors different cell populations located in specific sub-regions, for instance, NSC populations in the more rostral part are mainly taking part in the neurogenesis path to the olfactory bulb. Taking into account advantages and disadvantages, we decided to submit rostro-caudal SVZ slices to OGD in order to analyse how hypoxia affects different NSC population.

Organotypic culture protocol was adapted from Plenz and Kitai (Plenz & Kitai, 1996). Cultures were prepared from P5-old Sprague-Dawley rat pups, the skull was cut through commissural lines and brains collected in cold Hank's balanced salt solution (Fig. 18). Meninges, cerebellum and olfactory bulb were removed and the brain was sliced in 350 µm coronal sections with a Leica VT 1200 S vibratome (Leica Microsystems). Rostral slices, intermediate slices and caudal slices were collected once lateral ventricles, third ventricles and hippocampus respectively become evident. All slices with lateral ventricles were cultured from both hemispheres (6 slices per animal approximately). Slices were plated in liquid-air interphase 0.4 µm membrane (Millicell CM culture insert, Millipore, Schwalbach, Germany) with the organotypic medium (50% Neurobasal-B27, 25% HBSS, 25% inactive horse serum (Gibco, Eggenstein, Germany), 1 mM L-glutamine (Biochhrom, Berlim, Germany), 25 mg/ml penicillin/streptomycin mix and 5.5 mM glucose). The medium was replaced the second day and every two-three days thereafter. OGD was performed after one week of the preparation and two weeks later, were fixed for 40 minutes in 4% PFA for Immunofluorescence (see protocol below).

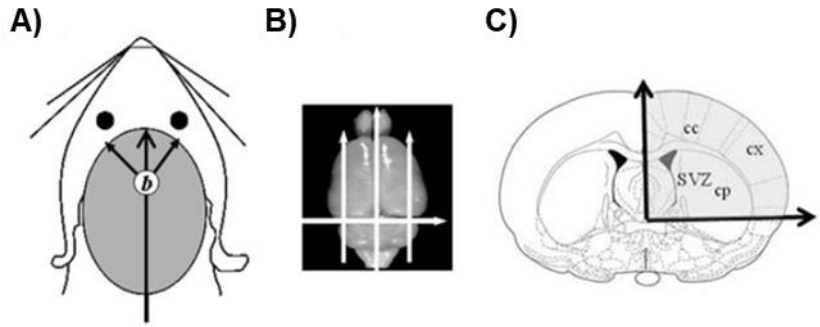

***Figure 18*. Schematic view of organotypic culture preparation.** A) Lines indicate the location and direction of cut to open the skull and remove the brain for further dissection. b inside the circle indicates the Bregma point. B) The outer third of the lateral cortex and the entire cerebellum were removed (arrows). C) Schematic view of explant structure, which includes corpus callosum (cc), cerebral cortex (cx), subventricular zone (SVZ) and striatum-caudate putamen (cp).

1.2. Techniques

1.2.1. *In vitro* immunofluorescence protocol

Cells were fixed with 4% PFA and after one wash with PBS, unspecific epitopes were blocked with the blocking solution (PBS 1X, 0.1% Triton and 10% Normal Goat Serum) for one hour at room temperature. Primary antibodies (see Table 2 for specific working concentrations) were prepared in the same blocking solution and incubated overnight at 4°C with continuous shaking. After 3 washes of 10 minutes each with washing solution (PBS 1X 0.1% Triton), secondary antibodies diluted 1:500 in blocking solution were added and incubated for 1 hour at room temperature. After 3 washes with washing solution, DAPI was added for nuclei visualization. Finally, cells were rinsed with PBS 1X three times and mounted with Fluoromount-G mounting media (SouthernBiotech) in Microscope slides RS (RS FRANCE, #BPB019).

For HA visualization, the same immunofluorescence protocol was used with minimal changes. Triton detergent is extremely aggressive and disturb HA staining thus, it was replaced with saponine. Saponine is a less aggressive detergent that produces transient pores in the cell membrane. For this reason, saponine was freshly prepared and added at 0.1% and maintained in all steps. To avoid reflection disturbance, Mowiol (Millipore 4-88 reagent #475904) mounting media was used instead Fluoromount-G (SoutherBiotech) mounting media. Mowiol mounting media has a similar oil reflection and improve HA ultra-structure visualization.

Immunofluorescence protocol for organotypic slices was carried out in the same manner with minimal changes. Incubation in 4% PFA for fixation was increased to 40

minutes. Concentration of triton in the blocking solution was 0.5% instead of 0.1%. Following steps were performed as described before.

Table 2. Primary antibodies for *in vitro* immunofluorescence protocol

Antibody	Host	Isotope	Dilution	Reference	Company
Thbs4	Mouse	Monoclonal IgM kappa light chain	1/400	Sc-390734	Santa Cruz Biotechnology, USA.
βIII tubulin	Rabbit	Polyclonal	1/400	ab18207	Abcam, UK
GFAP	Rabbit	Polyclonal	1/4000	Z0334	Dako, Agilent Techonologies, Inc.
Nestin	Mouse		1/500	NES	Cell Signaling, Germany
Prominin 1	Rat	Monoclonal IgG1 kappa	1/300	14-1331-82	Invitrogen, Spain
BrdU	Rat	Monoclonal	1/400	MCA2060	Biorad, USA.
Biotinylated Hyaluronan Binding protein	-	-	1/100	385911	Millipore, Germany
MBP	Chicken	Polyclonal IgY	1/1000	AB9348	Millipore, Germany
MCT1	Chicken	Polyclonal IgY	1/1000	AB1286-1	Millipore, Germany
MCT4	Rabbit	Polyclonal IgG	1/200	AMT-014	Alomone, Israel
Iba1	Guinea Pig	Polyclonal IgG	1/500	234 004	Synaptic Systems, USA
iNOS	Mouse	Monoclonal IgG2a	1/100	#610329	BD Bioscience
Amigo2	Rabbit	Polyclonal IgG	1/200	bs-11450R	Bioss, USA
Ptx3	Rabbit	Polyclonal IgG	1/200	Bs-5783R	Bioss, USA

1.2.2. Fluorimetry assay (Matrix metalloproteinases assay)

Neurosphere-derived astrocytes were dissociated and seeded in 96-well plates pre-treated with 1 mg/ml of high molecular weight hyaluronic acid as previously described. The following day, OGD was performed in the hypoxic condition. One week before seeding the cells, Matrix Metallo-Proteinases (MMPases) assay was performed following manufacture's procedure (Abcam, ab112146). Briefly, MMPases presented in each condition were pre-activated for 3 hours and banded to a green substrate (light sensitive). Hoechst was added to normalize the green fluorescence intensity. Fluorescence was measured using a Synergy-HT fluorimeter (Bio-tek). Excitation wavelength used was 405 nm for Hoechst and 485 nm for the green substrate. Controls for APMA and pro-MMPases reagent was used in all experiments. Three independent experiments were performed with 4 wells per conditions. Data is represented as Relative Fluorescence Units (RFU) by Hoechst fluorescence intensity.

1.2.3. Fluorescence-Activated Cell Sorting

Fluorescence-Activated Cell Sorting (FACS) was performed on neurosphere-derived astrocytes after one week of differentiation, with or without OGD. Cells were detached using trypsin 0.05% EDTA (Gibco) for 5 minutes at 37°C, collected and

transferred to a 1.5 ml tube (Eppendorf). After centrifuging at 800G for 5 minutes, cells were fixed in suspension with 4% PFA for 10 minutes at 4°C. After several washes with PBS 1X, blocking buffer was added and incubated for 1 hour at room temperature in continuous orbital shaking. Primary antibodies for Thbs4 was diluted at 1:100 in blocking buffer and incubated overnight at 4°C. The following day, after three washes with PBS 1X, secondary antibodies diluted in blocking buffer was incubated for 1 hour at room temperature. Finally, after three washes with PBS 1X, cells were sorted using BD FACS Jazz™ Cell Sorting System (BD Biosciences). 488 nm (blue) laser was used to sort Thbs4 antibody positive cells (PE-CY7 secondary antibody).

1.2.4. Protein extraction and Western blot

Neurosphere-derived astrocytes were seeded in 35Ø petri dish (500.000 cells) and subjected to OGD as previously described. Seven days after OGD, proteins were extracted after cell lysis with RIPA buffer (RIPA, Thermo Fisher Scientific 89900), Protease and Phosphatase Inhibitor Cocktail 100X (Thermo Fisher Scientific) and stored at least one day at -20°C to allow complete cell disruption. Protein concentration was measured by chemioluminescence using RC DC™ Protein Assay (Bio-Rad). Forty micrograms of protein samples were denatured in reducing loading buffer contained β-mercaptoethanol (M3148, Sigma) and 0.0002% bromophenol blue at 95°C for 5 minutes and separated in pre-casted 12% or 7.5% Tris-Glycine polyacrilamine gel using the Criterion cell system (Biorad). Electrophoresis was conducted at 80 V in a Tris-Glycine buffer (25 mM Tris, 192 mM glycine, 0.1% SDS in dH_2O, pH 8.3). After complete separation, proteins were transferred to a nitrocellulose membrane (Biorad) using Trans-Blot® Turbo™ Transfer System (Bio-Rad). Nitrocellulose membranes were incubated in blocking solution (Tris-Buffer Solution (TBS), 0.1% Tween-20 and 5% BSA) for one hour at room temperature in a Duomax 1030 shaker (Heidolph Instruments, Germany). Primary antibodies (Table 3) were incubated overnight at 4°C in blocking solution.

Table 3. Primary antibodies for *in vitro* Western Blot

Antibody	**Host**	**Isotope**	**Dilution**	**Reference**	**Company**
Thbs4	Mouse	Monoclonal IgM kappa light chain	1/400	Sc-390734	Santa Cruz Biotechnology, USA.
GAPDH	Mouse	Monoclonal, IgG1	1/1000	MAB374	Millipore, Germany
Nestin	Chicken	Polyclonal IgY	1/1000	NES	Aves Lab, EEUU
MCT1	Chicken	Polyclonal IgY	1/1000	AB1286-1	Millipore, Germany

After incubation, membranes were washed three times for 10 minutes with TBS-0.1% Tween. Horseradish peroxidase-conjugated secondary antibodies were incubated in blocking buffer for one hour at room temperature in a Duomax 1030 shaker (Heidolph

Instruments, Germany). After three washes with TBS, immunodetection was performed by electrochemical luminescence in a Chemidoc MP (Biorad).

2. *In vivo* experiments

2.1. Models, conditions and protocols

2.1.1. Animals and experimental groups

For *in vivo* experiments we used male and female wild-type C57BL6/J mice and Ai14-Rosa26-CAG-tdTomato$^{flx/flx}$ transgenic mice bred at the animal facility of UPV/EHU. Ai14-Rosa26-CAG-tdTomato$^{flx/flx}$ transgenic mice were kindly provided by Harold Cremer at Institut de Biologie du Développement de Marseille (IBDM). All animals for *in vivo* studies were handled in accordance with the European Communities Council Directive (2010/63/EU). All possible efforts were made to minimize animal suffering and the number of animals used. Animals were maintained under standard laboratory conditions with food and water ad libitum.

Experimental groups. For *in vivo* experiments, sham and ischemic mice were used as experimental groups (M20_2016_318_matute almau). Ischemic mice were analysed at different time points after brain ischemia (7, 15, 30 and 60 days after lesion). For adeno-associated virus experiments, two control groups were used to limit virus injection side effects. Experiments with specific time scale are described in each section.

2.1.2. Transient Middle Cerebral Artery Occlusion model

There are different brain stroke models to reproduce ischemic damage in the mice brain (Macrae, 2011). Among them, the transient Middle Cerebral Artery Occlusion (MCAO) is one of the most classical models to perform preclinical ischemic brain strokes. This procedure replicates core-penumbra areas through arresting blood flow proximal to the lenticulo-striate arteries using an intraluminal filament. This model generates specific lesions in mice cortex and striatum with correspondent motor deficits. To better reproduce the canonical brain stroke, transient occlusion was followed by blood reperfusion in the ischemic area. MCAO model was performed according with Gelderblom et al., (2009) with mice weighting between 23-27 grams (approximately 3-4 months old). Animals were anesthetized with 4% isofluorane (1 L/min vol oxygen) and maintained in 1.5-2% isofluorane (0.4L/min oxygen) using a vaporizer system (Harvard Apparatus Isoflurane Funnel-Fill Vaporizer). Following anaesthesia induction, mice were placed face up under magnifying glass and head was attached to the vaporizer mask to

maintain the anaesthetic status. Body temperature was maintained at 37°C during the surgery using a heating plate.

Firstly, neck fur was removed and skin disinfected with 30% ethanol. A 1mm midline incision was made in the neck, salivary glands were pulled apart and windpipe exposed. The left common carotid artery (CCA) was isolated and the bifurcation identified without harming the vagal nerve. A first knot was temporary done in the CCA with 6-0 silk thread (B. Braun) to avoid blood perfusion. Another temporary knot was done in the internal carotid artery (ICA) with 6-0 silk thread to avoid blood reperfusion. Finally, two fixed knots were done in the external carotid artery (ECA) to allow monofilament introduction through a small hole between them. For 25 grams mice, we used a filament with 0.2-0.22 mm of diameter and 10 mm of length (Doccol Corporation, 602223PK10). Monofilament was introduced and redirected toward the ICA. Ten mm-length monofilament blocked blood flow in the Middle Cerebral Artery (MCA) level. Thus, ECA ligations remain in the animal as a side effect of the MCAO model although reperfusion is possible thanks to this. After one hour of occlusion, filament was extracted and temporary knots from CCA and ICA removed to allow blood perfusion. Animals were sutured and kept at 37°C until animal recovery. Representative cartoon about MCAO surgery is shown in Fig. 19.

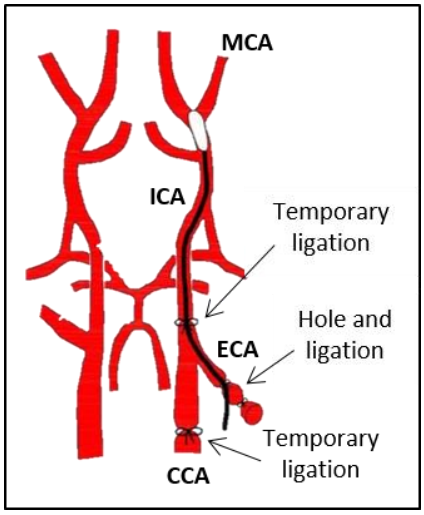

***Figure 19*. Caudal view of vessel architecture in the mice brain.** Monofilament of 0.2-0.22 mm emboli diameter and 10mm length was introduced in the ECA and redirected to ICA. MCA was blocked at the proximal level.

In addition, analgesia was underwent using 0.03 mg/kg buprenorphine (Animalcare Ltd, Nether Poppleton, United Kingdom) injected intraperitoneally (i.p.) every 12 hours for 24 hours. Weight and neurological scores were controlled and

recorded for all animals and every day until sacrificing them. Sham group were exposed to isofluorane anesthesia and common carotid artery was identified without ligation and filament introduction. ECA was ligated to reproduce MCAO model side effects.

- Clinical scores

In order to evaluate the Middle Cerebral Artery (MCA) occlusion and animal health, motor deficits and body weigh was assessed in each animal one hour after MCAO and later, every 24 hours until the day of perfusion. Those animals with a high weight loss were treated with physiological serum until weight gain. Animals without neurological deficits were excluded from the study.

Neurological scores from motor deficits was registered in a system of five-point scale with grade (Table 4).

Table 4: Neurological score scale

Grade 0	No observable deficit. The animal is active.
Grade 1	Failure to extend right paw.
Grade 2	Decreased resistance to lateral push and circling to the right.
Grade 3	Falling to the right. The animal presents rotating or revolving.
Grade 4	Unable to walk spontaneously.
Grade 5	Dead animal.

- Infarct volume measure

To measure infarct volume and evaluate the efficiency of the MCAO surgery, we performed different staining techniques: 2,3,5-triphenyltetrazolium chloride staining (TTC) cresyl violet and immunofluorescence for nestin expression (described in *2.2.5 section*), especially used to better visualize the glial scar.

- Histology staining. 2,3,5-triphenyltetrazolium chloride (TTC)

Infarct volume indicated the efficiency of MCAO model. This parameter is fundamental to understand the severity grade of the ischemic damage in the mice. There are several procedures to measure infarct volume. Among them, 2,3,5-triphenyltetrazolium chloride (TTC) staining induces an intense red color in the living tissue whereas is pale pink in the dead regions. This phenomenon happens because TTC is enzymatically reduced to a red formazan product by dehydrogenases, which is more abundant in living mitochondria. As a result, viable tissues are stained red whereas dead tissues remain unstained. TTC was dissolved at 1% in PBS 1X solution and kept at 37°C before its use. After MCAO, animals were sacrificed, brains collected and cut 1 mm thick using a mouse brain matrice stainless steel. Slices were immersed in TTC

solution for 5 minutes and quickly placed in a scale surface. Pictures were taken using a sony alpha 230 camera. Infarcted area was visualized delimitating the stained tissue using ImageJ software. Analysis was performed in both hemispheres. Infarct volume was calculated according to Storini (Storini et al. 2006). In this equation the ischemic area and the percentage of swelling were determined by subtracting the area of the healthy tissue in the ipsilateral hemisphere from the contralateral hemisphere on each section.

- Cresyl violet staining

Cresyl violet staining is one of the most useful protocols because it allows to measure infarct volume in each experimental animal and exclude non-infarcted animals from the statistics. Cresyl violet protocol was performed in 40 µm slices from perfused MCAO animals. 6 serial sections of 1mm were stained for any animal. Slices were placed in superfrost slides and dried for 1 hour at room temperature. Tissue was submerged in distilled water and then, in cresyl violet solution (0.5% cresyl acetate solution ACROS #405760100, 25% methanol and 75% distilled water) for 5 minutes. After that, tissue were dehydrated in an increasing concentration of alcohols (70%, 96% and 100% ethanol) and fixed in xylol for 2 minutes before mounting with DPX Mountant for Histology (Sigma).

2.1.3. 5-bromo-2'-deoxyuridine treatment

Administration of 5-bromo-2'-deoxyuridine (BrdU) is commonly used to assess proliferation in the neurogenic niches. In order to evaluate proliferation in different NSC pool of the SVZ, we performed two different BrdU protocols:

Total cell proliferation

To stain total cell proliferation in the SVZ we decided to use an acute BrdU treatment (Fig. 20). Fifty mg/kg BrdU was injected i.p. three times every two hour the day before the MCAO. Total BrdU cell number was quantify in the sham and MCAO groups 24 hours after the surgery.

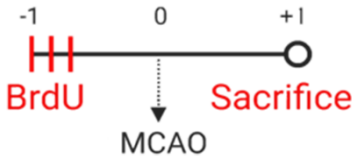

Figure 20. **Experiment design of acute BrdU treatment protocol for assessing SVZ proliferation.** Three BrdU injections of 50 mg/kg were applied every 2 hours. The following day, MCAO model was performed and mice were sacrificed in the followed 24 hours.

Quiescent NSC staining

Quiescent NSCs were stained by chronic BrdU incorporation using the protocol by Codega et al. (2014). To analyze the cellular origin of the Thbs4^{+} astrocytes, we labelled the whole pool of proliferating cells with 1% of BrdU in drinking water with sucrose during 14 days before the MCAO. One month after MCAO in the SVZ, BrdU stained only slow proliferative cells like type B cells whereas BrdU in rapid transit-amplifying cells (type C) was washed away. Three mice were sacrificed every 3, 7 and 15 days after occlusion. Moreover, Type C cells were labelled with 50 mg/Kg of 5-iodo-2′-deoxyuridine (IdU) 24 hours before perfusion (Fig. 21). Finally, Prominin 1 and nestin markers for quiescent and active NSC respectively were visualized by immunofluorescence to corroborate the identity of BrdU^{+} cells as quiescent or activated NSC respectively.

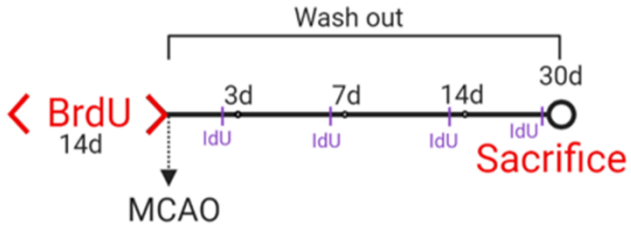

***Figure 21*. Experimental design of chronic BrdU treatment for quiescent NSC identification.** Animals were treated with 1% BrdU in the drinking water for 14 days before performing the MCAO model. To wash out all BrdU in fast-cycling cells, animals were kept for 30 days after MCAO protocol. In addition, three animals were sacrificed 3, 7 and 14 days after MCAO protocol as experimental controls for the BrdU treatment. Finally, IdU was injected at 50 mg/kg the day before sacrificing the animals to label all proliferative cells in that moment.

2.1.4. Subcloning protocol

In order to analyze the Thbs4 positive cells in the SVZ, subcloning protocol was performed to create a new plasmid based on two previous ones. PGL3-basic backbone with a mouse +/- 2000 bp of Thbs4 protein sequence as a promoter was kindly provided by Muppala et al. (2018). Using a pCMV-eGFP N1 provided by Prof. Zugaza from Achucarro Basque Center for Neuroscience, eGFP sequence was subcloned in the Thbs4 promoter plasmid using NcoI and XbaI enzymes. To verify subcloning efficiency, miniprep assay (Qiagen, Cat. 27104) was done and control digestion with NcoI and XbaI enzymes were performed. Control transfection in HEK cells were also performed to corroborate subcloning efficacy.

2.1.5. *In vivo* postnatal electroporation

To confirm that Thbs4^{+} astrocytes were recruited in the lesion from the SVZ progenitor cells, we performed an *in vivo* post-natal electroporation. Ai14-Rosa26-CAG-tdTomato$^{fl/fl}$ transgenic mice, kindly provided by Harold Cremer from Institut de Biologie du Développement de Marseille (IBDM), were dorsally electroporated with pCX-CRE using a BTX ECM399 electroporator system (Thermo Fisher Scientific) after anesthesia. P1 pups were anesthetized in ice for 1 minutes and pCX-CRE plasmid was injected in the left lateral ventricle using an air-flow pressure tube attached to a glass capillarity. Electroporation parameters were 95V, 950 ms interval and 5 pulses. pCX-CRE plasmid, also kindly provided by Harold Cremer (IBDM), was designed using CAG promoter and Cre sequence for LoxP recombination.

After plasmid injection, heads were immediately placed between a 7 mm tweezers electrode. Anode electrode was situated caudally and cathode dorsally. Electroporation targeted mainly the dorsal SVZ progenitor cells that could successfully express the fluorescent protein tdTomato. MCAO model was performed 3-4 months later and sham and MCAO animals were perfused 7, 30 and 60 days after the MCAO. To confirm the efficiency of electroporation, olfactory bulb was sliced coronally in 40 µm and tdTomato (tdTOM) positive cells migrating from the dorsal SVZ to the olfactory bulb (OB) were visualized under physiological conditions (Platel et al., 2019) by fluorescence microscopy. Experimental design is shown Fig. 22.

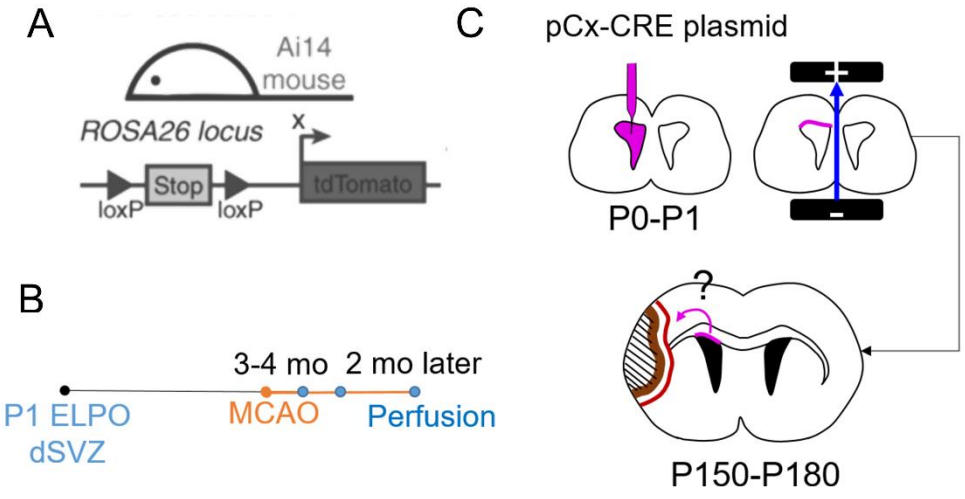

***Figure 22*. Electroporation protocol design**. Sequence encoded in the transgenic mice cells (A). Temporal scale of the electroporation experiment (B). Cartoon showing electroporation steps and hypothesis/aim (C).

Previously produced plasmid, pThbs4-GFP vector, was also electroporated in P1 mouse pups to further corroborate Thbs4 expression in the SVZ at postnatal stages. Pups were anesthetized with ice and 2.5 µg of pThbs4 plasmid was injected in the lateral ventricle. Immediately, pup head was placed between tweezers electrode and dorsal electroporation was performed with the same parameters described before. Pups were maintained at 37°C until total recovery and later returned to the mother box. Mice were perfused the following day to assess Thbs4 expression in the post-natal SVZ.

2.1.6. Adeno-associated viral injection

To confirm that Thbs4^{+} astrocytes were recruited from the SVZ to the damaged area to modulate the glial scar, we simulated an ischemic scar by overexpressing HMW HA in Sham and ischemic mice. HMW HA was overexpressed in the striatum by Adeno-Associated Viral injection of Hyaluronic Acid Synthase 2 (AAV2/9-CAG-HAS2-Flag). HAS2 adeno-associated virus was injected in the striatum of 3-4-month-old C57BL6/J mice. Animals were anesthetized using a vaporizer anesthesia system (Harvard Apparatus Isoflurane Funnel-Fill Vaporizer) attached to the stereotaxic frame. Injection was performed using a glass capillary pipette attached to Nanoject II nanoliter injector (Drummond Scientific). After the injection of 1 µl of HAS2 adeno-associated virus in the striatum (AP: +1.8; ML: -1.0; DV: -3.2), animals were maintained in analgesia, placed at 37°C until total recovery and lately returned to post-surgery standard animal facility. HAS2 adeno-associated virus was kindly provided by Federico N. Soria and created by Nathalie Dutheil from the Institut des Maladies Neurodégénératives (Bordeaux) using CAG promoter, FLAG sequence, tata fusion protein sequence and a HAS2 cDNA obtain from Vera Gorbunova (Tian et al., 2013; Fig. 23).

***Figure 23*. AAV2/9-CAG-HAS2-Flag virus scheme map.**

In MCAO group, ischemia was performed two weeks after injecting the AAV2/9-CAG-HAS2-Flag in the contralateral hemisphere to synchronize the pseudo-lesion and the ischemic scar. Thbs4^{+} astrocytes were visualized by immunofluorescence 30 days after MCAO. The control group for viral infection was injected with 1 µl of the same backbone adeno-associated virus.

2.2. Techniques

2.2.1. Wholemount assay

Fresh brain was collected from sham and 24 hours post-MCAO animals in order to isolate SVZ as described in Mirzadeh et al., (2010). Contralateral hemisphere, olfactory bulb and cerebellum was removed. One-two mm of caudal brain was cut, in order to expose the posterior tail of the hippocampus. Using a scalpel, hippocampus was removed and the rest of the brain was fixed in 2% paraformaldehyde with 0.5% triton at 4°C. After 24 hours, tissue was washed with PBS and SVZ was isolated from the cortex, striatum and midbrain. SVZ slide of 200-300 µm was stored in PBS Azide (0,01%) for short time or in cryoprotective solution for longer time.

2.2.2. Protein extraction and Western blot

SVZ and injured areas were isolated from fresh brains of sham and 15 days post-MCAO animals (as previously described in *wholemount section*). Tissues were mechanical disrupted and minced in lysis buffer (RIPA buffer (Thermo Fisher Scientific #89900) and Protease and Phosphatase Inhibitor Cocktail 100X (Thermo Fisher Scientific). Samples were lysed in ice for 10 minutes following a 0.6 cycle of sonication and 80% amplitude using an Ultrasonic Processor (Hielscher Ultrasound Technology). Sonicated tissues were centrifuged at 1200 rpm for 10 min and 4°C to remove insoluble fragments. Protein concentration, protein separation and Western blot analysis were performed as described previously in *1.2.4 section*.

2.2.3. RNA extraction and Real Time-Polymerase Chain Reaction

Fresh SVZ tissue from ipsilateral hemisphere was isolated as previously described from sham, 15 and 30 days after MCAO animals to analyse the expression of several genes (Table 5). RNA was extracted from the tissue after mechanical trituration following the manufacturer´s protocol (NZYTECH Total RNA Isolation kit protocol (NZYTECH, MB13402). RNA concentration was measured by spectrophotometry using the Nanodrop 2000c spectrophotometer (Thermo-Scientific, USA).

Real time polymerase chain reaction (RT-PCR) from 10 ng of RNA was performed using the One-step NZYTECH RT-qPCR Green kit according to manufacturer´s protocol (NZYTECH, MB34302). RT-PCR was normalized using the housekeeping genes hypoxanthine phosphoribosyl-transferase 1 (HPRT1, Qiagen QuantiTect Primer Assay, Barcelona, Spain). Specificity of each amplification was confirmed by melting curve analysis. PCR reactions were performed in a CFX96

Detection System (BioRad, Madrid, Spain). Semi-quantification was performed using the 2-ΔΔCt algorithm. Unsupervised hierarchical distance matrix and distance matrix map was developed using Orange3 software (Python v3.0).

Table 5. Primer sequences used for RT-PCR protocol.

Name	Sequence	Scale	Purification
Hyal1_FW	GTGCCAAGCCCTATGCTAATAAG	25nm	STD
Hyal1_REV	GCATGTCCATTGCAAAGACTGA	25nm	STD
Hyal2_FW	GTCCCACATACACCCGAGGA	25nm	STD
Hyal2_REV	GGCACTCTCACCGATGGTAGA	25nm	STD
Hyal3_Ffw	GGACGACCTGATGCAGACTATTG	25nm	STD
Hyal3_REV	GGTCCCCCCAGAGTACCACT	25nm	STD
Has1_FW	AGGGCTCTTAAAGGAGGAGTCC	25nm	STD
Has1_REV	AGAAGGTAAACTGAGTCCCCAGAA	25nm	STD
Has2_FW	CAAAGAGGTTCGTTCAAGTTCTGA	25nm	STD
Has2_REV	TGTGTTTGTTTCCCACTAGCTCTC	25nm	STD
Has3_FW	CTGGTCTATCTCCTCCAACAGCTT	25nm	STD
Has3_REV	GCTGGGATAATGAAGAGCTACAGAA	25nm	STD
Mmp2_FW	ACCGTCGCCCATCATCAA	25nm	STD
Mmp2_REV	TTGC ACTGCCAACTCTTTGTCT	25nm	STD
Mmp3_FW	CTG GAA TGG TCT TGG CTC AT	25nm	STD
Mmp3_REV	CTG ACT GCA TCG AAG GAC AA	25nm	STD
Mmp9_FW	TCGAAGGCG ACCTCAAGTG	25nm	STD
Mmp9_REV	TTCGGTGTAGCTT TGGATCCA	25nm	STD
Mmp14_FW	CGGGCGGATCCACCAT	25nm	STD
Mmp14_REV	GCCAGGCTTCGGGGCT	25nm	STD
Mmp15_FW	CTTGCAGAGATGCAGCGCTTCTAC	25nm	STD
Mmp15_REV	CTGGATGCTAAAGGTCAGATGGTG	25nm	STD
Mmp16_FW	CAG CTC TGG AAG AAG GTT GG	25nm	STD
Mmp16_REV	GAG CTG CCT CTT GTT TGG TC	25nm	STD
Hif1a_FW	CATAAAGTCTGCAACATGGAAGGT	25nm	STD
Hif1a_REV	ATTTGATGGGTGAGGAATGGGTT	25nm	STD
HPRT1_FW	TGATAGATCCATTCCTATGACTGTAGA	25nm	STD
HPRT1_REV	AAGACATTCTTTCCAGTTAAAGTTGAG	25nm	STD

2.2.4. Tissue fixation and dissection

Mice from **sham and MCAO** groups were perfused with 4% PFA in 0.1M PB, brains were collected and post-fixed for 4 hours in the same solution. After several washes to remove paraformaldehyde, brains were embedded in 30% sucrose solution until decanted and later stored in cryoprotection solution (30% glycerol, 30% ethylene glycol, 10% 0.4M PB, 30% water) at -20°C until use. Brains were cut in coronal sections of 40 µm using a Leica VT 1200 S vibratome (Leica Microsystems). Slices were stored

in PBS 0.01% Azide for no more than one month or in cryoprotection solution for longer storage.

Ai14-Rosa26-CAG-tdTomato$^{fl/fl}$ transgenic mice brains were washed in PBS 1X and embedded in 30% sucrose solution in PBS 1X until decanted. Brains were cut in coronal sections of 50 µm of thickness using an Epredia™ HM 450 Sliding Microtome (Thermo Fisher Scientific). Slices were stored in PBS Azide or cryoprotection solution as described above.

Olfactory bulb from Ai14-Rosa26-CAG-tdTomato$^{fl/fl}$ transgenic mice were extracted after perfusion and cryoprotected in 15% sucrose (Panreac) for 24-48 hours. Then, samples were embedded in 7% gelatin (Sigma-Aldrich), 15% sucrose and PB solution and stored at -80ºC until use. Embedded samples were frozen at -64ºC in 2-Methylbutane (Honeywell Research Chemicals) for 2 minutes before cryostat cutting. Samples were cut at 12 µm using a cryostat CM1950 (Leica Mycrosystems). Slices were attached to superfrost slides (Thermo Fisher Scientific) and stored at -20ºC until use.

2.2.5. Immunofluorescence protocol for *in vivo* experiments

Standard immunofluorescence

Standard immunofluorescence protocol for *in vivo* experiments was performed in floating slices. Tissues were rinsed in PBS 1X three times to wash out Azide or cryoprotective solution before starting the immunolabeling. Slices were incubated with blocking solution and permeabilized with PBS 1X, 0.1% Triton, 10% Normal Goat Serum (NGS) for one hour at room temperature. Primary antibodies were used at different working concentrations (Table 6) in blocking solution overnight at 4ºC. After three washes with PBS, 0.1%Triton, secondary antibodies (Table 7) and DAPI (5 mg/ml) were added for one hour at room temperature. Slices were washed three times with PBS 1X and mounted with Fluoromount-G (SouthernBiotech) in superfrost slides (Thermo Fisher Scientific). When necessary, antigen retrieval was performed as specified in the manufacturer specifications (Vector #H3300).

Thrombospondin 4 immunofluorescence

Thbs4 antibody immunofluorescence was performed as previously described with minimal changes. Slices were rinsed in PBS 1X to wash out Azide or cryoprotective solution before blocking the secondary antibodies unspecific binging and permeabilized with PBS 1X 0.1% Triton 1% BSA 5% Donkey serum for one hour at room temperature

and in a rotating shaker (Duomax 1030 shaker, Heidolph Instruments, Germany). After that, slides were incubated with primary antibodies diluted in the same blocking solution overnight at 4°C. After three washes with PBS 0.1%Triton for 10 minutes each, donkey secondary antibody for goat α-Thbs4 antibody was diluted in blocking medium and incubated for one hour at room temperature. After three washes with PBS 1X 0.1% triton, goat secondary antibodies and DAPI reagent were diluted in the same blocking media and incubated for another hour at room temperature. Following three washes with PBS 1X, slices were mounted in superfrost slides (Thermo Fisher Scientific) using Fluoromount-G (SouthernBiotech) mounting medium.

Wholemount immunofluorescence

For wholemount immunofluorescence protocol, tissue was incubated in blocking buffer (PBS 1X 0.5% Triton and 1%BSA) for 2 hour at room temperature. Primary antibodies diluted in blocking buffer was incubated 72 hours at 4ºC. After three washes with PBS 0.1% Triton, tissue was incubated with donkey secondary antibody diluted in blocking buffer for one hour at room temperature. After three washes with PBS 1X 0.1% triton, goat secondary antibodies and DAPI were incubated another hour at room temperature. Lateral SVZ wholemount was mounted in Fluoromount-G (SouthernBiotech) and dried in the dark for at least 48 hours at room temperature.

BrdU immunofluorescence

For BrdU immunofluorescence unspecific cytoplasmic BrdU was eliminated and specific incorporation into DNA was enhanced by DNA hydrolysis with 2N hydrogen chloride (HCl). Before primary antibody binding, slices were incubated in pre-heated 2N HCl for 20 minutes at 37ºC. After HCl treatments the pH solution was neutralized by 10 minutes washing with 1 mM sodium tetraborate at room temperature. After one further wash with PBS 1X the immunofluorescence was performed as for standard protocol.

Hyaluronic acid binding protein staining

For hyaluronic acid labelling, endogenous biotins were pre-blocked using Strep/Biotin blocking solution (Palex, #416539) following manufacturer´s instructions. Slices were first incubated in streptavidin blocking solution for 20 minutes at room temperature. After three washes with PBS 1X, slices were incubated in biotin blocking solution for another 20 minutes at room temperature. Biotin blocking solution was removed washing the slices with PBS 1X before incubation with blocking buffer (PBS 1X

Table 6. Primary antibodies used for *in vivo* immunofluorescence protocol.

Antibody	Host	Isotope	Dilution	Reference	Company
Thbs4	Mouse	Monoclonal IgM kappa light chain	1/400	Sc-390734	Santa Cruz Biotechnology, USA.
Thbs4	Goat	Polyclonal IgG	1/200	AF2390	R&B systems, USA
S100β	Rabbit	Polyclonal	1/400	Z0311	Dako, Agilent Techonologies, Inc.
S100β	Mouse	Monoclonal IgG2a	1/1000	MA5-12969	Invitrogen, Spain
GFAP	Mouse	Monoclonal IgG1	1/1000	MAB3402	Sigma, Spain
GFAP	Rabbit	Polyclonal	1/4000	Z0334	Dako, Agilent Techonologies, Inc.
βIII tubulin	Rabbit	Polyclonal	1/400	ab18207	Abcam, UK
NeuN	Mouse	Monoclonal IgG1	1/1000	MAB377	Milipore, Germany
DCX	Rabbit	Polyclonal IgG	1/500	ab18723	Abcam, UK
Nestin	Chicken	Polyclonal IgY	1/1000	NES	Aves Lab, EEUU
Prominin 1	Rat	Monoclonal IgG1 kappa	1/300	14-1331-82	Invitrogen, Spain
EGFR	Mouse	Monoclonal	1/400	SAB4200809	Abcam, UK
BrdU	Rat	Monoclonal	1/400	MCA2060	Biorad, USA.
BrdU	Mouse	Monoclonal IgG1, kappa	1/500	03-3900	Invitrogen, Spain
IdU	Mouse	Monoclonal IgG2b	1/100	MA5-24879	Invitrogen, Spain
Ki67	Rabbit	Polyclonal IgG	1/400	Ab15580	Abcam, UK
Cleaved-Caspase 3	Rabbit	Monoclonal IgG	1/300	#9664	Cell Signaling, Germany
Biotinylated Hyaluronan Binding protein (HABP)	-	-	1/100	385911	Milipore, Germany
CD44	Rat	Monoclonal IgG2b	1/500	MA517875	Invitrogen, Spain
FLAG	Mouse	Monoclonal IgG1	1/500	F1804	Sigma, Spain
Olig2	Mouse	Monoclonal IgG2aκ	1/1000	MABN50	Milipore, Germany
MCT1	Chicken	Polyclonal IgY	1/1000	AB1286-1	Milipore, Germany
CD31	Rabbit	Polyclonal IgG	1/100	Ab28364	Abcam, UK

Table 7. Secondary antibodies used for *in vivo* immunofluorescence protocol.

Antibody	Host	Dilution	Reference	Company
Alexa Fluor 488	Donkey α-goat	1/1000	A10055	Invitrogen, Spain
Alexa Fluor 555	Donkey α-rabbit	1/1000	A31572	Invitrogen, Spain
Alexa Fluor 594	Donkey α-goat	1/1000	A11058	Invitrogen, Spain
Alexa Fluor 680	Donkey α-mouse	1/1000	A10038	Invitrogen, Spain
Alexa Fluor 488	Goat α-mouse IgG2a	1/1000	A21131	Invitrogen, Spain
Alexa Fluor 488	Goat α-rabbit	1/1000	A11008	Invitrogen, Spain
Alexa Fluor 546	Goat α-chicken	1/1000	A11040	Invitrogen, Spain
Alexa Fluor 555	Goat α-rat	1/1000	A21434	Invitrogen, Spain
Alexa Fluor 555	Goat α-chicken	1/1000	A21437	Invitrogen, Spain
Alexa Fluor 568	Goat α-rat	1/1000	A11077	Invitrogen, Spain
Alexa Fluor 594	Goat α-rabbit	1/1000	A11012	Invitrogen, Spain
Alexa Fluor 594	Goat α-guinea pig	1/1000	A11076	Invitrogen, Spain
Alexa Fluor 594	Goat α-mouse IgG1	1/1000	A21125	Invitrogen, Spain
Alexa Fluor 594	Goat α-mouse IgG2b	1/1000	A21145	Invitrogen, Spain
Alexa Fluor 633	Goat α-rabbit	1/1000	A21070	Invitrogen, Spain
Alexa Fluor 647	Goat α-chicken	1/1000	A21449	Invitrogen, Spain
Alexa Fluor 647	Goat α-rat	1/1000	A21248	Invitrogen, Spain
Streptavidin ATTO-647N conjugated		1/1000	S000-56	Rockland

0.1% Saponine 1% BSA) for one hour at room temperature. Primary antibodies and biotinylated Hyaluronic Acid Binding Protein (HABP, #385911 Millipore) were incubated for 72 hours at 4°C or 24 hours at room temperature. After three washes with PBS 1X 0.1% Saponine, donkey secondary antibody diluted in the same blocking buffer was incubated for one hour at room temperature. After three washes with PBS 1X 0.1% Saponine, goat secondary antibodies and DAPI diluted in blocking media were incubated for another hour at room temperature. Three final washes with PBS 1X 0.1% Saponine were done and slices were mounted with Mowiol (Millipore 4-88 reagent #475904) in superfrost slides (Thermo Fisher Scientific) and #1.5 coverslips.

3. Image acquisition and processing

Images were acquired using a Zeiss AxioVision fluorescence microscope, a Leica TCS STED SP8 laser scanning confocal microscope and a 3DHISTECH panoramic MIDI II digital slide scanner (all from Achucarro Basque Center for Neuroscience). Settings were adjusted for each individual experiment and kept for all conditions. Image processing was performed using CellProfiler, ImageJ, CaseViewer and Hyugens softwares. Data processing was performed using Microsoft Excel (Microsoft), Prism 8.0 (GraphPad) and Orange 3 v3.29.3 (Miniconda platform, Python v3.9.1). Statistical analysis was done using Prism 8.0 (GraphPad).

3.1. *In vitro* images acquisition and processing

In vitro pictures were taken using a Zeiss microscope except for hyaluronan assay, which were taken in a Leica TCS STED SP8 laser scanning confocal microscope. Value comprised the average of five random fields per condition from scattered and dense populated areas. Each experiment was replicated at least three times to obtain representative values.

In vitro image analysis

In vitro images were acquired with a Zeiss microscope using 63X oil-immersion objective (1.4 NA). Microscope settings included fixed wavelength filterer for GFP, DAPI, Texas Red and Cy5 wavelength. Emission time was adjusted for each independent experiment and maintained for all conditions.

Image quantification was done using CellProfiler software for Thbs4 fluorescence intensity. The pipeline implicated several mask to identify the nuclei and the $Thbs4^{+}$ cell among all $GFAP^{+}$ ones per picture. Inside Thbs4 mask, fluorescence intensity was

measured only in the positive cells. Default algorithm was used to threshold the Thbs4 positive population. Fluorescence intensity for each picture was averaged per condition and compare between them.

Image quantification for colocalization of markers was done with ImageJ, manually adjusted using a default threshold and 30% area covered was considered them as positive co-expressing. $GFAP^+$ cell mask was used to quantify all progenitor cells. Prominin 1 and nestin markers were used to quantify quiescent NSC ($Prom1/GFAP^+$ cells) and active NSC ($Nestin/GFAP^+$ cells). Prominin 1 and nestin markers channels were thresholded using the default algorithm and area was measure inside $GFAP^+$ progenitor cell mask (Area fraction).

For quantification of individual markers, a minimum of 80% area covered surrounding the nuclei was established for positive cells. For βIII-tubulin and Thbs4 markers in the neurosphere-dissociated cells, a band of 1 µm surrounding the nucleus was used to measure the area of both markers. Those cells with 80% or more βIII-tubulin or Thbs4 expression in the 1 µm-surrounded band were included for Thbs4 or neuron population. Ki67 marker was measured by hand in all images and conditions.

In vitro HABP image analysis

To analyse HABP (Hyaluronan) spots in the Thbs4-positive population, we used Leica TCS STED SP8 laser scanning confocal microscope to achieve maximal diffraction-limited resolution. Z-stack images were acquired using 63X oil-immersion objective (1.4 NA). Each image contained a total of 13 planes with 0.5 µm interspace. A pulsed white-light laser with tunable acousto-optic filters (AOTFs) was used for excitation. To collect emitted light, highly-sensitive hybrid filters or photomultipliers (PMTs) were manually adjusted (bandwidth) to record DAPI, Alexa Fluor 488, Alexa Fluor 594, ATTO 647N.

HABP quantification was done using ImageJ software. We developed an IJ1 JAVA script to measure intracellular, extracellular and membrane-bound HABP spots. Macro is available in the Github repository (https://github.com/MariArdaya/Hyaluronan_v2). Cell region of interest (ROI) was extracted from binary Thbs4 channel image and membrane ROI was done by creating a band selection 1 µm inside and outside the cell ROI limit. Extracellular ROI was created from the external line of membrane ROI. Defined threshold for HABP channel made a binary image that was median filtered with 1 pixel to filter out electronic noise. HABP binary images were sorted in each ROI compartment and the number of spots was

quantified. Data is shown as HABP spots per ROI divided by total HABP spots to obtain the proportion in each space.

3.2. *In vivo* images acquisition and processing

In vivo images were acquired using a Leica TCS STED SP8 laser scanning confocal microscope (Achucarro Basque Center for Neuroscience) and 3DHISTECH panoramic MIDI II digital slide scanner (Achucarro Basque Center for Neuroscience). Five-six animals were used in almost all experimental conditions although 3 animals were used as minimal samples in some experiments in addition to the protocol controls. Although certain experiments with minimal image processing were analysed manually, the majority of image analysis was performed semi-automatically with the aid of custom tailored scripts. In all cases, GFAP/Thbs4 positive colocalization was analysed to exclude peripheral Thbs4$^+$ cells as monocytes (Rahman et al., 2020). Only the Thbs4$^+$ cells that also expressed GFAP were included as Thbs4 positive population.

SVZ images acquisition and processing

SVZ images were acquired with the Leica TCS STED SP8 laser scanning confocal microscope using a 20X objective (0.8 NA). SVZ images were reconstructed using the tile-scan tool (LasX software, Leica). SVZ layer was delimited by hand and marker expression was measured in the SVZ ROI. Values were represented as percentage of area labelled with the marker divided by the total area of the SVZ ROI (area fraction, %). Several reconstructed SVZ per animal were averaged.

Thrombospondin 4 images acquisition and processing

Thbs4$^+$ astrocytes were quantified using Leica TCS STED SP8 laser scanning confocal microscope images. Pictures were acquired using z-stack tool established for 13 stacks with 0.7 µm of interspace between them. Microscope settings included also 40X oil immersed objective (1.3 NA) and wavelength sequentially acquired to minimize channel bleeding. DAPI/Alexa Fluor 594 (GFAP marker) wavelength in the first sequence and Alexa Fluor 488 (Thbs4 marker) wavelength in the second sequence. Emission laser potency was adjusted for every channel and maintained throughout all experimental set with the same microscope settings. Five pictures per area were taken in every slice. At least 6 representative slices were quantified per animal. Analysed areas included SVZ, cortex, striatum and corpus callosum.

Thbs4/GFAP positive colocalization was measured using ImageJ software. Positive cell number was measured using an IJ1 JAVA code macro. A 1 µm band was done in every nuclei and GFAP expression was measured inside it. At least 80% area of 1 µm nuclei-surrounded band was needed to consider the cells as GFAP positive ones. In addition, to consider them as $Thbs4^{+}$ cells, binary image was done in the GFAP channel using a default algorithm threshold to delimitate the cell mask. Based on experimental data, a minimum of 30% cell mask area covered by Thbs4 marker was required for counting them as positive ones. GFAP and Thbs4/GFAP positive cells were quantified in each condition.

Nestin glial scar images acquisition and processing

Same microscope parameters were used except for adding a new manually established wavelength for Nestin marker (Alexa Fluor 647). Emission laser potency for Alexa Fluor 647 was adjusted and maintained through all experimental set with the same microscope settings. Lesion area images were reconstructed using Navigator plug-in (LasX, Leica) and analyzed using ImageJ software. Deconvolution process was performed using the Huygens software, to improve signal-to-noise ratio of Nestin labeling. Glial scar ROI was created manually based on nestin expression using ImageJ software. Thbs4, GFAP and Nestin markers were quantified in the glial scar ROI and expression area was normalized by the total glial scar region (Area fraction, %).

Hyaluronan images acquisition and processing

Analyzed samples for HABP quantification were mounted using Mowiol (refraction index 1.47) and #1.5 glass coverslips to reduce refraction artifacts and improve resolution. Images were acquired with Leica TCS STED SP8 laser scanning confocal microscope using 63X oil-immersion objective (1.4 NA) and 2048x2048 image size (0.09 µm/pixel). Line average of 2 were used to avoid electronic noise in all sequences. Sequences were the same as previously described only with the exception of the ATTO 647N instead Alexa Fluor 647. Excitation laser power was re-adjusted for each channel and maintained in all conditions.

Image processing was carried out with a semi-automated approach using two different IJ1 JAVA code macro in the ImageJ software. The first code was used for HABP spots quantification in two cell compartment and the second one for HABP skeleton analysis. CD44 and HAS2 adeno-associated virus experiment were analysed manually using the ImageJ software.

Materials and methods

HABP spots were quantified in the intracellular space and cell membrane of Thbs4/GFAP and GFAP positive cells. Membrane and cell ROI were done via automatic thresholding using the Intermodes algorithm. Positive Thbs4 population was measured as previously described using a 30% area occupied in the GFAP cell mask. Cell membrane ROI was created using GFAP marker for both population ($Thbs4^+$ astrocytes and local astrocytes). 0.5 µm length was added outside and inside cell mask boundary. Thus, 1 µm band was created in the membrane of all GFAP positive cells. Threshold for HABP marker was performed and binary image was filtered with 1 pixel median value. "Analyze particles" tool was used to sort HABP spots in the cell membrane ROI and intracellular ROI (created by subtracting 0.5 µm to cell membrane ROI). HABP spot number per compartment and population was exported to excel and data was normalized dividing HABP spots per ROI by total HABP spots.

Next, skeletonize analysis were done. Binary image was created in the HABP marker channel using a threshold. As before, 1 pixel median filter was used to reduce speckles from electronic noise. Skeletonize analysis was performed through IJ1 JAVA code developed previously by Federico N. Soria (beta version, unpublished). HABP skeleton number and skeleton size was recorded for every picture. All pictures comprised one condition was averaged to easily compare among groups. Cumulative Frequency distribution analysis was made to assess HA size. In addition, fractal dimension from HABP skeleton was measured for every picture. Both analysis were made in order to understand how extracellular matrix connectivity is disrupted after MCAO stroke model

Slide reconstruction for fluorescence intensity profile

Slice reconstruction of whole ipsilateral hemisphere was performed using the Navigator plug-in (LasX software, Leica). Images were acquired using 40X oil-immersion objective (1.3 NA), 1024x1024 image size (0.18 pixel/µm) and wavelength sequentially acquired. GFAP, Thbs4, Nestin, DCX and HABP fluorescence intensity were plotted in the slice reconstruction to analyse marker location across the lesion. All markers were imaged with the same resolution size.

IJ1 JAVA code macro, developed previously by Federico N. Soria (beta-version, unpublished), was used to analyze the fluorescence spatial distribution of all markers in the core-penumbra area. In brief, two 250 pixel-thickness lines were traced from core of the lesion to the penumbra/healthy tissue. Fluorescence intensity from markers analyzed was collected in X (distance) and Y (fluorescence intensity) values. Several profiles were acquired per animal and averaged to easily compare animal conditions. Because lesion

size or region varies between individuals, values were normalized using a relative distance scale (for *x* values) and relative fluorescence (for *y* values). Fluorescence values were also normalized to background signal to evaluate the spatial distribution between markers regardless of dissimilar signal-to-noise ratios.

Slide scanner

Whole slide images were taken for representative images using a 3DHISTECH panoramic MIDI II digital slide scanner. No images from these were used for quantification. Images were processed for better visualization enhanced contrast and brightness parameters using CaseViewer software (3DHISTECH Company).

3.3. Western blot images processing

Western blot images were acquired using a Chemidoc MP (Biorad). Images were exported as tiff and processed with ImageJ software and ImageLab software. Western blot immunoblot were quantified using ImageJ software applying threshold default algorithm to delimitate the band and mean gray value (MGV) from each band was measure. Protein quantification with ImageLab were done using the adjusted volume of a band after background subtraction (Adj. Vol. (Int)). All quantifications were normalized with the housekeeping values.

4. Statistical processing

Statistical analysis were done using GraphPad Prism software (version 8.0; GraphPad software).

In vitro data are presented as means ± SEM. Statistical analysis was performed using paired Student's t-test comparing experimental conditions. P-value is considered significant where statistical differences shown $p < 0.05$. Representative images were selected to visual reproduce experimental data.

In vivo data are presented as means ± SEM. Statistical analysis was performed using unpaired Student´s t-test for independent conditions and paired Student´s t-test for dependent conditions. In addition, one-way, two-way ANOVA or mixed model were also performed to compare more than 2 groups among them. Tukey and Dunnett post-hoc test were used. For HABP skeleton analysis, Kruskal-Wallis analysis was performed to compare cumulative frequency accumulation (%) in more than 2 groups. P-value is

considered significant where statistical differences shown $p < 0.05$. Representative images were selected to visual reproducing experimental data.

RESULTS

BRAIN ISCHEMIA ACTIVATES THE SVZ

1. MCAO model characterization

According to the protocol previously published (Gelderblom et al., 2009), the lesion size and location after Middle Cerebral Artery Occlusion (MCAO) model in mice, can manifest large heterogeneity and differences in neurological deficits. First of all, we set up the MCAO parameters to obtain representative and homogeneous damaged areas in all experimental mice. Sixty minutes of MCAO caused neuronal damage in the cortex and striatum as observed by cresyl violet staining (Fig. 24A) and NeuN immunofluorescence staining (Fig. 24B). Survival rate of this model calculated at 28 days post-lesion was around 50% of all infarcted mice (Fig. 24C). Moreover, motor deficits and animal weight of ischemic mice were followed every day after MCAO during 30 days (Fig. 24D-E respectively). Based on neurological scores and animal weight, we could estimate the lesion magnitude in each mice. Mice with deviated neurological punctuation were later histologically analysed to confirm the lesion.

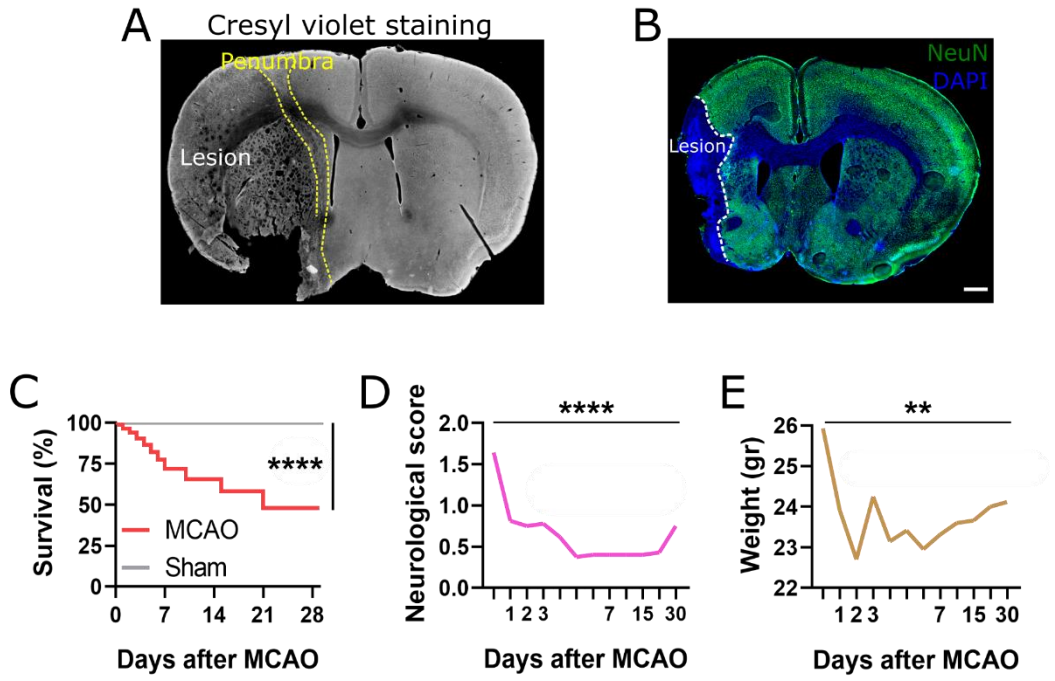

***Figure 24.* MCAO characterization.** A. Representative ipsilateral hemisphere damage using cresyl violet staining. B. Neuronal damage in the ipsilateral hemisphere using NeuN immunofluorescence staining. Mice survival rate (C), neurological scores for motor deficits (D) and animal weight (E) recorded between 28-30 days after MCAO. Scale bar = 1000 µm. **p<0.01, ****p<0.0001.

2. MCAO model induced proliferation in the SVZ

Following MCAO characterization, we analysed and characterised the SVZ response to MCAO. To study the cell proliferation in the SVZ, we administrated 50mg/kg BrdU i.p. every two hours (3 doses in total) the day before the MCAO surgery (Fig. 25A). Total cell proliferation in the SVZ was quantified 24 hours after MCAO by immunofluorescence as means of $BrdU^+$ cells (Fig. 25B). We observed an increase of total SVZ $BrdU^+$ cells (Fig. 25B-C) but differential analysis of different SVZ regions (dorsal, lateral, ventral and medial) evidenced a more significative increase in dorsal and lateral SVZ regions (Fig. 25D). These data suggest that MCAO induced a fast and specific proliferative response in the SVZ.

Results obtained after BrdU labelling were confirmed by Ki67 staining. BrdU and Ki67 are broadly used as proliferation markers and usually show similar expression patterns, however they stain different groups of proliferating cells. BrdU labels cells during the S phase, whereas Ki67 labels cells in the G1, S, G2, and M phases. Ki67 immunofluorescence in the whole-mount preparation of lateral SVZ, showed a ten fold increase of $Ki67^+$ cells 24 hours after MCAO (Fig. 25E-G) confirming that ischemic insult triggered the SVZ proliferation.

Finally, to assess the cell loss in the SVZ following ischemia we analysed apoptotic death in the SVZ by immunofluorescence with cleaved-Caspase 3 (c-Casp3) 24 hours after MCAO. SVZ showed a significant increase in the $c\text{-}Casp3^+$ cells 24 hours post-lesion (Fig. 25H-I). After differential analysis in the SVZ regions, apoptotic cells ($c\text{-}Casp3^+$) increased in dorsal and medial SVZ after MCAO (Fig. 25J). These data showed that MCAO sustains SVZ NSC activation 24 hours after the insult via proliferative process.

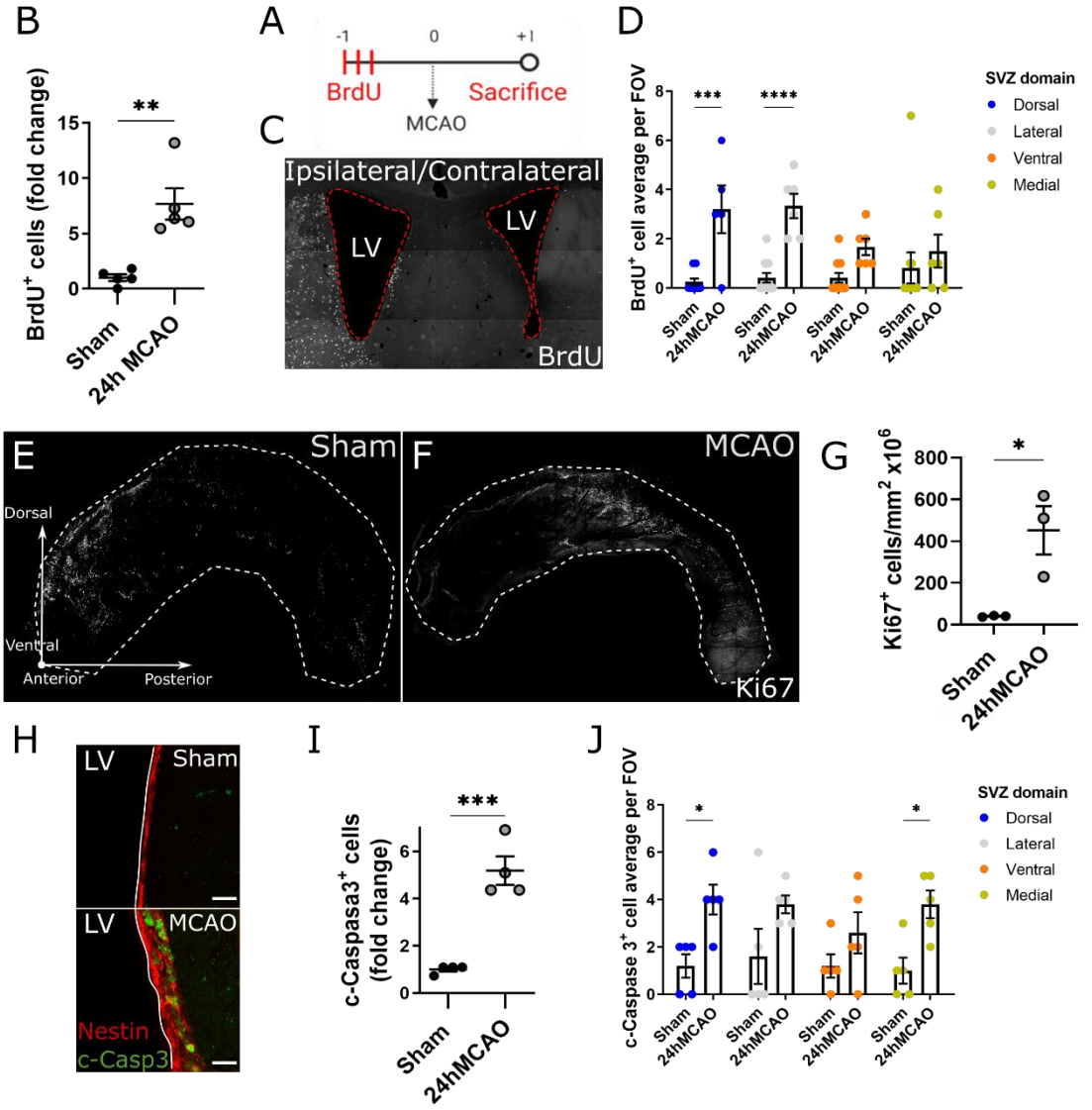

Figure 25. **SVZ cell proliferation after MCAO.** Experimental design (A). BrdU staining showed a general increase in the SVZ after MCAO (B) in (C) a representative image of BrdU staining. Analysis of different SVZ regions showed that MCAO increased the $BrdU^+$ cell number especially in dorsal and lateral SVZ (D). Immunofluorescence of Whole-mount preparation of lateral SVZ with Ki67 (E-F) showed an increase of cell proliferation after MCAO (G). Nestin staining, in red, was used to line the SVZ (H). c-$Casp3^+$ cells quantification in the whole SVZ (I) or in its regions (J) after MCAO. Scale bar = 15 µm. LV = Lateral Ventricle. *p<0.05, **p<0.01, ***p<0.001, ****p<0.0001.

BRAIN ISCHEMIA ACTIVATES THE ASTROGLIOGENESIS IN THE SVZ

3. MCAO model induced Thbs4$^+$ astrogliogenesis from SVZ neural stem cells

Thbs4 expression in the SVZ under physiological conditions. As described by other authors (Benner et al, 2013; Girard et al, 2014; Pous et al, 2020), Thbs4 is highly expressed in the SVZ and RMS (Fig. 26A). Together with SVZ and RMS, Thbs4 can be expressed also in the granular layer of the cerebellum and the ventral-tegmental area (Fig. 26A), being associated with non-classical neurogenic regions (Wojcinski et al, 2017).

Under physiological conditions, expression of Thbs4 in the SVZ was associated to cells with different morphologies (Fig. 26B). We observed Thbs4$^+$ cells with small primary apical process touching the ventricle and the BV in the parenchymal region or rounded NSC-like cells in the dorso-lateral SVZ horn. Among all the SVZ cells, Thbs4$^+$ cells represented 21,4 % (Fig. 26C), which mostly (more than 60%) have a type B-like morphology (Fig. 26D). To confirm our morphological observation, we labelled the SVZ with pThbs4-eGFP after postnatal (P1) electroporation. pThbs4-eGFP plasmid expressed the green fluorescent protein under the control of the Thbs4 promoter so green fluoresce positive cells would be Thbs4$^+$ cells. Twenty four hours after electroporation, almost 20% of dorsal SVZ cells were positive for GFP (Fig. 26E-F), with a greater extent in the most rostral SVZ (Fig. 26G). These results suggested that in physiological conditions, Thbs4$^+$ cells were mainly restricted to the neurogenic niche of the SVZ and evidenced a type B-like morphology.

Thbs4 expression in the SVZ under ischemic conditions. To quantify the activation of astrogliogenesis in the SVZ following brain ischemia, we analysed the expression of Thbs4 in the SVZ in combination with Nestin, a NSC marker, and Doublecortin (DCX), a marker of neuroblasts. SVZ was analysed in sham and ischemic mice 7, 15 and 30 days post-lesion. The immunofluorescence analysis of the SVZ (Fig. 27A-B) showed a transient decrease of Nestin and Doublecortin (DCX) positive cells but an increase of Thbs4$^+$ astrocytes up to day 15 after MCAO (Fig. 27C-E). The increase of Thbs4$^+$ astrocytes was demonstrated by immunofluorescence also using a whole-mount preparation of the SVZ from sham and ischemic mice, 15 days after MCAO (Fig. 27F-H). Also nestin and Thbs4 proteins were modulated by the MCAO. Western blot analysis of total SVZ proteins confirmed the down regulation of the Nestin (Fig. 27I-J) and the upregulation (Fig. 27J-K) of Thbs4 proteins respect to the sham animals. All these data suggested that brain ischemia activated the astrocyte production in the SVZ.

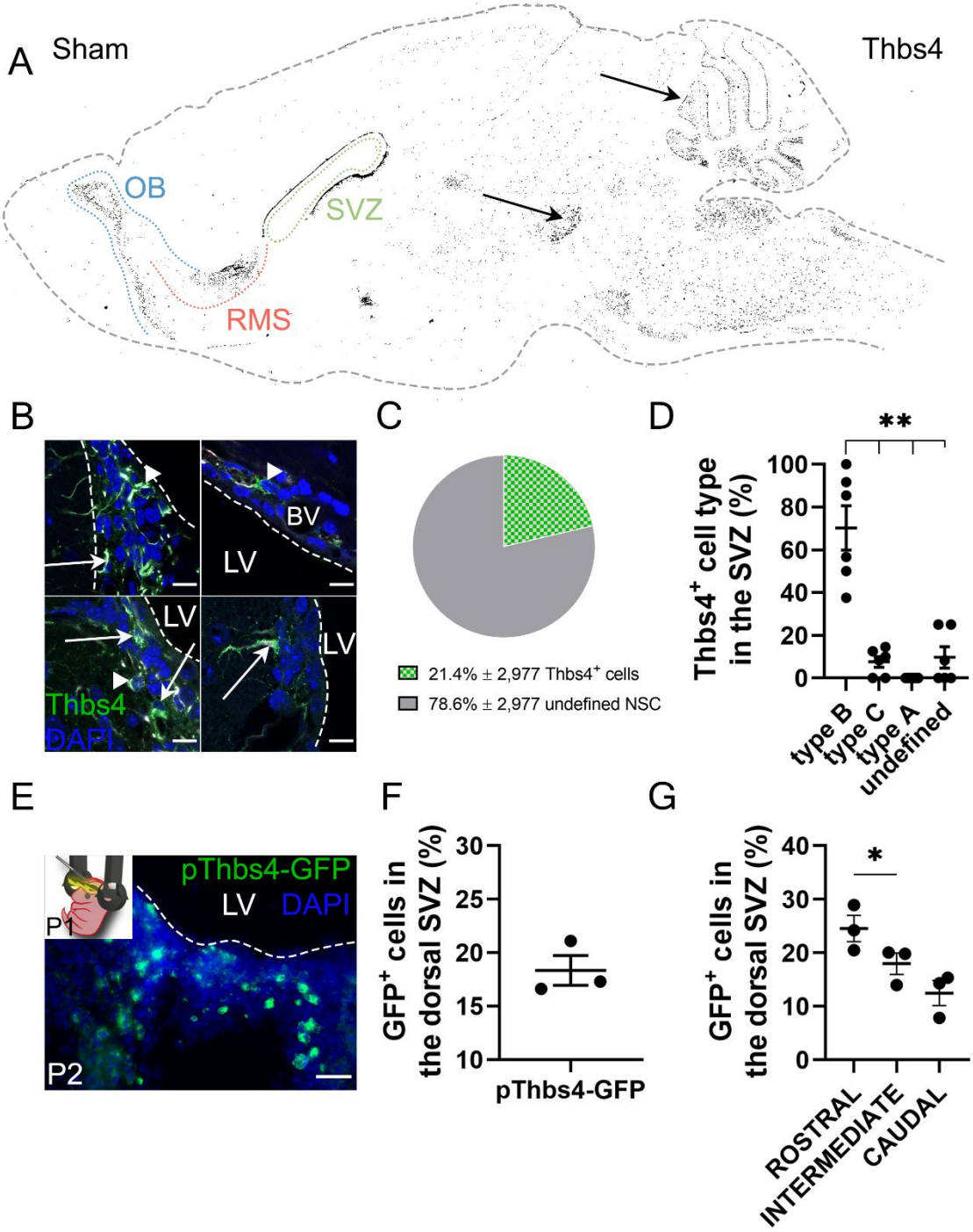

***Figure 26.* Thbs4⁺ cells characterization in the SVZ in physiological conditions.** Thbs4 was mainly expressed in the SVZ, RMS and OB but also in the cerebellum and ventral tegmental area (arrows) (A). In the SVZ, Thbs4⁺ cells displayed type B and type C cells morphology as indicated respectively by arrows and arrow heads (B). After total count by immunofluorescence, 21% of total SVZ cells were positive for Thbs4 (C). Among all Thbs4⁺ cells, more than 60% presented a type B NSC morphology (D). After pThbs4-eGFP electroporation in P1 mice (E), almost 20% of the dorsal SVZ were positive for GFP fluorescence 24 hours later (F). GFP⁺ cells were mainly present at rostral SVZ (G). LV = Lateral Ventricles. Scale bar = 10 µm in B and 50 µm in E. *p<0.05; **p<0.01.

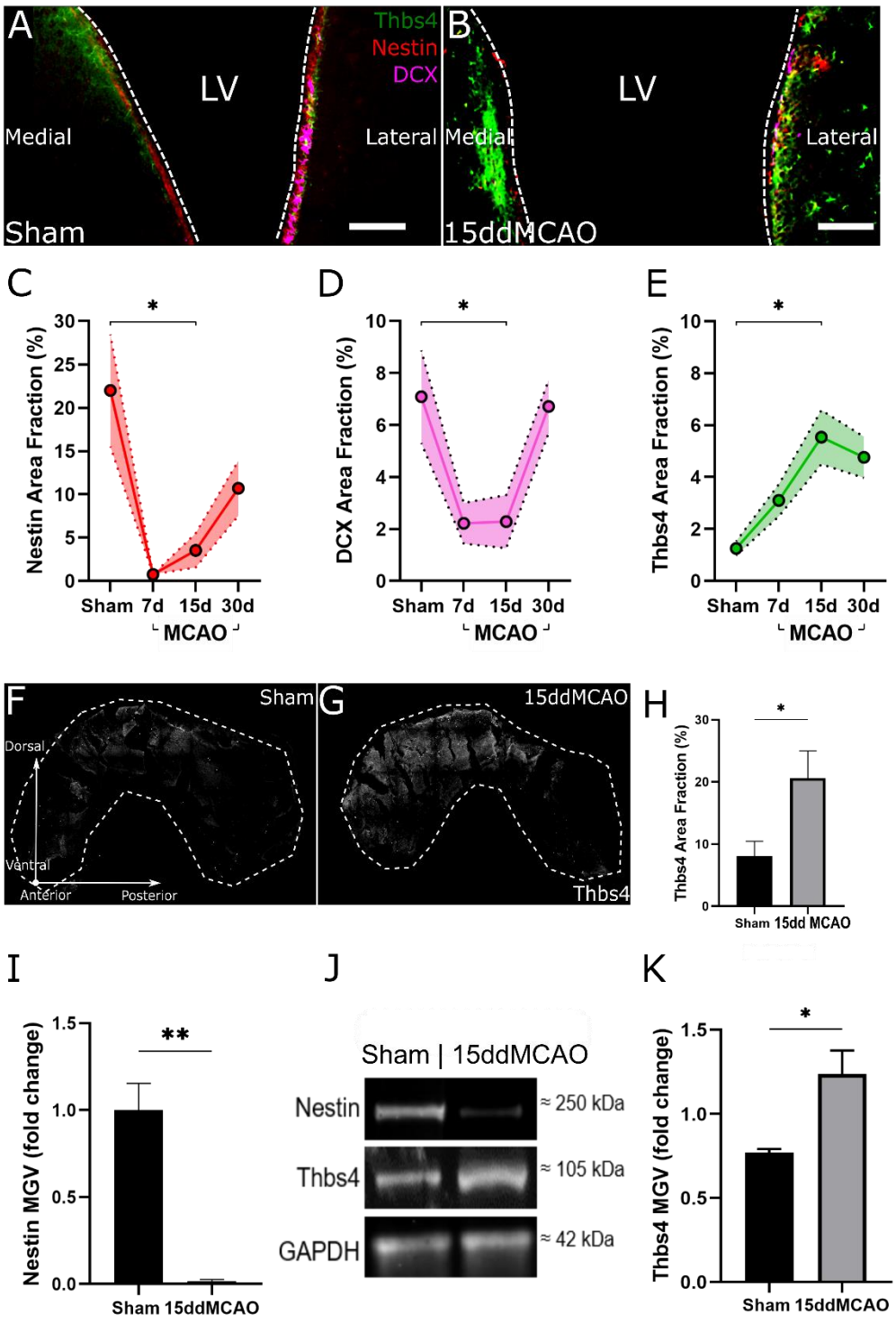

Figure 27. **Thbs4⁺ cells characterization in the SVZ after MCAO.** Representative immunofluorescence of Nestin (red), DCX (pink) and Thbs4 (green) in Sham and ischemic SVZ 15dd post-MCAO (A & B). Quantification of Nestin⁺ NSC (C), DCX⁺ neuroblasts (D) and Thbs4⁺ astrocytes 7, 15 and 30 days after MCAO. Data are expressed as % of area fraction. Thbs4⁺ astrocytes analysis (F-G) and quantification (H) in the whole-mount SVZ preparation. Western blot analysis and quantification of Nestin (I-J) and Thbs4 protein expression (J-K) 15 days after MCAO. LV = Lateral Ventricle. MGV = Mean Gray Value. Scale bar = 100 µm in A. *p<0.05, **p<0.01.

CELL AND REGIONAL ORIGIN OF THE ASTROGLIOGENESIS IN THE SVZ AFTER BRAIN ISCHEMIA

4. Cell origin in the SVZ

To characterize the different cell populations of the SVZ, we labelled the whole pool of proliferating cells with 1% of BrdU in drinking water during 14 days before the MCAO (Codega et al., 2014). One month after MCAO, BrdU in the SVZ only stained slow proliferative cells like type B cells whereas BrdU in rapid transit-amplifying cells (type C) was washed away. Type C cells were labelled i.p. with 50mg/Kg of 5-Iodo-2′-deoxyuridine (IdU) 24 hours before animals perfusion (Fig. 28A; see *2.1.3 section* for protocol).

To identify the cell origin of newborn astrocytes, we analysed SVZ 30 days after MCAO by immunofluorescence of co-labelling Thbs4 and GFAP together with BrdU or IdU. The total amount of $BrdU^+$ cells was increased in the SVZ 30 days after MCAO (Fig. 28B) whereas we did not observe any change in the number of IdU^+ cells (Fig. 28C). After MCAO, Thbs4/GFAP colocalization with BrdU (slow proliferative NSC) increased linearly after MCAO (Fig. 28D), whereas Thbs4/GFAP colocalization with IdU (activated NSC) did not show any significative changes (Fig. 28E). These results suggested that $Thbs4^+$ astrocytes derived from the slow proliferative cells.

5. SVZ regional origin

SVZ is a neurogenic niche with a complex structure where different NSC populations can populate specifically different regions. Depending on their location, NSCs are committed to different cell fate (Fiorelli et al, 2015). To identify the regional origin of Thbs4/GFAP/BrdU positive cells in the SVZ we analysed the dorsal, lateral, ventral and medial SVZ regions 30 days after MCAO (Fig. 29A-B). Topographic analysis of the SVZ showed a significant increase of co-labelled Thbs4/GFAP/$BrdU^+$ cells only in the dorsal region (Fig. 29C-D); whereas we did not observe any significant modulation of Thbs4/GFAP/IdU^+ cells at any SVZ region (Fig. 29E). Data suggested that ischemia-induced $Thbs4^+$ astrocytes arose from quiescent type B cells in the dorsal SVZ.

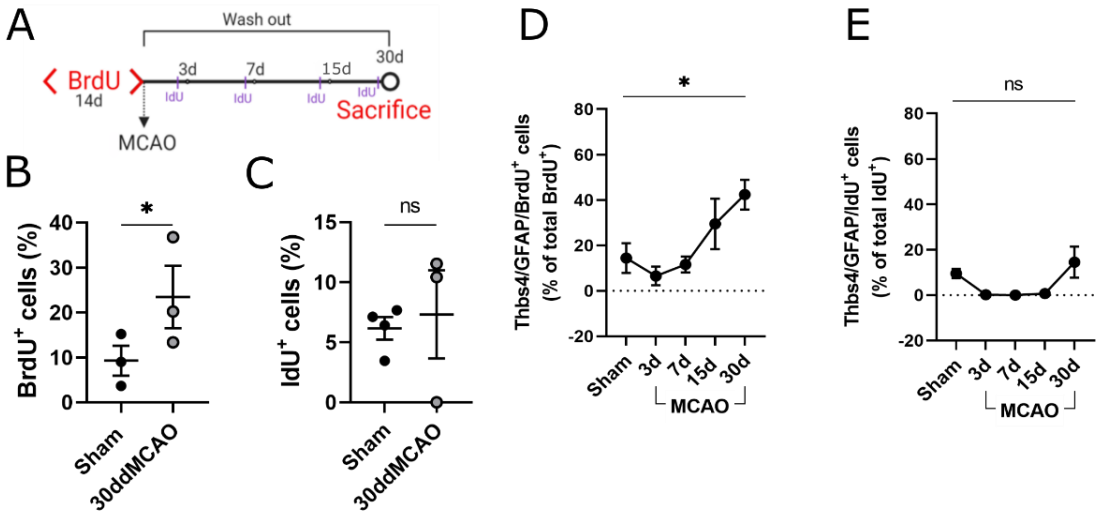

Figure 28. **Cellular origin of astrocytes after MCAO in the SVZ.** Experimental protocol (A). Number of total $BrdU^+$ (B) and IdU^+ (C) cells in the SVZ of sham and ischemic mice 30 days post-lesion. Thbs4/GFAP/$BrdU^+$ cells (slow proliferative cells) increased in the SVZ 30 days after MCAO (D). Thbs4/GFAP/IdU^+ cell number (high proliferative cells) in the SVZ did not change after MCAO (E). Cell labelling was performed 3 days (3d), 7 days (7d) 15 days (15d) and 30 days (30d) after MCAO in the SVZ. *p<0.05.

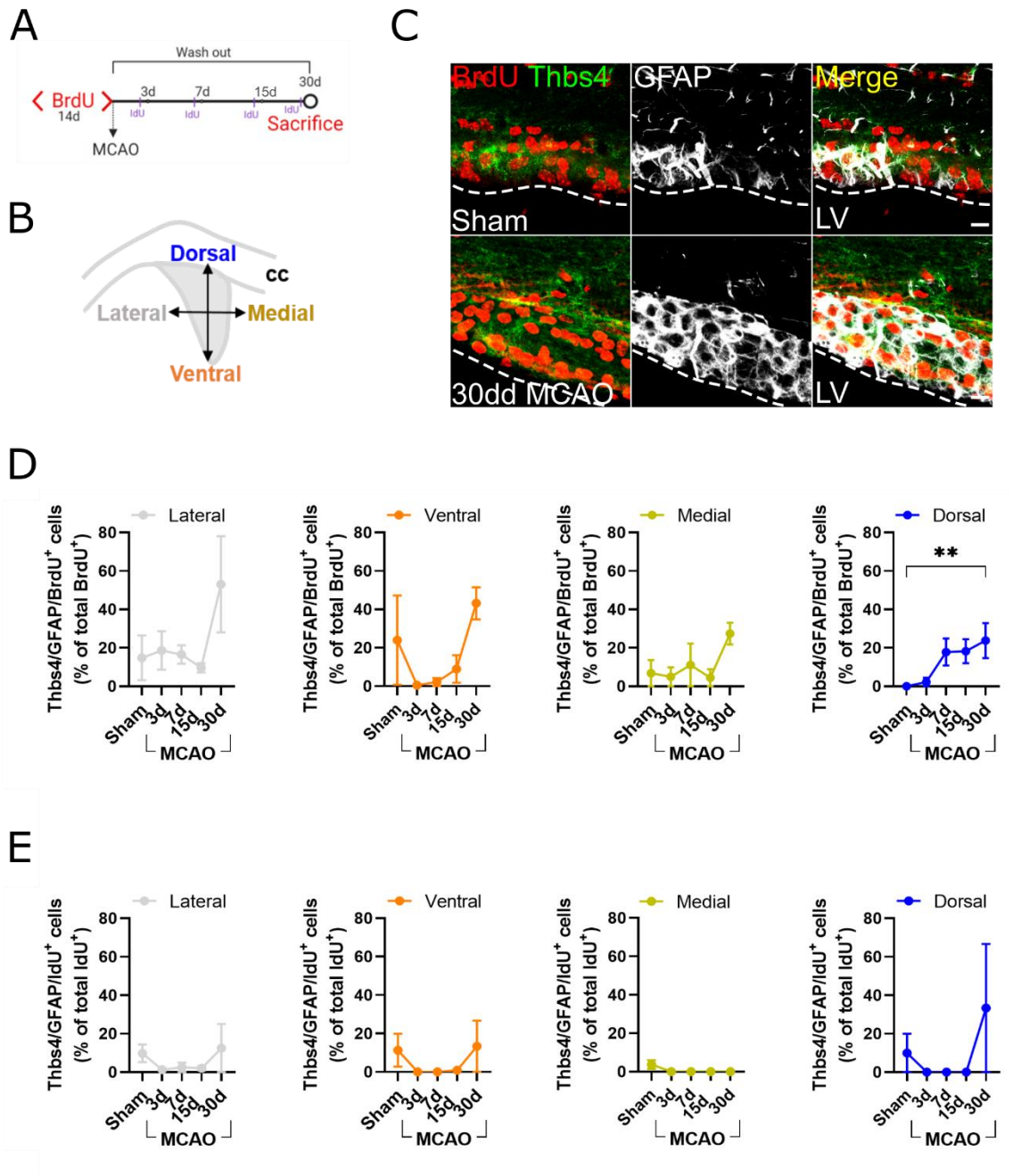

Figure 29. **SVZ regional origin of Thbs4⁺ astrocytes.** Experimental protocol (A) and SVZ regions analysed (B). Representative image of Thbs4 expression and BrdU incorporayion in the dorsal SVZ of sham animals and 30 days after MCAO (C). MCAO increased the number of Thbs4/GFAP/BrdU⁺ cells only in the dorsal SVZ 30 days after the insult (D) whereas we did not see any changes in the Thbs4/GFAP/IdU⁺ cells in the SVZ at the same time point (E). Cell labelling was performed 3 days (3d), 7 days (7d) 15 days (15d) and 30 days (30d) after MCAO in the SVZ regions described in B. Scale bar = 10 µm. **p<0.01.

Thbs4^{+} ASTROCYTES RECRUITMENT TO THE ISCHEMIC REGION

6. *Kinetic of glial scar formation and migration of Thbs4^{+} astrocytes after brain ischemia*

Nestin, beside its role in the neurogenic niches, is also rapidly and locally expressed by reactive astrocytes and participates in the glial scar formation (Frisén et al., 1995). Thus, we used the Nestin immunofluorescence as a tool to identify the glial scar (Fig. 30A). Identification of the scar with Nestin was also compared with more classical methodologies like TTC staining (Fig. 30B-C). Unlike the TTC staining, that can only be performed hours after the lesion (the infiltration of peripheral immune cells avoids the exposure of the pale pink area), the visualization of the glial scar with Nestin immunofluorescence allowed us to analyse a wider time frame of the lesion.

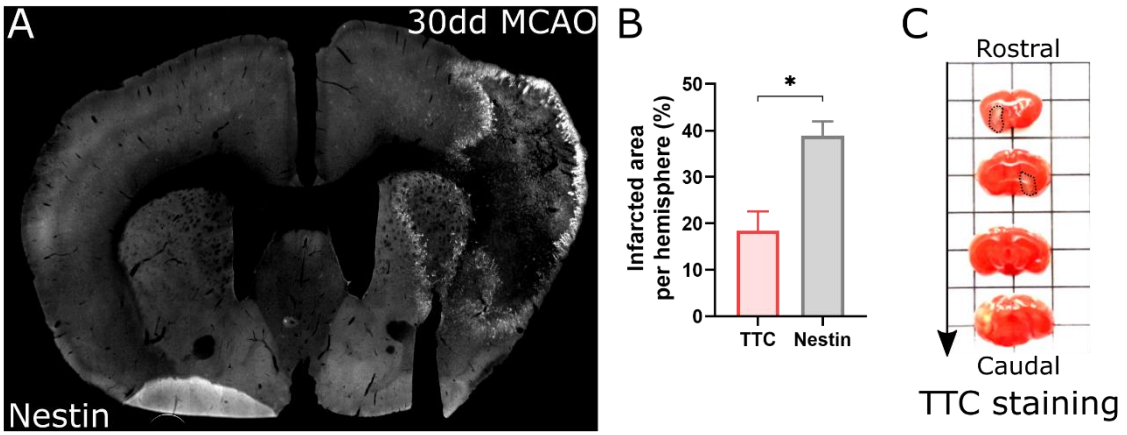

***Figure 30*. Characterization the glial scar using Nestin immunofluorescence and TTC staining.** Nestin immunofluorescence and damage delimitation 30 days after MCAO (A). Infarcted area quantification after TTC staining (B). TTC staining of serial brain slices showed infarcted area as a pale pink (C). *p<0.05.

Using the Nestin immunofluorescence we observed a rapid formation of the glial scar already 7 days after the MCAO (Fig. 31A-B). Analysing the expression of the two astrocytic markers, Thbs4 and GFAP, we observed a different kinetic and localization between them. GFAP expression was observed rapidly after 7 days and within the glial scar, whereas Thbs4 was observed later, 15 days post ischemia, at the border of the glial scar (Fig. 31B-D). This delay suggested that the glial scar is composed by two different astrocytic sub-populations expressing only GFAP or GFAP/Thbs4. To analyse the spatial location of GFAP and Thbs4 markers within the Nestin border, we measured the fluorescence intensity profile of damaged area 30 days after the MCAO. Thbs4

fluorescence intensity was mainly restricted to the Nestin glial scar (Fig. 31C-D), whereas GFAP fluorescent intensity was also found in the lesion core (Fig. 31D).

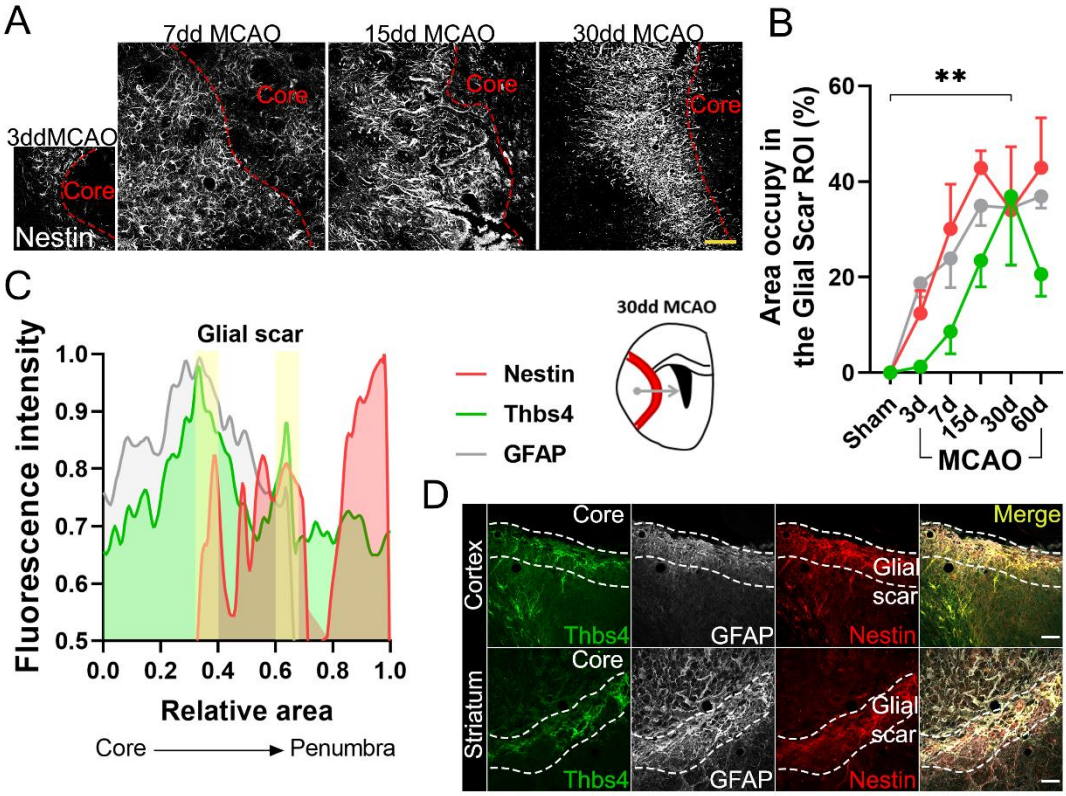

Figure 31. **Glial scar characterization after MCAO.** Time course of Nestin expression and scar delimitation in the core-penumbra area 3, 7, 15 and 30 days post-lesion (A). Using Nestin as a glial scar marker, Thbs4 and GFAP fluorescence was quantified inside the glial scar in sham animals and different days after MCAO (B). Fluorescence intensity profile of Thbs4, GFAP and Nestin in the glial scar (C). Thbs4 is mainly localized in the outer and inner glial scar defined by Nestin. Representative images of Thbs4 (green), GFAP (white) and Nestin (red) immunofluorescence in the infarcted cortex and infarcted striatum of 30 days after MCAO mice (D). Scale bar = 100 µm in A and 50 µm in D. **p<0.01.

7. Detailed analysis of Thbs4⁺ astrocytes in the infarcted areas

Analysis and kinetic of Thbs4⁺ astrocytes migration was further performed in corpus callosum (CC), striatum (Str) and cortex (Ctx) (Fig. 32A). We observed a linear increase of Thbs4⁺ astrocytes from 7 to 60 days after MCAO, both in the Ctx and Str (Fig. 32B). Migration occurred mainly through the corpus callosum. Among the total GFAP⁺ astrocytes, 36.5% were also positive for Thbs4, suggesting that almost one third of the astrocytes in the glial scar derived from the SVZ (Fig. 32C). In fact, Thbs4⁺ astrocytes were visualized at the damaged area 30 days after the lesion and occupied

the glial scar territory (Fig. 32A). All in all, these data demonstrated that the Thbs4$^+$ astrocytes found in the glial scar are a different population deriving from the SVZ, moving through the corpus callosum with their own kinetic and positioning at the border of the ischemic glial scar.

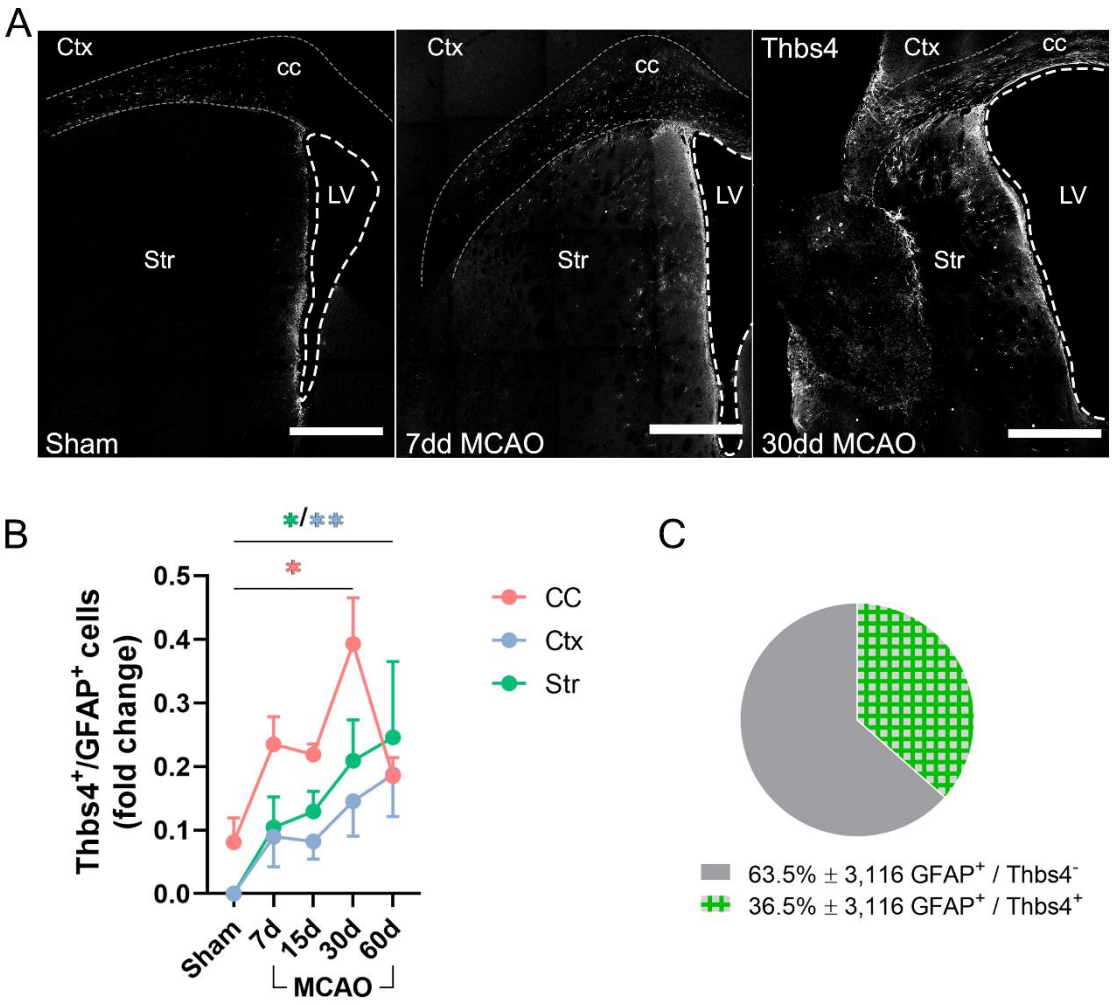

Figure 32. **Thbs4/GFAP immunofluorescence in the ischemic tissues.** In sham animals, the Thbs4/GFAP$^+$ astrocytes were restricted to the SVZ. In ischemic mice, Thbs4/GFAP$^+$ astrocytes started to migrate to the ischemic lesion already after 7 days and finally invaded the glial scar 30 days after MCAO (A). Time course quantification of Thbs4/GFAP$^+$ immunofluorescence in the corpus callosum (CC), cortex (Ctx) and striatum (Str) (B). 36.5% of total GFAP$^+$ astrocytes also co-expressed Thbs4 (C). LV = Lateral Ventricle. Scale bar = 500 µm. *p<0.05, **p<0.01.

8. MCAO re-direct olfactory bulb neurogenesis to the ischemic infarct

To further confirm the cell recruitment from the SVZ to the ischemic infarct, we decided to analyse if ischemia could redirect the neurogenesis in the OB to the ischemic

lesion. We labelled the proliferative cells as shown in Fig. 33A and analysed the OBs of sham and ischemic mice 7, 15 and 30 days after MCAO. BrdU$^+$ cells and neuroblasts (DCX$^+$) were analysed by immunofluorescence in each OB layer (Fig. 33B-F). We observed a strong decrease in the number of BrdU$^+$ cells only in the glomerular layer 30 days after MCAO (Fig. 33D). Number of DCX$^+$ cells dramatically decreased 15 days after the lesion in all OB layer with a slight recovery 30 days after the insult (Fig. 33E). Colocalization of BrdU with DCX markers showed a significant decreased of ischemia-induced neuroblasts in the RMS 30 days post-lesion (Fig. 33F), suggesting that ischemia, induced a change in the neuroblasts ectopic migratory pathway, depriving the OB layers of SVZ new-born neurons.

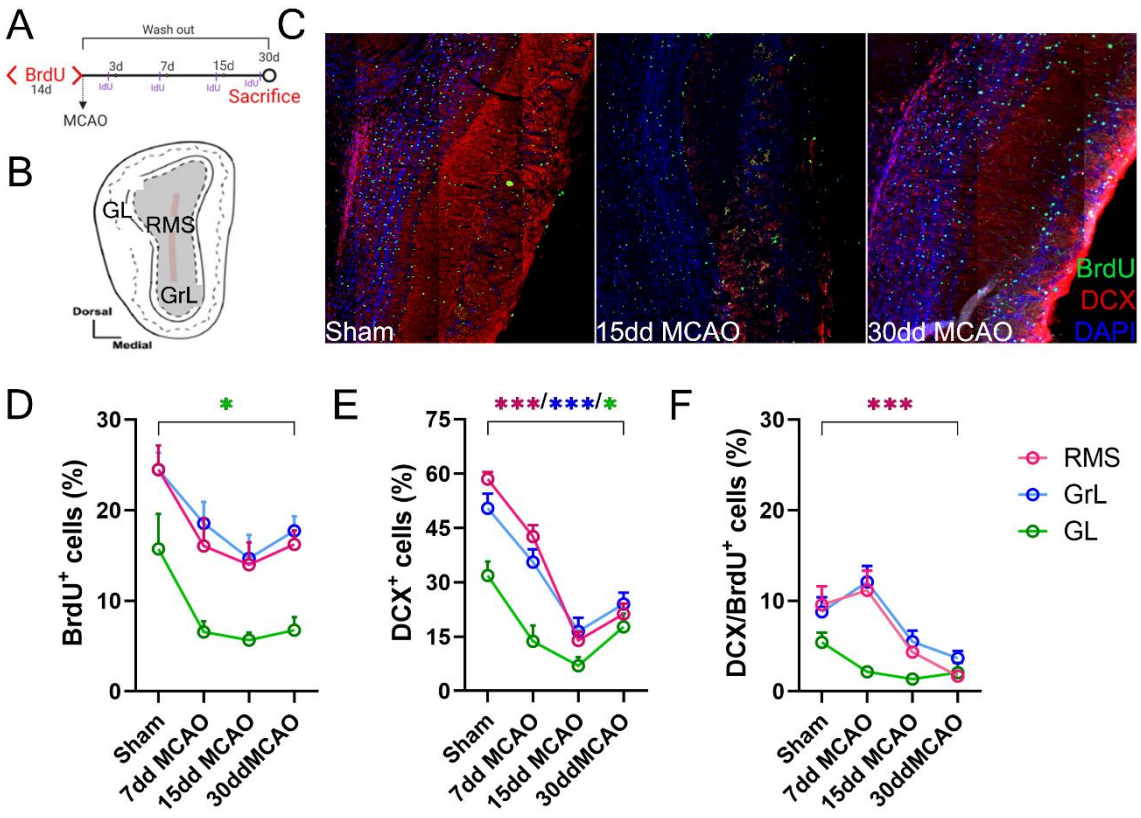

Figure 33. **Reduced neurogenesis in the OB after brain ischemia.** Experimental design (A) and scheme of OB layers (B). RMS, rostral migratory stream; GrL, granular layer; GL, glomerular layer. Representative images of DCX (red), BrdU (green) immunofluorescence and DAPI staining in sham and ischemic mice, 15 and 30 days after MCAO (C). BrdU$^+$, DCX$^+$ and BrdU/DCX$^+$ cell number quantification in sham and ischemic mice in the different OB layers (D-F). *p<0.05, ***p<0.001.

To confirm that ischemic brain insult changed the ectopic migratory pathway of neuroblasts from SVZ to OB, we analysed in parallel the neurogenesis in ischemic areas. We confirmed a transient reduction of DCX$^+$ neuroblasts in the SVZ, 7 and 15 days after

MCAO, as shown in Fig. 27D. Furthermore, we observed a slight increase of the DCX$^+$ cells in the infarcted areas 30 days after MCAO (Fig. 34A-D) suggesting that the neurogenic program in the SVZ can be restored lately after the brain ischemia.

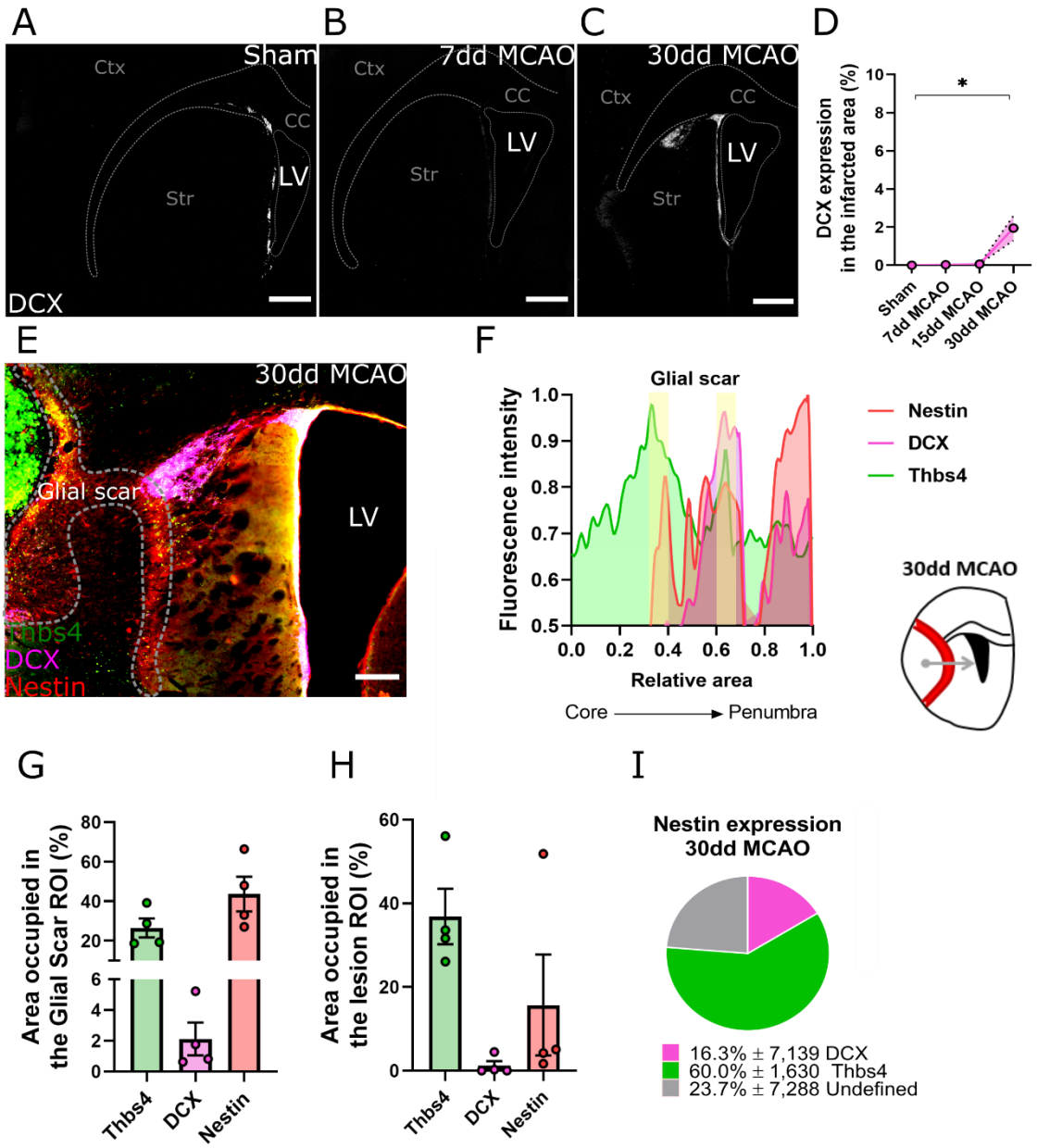

***Figure 34*. Neurogenesis and DCX$^+$ neuroblasts analysis in the damaged areas.** Representative images of DCX staining in sham (A) and ischemic animals 7 (B) and 30 days after MCAO (C). DCX quantification after MCAO overtime (D). Representative image of Thbs4/Nestin/DCX staining 30 days after MCAO (E). Fluorescence intensity profile of Thbs4, Nestin and DCX markers in the lesion 30 days after MCAO (F). Area occupied by Thbs4, Nestin and DCX in the glial scar 30 days after the lesion (G). Area occupied by Thbs4, Nestin and DCX in the core of the lesion 30 days after the lesion (H). Colocalization between Nestin with Thbs4 (green), DCX (pink) markers or with undefined cells (gray) 30 days after the MCAO (I). LV = Lateral Ventricle; cc = corpus callosum; Ctx = Cortez; Str = Striatum. Scale bar = 500 µm in A, B, C and 200 µm in E. *p<0.05.

To better characterize the cell populations activated after brain ischemia we performed a triple immunofluorescence for Nestin, Thbs4 and DCX (Fig. 34E). Ischemic areas were analysed 30 days after MCAO and compared with the sham group. Using an immunofluorescence profile, we observed that Thbs4 fluorescence intensity was limited to the glial scar compartment (Fig. 34F) whereas DCX fluorescence intensity was restricted to the outer space of the lesion (Fig. 34E-F).

Next, we created a glial scar ROI using the Nestin marker and we measured the Thbs4 and DCX expression inside the glial scar. We observed around 2% of the glial scar was covered by the DCX labelling whereas 20% was covered by Thbs4 (Fig. 34G). We did not see any DCX^+ cells inside the lesion (Fig. 34H) suggesting that DCX^+ neuroblasts did not cross the glial scar tissue. However, part of the Thbs4 labelling (37%) was found inside the damaged area (Fig. 34H). Finally, we analysed the colocalization between Nestin marker and Thbs4/DCX markers. More than 60% of $Nestin^+$ cells also expressed Thbs4 marker whereas only 16% expressed DCX marker 30 days after the lesion (Fig. 34I).

These data suggest SVZ stops producing neuroblasts and generates $Thbs4^+$ astrocytes in response to the brain ischemia. However, SVZ starts producing neuroblasts which migrate to infarcted regions at chronic stages of the disease.

9. Ischemia-induced $Thbs4^+$ astrocytes reached the damaged areas from the SVZ niche

To confirm that $Thbs4^+$ astrocytes derived from type B cells of dorsal SVZ, we labelled NSCs of dorsal SVZ by electroporating the pCAGGSx-CRE plasmid in P1 Ai14 Rosa26-CAG-tdTomato transgenic mice (see Fig. 35A and *2.1.5. section* for protocol). Plasmid electroporation induced the tdTOM expression by Cre recombination so we could trace the cell fate of NCS from the dorsal SVZ. After 3-4 months from the electroporation, we performed the MCAO and tdTOM fluorescence was analysed 7, 30 and 60 days after MCAO. To confirm that electroporation protocol worked properly and labelled NSCs, we followed the tdTOM fluorescence in the OB (Fig. 35B). Only those animals with a proper number of $tdTOM^+$ cells in the OB were took into account for later analysis. $tdTOM^+$ cells could be observed in the OB starting 3 weeks after electroporation (Platel et al. 2019). After quantification of $tdTOM^+$ NSCs 7, 30 and 60 days after MCAO, we observed a significant decrease of $tdTOM^+$ cells in the SVZ of

ischemic animals respect to sham animals (Fig. 35C-D). In addition, the decrease of tdTOM$^+$ NSCs was observed in all SVZ axis analysed, as shown in Fig. 35E.

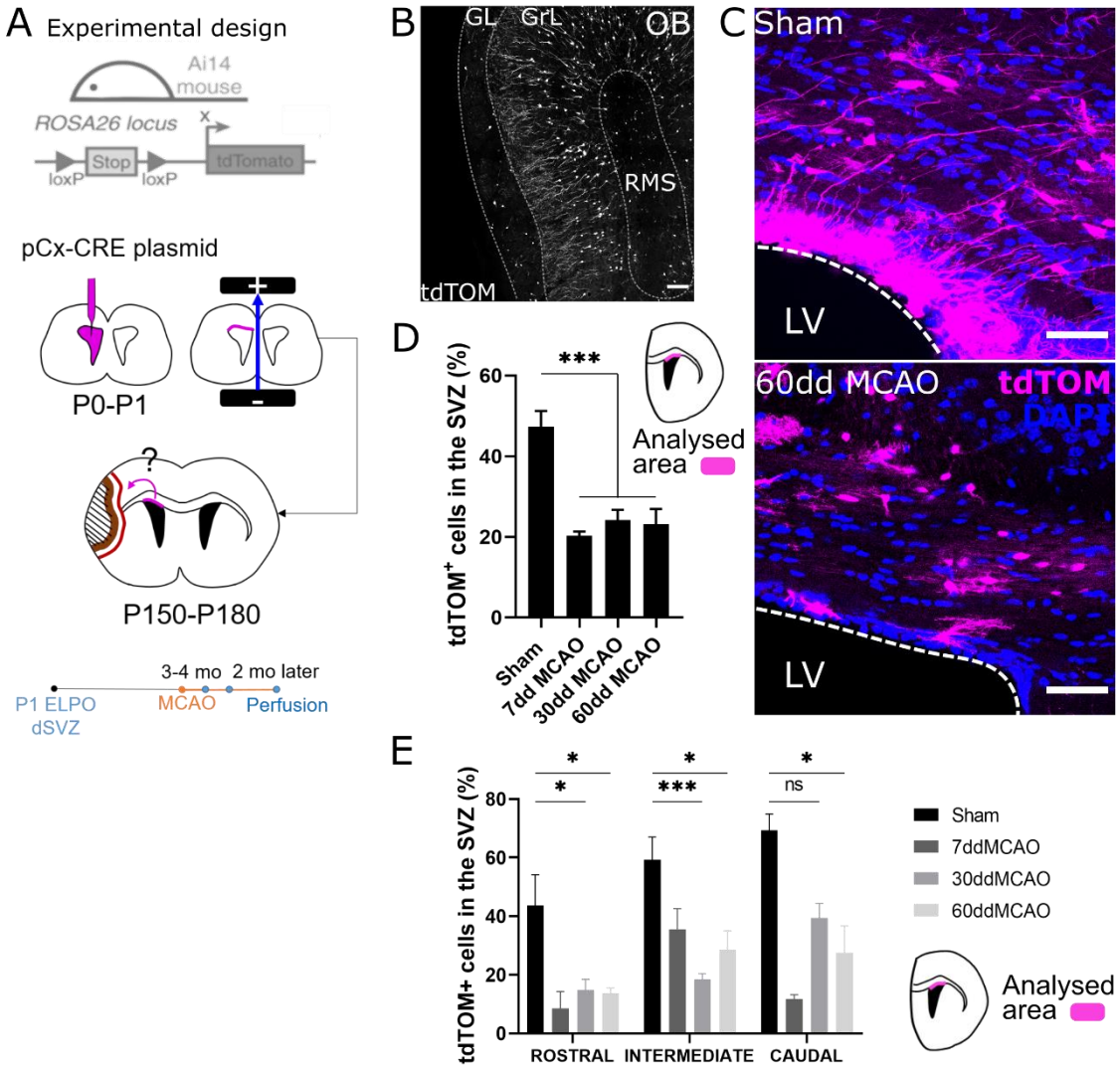

***Figure 35.* Characterization of pCAGGSx-CRE electroporation for SVZ NSC tracing.** Experimental design (A). P1 Ai14-ROSA26-tdTomato$^{fl/fl}$ mice were electroporated (ELPO) with a PCAGG-CRE plasmid. After 3-4 months (mo), MCAO was performed and animals were analysed 7, 30 and 60 days after the lesion. tdTOM fluorescence in the OB was used as a positive control for ELPO (B). The number of electroporated cells decreased in the SVZ after MCAO respect to sham mice (C-D) in all SVZ regions (E). RMS = Rostral Migratory Stream; GL = Glomerular Layer; GrL = Granular Layer; LV = Lateral Ventricle. Scale bar = 100 µm in B and 50 µm in D. *p<0.05, ***p<0.001.

After MCAO, together with the reduction of electroporated cells in the SVZ we observed a general increase of labelled cells outside the SVZ, especially in the Intermediate and Caudal axis of the whole brain respect to sham animals (Fig. 36A-B). This would suggest that brain ischemia induced a migration of dorsal SVZ cells. The

preferential way of migration is the corpus callosum through its intermediate/Caudal pathway (Fig. 36C). At deeper analysis we confirmed that labelled cells after MCAO migrated to the cortical and striatal ischemic area (Fig. 36D) with a greater significative increase in their Intermediate and Caudal axis (Fig. 36E). This experiment confirmed that brain ischemia activated the astrogliogenesis in the dorsal SVZ and their migration to the infarcted areas.

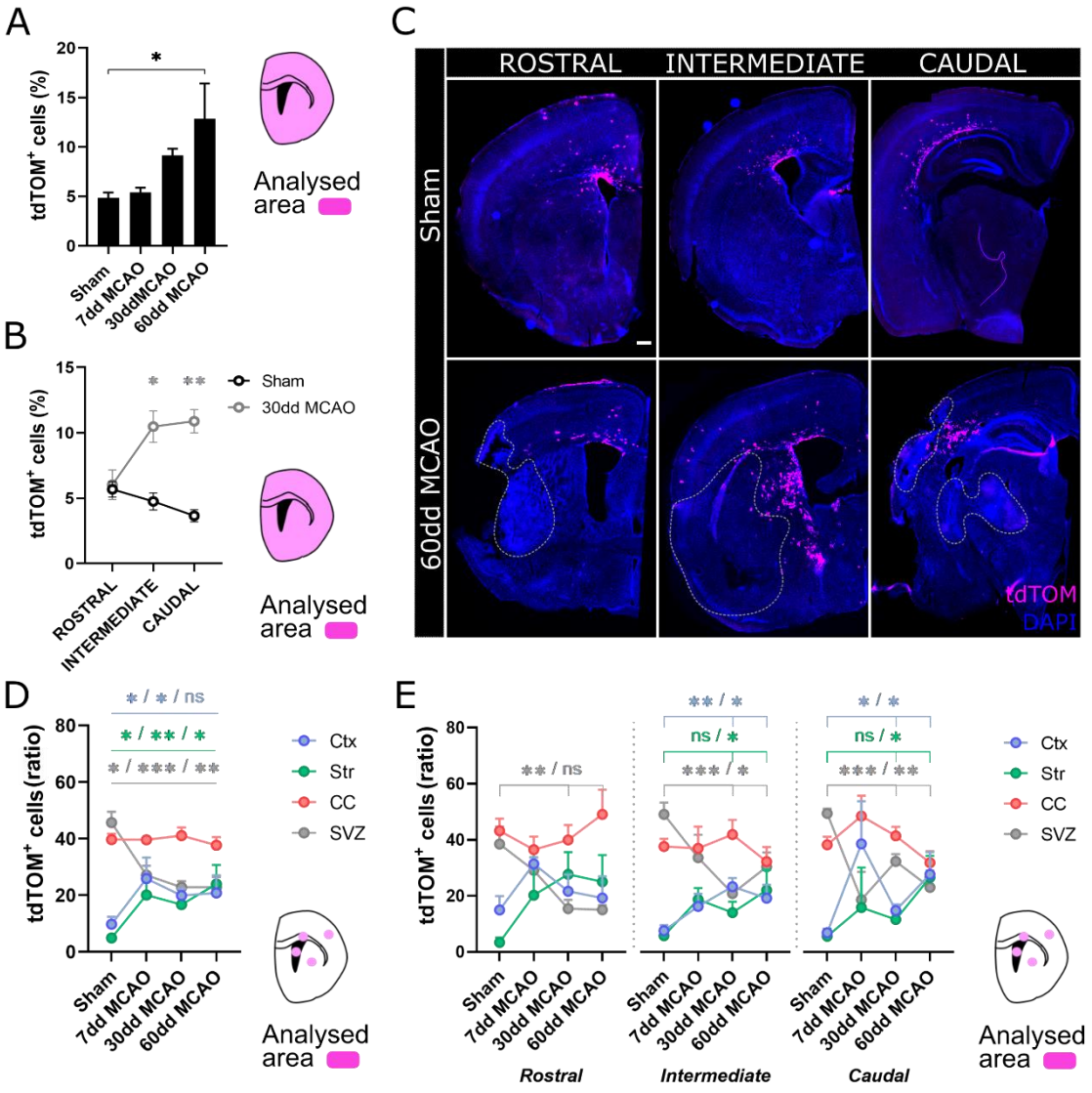

Figure 36. **Effect of MCAO on electroporated cells.** Quantification of tdTOM+ cells in the whole brain after MCAO (A) and in the Rostral, Intermediate and Caudal axis (B). Visualization of tdTOM+ cells in the rostral/caudate axis in sham animals and 60 days after MCAO (C). Quantification of the tdTOM+ cells in the cortex (Ctx), striatum (Str), corpus callosum (CC) and SVZ, 7, 30 and 60 days after MCAO and in sham animals (D) and divided into Rostral, Intermediate and Caudal axis (E). Scale bar = 1000 µm. *p<0.05, **p<0.01, ***p<0.001.

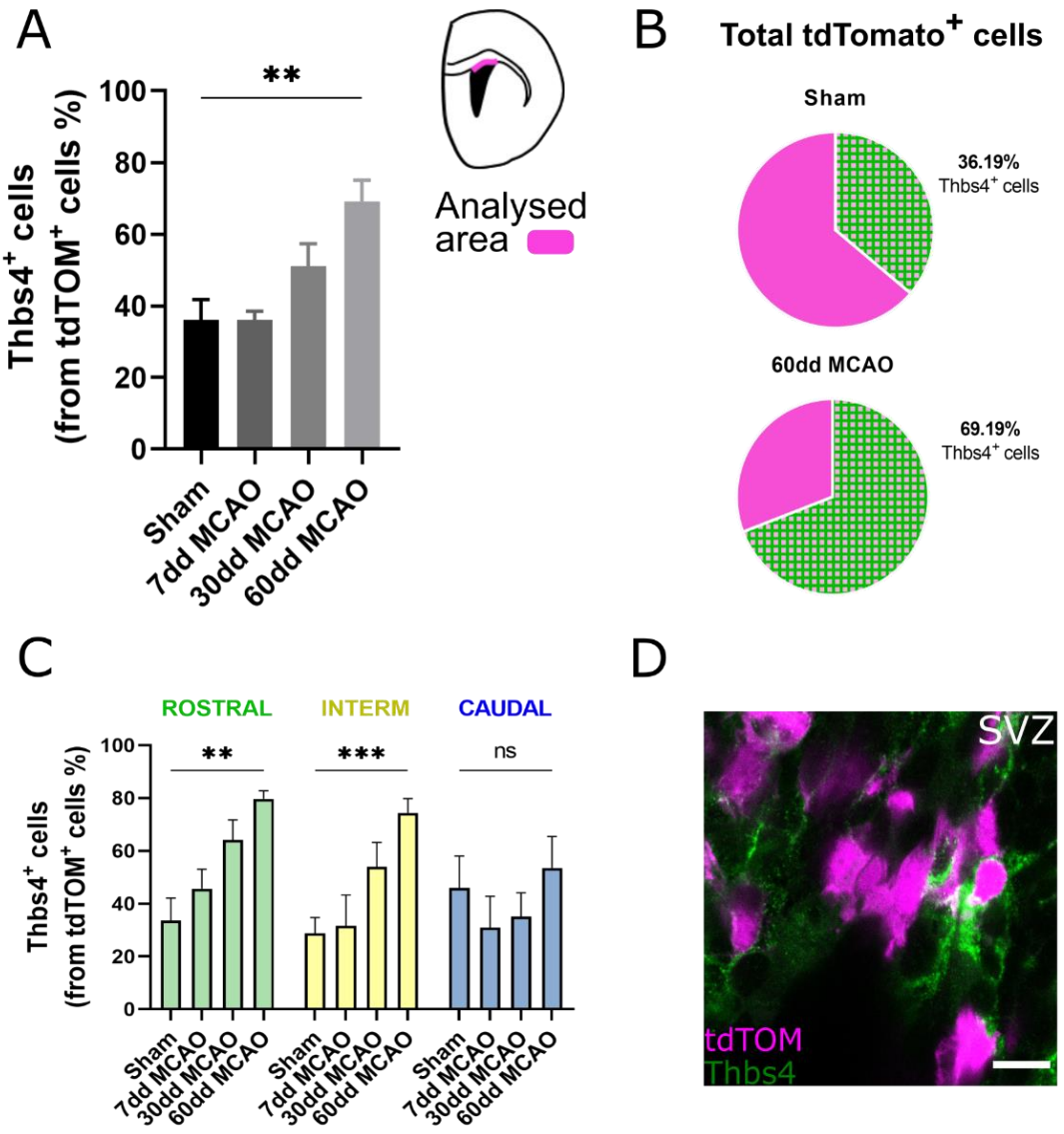

Figure 37. **Thbs4 localization in electroporated cells after MCAO in the dorsal SVZ.** TdTOM$^+$ cells co-expressing Thbs4 in the dorsal SVZ increased overtime after MCAO (A). Fraction and quantification of tdTOM$^+$ cells co-expressing Thbs4 (green) in sham and 60 days after MCAO animals (B). Thbs4/tdTOM$^+$ cells increased progressively in the rostral and intermediate SVZ after MCAO (C). Representative image of tdTOM$^+$ cells co-expressed Thbs4 in the SVZ (D). Scale bar = 10 µm. **p<0.01, ***p<0.001.

To identify the portion of NSCs that differentiated to Thbs4$^+$ astrocytes following ischemia we analysed the co-expression of Thbs4 with tdTOM after MCAO (Fig. 37A-D). Regardless the general decrease of tdTOM$^+$ cells in the SVZ, the Thbs4/tdTOM positive cells increased already 30 days after the brain ischemia respect to sham animals (Fig. 37A). In sham animals, we observed that 36% of tdTOM$^+$ cells expressed Thbs4, increasing to 69% sixty days after MCAO (Fig. 37B). The number of Thbs4/tdTOM$^+$ astrocytes in the SVZ increased especially in its rostral and intermediate axis (Fig. 37C),

suggesting that brain ischemia activated the generation of Thbs4 astrocytes especially in the dorso-rostral and dorso-intermediate SVZ.

Finally, after characterizing the ischemic response of Thbs4 astrocytes in the SVZ, we analysed the Thbs4$^+$ astrocytes recruitment to the ischemic regions. More than a half of total tdTOM$^+$ cells in the infarcted area expressed the Thbs4 marker 60 days after MCAO (Fig. 38A). However, not all Thbs4$^+$ astrocytes overlapped with tdTOM fluorescence (Fig. 38B-B´): we suppose because electroporation protocol only labelled part of the NSC in the SVZ. Even though, the analysis of Thbs4/tdTOM colocalization in the infarcted areas supported our hypothesis that ischemia activated the astrogliogenesis in the SVZ, from the type B cells and that Thbs4$^+$ astrocytes migrate to the ischemic areas.

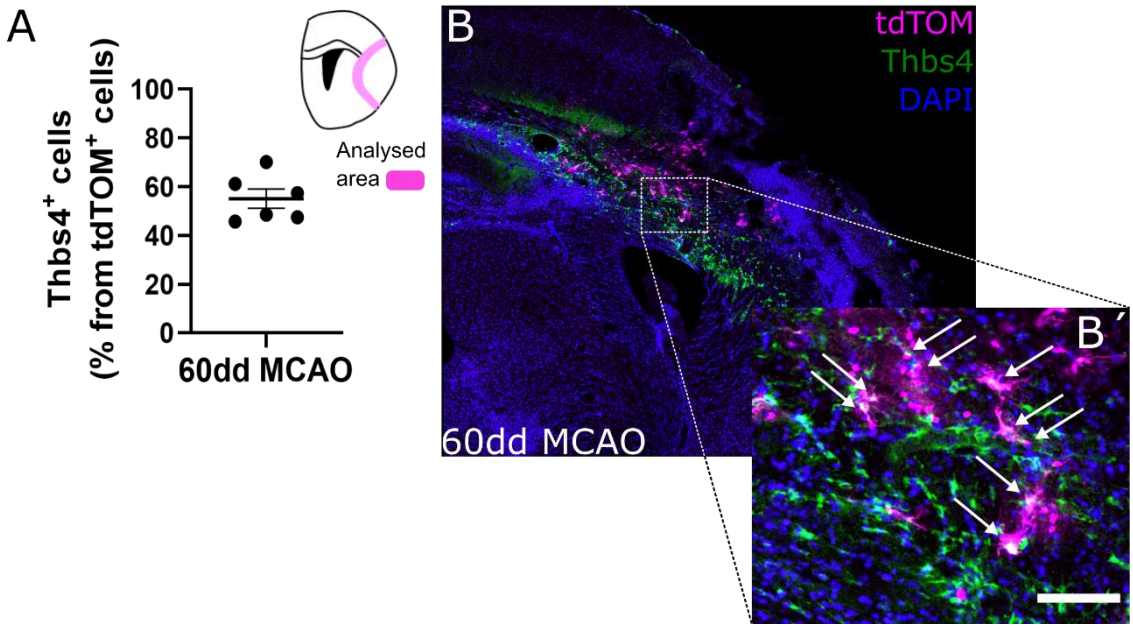

Figure 38. **Electroporated NSCs also expressing Thbs4 were found in the damaged areas 60 days after MCAO.** About a half of tdTOM$^+$ cells found in the infarcted areas 60 days after the lesion also expressed Thbs4 (A). Representative image of tdTOM and Thbs4 immunofluorescence and DAPI staining 60 days after MCAO (B). Magnification of previous image in the area between SVZ and the lesion (B´). Arrows point to double labelled cells. Scale bar = 100 µm.

ROLE OF Thbs4⁺ ASTROCYTES IN THE ISCHEMIC LESION

10. Ischemia-induced extracellular space disruption. Thbs4⁺ astrocytes modulate the hyaluronic acid production in the glial scar

To study the role of Thbs4 astrocytes in the glial scar, we analysed the hyaluronan (HA), the main compound of the ECM, and we used the hyaluronic binding protein (HABP) as a marker. It is described that when local astrocytes react to the ischemic damage, they do not only change their morphology to a fibrotic stage, but they also produce HA to form the glial scar and isolate the healthy from the damaged tissues (Preston & Sherman, 2011). Our hypothesis is that ischemia-induced Thbs4⁺ astrocytes derived from SVZ may play a role in modulating the HA formation in the glial scar.

First of all, we analysed how brain ischemia modulated the HA deposition in the corpus callosum and the infarcted areas. HA was visualized by immunofluorescence with HABP in sham animals and 7, 15 and 30 days after the MCAO (Fig. 39A). In order to analyse HA size, we performed the skeletonize analysis to measure the HABP spots size and structure (Fig. 39A1-2; see *3.2 section* for method). Fractal dimension, that measure the skeletonize analysis of HA structure, was disrupted in the infarcted areas overtime (Fig. 39B). Moreover, we did not observed any change in the proportions of HABP spots size in the corpus callosum at any time after MCAO model (Fig. 39C). Nevertheless, HABP spots were larger as more days pass after the MCAO in the damaged areas (Fig. 39D) suggesting the formation of anti-inflammatory HMW HA structures like glial scar tissue after the insult (Moshayedi & Carmichael, 2013). This data confirmed that MCAO induced an alteration in the HA of ECM.

Thirty days after the MCAO, we observed Thbs4⁺ astrocytes in the ischemic scar, in the proximity of the HABP (Fig. 40A-B). To further understand the role of Thbs4⁺ astrocyte in the glial scar formation and whether they produce or degrade the ECM, we developed an ImageJ script for HABP quantification in the cell membrane of Thbs4⁺ astrocytes (Fig. 40C-D). In fact, HA is produced only in the cell membrane of neurons during the embryonic development or astrocytes during the adulthood (Zimmermann & Dours-Zimmermann, 2008; Peters & Sherman, 2020). Although HABP area increased in the Thbs4⁺ astrocyte membrane in all analysed areas (corpus callosum, infarcted cortex and striatum) and all time points (7, 15, 30 and 60 days) after MCAO (Fig. 40E), HABP spots only increased significantly 60 days after MCAO (Fig. 40F). This result suggested Thbs4⁺ astrocytes were surrounded by HMW HA after MCAO until late stages of the disease where it was already fragmented.

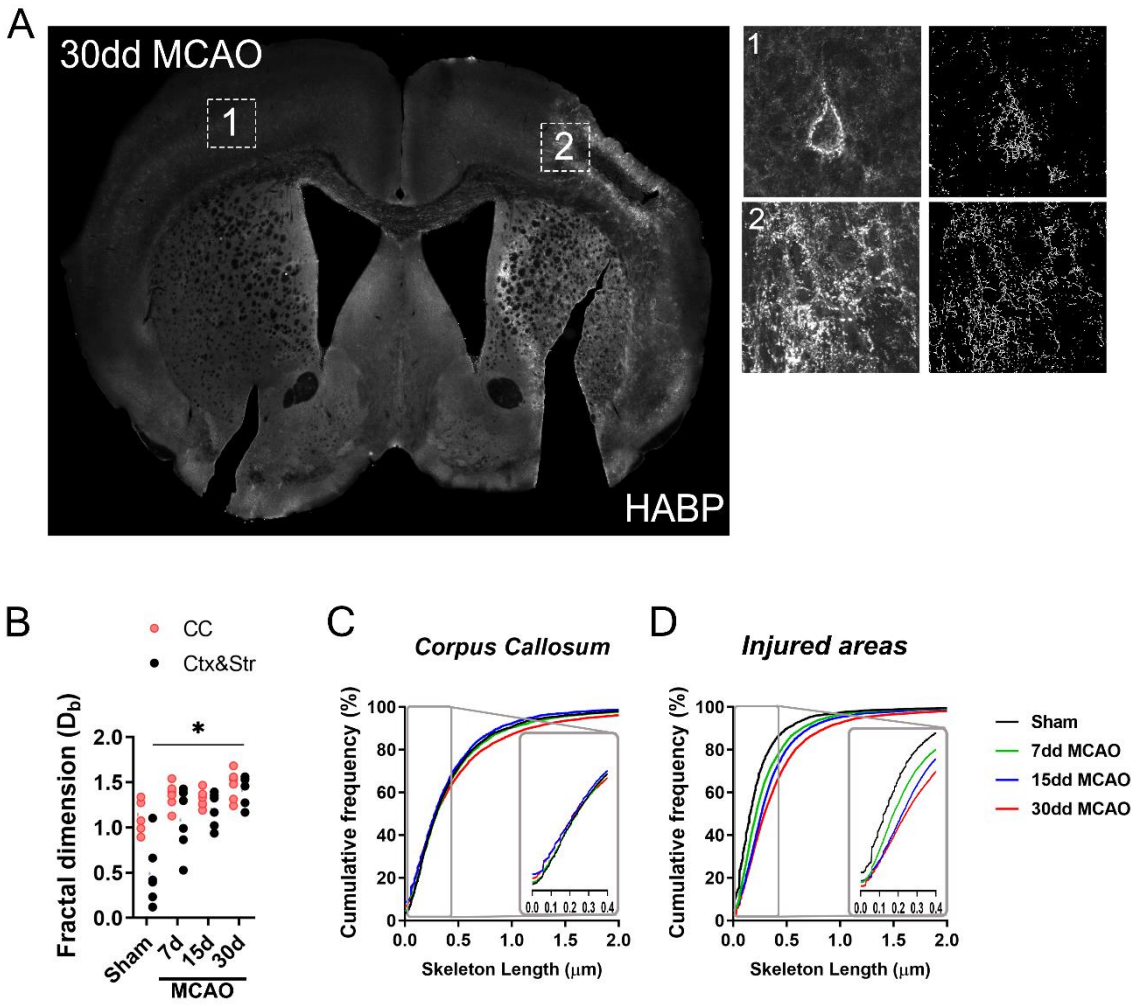

Figure 39. **Glial scar characterization by hyaluronan analysis after MCAO.** Visualization of Hyaluronic Acid Binding Protein (HABP) staining 30 days after MCAO (A). Representative skeletonized images used for HABP spots size analysis in the healthy tissue (1) and damaged area (2). Fractal dimension, a hyaluronan structure parameter, was disrupted after MCAO model overtime in all analysed areas (B). Cumulative frequency distribution of HABP spots size in the sham, 7, 15 and 30 days after MCAO mice in the corpus callosum (C) and damaged areas (D). *p<0.05; All time points in graph D were ****p<0.0001. No differences were observed in the corpus callosum.

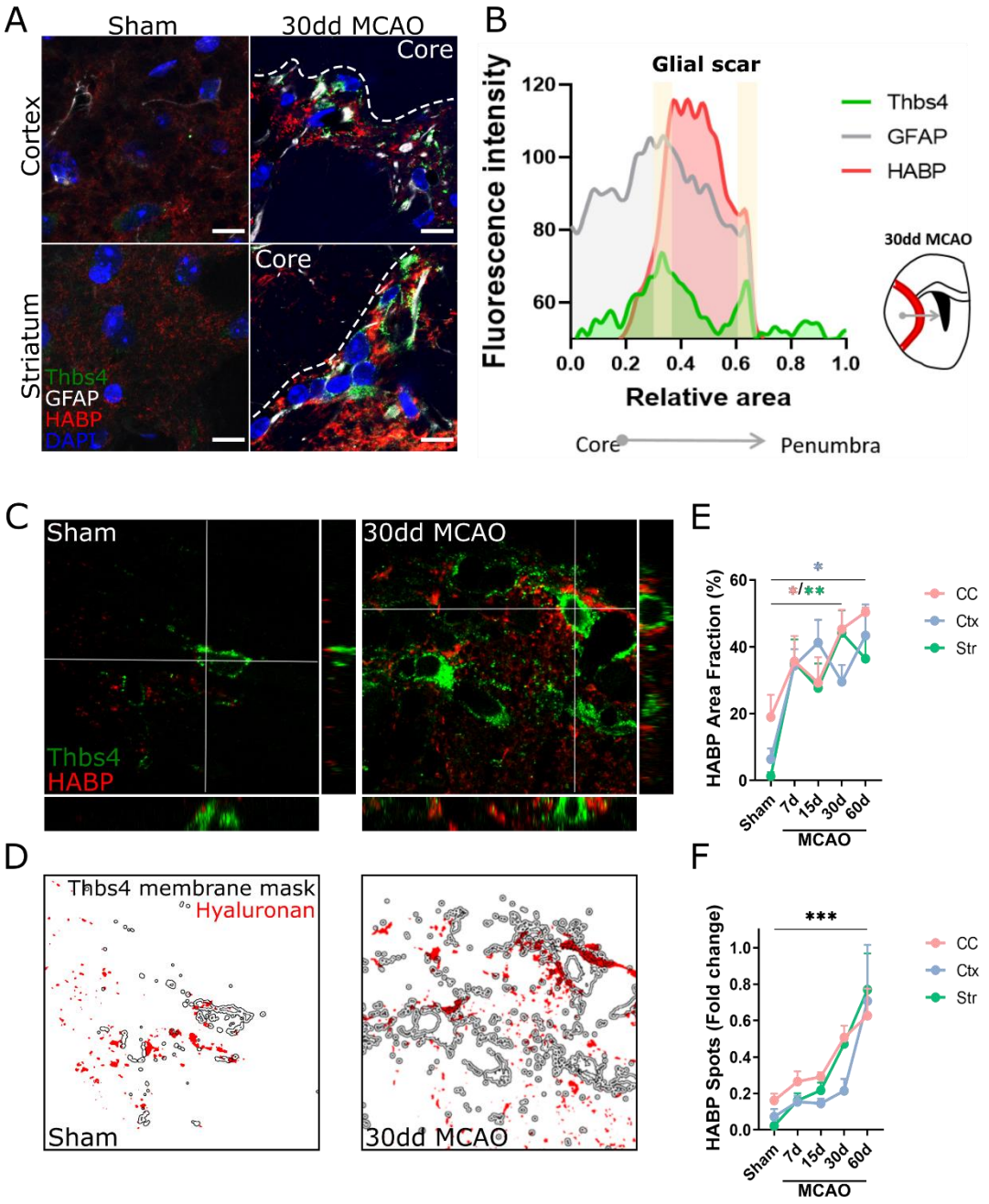

Figure 40. **HABP and Thbs4 immunofluorescence in the ischemic area.** Representative images of cortex and striatum from sham and ischemic mice (30dd after MCAO) labelled with Thbs4, GFAP, and HABP and counterstained with DAPI (A). Fluorescence lesion profile of HABP, GFAP and Thbs4 markers 30 days after MCAO (B). HABP profile mainly spans with Thbs4. Orthogonal representative images of Thbs4$^+$ cells and HABP co-localization in the sham mice and 30 days after MCAO (C). Binary mask of (C) images showing membrane ROI in black and hyaluronan in red in sham animals and 30 days after MCAO (D). HABP area fraction inside Thbs4$^+$ cell membrane increased dramatically in the corpus callosum and infarcted areas after MCAO (E). The number of HABP spots inside Thbs4$^+$ cell membrane increased progressively in all analysed areas after MCAO (F). Scale bar = 10 µm for all picttures. *p<0.05, **p<0.01, ***p<0.001.

11. Thbs4⁺ astrocytes internalize hyaluronic acid in the ischemic glial scar

To study if astrocytes can degrade HA, we analysed the intracellular HABP spots in Thbs4⁺ astrocytes. Although ECM remodeling is an extracellular process, HA can be internalized for later degradation, ECM recycling and remodeling (Zimmermann & Dours-Zimmermann, 2008; Peters & Sherman, 2020). Intracellular HABP spots were analysed in the Thbs4⁺ astrocytes and local astrocytes labelled only with GFAP marker (Fig. 41A). Thirty days after MCAO, Thbs4⁺ astrocytes showed more area filled by intracellular HABP compared with local astrocytes in the infarcted cortex (Fig. 41B). However, HABP spots number was higher in the local astrocytes of infarcted cortex (Fig. 41C) suggesting Thbs4⁺ astrocytes were able to internalize HMW HA. HABP area did not present any change between both populations in the infarcted striatum 30 days after MCAO (Fig. 41D), although HABP spots were higher in the local astrocytes compared with the Thbs4⁺ astrocytes (Fig. 41E), suggesting Thbs4⁺ astrocytes internalized larger hyaluronan fragments in the infarcted areas.

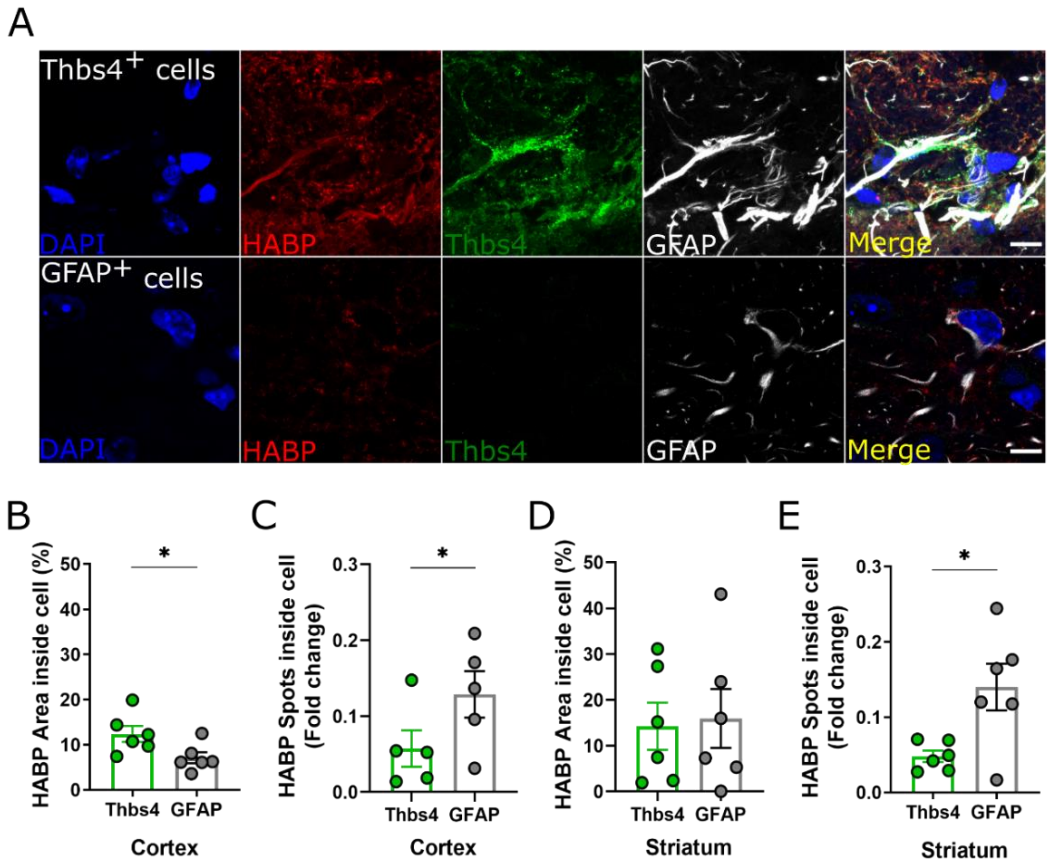

Figure 41. **HABP quantification inside Thbs4⁺ astrocytes and GFAP⁺ local astrocytes after MCAO.** Representative images of HABP spots inside Thbs4⁺ cells and GFAP⁺ local astrocytes (A). Quantification of HABP area (B) and HABP spots (C) inside Thbs4⁺ astrocytes and GFAP⁺ local astrocytes in the infarcted

cortex 30 days after the lesion. Quantification of HABP area (D) and HABP spots (E) inside Thbs4$^+$ astrocytes and GFAP$^+$ local astrocytes in the infarcted striatum 30 days after the lesion. Scale bar = 50 µm. *p<0.05 vs GFAP paired Student´s t-test.

To assess that astrocytes were degrading HA we performed an immunofluorescence analysis of CD44 (Fig. 42A). CD44 is a transmembrane glycoprotein receptor whose main function is the HA degradation and ECM remodeling (Dzwonek & Wilczynsk, 2015). We showed that Thbs4$^+$ astrocytes highly expressed CD44 receptor and their colocalization was around 80% of the total Thbs4$^+$ astrocytes in the corpus callosum 30 days after MCAO model (Fig. 42B). Despite CD44 spots inside the Thbs4$^+$ astrocytes differed depending on analysed area (corpus callosum, infarcted cortex and infarcted striatum, Fig. 42C), global CD44 spots were around 40% in the infarcted areas 30 days after the lesion (Fig. 42D). These results suggest Thbs4$^+$ astrocytes express the potential machinery to both produce and degrade the HMW HA.

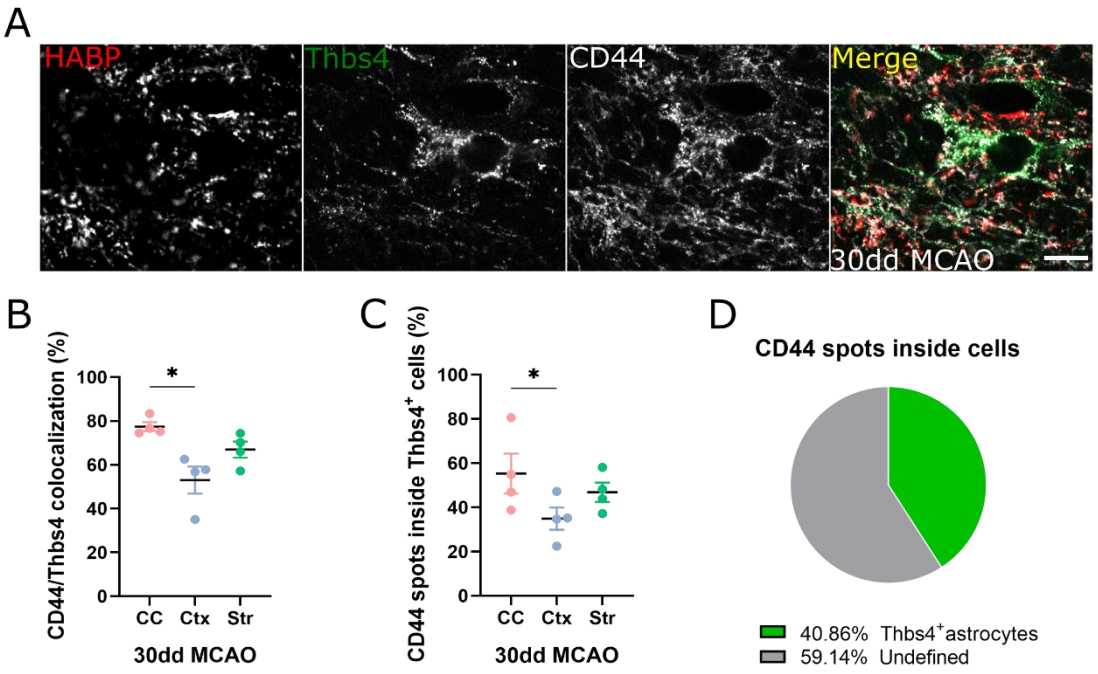

Figure 42. **Thbs4$^+$ astrocytes expressed the hyaluronan receptor CD44.** Representative image of HABP, Thbs4 and CD44 immunofluorescence in ischemic brain, 30 days after MCAO (A). Quantification of CD44/Thbs4 colocalization in the corpus callosum (CC, pink), infarcted cortex (Ctx, blue) and striatum (Str, green) 30 days after MCAO (B). Quantification of CD44 spots inside Thbs4$^+$ astrocytes in the ischemic areas 30 days after MCAO (C). Fraction of CD44 spots inside Thbs4$^+$ astrocytes in injury (D). Scale bar = 10 µm. *p<0.05.

12. In vitro Thbs4⁺ astrocytes internalized more hyaluronan spots after OGD protocol

In order to validate the results obtained *in vivo* after MCAO, we performed an *in vitro* assay for HABP uptake into Thbs4⁺ astrocytes. NSC from neurosphere cultures were seeded in 100% HA (1mg/ml) or 50% HA in Poly-L-Ornithine pretreated plates; 100% Poly-L-Ornithine were used as a control. After 7 days *in vitro*, Thbs4⁺ astrocytes cultured in 100% HA showed the most evident HABP spot modulation after HABP immunofluorescence (Fig. 43A-B).

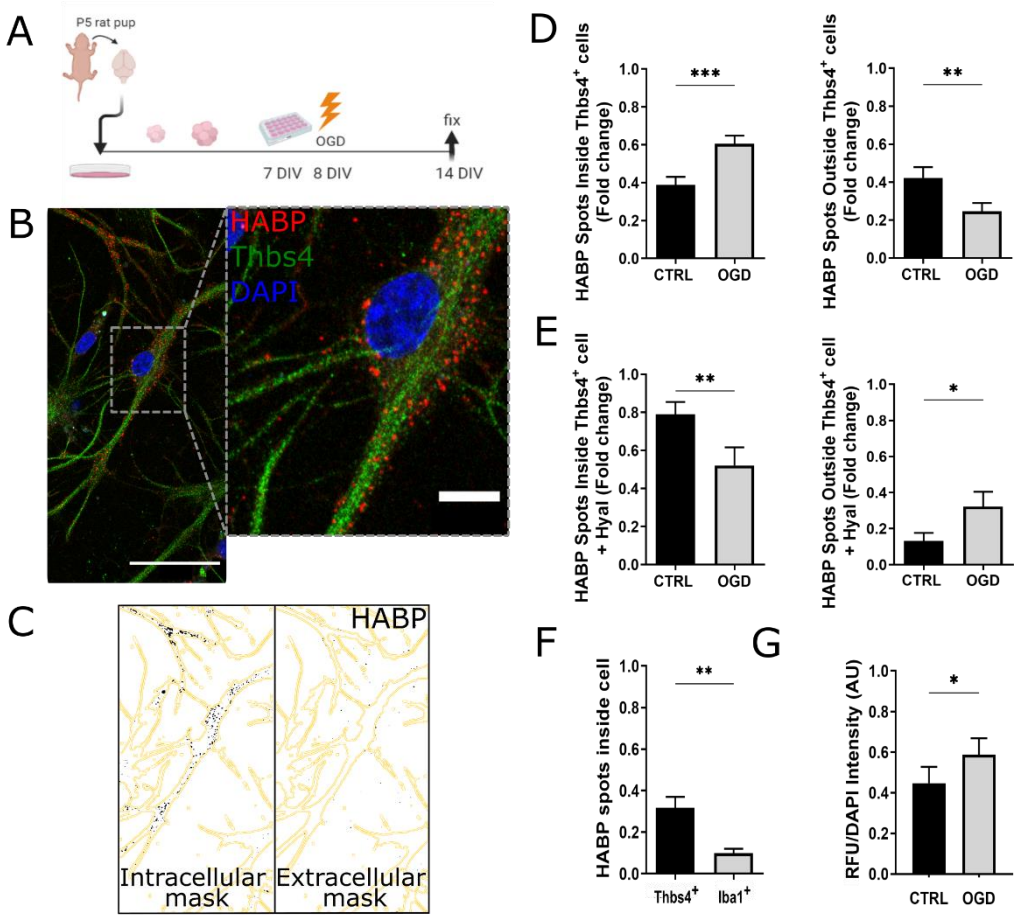

***Figure 43. In vitro* validation of HA internalization after OGD.** Experimental design (A). Representative immunofluorescence of HABP spots (red) co-localizing with Thbs4 (green) (B). Cell mask in yellow used to analyse the intracellular and extracellular HABP spots (C). Quantification of HABP spots inside and outside the Thbs4⁺ astrocytes, before (CTRL) and after OGD (D). Quantification after Hyaluronidases exposure (E). Intracellular HABP spots in co-culture experiments were quantified in Thbs4⁺ astrocytes and microglia (Iba1) as a control condition (F). MMPases activity (RFU/DAPI intensity) in Thbs4⁺ astrocytes increase after OGD (G). Scale bar = 50 µm and 10 µm (B and zoom respectively). RFU = Relative Fluorescence Units. *p<0.05, **p<0.01, ***p<0.001.

HABP spots were analysed by ImageJ scripts inside and outside Thbs4^{+} cells, before and after OGD (Fig. 43C). OGD induced a greater internalization of HA into the Thbs4^{+} astrocytes compared with the control condition (Fig. 43D). As a control, we performed another experiment where we used hyaluronidases to digest the extracellular HA. Thbs4^{+} astrocytes exposed to OGD condition were able to revert the HABP internalization (Fig. 43E), suggesting a Thbs4^{+} astrocytes-hyaluronan interplay based on external stimulus.

To rate the HA internalization in Thbs4^{+} astrocytes, we compared the HABP spots in astrocytes with the spots in microglia in a co-culture system. Surprisingly, we observed a major efficacy of astrocytic internalization respect to the microglial phagocytosis (Fig. 43F). Finally, to confirm the ability of Thbs4^{+} astrocytes in digesting HA, we assayed the Metalloproteinases (MMPases) activity after OGD (Fig. 43G). All these data suggest Thbs4^{+} astrocytes can internalize and degrade HA in response to OGD.

13. Matrisome analysis in the SVZ after MCAO model

The *matrisome* is defined as the set of transcripts that contribute to form the ECM. To analyse the transcripts that contribute the most to the generation of ECM we analysed the matrisome induction after MCAO. We studied the mRNA transcripts from fresh SVZ tissue of sham and 15 and 30 days after MCAO (Fig. 44A). MCAO modulated especially the hyaluronidase (Hyal1-3) and hyaluronan synthase Has1-2 transcripts (Fig. 44B). As a control of the ischemic insult we confirmed an increment of Thbs4 and hypoxia inducible factor 1a (Hif1a) transcript. Interestingly, the Hyal1-3, that are involved in the matrix degradation, were more upregulated 15 days after the MCAO whereas the Has 1-2 were more upregulated 30 days after the insult (Fig. 44B), suggesting that SVZ activation may modulate the extracellular stiffness. Further analysis of gene modulation by hierarchical distance matrix (Fig. 44C) also suggested that Thbs4 transcription is closer to the hyaluronidases than to the synthases. These data confirm that HA degradation is a favorable event for SVZ activation following brain ischemia.

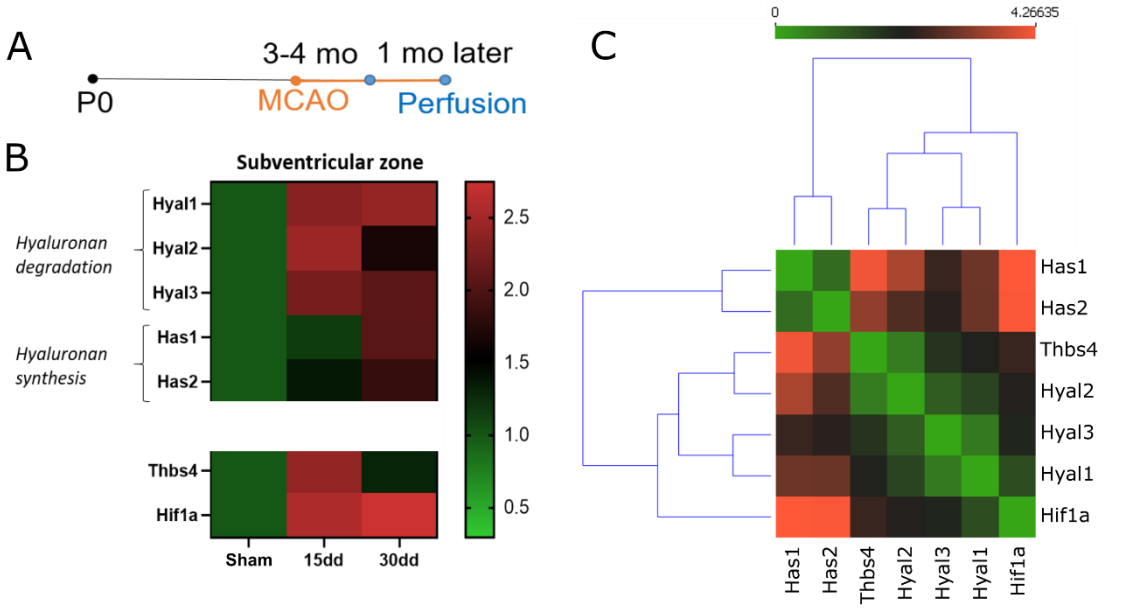

Figure 44. **Matrisome analysis of the SVZ after MCAO by qRT-PCR.** Fresh SVZ tissue was extracted from sham mice and 15 and 30 days after MCAO as depicted in (A). Hyaluronidase 1-3 (Hyal1, Hyal 2 and Hyal3) and Hyaluronan synthase 1-2 (Has1 and Has2) transcripts were the most modulated after MCAO. Thbs4 and hypoxia inducible factor 1a (Hif1a) were used as controls for the brain ischemia (B). Hierarchical matrix distance analysis and genes distances (C). All genes showed significative differences (*p<0.05) after MCAO.

14. Hyaluronan accumulation was sufficient but not exclusive for Thbs4$^+$ astrocytes recruitment in damaged areas

Finally, to confirm that the HA of ischemic scar may represent a signal for the Thbs4$^+$ astrocyte migration, we simulated the ischemic scar by overexpressing the HAS2 after AAV2/9-CAG-HAS2-Flag infection in the striatum. HAS2 is poorly expressed in the brain in physiological conditions because its main function is the production of HMW HA (Kwok et al. 2011). First at all, we optimized the AVV protocol in order to know the proper concentration to induce HAS2 overexpression. Two microliters of AAV2/9-CAG-HAS2-Flag injected in the striatum (AP: +1.8; ML: -1.0; DV: -3.2) avoided the local neuroinflammation and it was sufficient to induce HAS2 overexpression (Fig. 45A) and HA accumulation in the injected site. Most of the infected cells were neurons that produced HA perineuronal nets whereas only few Thbs4$^+$ astrocytes were infected by AAV2/9-CAG-HAS2-Flag. (Fig. 45B-C).

HAS2 overexpression and subsequently HMW HA production is an experimental reproduction of the scar formed after brain ischemia (Fig. 46A-G). This experimental approach was sufficient to recruit the Thbs4$^+$ astrocytes from the ipsilateral SVZ 45 days

after the injection of 1 µl of AAV2/9-CAG-HAS2-Flag (Fig. 46A, C, F), with a time frame similar to the ischemic model. Nevertheless, when we produced the ischemic lesion by MCAO together with the viral overexpression of HA in the contralateral hemisphere, we observed that Thbs4^{+} astrocytes preferentially migrated from the SVZ to the glial scar generated by the MCAO (Fig. 46D-G).

These results suggested that accumulation of HMW HA *per se* is sufficient to activate and recruit the Thbs4^{+} astrocytes from the SVZ to the damaged areas. However, we hypothesize that there are more biochemical signals that contribute to the activation of the SVZ gliogenesis and the recruitment of the newborn astrocytes to the damaged areas.

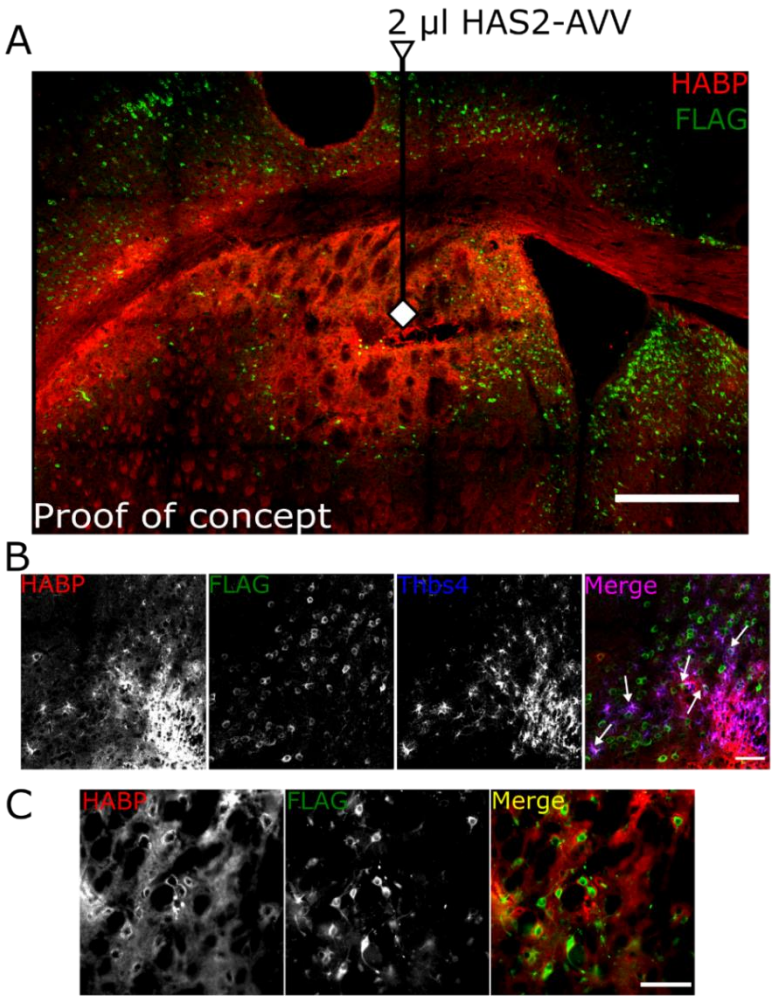

Figure 45. **Simulation of a glial scar by AAV2/9-CAG-HAS2-Flag infection: proof of concept.** The infection with AAV2/9-CAG-HAS2-Flag generated a scar with hyaluronan deposition similar to that observed after MCAO. Representative image of HAS2-AVV injection in the striatum (AP: +1.8; ML: -1.0; DV: -3.2) and HABP expression after 45 days (A). Thbs4^{+} astrocytes reacted to the HA accumulation due to HA synthase (HAS2) overexpression (B). Infected cells were mainly neurons which produced HA to create perineuronal nets (C). HABP in red to visualize hyaluronic acid; Thbs4 in blue and FLAG in green as HAS2-AVV tag. Scale bar = 500 µm in A and 100 µm in B, C.

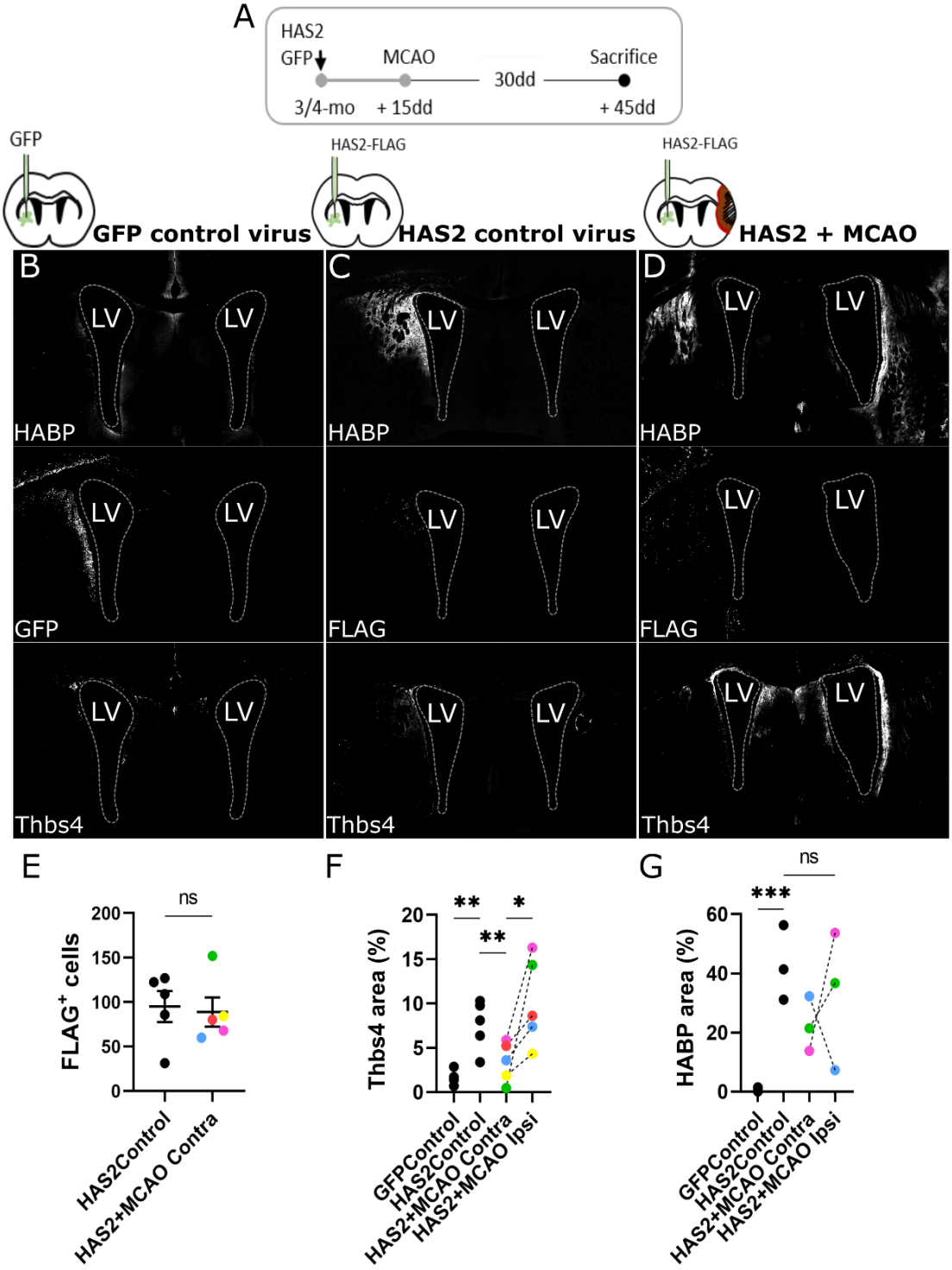

Figure 46. **HA accumulation is necessary but not sufficient fot Thbs4⁺ astrocytes activation.** Experimental design: AAV2/9-CAG-HAS2-Flag was injected in 3-4-month old mice, MCAO performed after 15 days and mice sacrificed 30 days after the surgery (A). Three groups of mice were used: mice infected with mocked virus (GFP), AAV2/9-CAG-HAS2-Flag (HAS2 control virus) and AAV2/9-CAG-HAS2-Flag + MCAO (HAS2 + MCAO). Representative images from GFP (B), HAS2 control virus (C) and HAS2 + MCAO (D) groups. FLAG was measured in the HAS2 groups in order to rule out external issues (E). Thbs4 expression increased only in response to the HAS2 overexpression (F). However, Thbs4 was even higher in the case of HAS2 + MCAO than HAS2 control virus (F). HABP area was increased in both HAS2 groups (HAS2 control virus and HAS2+MCAO) but not in the GFP (G). *p<0.05, **p<0.01, ***p<0.001.

DISCUSSION

1. NSC proliferate and differentiate mainly into astrocytes following the ischemic stroke

Our results showed that the **adult neurogenic niche at the SVZ responded early after the ischemic stroke by proliferating and differentiating into astrocytes**. SVZ stem cells proliferate fast as a response to the ischemic stroke as revealed by immunofluorescence to BrdU, Ki67 and cleaved-Caspase 3 markers only 24 hours after the injury. Unlike previous results from other groups, showing that NSC responded and contributed to the brain protective responses lately after the insult (Zhang et al., 2001; Arvidsson et al., 2002; Parent et al., 2002), **our results evidenced the faster response of the SVZ NSC to the brain ischemia**, supporting the data from others (Jin et al., 2003; Zhang et al., 2004; Saha et al., 2013). The early proliferative response of the SVZ to the brain ischemia allowed a faster glial recruitment also in the infarcted areas.

Using *in vitro* and *in vivo* approaches and by immunofluorescence, western blot and FACS techniques we observed that **brain ischemia mainly activated astrogliogenesis from the SVZ**. Analysis by immunofluorescence revealed an evident decrease of progenitor cells (Nestin) and neuroblasts (DCX) but increase of astrocytes (Thbs4/GFAP) between 7 and 15 days after the lesion. Our data showed that NSC in the SVZ started to produce astrocytes in detriment to immature neurons after brain ischemia. We demonstrated that after 15 days, brain ischemia re-routed the cell migration from the physiological SVZ-RMS-OB path to the pathological cortex and striatum affected. In contrast with our results, the majority of researchers who study this event have shown that NSC produced DCX^+ neuroblasts after the ischemic injury (Jin et al., 2001; Zhang et al., 2001; Arvidsson et al., 2002; Yamashita et al., 2006; Thored et al., 2007; Saha et al., 2013; Palma-Tortosa et al., 2017; Liang et al., 2019; Santopolo et al., 2020). However, most of these papers analysed NSC differentiation at later time points after the ischemic insult. Our findings regarding ischemic-induced new generated astrocytes from NSC in the SVZ were analysed at shorter time points after the insult so that they can be complemented with the previous observations at later stages. Moreover, even some papers showed that NSC differentiate also into astrocytes, the main focus of these papers is on the new neuroblasts production following the ischemic stroke (Yamashita et al., 2006; Carlen et al., 2009). Of course, the principal interest of cell restoring after brain ischemia is focused in the neurogenesis and its ability to repopulate the penumbra tissue. Likewise, those publications which focused in the neuronal production have shown that these immature neurons integrate in the pre-established neuronal network and develop functional activity. However, few of these neuroblasts survive at longer

stages of the disease and functional recovery induced by the SVZ neurogenesis is limited (Arvidsson et al., 2002; Yamashita et al., 2006).

Astrogliogenesis after brain ischemia is also demonstrated by other groups (Li et al., 2010; Young et al., 2012; Benner et al., 2013; Faiz et al., 2015; Laug et al., 2019). Nevertheless, among publications discrepancy exit about how astrogliogenesis is characterized and quantified. Some authors only used GFAP or Nestin markers to identify new generated astrocytes in SVZ but NSC can also express these markers (Young et al., 2012; Laung et al., 2019). The gold techniques to assess if NSC from SVZ produce astrocytes instead of new-born neurons are cell tracing techniques that take advantages of transgenic mice or viral infection of the NSC to exclude parenchymal astrocytes contribution (Yamashita et al., 2006; Li et al., 2010; Faiz et al., 2015). Some papers also used Thbs4 marker to label new generated astrocytes from the SVZ (Benner et al., 2013; Laug et al., 2019; Pous et al., 2020). In our work we combined two of the methodologies used to characterize the astrogliogenesis from the SVZ: the Thbs4 labelling and cell tracer by *in vivo* electroporation.

Our results showed that Thbs4 is an accurate marker for the identification of new astrocytes generated from the SVZ. Under physiological conditions, Thbs4 is expressed by a specific NSC population in the SVZ as demonstrated by other authors using immunofluorescence and RNA-seq techniques (Codega et al., 2014; Llorens-Bobadilla et al., 2015; Zywitza et al., 2018; Basak et al., 2018; Mizrak et al., 2019; Zamboni et al., 2020; Cebrían-Silla et al., 2021). Codega et al. (2014) and Llorens-Bobadilla et al. (2015) both demonstrated that Thbs4 is mainly expressed by cells derived from NSC and at very lower extent, by other parenchymal cell populations. Expression of Thbs4 in the neurogenic niche was also documented in NSC pre-programmed for responsing to injury (Basak et al., 2018; Mizrak et al.,2019) and quiescent NSC located in dorsal and caudal SVZ regions (Cebrían-Silla et al., 2021). These data in accordance with our results suggest SVZ harbour a specific NSC population expressing the Thbs4 marker.

The use of Thbs4 marker has become useful for measuring the SVZ astrogliogenesis after pathological conditions such as ischemic stroke or TBI (Benner et al., 2013; Laug et al., 2019; Zhao et al., 2020; Pous et al., 2020). Benner et al. (2013) showed that Thbs4 expression is restricted to the new pool of astrocytes generated from NSC in the SVZ following brain ischemia and increase of Thbs4 marker in the SVZ is mediated by Notch signalling like reported by Laung et al. (2019). Notch signalling is known for its role in the maintenance of the quiescence state of NSC and its suppression

drive the differentiation of the NSC into neurons (Gaiano & Fishell, 2002). Data suggest an involvement of Notch signalling in our ischemic model.

Finally, in contrast with previous studies where authors have shown that Thbs4 expression is restricted to the SVZ extracellular space (Beckervordersandforth et al., 2010; Kjell et al., 2020) or to RMS (Girard et al., 2014), our results suggest Thbs4 glycoprotein is expressed by specific NSC pool and in the extracellular space or in the RMS as described previously (Codega et al., 2014; Llorens-Bobadilla et al., 2015; Zywitza et al., 2018; Basak et al., 2018; Mizrak et al., 2019; Zamboni et al., 2020; Cebrían-Silla et al., 2021).

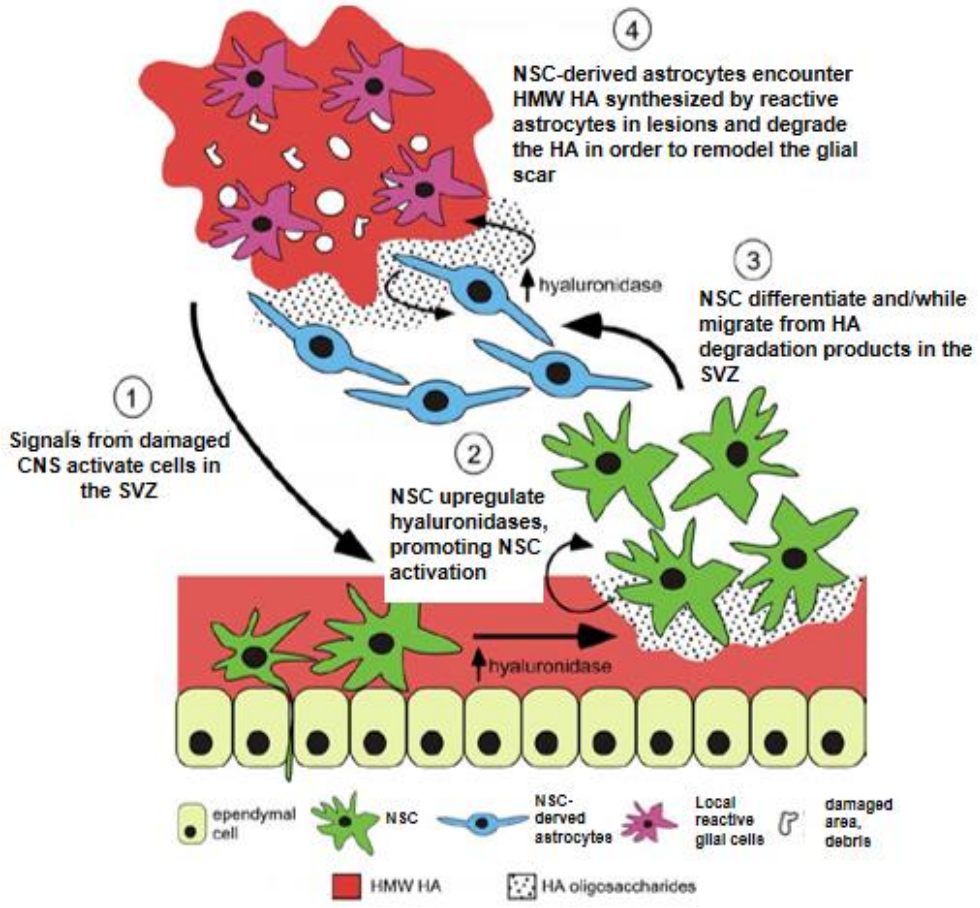

Figure 47. **HA digestion is needed for NSC activation following brain injury.** NSC response is modulated by external and internal factors from SVZ until damage area. Modified from Preston & Sherman (2011).

Specific Thbs4 positive NSC population covers a relevant role in the extracellular space of the SVZ. SVZ harbour a special ECM niche because the hyaluronan is absent inside the NSC layer but it is overexpressed in the lining and limiting the SVZ from the

striatum. As described in detail in the *Introduction section*, the particular SVZ environment conserves NSC population and avoids the exhaustion of the niche (Peters & Sherman, 2011; Khaing & Seidlits, 2015; Kjell et al., 2020). Our results using immunofluorescence staining for hyaluronan and Thbs4 glycoprotein showed a close interplay between both elements. HABP is reduced in the dorsal SVZ following the ischemic stroke. Skeletonize analysis showed hyaluronan degradation 7 days after the ischemic stroke in the dorsal SVZ but not in other SVZ domains. In addition, matrisome gene analysis revealed an increase of hyaluronidases in the SVZ after the ischemic stroke. The degradation of hyaluronan in the dorsal SVZ coincides with the activation and production of Thbs4 positive astrocytes between 7 and 15 days following the ischemic stroke. Taking all these data together, our results suggest that hyaluronan degradation is needed to allow dorsal NSC activation in the SVZ and the production of Thbs4^{+} astrocytes after the stroke model as proposed previously (Fig. 47; Peters & Sherman, 2011; Kjell et al., 2020).

Altogether, Thbs4 is postulated as a potential and accurate marker for identifying new generated astrocytes from SVZ. All these findings suggest Thbs4 is expressed by a specific quiescent NSC population that is programmed for responding to injury.

2. Ischemia-induced Thbs4^{+} astrocytes derive from specific NSC population of the SVZ

Once we had demonstrated that brain ischemia activated NSC in the SVZ to generate new astrocytes, we studied in detail the cell and regional origin of the Thbs4^{+} astrocytes. We demonstrated that Thbs4^{+} astrocytes derived from specific progenitor cells along rostro-caudal and dorso-ventral axis that migrated in response to brain ischemia. By using BrdU chronic treatment to identify quiescent NSC (Codega et al., 2014) we observed that almost 40% of the BrdU^{+} quiescent NSC express the Thbs4 glycoprotein 30 days after ischemia. Moreover, in accordance with Cebrián-Silla et al. (2021), our result showed that Thbs4/BrdU double positive cells were more present in the dorsal SVZ and predominantly enriched in quiescent NSC pool. Activation of the Thbs4 quiescent NSC pool was also corroborated by immunofluorescence for EGFR, a marker for active NSC (Doetsch et al., 2002). Indeed, Thbs4 expression was induced in a NSC population that did not express EGFR marker between 7 and 15 days after the ischemia. Whether Thbs4 are generated *de novo* from quiescent NSC (Codega et al., 2014; Llorens-Bobadilla et al., 2015; Zywitza et al., 2018; Zamboni et al., 2020; Cebrían-Silla et al., 2021) or come from a primed NSC population (Basak et a., 2018; Mizrak et al., 2019) is still unknown but what seem to be clear is that Thbs4^{+} astrocytes represent

a direct progeny of the quiescent NSC. Other indirect evidence of our findings are that brain ischemia induced a deprivation of neuroblasts in the periglomerular layer of OB that is normally furnished by the NSC population coming from the dorsal SVZ (Young et al., 2007; López-Juárez et al., 2013; Fiorelli et al., 2015; Chaker, Codega & Doetsch, 2016). Taking all together, these data support the evidence that ischemic-induced Thbs4^{+} astrocytes are produced by dorsal quiescent NSC populations being a potential target for preclinical therapeutic strategies.

Even if in slight contradiction with other studies that did not show the presence of NSC in dorso-caudal regions of the SVZ (Doetsch, García-Verdugo & Álvarez-Buylla, 1997; Mirzadeh et al., 2008; Fiorelli et al., 2015), we coincide with others (Bordiuk et al., 2014, Cebrían-Silla et al., 2021) showing striking evidence of Thbs4^{+} NSC in this region. One explanation may derive from the natural migration of these populations from the dentate gyrus of the hippocampus, lining the lateral ventricles (Bordiuk et al., 2014).

The presence of a NSC population expressing the astroglial marker Thbs4, lead us to investigate if this population may be activated by brain ischemia to differentiate into astrocytes. Labelling and tracing the dorsal SVZ NSC by postnatal electroporation, we were able to demonstrate that brain ischemia induced differentiation of this dorsal SVZ population into astrocytes that later migrated to the ischemic damage. Using this strategy we could unmask an underrepresented mechanism of the gliogenesis from the SVZ showing not only oligodendrocytes but also astrocyte differentiation (Menn et al., 2006; Ge et al.; 2012; Sohn et al., 2015). Our results suggested that more than a cell population can be represented in the SVZ and activated following brain ischemia. Presence and characterization of a reactive cell population responding to the ischemia will be of great interest to direct pharmacological treatment to a specific SVZ cell population.

3. *New-generated Thbs4^{+} astrocytes migrate from SVZ to the infarcted areas*

After characterizing the cell and regional origin of SVZ astrocytes we investigated if ischemic tissues can recruit newly differentiated astrocytes. We developed two experimental paradigms to study migration of these astrocytes toward the injured area. As a first attempt we labelled the SVZ NSC by chronic treatment with BrdU (see *2.1.3. section* for protocol) and analysed the brain tissues after 30 days washing. We also co-labelled the proliferating cells with IdU allowing the labelling of type C cells. Using this protocol we observed an increase in the number of BrdU positive cells in the infarcted areas suggesting the migration of NSC-derived cells from SVZ toward the injury. Almost 40% of these BrdU^{+} cells also expressed Thbs4 glycoprotein in the lesion suggesting

that quiescent NSC gave rise to Thbs4$^+$ astrocytes that migrated to the infarcted area. In addition, the deprivation of BrdU$^+$ cells in the periglomerular OB layer after ischemia suggested that mainly dorsal SVZ cell populations responded to the injury re-routing their physiological pathway from the OB to the injury.

Actually the BrdU/IdU protocol still not shed light on the real origin and destination of the Thbs4$^+$ astrocytes after brain ischemia. Thus, we decided to confirm our first observations labelling and tracing the dorsal SVZ NSC by electroporation with pCMV-Cre plasmid in *R26-CAG-tdTomato* transgenic mice. After brain ischemia, regardless of few labelled cells that remained in the site of electroporation, most of labelled cells migrated to the injured areas. Indeed, the kinetic of the dorsal SVZ activation evidenced first an increase of tdTOM cells in the dorsal SVZ, later, 15 days after the ischemic insult, SVZ was depleted of tdTOM cells with a progressive increase of tdTOM cells at the injured areas. This experiment demonstrated that NSC proliferated and migrated outside the SVZ niche recruited by the ischemic environment.

When we characterized the tdTomato in the SVZ, we observed an elevated number of tdTOM cells co-expressing the Thbs4 glycoprotein following the brain ischemia suggesting that NSC in the dorsal SVZ could differentiate into Thbs4$^+$ astrocytes. Electroporation protocol was instrumental to demonstrate that dorsal NSC-derived astrocytes were able to move toward injury. We can not exclude that Thbs4$^+$ astrocytes could differentiate also in the injured tissues, after NSC migration. Using viral and transgenic approaches, Faiz et al (2015) observed the migratory pathway of NSC from SVZ to the injury and, once there, the differentiation into astrocytes primed by extracellular environment (Laung et al., 2019; Pous et al., 2020). However, according with Benner and other laboratories (Yamashita et al., 2006; Li et al., 2010; Benner et al., 2013; Zhang et al., 2014; Faiz et al., 2015; Santopolo et al., 2020; Pous et al., 2020) we sustain the hypothesis that Thbs4$^+$ astrocytes, once differentiated in the SVZ, migrated to the ischemic lesion as demonstrated by the kinetic of electroporated SVZ cells (Fig. 37). Migration of specific Thbs4$^+$ cells to the infarcted area was well documented by other authors. Benner et al., (2013) observed that NSC differentiate into astrocytes and migrate to the infarcted area also using Thbs4 marker to identify new generated astrocytes from SVZ.

Our data showed that Thbs4$^+$ astrocytes started to migrate 7 days after ischemic protocol and use the radial migratory stream under the corpus callosum until arriving to the lesion. The major peak in the Thbs4$^+$ astrocytes migration was observed around 30 days after lesion even though incorporation of this particular astrocytes population

continue increasing in the infarcted areas 30 and 60 days post-lesion. Reduction in the amount of Thbs4^{+} astrocytes in the corpus callosum 60 days after the MCAO model suggested that NSC stop to produce this population of astrocytes to produce neuroblasts (Sierra et al., 2014). When we characterized the cell type originated by the tdTomato cells we also observed an increase of oligodendrocytes. However, the increase of double positive Olig2/tdTomato cells were significant only in white matter areas (corpus callosum and striatum) (see *Annex 2. A2.4*).

As suggested by other authors (Faiz et al., 2015; Sultan et al., 2015) the possible function and the kinetic of the new Thbs4^{+} astrocytes after the brain ischemia could be the buffering of the unfavourable environment to promote the neuronal repopulation and survival. Overall, our results demonstrated that Thbs4^{+} astrocytes are generated from quiescent NSC in the dorsal SVZ and migrated to the lesion (Fig. 48).

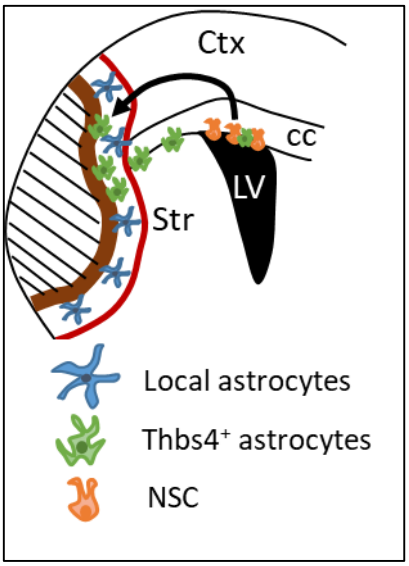

Figure 48. **Our proposed model.** Thbs4^{+} astrocytes differentiate from dorsal SVZ NSC and migrate to the injured areas occupying the borders of the glial scar together with local reactive astrocytes.

4. *SVZ-derived Thbs4^{+} astrocytes take part in the glial scar formation*

The last objective of our study was to investigate the role of Thbs4^{+} astrocytes during an ischemic event. We showed by immunofluorescence profile assay that Thbs4^{+} astrocytes migrated and occupied the borders of the glial scar territory. We also demonstrated that glial scar begin to be formed two weeks after the lesion coinciding with the arrival of Thbs4^{+} astrocytes. Robust expression of Nestin in the glial scar makes this marker extremely useful to identify the injured areas and it should be taken into account for this kind of analysis. Moreover, using Nestin as a marker for the ischemic

scar, we can identify more accurately the damage tissue compared with TTC or Cresyl violet staining. HABP is another marker we used to define the ischemic scar regardless of its faint staining.

Local reactive astrocytes are known for their faster response to the ischemic stroke and their function is thought to be beneficial for the resolution of the disease (Zamanian et al., 2012; Liddelow et al., 2017). However other publications pointed to another effect of the glial reactivity suggesting that prolonged activation of astrocytes inhibits the repopulation of new neurons, axonal sprouting and regrowth in the damaged area (Schwab, Kapfhammer & Bandtlow, 1993; Frisén, 1997). We showed that Thbs4$^+$ astrocytes represented around 36% of total astrocytes in the perilesional area what suggesting a beneficial role of these SVZ-derived astrocytes. Indeed, genetic removal of Thbs4$^+$ astrocytes can increase the ischemic oedema volume and trigger a worse progression of the disease (Benner et al., 2013). In our model, Thbs4$^+$ astrocytes occupied the closest part of the glial scar to the lesion that may represent a suitable control of excitotoxicity avoiding the expansion of injury, as already demonstrated also in the spinal cord injury (Frisén, 2016).

The SVZ-derived astrocyte population may represent a valid tool to allow the neuronal repopulation. In fact, DCX$^+$ neuroblasts migrate to injury lately, 30 days after the ischemic lesion and occupied perilesional areas. Understanding the differences between both local reactive astrocytes and Thbs4$^+$ astrocytes is instrumental to know the potential role of the SVZ-derived astrocytes population. Different hypothesis suggest that new generated astrocytes are needed to further allow the repopulation by new-born neuroblasts from the SVZ or themselves re-differentiated into neuroblasts to later repopulate the infarcted area (Faiz et al., 2015).

5. Ischemia-induced Thbs4$^+$ astrocytes participate in the glial scar remodelling

Massive presence of Thbs4$^+$ astrocytes in the ischemic scar and the close relation between HA and Thbs4, led us to investigate if these astrocytes could participate in the modulation of the glial scar after ischemia. Using *in vivo* and *in vitro* paradigms, we found that Thbs4$^+$ astrocytes were able to both synthesize and degrade HA (especially HMW HA). Renewal of HA is an important step to allow axonal regrowth and neuron repopulation at later stages of the disease. Moreover, CD44 expression is a marker that indicates HMW HA degradation and is highly expressed in the NSC (Khaing & Seidlits, 2015; Su et al., 2017). A huge percentage of CD44 spots were observed also in the Thbs4$^+$ astrocytes suggesting that this particular population can degrade HMW

HA. Moreover, our *in vitro* studies showed that Thbs4$^+$ astrocytes derived from the SVZ stem cells degraded HA and up-regulated MMPs after the OGD.

HMW HA is well-known to inhibit neural plasticity in healthy and pathological brain (Peters & Sherman, 2020). In the ischemic stroke, HA is accumulated after ischemia to create a physical barrier between the lesion core and healthy tissues (Lindwall et al., 2013; Greda & Nowicka, 2020). HMW HA covers two distinct roles at early and later stages after the scar formation. Early after the scar formation the HMW HA participates to build a physical barrier between damaged environment and healthy tissues. It represents an anti-inflammatory strategy avoiding the infiltration of peripheral immune cells and stopping the increase of the edema volume. Nonetheless, at later time glial scar impedes tissue regeneration and establishment of new neuronal networks from the SVZ. Hyaluronidases (HAase), a digestive enzymes of the HA, cover a central role in the degradation of the glial scar. It can be synthesised by the reactive astrocytes but its synthesis is slower, later after the scar formation (Greda & Nowicka, 2020). Thbs4$^+$ astrocytes can intervene at this time point, in fact whereas the HAase synthesis and CD44 activity in local reactive astrocytes are decreased, Thbs4$^+$ astrocytes that reach the glial scar could maintain a high production of HAase and CD44 (Lindwall et al., 2013). Participation of Thbs4$^+$ astrocytes can be relevant in this temporal window when upregulation of MMPs or HAase promote renewal of the HA that conform the glial scar.

Among HA synthetic enzymes (HAS), HAS2 is principally overexpressed in the injured areas and is mainly expressed by astrocytes at acute phases of the ischemic response (Greda & Nowicka, 2020). Indeed, HAS2 enzyme is well-known to produce HMW HA (Itano et al., 1999; Tian et al., 2013) and contribute to the scar tissue formation. Overexpressing HAS2 by AAV infection, we simulated the glial scar formation in non-ischemic animals. We found that Thbs4$^+$ astrocytes are not only attracted to the infarcted area because of HA accumulation. The mere overexpression of HAS2 in cortex and striatum induced the activation of Thbs4$^+$ astrocytes and their migration to the HMW hyaluronan area (the ischemic scar mode). However, when mice were exposed to both conditions (HAS2 overexpression and MCAO ischemia), Thbs4$^+$ astrocytes preferentially migrated to the ischemic hemisphere, suggesting that more elements are involved in the recruitment of Thbs4$^+$ astrocytes. Indeed, when the hyaluronan-based hydrogel is used to coat the lesion cavity after brain ischemia, different groups (Fujioka et al., 2017; Pous et al., 2020; Zhao et al., 2020) demonstrated a further activation of the SVZ NSC, suggesting that other ECM-related elements could be involved in the SVZ response and recruitment of NSC to injured areas.

Altogether our results suggest a close relationship between Thbs4^{+} astrocytes and HA in the infarcted tissue. Thbs4^{+} astrocytes modulate HMW HA to remodel the glial scar late after the ischemia (Fig. 49). Further experiments must be done to elucidate the interplay between the HA and the SVZ NSC in every phase of the vascular disease.

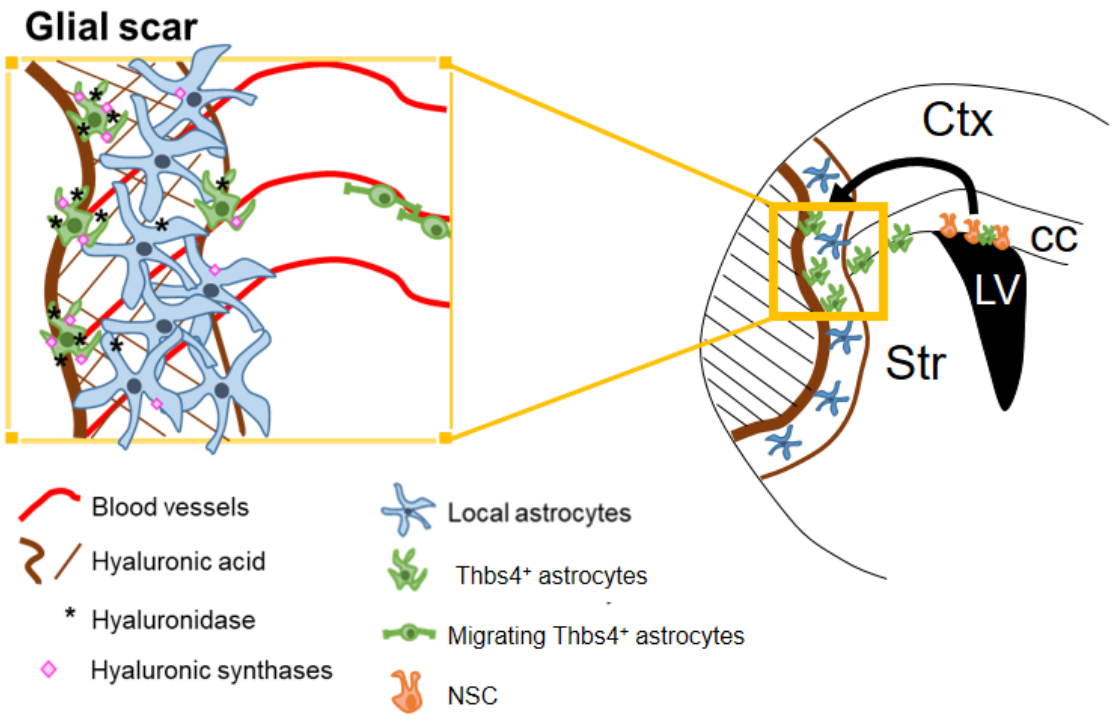

***Figure 49*. Thbs4^{+} astrocytes role in the glial scar remodeling.** SVZ-derived Thbs4^{+} astrocytes arrived to the lesion and occupied the glial scar territory at chronic stages of the disease. In this temporal window, hyaluronan synthesis and degradation is mediated by Thbs4^{+} astrocytes in the glial scar.

6. *Future studies. Thbs4^{+} astrocytes as a possible therapeutic tool against ischemic stroke: translation into the clinics*

In summary, our results suggest that Thbs4^{+} astrocytes are essential for the proper brain reactivation after ischemia. Their main role is to help to remodel the glial scar to facilitate the neuronal repopulation and axonal sprouting in the damage tissue. Even if the brain responses involve the production of new Thbs4^{+} astrocytes from the SVZ, this astrocytes population seems to have a limited capacity to improve the outcome of the disease. However, the activity of Thbs4^{+} astrocytes is essential for reducing the edema and protect the brain tissues after ischemia (Benner et al., 2013) suggesting that Thbs4^{+} astrocytes play a crucial role in ameliorating the brain injury after an ischemic insult. Unrevealing the potential role of Thbs4^{+} astrocytes in the lesion may help us to develop new therapeutic tools using this particular population against ischemic stroke.

Future studies include the overexpression of Thbs4 glycoprotein in the SVZ to understand if Thbs4$^+$ overproduction can improve the response to the ischemic stroke. Overexpression of Thbs4 can be performed using viral vectors or transgenic approaches. These tools could help to explain in detail how relevant the role of Thbs4$^+$ astrocytes are or how can improve motor and cognitive deficits after ischemia. Future preclinical approaches must focus in the development of different techniques to modulate the activation of Thbs4$^+$ astrocytes after ischemic stroke. Characterising all potential factors that could modulate Thbs4$^+$ astrocytes role is instrumental to develop suitable therapeutic strategies.

Because the SVZ and Thbs4$^+$ astrocytes are activated at mid and chronic stages after the ischemia (Fig. 50), a wide range of preclinical therapeutic tools can be developed to harness these particular NSC and astrocytes population. Furthermore, the development of therapeutic tools using these particular astrocytes as a preclinical target would increase the therapeutic temporal window because Thbs4$^+$ astrocytes role extend to several phases of the disease. In this way, we would be able to overcome the major issue in the ischemia treatment: the temporal window for therapy. For this reason, measuring if Thbs4 alterations may improve ischemic outcome is an opportunity to develop flexible therapeutic tools.

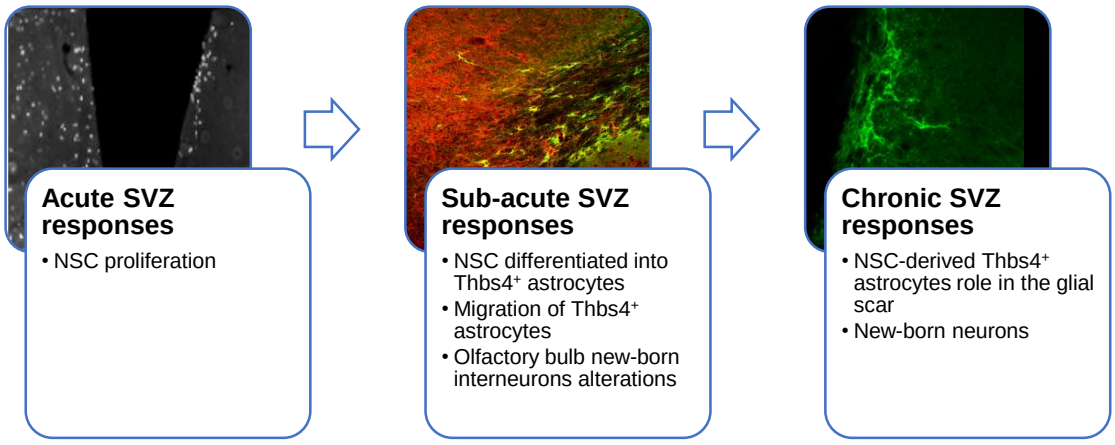

***Figure 50*. Acute, sub-acute and chronic stages of the ischemic stroke and their respective NSC responses.** Proliferation is the main feature of SVZ response after ischemic stroke in the acute phase. Astrogliogenesis and neurogenesis are upregulated and downregulated respectively in the SVZ at sub-acute phases of the ischemic stroke. Migration of SVZ-derived astrocytes is observed at this time point. At chronic stages, SVZ responses include the role of SVZ-derived astrocytes in the injured area.

CONCLUSIONS

The conclusions of this work are as follow:

1. **Ischemic stroke activates the SVZ and induces the proliferation of NSC early, 24 hours after the insult.**

2. **As a response to the ischemic stroke, SVZ stem cells differentiate into astrocytes to the detriment of neurogenesis. Thbs4 is an accurate marker to identify astrocytes derived from the SVZ and to distinguish this population from parenchymal astrocytes.**

3. **Ischemia-induced Thbs4^{+} astrocytes derive from quiescent NSC mainly located at the dorso-caudal axis of the SVZ.**

4. **Thbs4^{+} astrocytes transiently migrate from the SVZ to the infarcted areas through the corpus callosum. Their destination is the glial scar.**

5. **Thbs4^{+} astrocytes participate in the glial scar formation. Newly generated Thbs4^{+} astrocytes replace local reactive astrocytes in the glial scar.**

6. **Thbs4^{+} astrocytes participate in the glial scar remodelling. Ischemia-induced Thbs4^{+} astrocytes produce and degrade HMW hyaluronan.**

ANNEXES

ANNEX 1: Summary of publications about SVZ response to brain ischemia

Table 1. Summary of relevant works which study SVZ response after ischemic stroke.

Authors	Year	NSC fate	Ischemic model	Lesion place	NSC response phase
Zhang et al.	2001	NG	MCAO	Cortex & Striatum	Activation
Arvidsson et al.	2002	NG	MCAO	Cortex & Striatum	Migration
Parent et al.	2002	NG	MCAO	Cortex & Striatum	Activation & migration
Zhang et al.	2004	NG	MCAO	Cortex & Striatum	Integration
Yamashita et a.	2006	NG	MCAO	Striatum	Migration & Integration
Zhang et al.	2007	NG	MCAO	Cortex & Striatum	Migration
Liu et al.	2007	NSC	MCAO	Cortex & Striatum	Migration & integration
Thored et al.	2007	NG	MCAO	Striatum	Migration
Kolb et al.	2007	NSC	Permanent devascularisation	Cortex	Migration & Integration
Wang et al.	2007	NG	MCAO	Cortex & Striatum	Migration
Carlen et al.	2009	NG	MCAO	Cortex & Striatum	Activation
Kojima et al.	2010	NSC	MCAO	Cortex & Striatum	Migration
Li et al.	2010	AG	MCAO	Cortex & Striatum	Activation & Migration
Shen et al.	2010	NSC	MCAO	Cortex & Striatum	Activation & Migration
Zhang et al.	2011	NG	MCAO	Cortex & Striatum	Activation
Young et al.	2012	AG	MCAO	Cortex & Striatum	Activation
Saha et al.	2013	NG	Cortex aspirated	Cortex	Activation & migration
Benner et al.	2013	AG	Photothrombotic ischemia	Cortex	Activation, migration & integration
Zhang et al.	2014	NG	MCAO	Cortex & Striatum	Activation
Magnusson et al.	2014	AG	MCAO	Cortex & Striatum	Activation, migration & integration
Faiz et al.	2015	NSC AG	ET-1 and PVD Stroke	Cortex	Activation, migration & integration
Laterza et al.	2017	NG	MCAO	Cortex & Striatum	Activation
Palma-Tortosa et al.	2017	NG	MCAO	Cortex & Striatum	Activation & migration
Zhang et al.	2018	NG	MCAO	Cortex & Striatum	Activation & migration
Laug et al.	2019	AG	Photothrombotic ischemia	Cortex	Activation & migration
Pous et al.	2020	NSC AG	Photothrombotic ischemia	Cortex	Activation & integration
Santopolo et al.	2020	NG	MCAO	Striatum	Activation & migration
Tan et al.	2021	NG	MCAO	Cortex & Striatum	Activation

AG: Astrogliogenesis; NG: Neurogenesis; NSC: Neural Stem Cells

ANNEX 2: Methods characterization

A 2. 1. Oxygen and glucose deprivation and astrogliogenesis in *in vitro* NSC neurosphere cultures

To validate our ischemic model *in vitro*, we cultured NSC from rat SVZ and performed the OGD paradigm (Fig. A2.1A). 60 minutes of OGD with 3% O_2 did not induce cell death but activated the hypoxia inducible factor (HIF) and oxidative stress, as demonstrated by DAPI, ImageIT and MitoSox staining (Fig. A2.1A).

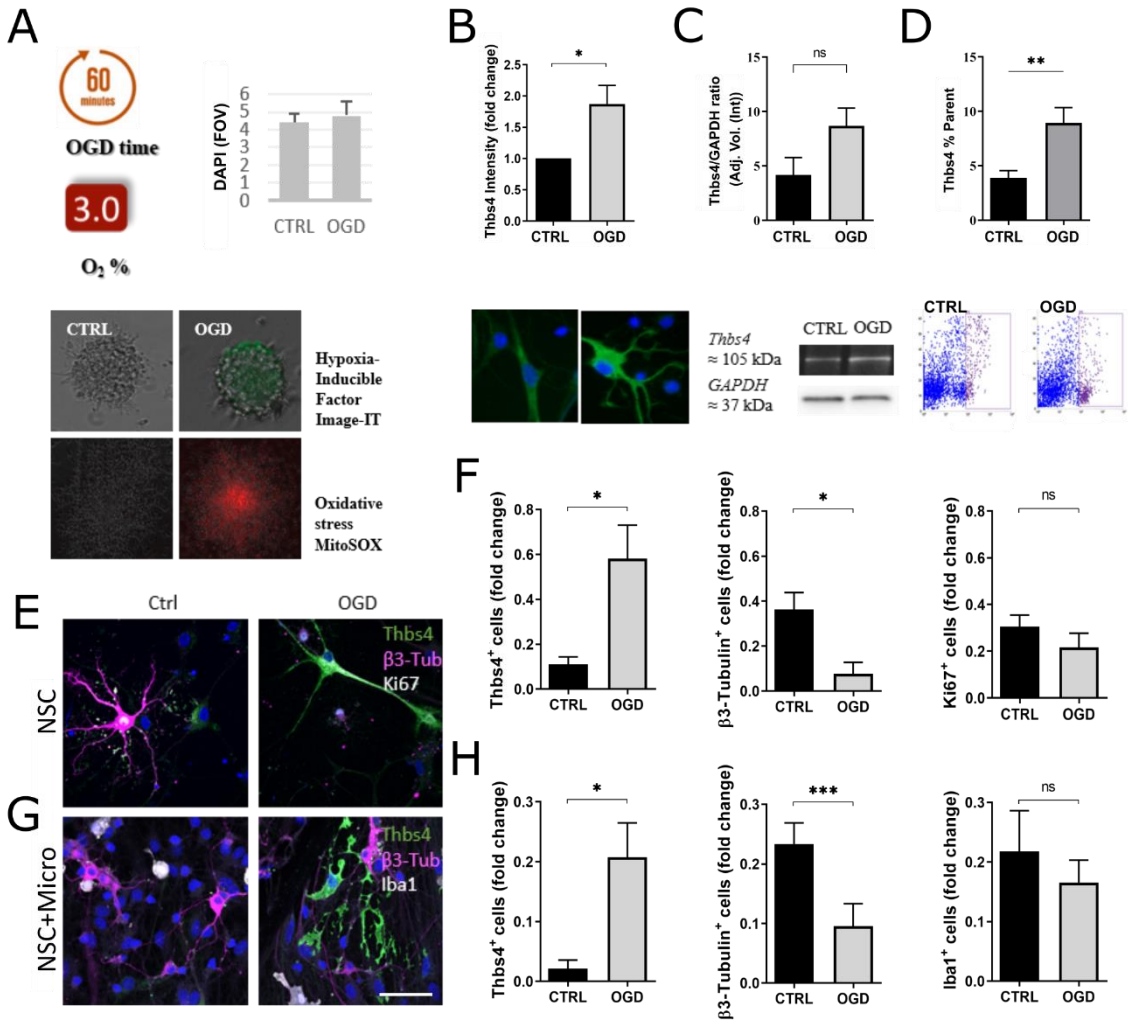

***Figure A2.1: In vitro* astrogliogenesis after OGD.** OGD protocol and its validation (A). NSC after 60 minutes of OGD (3% of oxygen) showed markers of activated hypoxia inducible factor (HIF), oxidative stress (MitoSOX) but did not show significative cell death as evidenced by DAPI. NSC differentiated into Thbs4$^+$ astrocytes after OGD evidenced by immunofluorescence (B), Western blot (C) and citofluorimetry assay (D). Astrogliogenesis, neuronal differentiation and cell proliferation was analysed by immunofluorescence with Thbs4, βIII tubulin and Ki67 antibodies in NSC cultures (E-F). Astrogliogenesis and neurogenesis in the NSC/microglia co-cultures (G). After immunofluorescence with Thbs4 and βIII tubulin, we did not observed

significant differences respect to the pure NSC cultures. The microglia marker Iba1 was not modulated by OGD (H). Scale Bar = 50 µm. *p<0.05, **p<0.01, ***p<0.001.

NSC from primary neurosphere cultures were differentiated to astrocytes for seven days after OGD. Analysis by immunofluorescence (Fig. A2.1B), Western blot (Fig. A2.1C) and cytofluorimetry analysis (Fig. A2.1D) evidenced almost six fold increase of Thbs4 staining respect to the normoxic control. Of note, after immunofluorescence we observed five fold decrease of βIII-tubulin$^+$ neurons whereas we could not detect any significant change in Ki67$^+$ cells (Fig. A2.1E-F). To study if astrogliogenesis induced by OGD could be conditioned by activated microglia, we induced OGD in a co-culture of NSC with microglia but we could not observe any significant variation respect to the pure NSC cultures (Fig. A2.1G-H). These results suggested that OGD activated the astrocyte differentiation from the SVZ that is not modulated by activated microglia.

A 2. 2. *In vivo* chronic BrdU treatment standardization

BrdU staining (quiescent NSC) was analysed 3, 7, 15 and 30 days after MCAO (Fig. A2.2A). Brain ischemia did not alter significantly the number of total BrdU or quiescent NSC (CD133$^+$ and BrdU$^+$) as visualised by immunofluorescence 3, 7 and 14 days after MCAO whereas active NSC (Nestin$^+$ and IdU$^+$) and total proliferating cells (Ki67) were upregulated (Fig. A2.2B). These results suggested MCAO did not alter the chronic BrdU treatment.

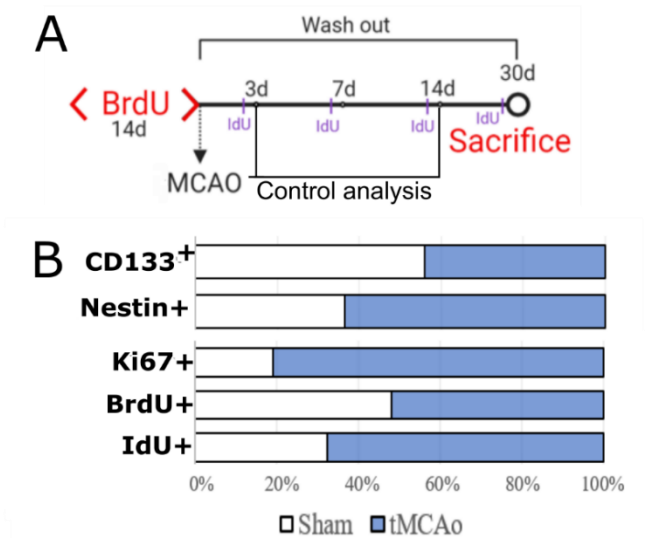

***Figure A2.2*. MCAO modulation of quiescent and activated NSC.** A. Experimental design. B. Quantifications of progenitor cell and proliferation markers in the sham (white) and MCAO (blue). Combination of markers corresponded to different NSC population (CD133$^+$/Nestin$^-$/BrdU$^-$: quiescent NSC; CD133$^+$/Nestin$^+$/BrdU$^+$: active NSC).

A 2. 3. *In vitro* SVZ organotypic cultures

We prepared organotypic slices from different SVZ sub-regions. SVZ from P5 rat pups were dissected in 300-µm slices from rostral to caudal lateral ventricle axis and cultured individually using a liquid/interphase membrane (Fig. A2.3A; see *1.1.6 section* for protocol). SVZ slices were classified in “Rostral”, “Intermediate” and “Caudal” axis including respectively the lateral ventricle, third ventricle and hippocampus (Fig. A2.3A). OGD in organotypic slices induced an increase of Thbs4/GFAP$^+$ astrocytes in the Rostral and the Intermediate slices two weeks after the insult (Fig. A2.3B). Each axis was analysed in dorsal, lateral and ventral regions (Fig. A2.3A). Topographic analysis of the SVZ displayed an increase of Thbs4/GFAP$^+$ astrocytes in the Rostro-ventral, Intermediate-ventral, Intermediate-dorsal and Caudal-medial SVZ (Fig. A2.3C). These data suggested that different NSC pools respond specifically to *in vitro* ischemic stimuli in the SVZ.

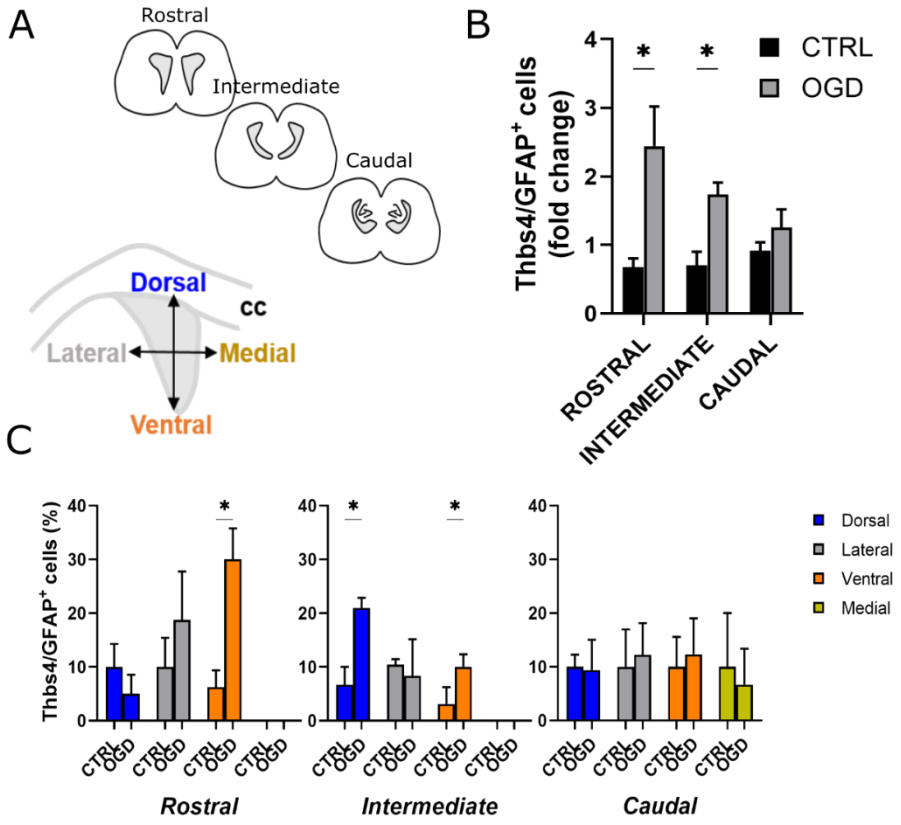

***Figure A2.3.* Topographic analysis of Thbs4 activation in SVZ organotypic cultures after OGD.** SVZ was analysed along rostro-caudal axis and in the dorsal, lateral, ventral and medial regions of the SVZ slices (A). In general, Thbs4/GFAP$^+$ astrocytes increased in the Rostral and Intermediate SVZ after OGD (B). Further analysis showed an increase of Thbs4/GFAP$^+$ cells in the Rostro-ventral, Intermediate-ventral, Intermediate-dorsal and Caudal-medial SVZ after OGD (C). cc = corpus callosum. *p<0.05.

A 2. 4. *In vivo* electroporation protocol characterization and tdTOM$^+$ cell type identification

Before analyzing Thbs4 and tdTOM co-localization, we decided to standardize the number of tdTOM$^+$ cells which differentiated into astrocytes or oligodendrocytes in sham and MCAO mice. GFAP and Olig2 immunofluorescence staining was performed to identify astrocytes and oligodendrocytes respectively. Analyzed areas were the corpus callosum, cortex and striatum. We could not see any change in the number of tdTOM$^+$ cells that also expressed GFAP in any area after MCAO (Fig. A2.4A-B). However, MCAO induced a progressive increase of tdTOM/Olig2$^+$ cells only in striatum and corpus callosum (Fig. A2.4A-B) suggesting that the increasing number of tdTOM$^+$ cells corresponded to oligodendrogenesis.

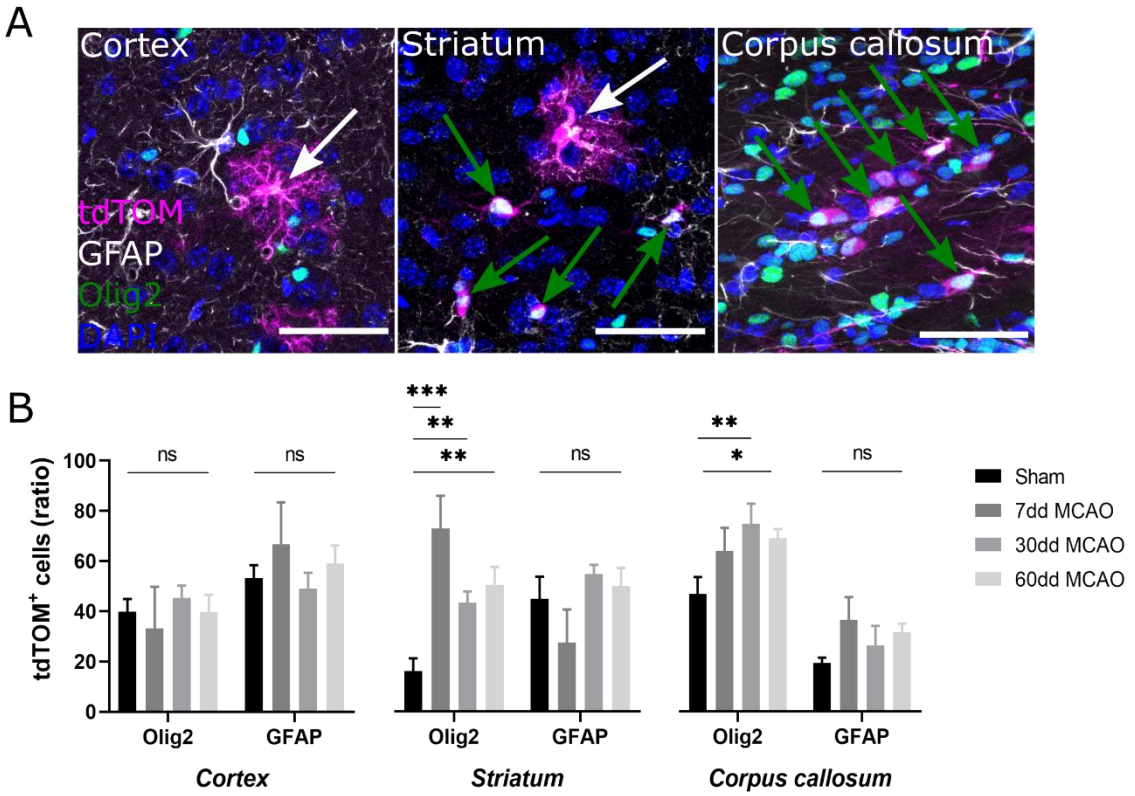

Figure A2.4. **Electroporated cells fate after MCAO.** GFAP and Olig2 immunofluorescence staining was performed to identify the tdTOM$^+$ cell phenotype in the corpus callosum and infarcted areas after MCAO (A). White arrows label tdTOM$^+$ astrocytes whereas green arrows label Olig2$^+$ oligodendrocytes. MCAO induced an increase of tdTOM/Olig2 colocalization in the infarcted striatum and the corpus callosum in time (B). However, tdTOM/GFAP$^+$ cells did not change in any time or any area after MCAO (B). Scale Bar = 50 µm. *p<0.05, **p<0.01, ***p<0.001.

ANNEX 3: Supplementary information

A 3. 1. *In vivo* chronic BrdU-treated mice analysis in the lesion

After characterizing the cellular origin of Thbs4$^+$ astrocytes in the SVZ, we analysed new-born astrocytes at corpus callosum and damaged areas (cortex and striatum) (Fig. A3.1A-B).Thirty days after MCAO, we observed an increase of total BrdU$^+$ cells in the lesion compared with sham animals where BrdU$^+$ cells in the cortex and striatum are rarely present (Fig. A3.1C). However, total IdU$^+$ cells did not increase after MCAO (Fig. A3.1D). Thbs4/GFAP/BrdU colocalization increased in corpus callosum and infarcted areas 30 days after MCAO (Fig. A3.1E) whereas Thbs4/GFAP/IdU$^+$ cells only increased in infarcted striatum (Fig. A3.1F). These results did not explained clearly if Thbs4$^+$ astrocytes in the lesion arose from SVZ even though suggest Thbs4$^+$ astrocytes gave rise from slow proliferative cells (BrdU$^+$) more than activated NSC (IdU$^+$).

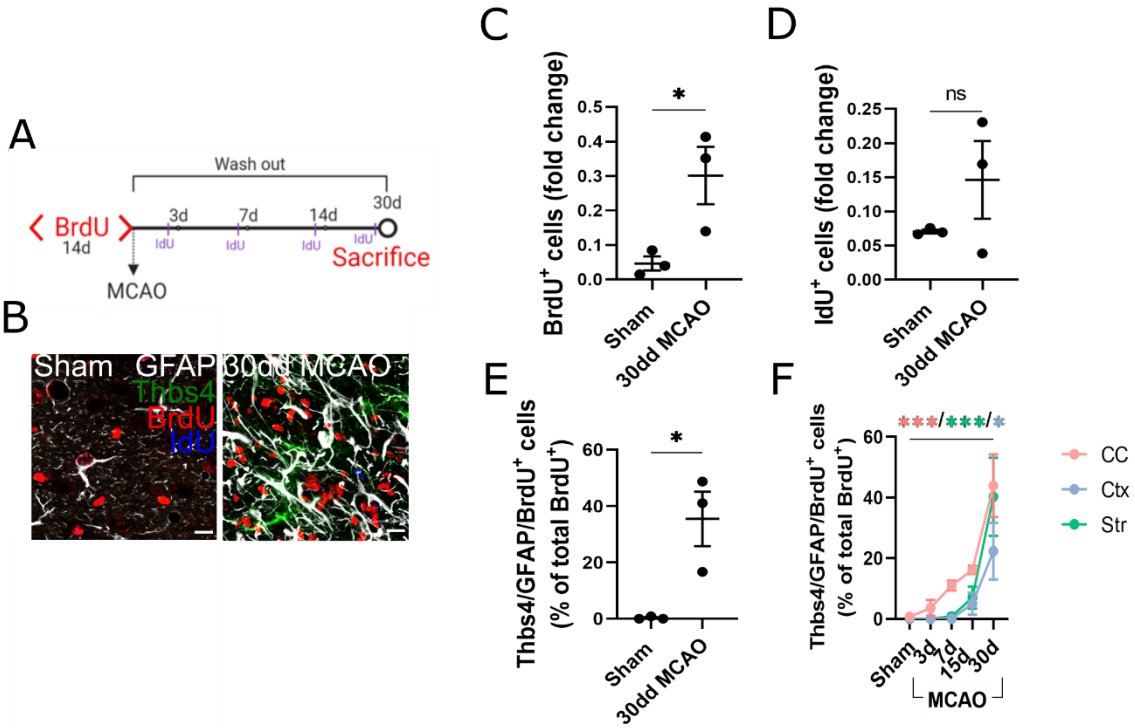

Figure A3.1. **Chronic BrdU treatment in the infarcted areas after MCAO.** Experimental scheme (A). B. Representative image of BrdU (red), IdU (blue), Thbs4 (green) and GFAP (white) from sham and 30 days MCAO. Total BrdU$^+$ cell number increased after MCAO (C). IdU$^+$ cells did not increase after MCAO (D). Triple colocalization of Thbs4/GFAP/BrdU increased 30 days after MCAO (E) and in all analysed areas (F). Scale Bar = 10 µm. *p<0.05, ***p<0.001.

A 3. 2. Cell origin in the SVZ

Type B NSC are classically divided in two groups depending on their proliferate state: quiescent (qNSC) and active NSC (aNSC), each population express specific markers: the receptor for epidermal growth factor (EGFR) (Doetsch et al., 2002) for aNSC and prominin 1 (CD133) for qNSC (Fig. A3.2A). We decided to analyse by immunofluorescence the expression of Thbs4 together with these two markers to further characterize the cellular origin of Thbs4 astrocytes. Total EGFR expression in dorsal SVZ increased linearly 30 days post-lesion (Fig. A3.2B). Early after MCAO (15 days) Thbs4 was mainly co-expressed with CD133 (activated NSC) and less with EGFR but later and until 30 days after MCAO Thbs4^{+} cells became activated increasing the number of Thbs4/EGFR^{+} cells (Fig. A3.2C-D). These results suggested that Thbs4 astrocytes derive from ischemia-activated qNSC in the dorsal domain of SVZ and confirmed the results presented in Fig. 29.

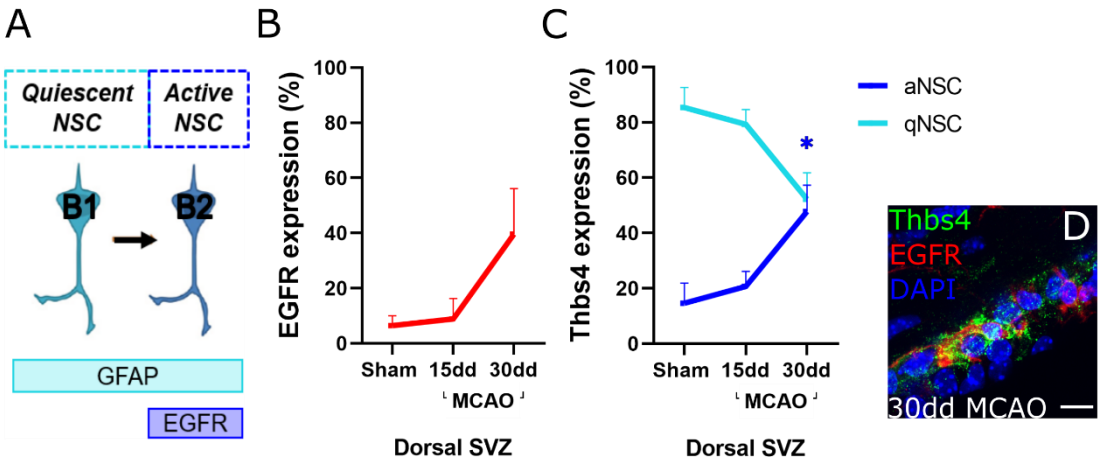

Figure A3.2. **EGFR immunofluorescence in dorsal SVZ after MCAO.** Expressed markers for quiescent or active NSC (A). EGFR expression increased concurrently in SVZ after MCAO (B). Thbs4 expression increased in aNSC (EGFR^{+}) after MCAO (C). Thbs4^{+} astrocytes in aNSC (blue) or qNSC (cyan) pool was identified using Thbs4^{+}/EGFR^{+}/GFAP^{-} or Thbs4^{+}/EGFR^{-}/GFAP^{+} colocalization. Representative image of Thbs4/EGFR^{+} cells in the SVZ of infarcted mice (D). Thbs4 in green; EGFR in red and DAPI in blue. Scale bar = 10 µm. *p<0.05.

A 3. 3. Thbs4 expression in the damaged area

Brain tissue close to the injury was freshly removed from sham and MCAO animals for protein analysis. We observed that Thbs4 expression increased 15 days after the MCAO by Western blot (Fig. A3.3A). This result corroborated immunofluorescence

quantification where we observed an increased in Thbs4 expression in the infarcted areas 15 days after MCAO (Fig. 32).

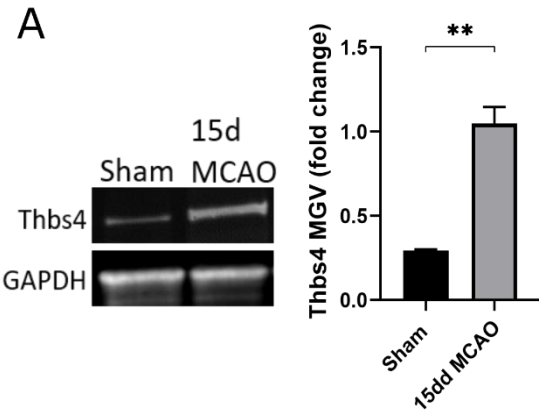

Figure A3.3. **Thbs4 expression in the infarcted areas.** Western blot analysis showed Thbs4 increased 15 days after MCAO (A). **p<0.01.

A 3. 4. Hyaluronan disruption in the SVZ after brain ischemia

HABP expression and HA structure was quantify in the SVZ after several days after MCAO (7, 15 and 30 days after the insult) in order to analyse, by skeletonize analysis, how ischemia can modulate HA structure (Fig. A3.4A). We analysed fractal dimension of HABP in dorsal, lateral, ventral and medial SVZ 7, 15 and 30 days after MCAO. We did not observed any significant changes except in dorsal SVZ where fractal dimension was reduced 7 days after the MCAO (Fig. A3.4B). Moreover, cumulative frequency distribution showed an alteration of HA structure 7 after MCAO (Fig. A3.4C) suggesting that MCAO induced fragmentation of HA in the SVZ.

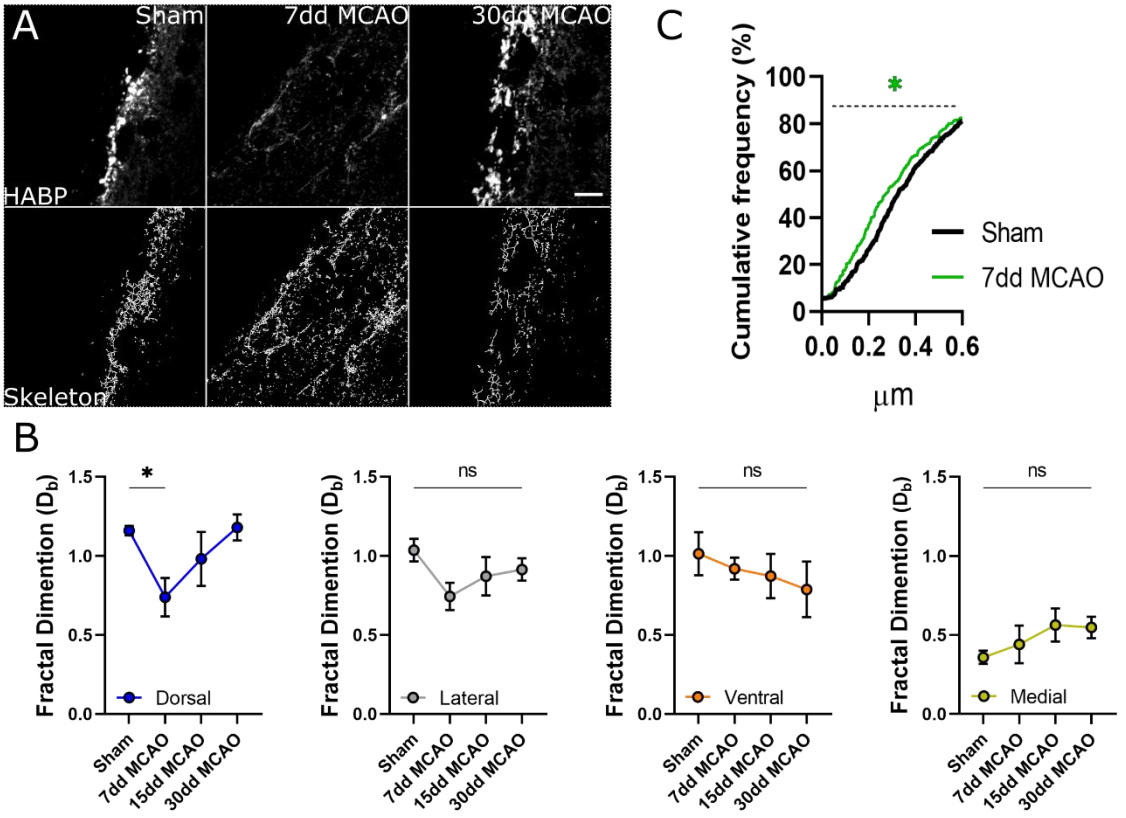

Figure A3.4. **HABP skeletonize analysis in SVZ 7, 15 and 30 days after MCAO.** Representative images of HABP skeletonize processes in sham, 7 and 30 days after MCAO (A). Fractal dimension analysis was down-regulated 7 days after lesion in dorsal SVZ whereas we did not see significant changes in lateral, ventral and medial SVZ in any time point after MCAO (B). Cumulative frequency distribution (%) of HABP skeletonizes in sham SVZ (black) and 7 days after MCAO (green) (C). HABP skeletonize were smaller at 7 days after MCAO in the SVZ, suggesting fragmentation of hyaluronan after the insult. Scale Bar = 10 µm. *p<0.05.

A 3. 5. Hyaluronan and Thbs4 interplay in the SVZ after brain ischemia

Thbs4 and HABP expression was measured by immunofluorescence in the SVZ after MCAO (Fig. A3.5A-B). Analysis of whole SVZ did not evidenced any significant change of HABP expression after MCAO whereas Thbs4 expression increased 15 and 30 days (Fig. A3.5C) as already demonstrated (see Fig. 27). When we analysed in detail the different SVZ regions, we observed a drastic decrease of HABP expression in dorsal SVZ 7 and 15 days after MCAO. Interestingly, HABP expression was restored to normal levels 30 days after MCAO (Fig. A3.5D). Altogether, structural analysis of HABP and Thbs4 in the SVZ suggested that ECM degradation after brain ischemia is needed for NSC activation before Thbs4 differentiation.

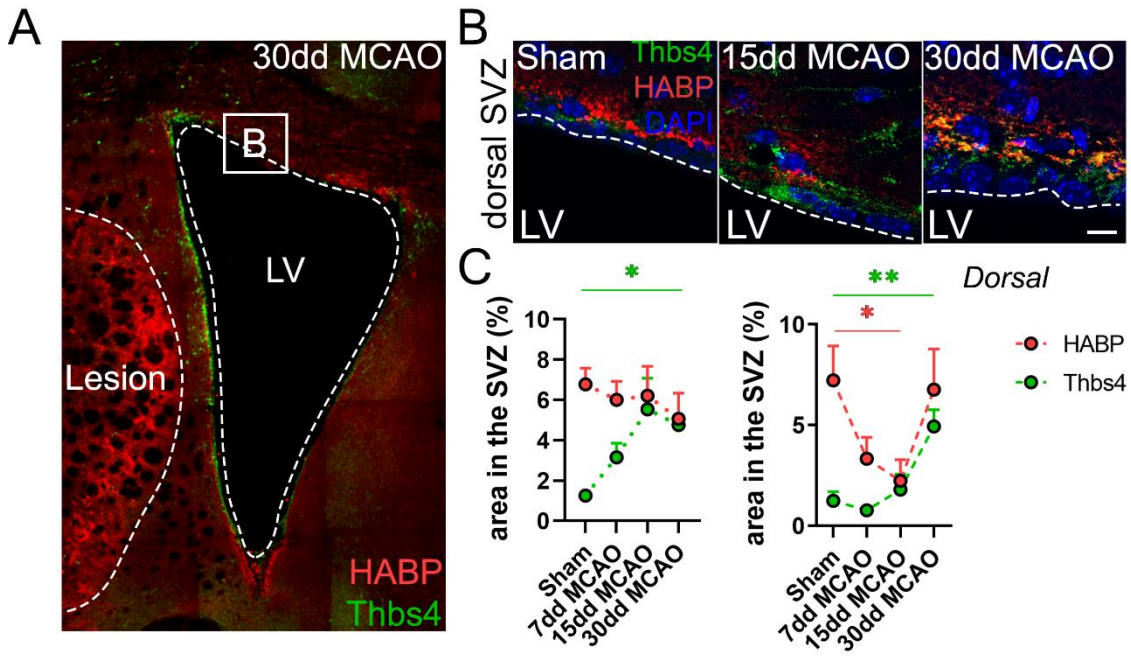

Figure A3.5. **Thbs4 and HABP expression in the SVZ after MCAO.** Representative image of Thbs4 and HABP expression in SVZ 30 days after MCAO (A). HABP and Thbs4 modulation after MCAO in the dorsal SVZ (B). Quantification of HABP and Thbs4 expression 7, 15 and 30 days after MCAO in whole (C) and dorsal (D) SVZ. Scale Bar = 10 µm. *p<0.05, **p<0.01.

A 3. 6. Thbs4^{+} astrocytes metabolism in the infarcted tissue

Monocarboxylate transporters 1 (MCT1) is a lactate transporter mainly found in endothelial and ependymal cells in mouse brain (Pierre & Pellerin, 2005). Metabolism path adopted from NSC at resting stages is mainly glycolytic of which final result is the energy consumed from lactate, a limited energy production process (Zheng et al., 2016). Glycolytic metabolism could be observed by immunofluorescence using lactate transporter markers. In this experiment, we analysed the monocarboxylate transporter 1 (MCT1) lactate transporter that is highly expressed in the SVZ cells (Fig. A3.6A; Pierre & Pellerin, 2005).

We analysed MCT1 expression in injury, we observed an increased in MCT1 expression overtime after MCAO (Fig. A3.6A-B). MCT1 and Thbs4 immunofluorescence was done to analyse the expression of the transporter in Thbs4^{+} astrocytes. We observed that Thbs4^{+} astrocytes, which arrived to the lesion 30 days after the insult, increased MCT1 expression (Fig. A3.6C) suggesting Thbs4^{+} astrocytes adopt a glycolytic metabolism like the SVZ stem cells.

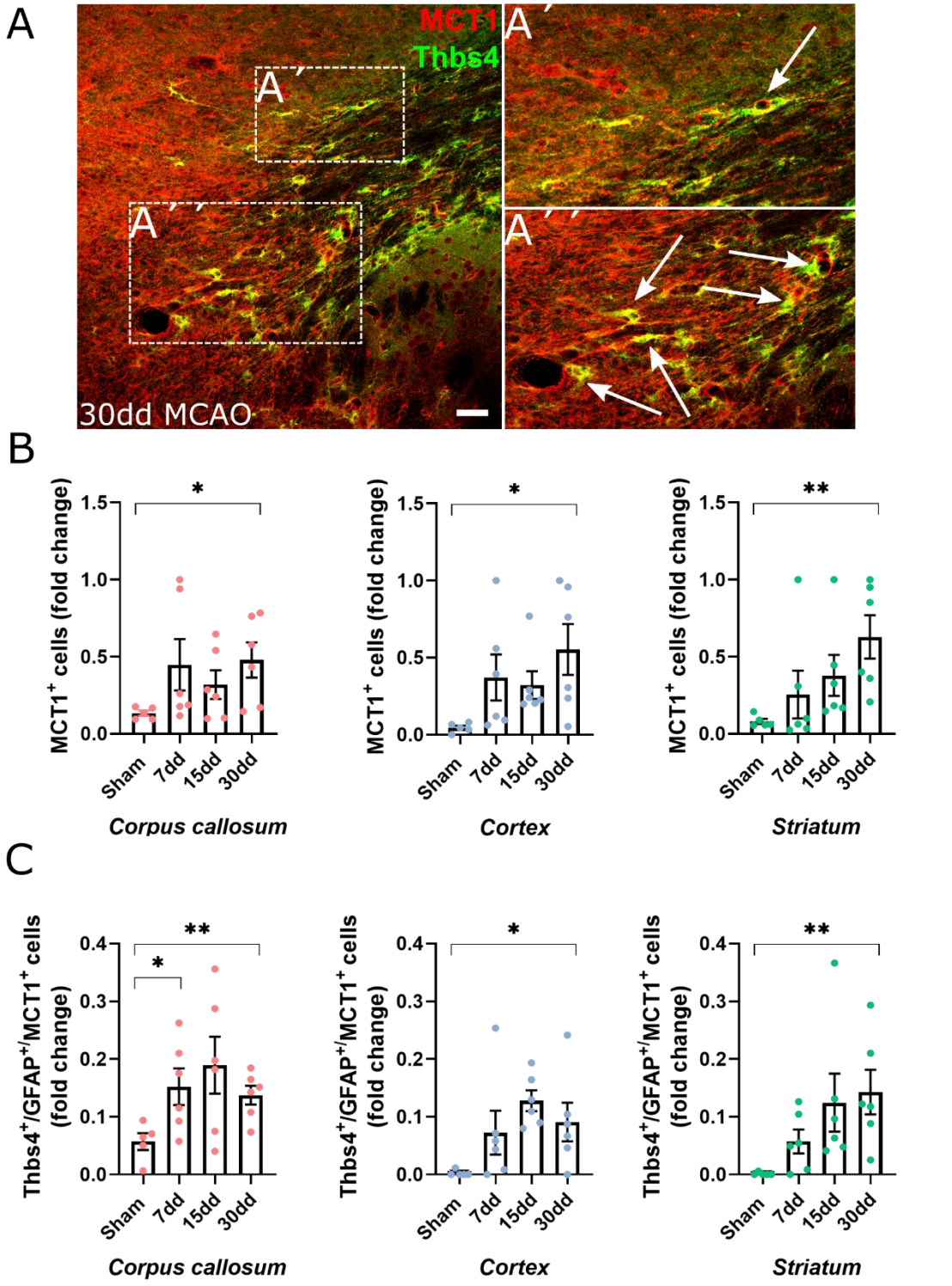

Figure A2.8. **MCT1 expression in Thbs4⁺ astrocytes in infarcted areas.** Thbs4/MCT1⁺ astrocytes 30 days after MCAO (A, A´, A´´). Arrows showed Thbs4/MCT1⁺ astrocytes. MCT1 expression increased in all analysed areas 30 days after the lesion (B). Moreover, colocalization of Thbs4 and MCT1 increased in corpus callosum and infarcted areas (cortex and striatum) 30 days after MCAO (C). Moreover, Scale Bar = 50 µm. *p<0.05, **p<0.01.

REFERENCES

Abbott, N. J., Patabendige, A. A. K., Dolman, D. E. M., Yusof, S. R., & Begley, D. J. (2010). Structure and function of the blood-brain barrier. *Neurobiology of Disease*, *37*(1), 13-25. https://doi.org/10.1016/j.nbd.2009.07.030

Adams, K. L., Riparini, G., Banerjee, P., Breur, M., Bugiani, M., & Gallo, V. (2020). Endothelin-1 signaling maintains glial progenitor proliferation in the postnatal subventricular zone. *Nature Communications*, *11*(1), 2138. https://doi.org/10.1038/s41467-020-16028-8

Ahmad, M. H., Fatima, M., & Mondal, A. C. (2019). Influence of microglia and astrocyte activation in the neuroinflammatory pathogenesis of Alzheimer's disease: Rational insights for the therapeutic approaches. *Journal of Clinical Neuroscience: Official Journal of the Neurosurgical Society of Australasia*, *59*, 6-11. https://doi.org/10.1016/j.jocn.2018.10.034

Al Qteishat, A., Gaffney, J. J., Krupinski, J., & Slevin, M. (2006). Hyaluronan expression following middle cerebral artery occlusion in the rat. *Neuroreport*, *17*(11), 1111-1114. https://doi.org/10.1097/01.wnr.0000227986.69680.20

Alia, C., Spalletti, C., Lai, S., Panarese, A., Lamola, G., Bertolucci, F., Vallone, F., Di Garbo, A., Chisari, C., Micera, S., & Caleo, M. (2017). Neuroplastic Changes Following Brain Ischemia and their Contribution to Stroke Recovery: Novel Approaches in Neurorehabilitation. *Frontiers in Cellular Neuroscience*, *11*, 76. https://doi.org/10.3389/fncel.2017.00076

Allen, N. J., & Barres, B. A. (2009). Glia—More than just brain glue. *Nature*, *457*(7230), 675-677. https://doi.org/10.1038/457675a

Altman, J. (1962). Are new neurons formed in the brains of adult mammals? *Science (New York, N.Y.)*, *135*(3509), 1127-1128. https://doi.org/10.1126/science.135.3509.1127

Altman, J., & Das, G. D. (1965). Autoradiographic and histological evidence of postnatal hippocampal neurogenesis in rats. *The Journal of Comparative Neurology*, *124*(3), 319-335. https://doi.org/10.1002/cne.901240303

Alvarez, J. I., Katayama, T., & Prat, A. (2013). Glial influence on the blood brain barrier. *Glia*, *61*(12), 1939-1958. https://doi.org/10.1002/glia.22575

Alvarez-Buylla, A., & Garcia-Verdugo, J. M. (2002). Neurogenesis in adult subventricular zone. *The Journal of Neuroscience: The Official Journal of the Society for Neuroscience*, *22*(3), 629-634.

Amulic, B., Cazalet, C., Hayes, G. L., Metzler, K. D., & Zychlinsky, A. (2012). Neutrophil function: From mechanisms to disease. *Annual Review of Immunology*, *30*, 459-489. https://doi.org/10.1146/annurev-immunol-020711-074942

Anderson, M. A., Burda, J. E., Ren, Y., Ao, Y., O'Shea, T. M., Kawaguchi, R., Coppola, G., Khakh, B. S., Deming, T. J., & Sofroniew, M. V. (2016). Astrocyte scar formation aids central nervous system axon regeneration. *Nature*, *532*(7598), 195-200. https://doi.org/10.1038/nature17623

Andreu-Agulló, C., Morante-Redolat, J. M., Delgado, A. C., & Fariñas, I. (2009). Vascular niche factor PEDF modulates Notch-dependent stemness in the adult subependymal zone. *Nature Neuroscience*, *12*(12), 1514-1523. https://doi.org/10.1038/nn.2437

Androutsellis-Theotokis, A., Rueger, M. A., Park, D. M., Boyd, J. D., Padmanabhan, R., Campanati, L., Stewart, C. V., LeFranc, Y., Plenz, D., Walbridge, S., Lonser, R. R., & McKay, R. D. G. (2010). Angiogenic factors stimulate growth of adult neural stem cells. *PloS One*, *5*(2), e9414. https://doi.org/10.1371/journal.pone.0009414

Arai, K., & Lo, E. H. (2009). Experimental models for analysis of oligodendrocyte pathophysiology in stroke. *Experimental & Translational Stroke Medicine*, *1*, 6. https://doi.org/10.1186/2040-7378-1-6

Argaw, A. T., Gurfein, B. T., Zhang, Y., Zameer, A., & John, G. R. (2009). VEGF-mediated disruption of endothelial CLN-5 promotes blood-brain barrier breakdown. *Proceedings of the National Academy of Sciences of the United States of America*, *106*(6), 1977-1982. https://doi.org/10.1073/pnas.0808698106

Arulmoli, J., Pathak, M. M., McDonnell, L. P., Nourse, J. L., Tombola, F., Earthman, J. C., & Flanagan, L. A. (2015). Static stretch affects neural stem cell differentiation in an extracellular matrix-dependent manner. *Scientific Reports*, *5*, 8499. https://doi.org/10.1038/srep08499

Arvidsson, A., Collin, T., Kirik, D., Kokaia, Z., & Lindvall, O. (2002). Neuronal replacement from endogenous precursors in the adult brain after stroke. *Nature Medicine*, *8*(9), 963-970. https://doi.org/10.1038/nm747

Asahi, M., Sumii, T., Fini, M. E., Itohara, S., & Lo, E. H. (2001). Matrix metalloproteinase 2 gene knockout has no effect on acute brain injury after focal ischemia. *Neuroreport*, *12*(13), 3003-3007. https://doi.org/10.1097/00001756-200109170-00050

References

Augestad, I. L. (2018). *Combinatory strategies for promoting tissue remodelling and endogenous plasticity after experimental ischemic stroke*. NTNU. https://ntnuopen.ntnu.no/ntnu-xmlui/handle/11250/2562475

Azim, K., Fiorelli, R., Zweifel, S., Hurtado-Chong, A., Yoshikawa, K., Slomianka, L., & Raineteau, O. (2012). 3-dimensional examination of the adult mouse subventricular zone reveals lineage-specific microdomains. *PloS One*, *7*(11), e49087. https://doi.org/10.1371/journal.pone.0049087

Bacigaluppi, M., Russo, G. L., Peruzzotti-Jametti, L., Rossi, S., Sandrone, S., Butti, E., De Ceglia, R., Bergamaschi, A., Motta, C., Gallizioli, M., Studer, V., Colombo, E., Farina, C., Comi, G., Politi, L. S., Muzio, L., Villani, C., Invernizzi, R. W., Hermann, D. M., … Martino, G. (2016). Neural Stem Cell Transplantation Induces Stroke Recovery by Upregulating Glutamate Transporter GLT-1 in Astrocytes. *The Journal of Neuroscience: The Official Journal of the Society for Neuroscience*, *36*(41), 10529-10544. https://doi.org/10.1523/JNEUROSCI.1643-16.2016

Bailey, K. J., Maslov, A. Y., & Pruitt, S. C. (2004). Accumulation of mutations and somatic selection in aging neural stem/progenitor cells. *Aging Cell*, *3*(6), 391-397. https://doi.org/10.1111/j.1474-9728.2004.00128.x

Baker, S. A., Baker, K. A., & Hagg, T. (2004). Dopaminergic nigrostriatal projections regulate neural precursor proliferation in the adult mouse subventricular zone. *The European Journal of Neuroscience*, *20*(2), 575-579. https://doi.org/10.1111/j.1460-9568.2004.03486.x

Bakiri, Y., Káradóttir, R., Cossell, L., & Attwell, D. (2011). Morphological and electrical properties of oligodendrocytes in the white matter of the corpus callosum and cerebellum. *The Journal of Physiology*, *589*(Pt 3), 559-573. https://doi.org/10.1113/jphysiol.2010.201376

Bardella, C., Al-Shammari, A. R., Soares, L., Tomlinson, I., O'Neill, E., & Szele, F. G. (2018). The role of inflammation in subventricular zone cancer. *Progress in Neurobiology*, *170*, 37-52. https://doi.org/10.1016/j.pneurobio.2018.04.007

Barkho, B. Z., Song, H., Aimone, J. B., Smrt, R. D., Kuwabara, T., Nakashima, K., Gage, F. H., & Zhao, X. (2006). Identification of astrocyte-expressed factors that modulate neural stem/progenitor cell differentiation. *Stem Cells and Development*, *15*(3), 407-421. https://doi.org/10.1089/scd.2006.15.407

Barnabé-Heider, F., Göritz, C., Sabelström, H., Takebayashi, H., Pfrieger, F. W., Meletis, K., & Frisén, J. (2010). Origin of new glial cells in intact and injured adult spinal cord. *Cell Stem Cell*, *7*(4), 470-482. https://doi.org/10.1016/j.stem.2010.07.014

Basak, O., Krieger, T. G., Muraro, M. J., Wiebrands, K., Stange, D. E., Frias-Aldeguer, J., Rivron, N. C., van de Wetering, M., van Es, J. H., van Oudenaarden, A., Simons, B. D., & Clevers, H. (2018). Troy+ brain stem cells cycle through quiescence and regulate their number by sensing niche occupancy. *Proceedings of the National Academy of Sciences of the United States of America*, *115*(4), E610-E619. https://doi.org/10.1073/pnas.1715911114

Beckervordersandforth, R., Tripathi, P., Ninkovic, J., Bayam, E., Lepier, A., Stempfhuber, B., Kirchhoff, F., Hirrlinger, J., Haslinger, A., Lie, D. C., Beckers, J., Yoder, B., Irmler, M., & Götz, M. (2010). *In vivo* fate mapping and expression analysis reveals molecular hallmarks of prospectively isolated adult neural stem cells. *Cell Stem Cell*, *7*(6), 744-758. https://doi.org/10.1016/j.stem.2010.11.017

Benito-Muñoz, M., Matute, C., & Cavaliere, F. (2016). Adenosine A1 receptor inhibits postnatal neurogenesis and sustains astrogliogenesis from the subventricular zone. *Glia*, *64*(9), 1465-1478. https://doi.org/10.1002/glia.23010

Benner, E. J., Luciano, D., Jo, R., Abdi, K., Paez-Gonzalez, P., Sheng, H., Warner, D. S., Liu, C., Eroglu, C., & Kuo, C. T. (2013). Protective astrogenesis from the SVZ niche after injury is controlled by Notch modulator Thbs4. *Nature*, *497*(7449), 369-373. https://doi.org/10.1038/nature12069

Bergmann, O., Spalding, K. L., & Frisén, J. (2015). Adult Neurogenesis in Humans. *Cold Spring Harbor Perspectives in Biology*, *7*(7), a018994. https://doi.org/10.1101/cshperspect.a018994

Berninger, B., Costa, M. R., Koch, U., Schroeder, T., Sutor, B., Grothe, B., & Götz, M. (2007). Functional properties of neurons derived from *in vitro* reprogrammed postnatal astroglia. *The Journal of Neuroscience: The Official Journal of the Society for Neuroscience*, *27*(32), 8654-8664. https://doi.org/10.1523/JNEUROSCI.1615-07.2007

Bignami, A., & Asher, R. (1992). Some observations on the localization of hyaluronic acid in adult, newborn and embryonal rat brain. *International Journal of Developmental Neuroscience: The Official Journal of the International Society for Developmental Neuroscience*, *10*(1), 45-57. https://doi.org/10.1016/0736-5748(92)90006-l

Bignami, A., Hosley, M., & Dahl, D. (1993). Hyaluronic acid and hyaluronic acid-binding proteins in brain extracellular matrix. *Anatomy and Embryology*, *188*(5), 419-433. https://doi.org/10.1007/BF00190136

Boison, D., Chen, J.-F., & Fredholm, B. B. (2010). Adenosine signaling and function in glial cells. *Cell Death and Differentiation*, *17*(7), 1071-1082. https://doi.org/10.1038/cdd.2009.131

Boldrini, M., Fulmore, C. A., Tartt, A. N., Simeon, L. R., Pavlova, I., Poposka, V., Rosoklija, G. B., Stankov, A., Arango, V., Dwork, A. J., Hen, R., & Mann, J. J. (2018). Human Hippocampal Neurogenesis Persists throughout Aging. *Cell Stem Cell*, *22*(4), 589-599.e5. https://doi.org/10.1016/j.stem.2018.03.015

Bordiuk, O. L., Smith, K., Morin, P. J., & Semënov, M. V. (2014). Cell proliferation and neurogenesis in adult mouse brain. *PloS One*, *9*(11), e111453. https://doi.org/10.1371/journal.pone.0111453

Borrell, V., & Götz, M. (2014). Role of radial glial cells in cerebral cortex folding. *Current Opinion in Neurobiology*, *27*, 39-46. https://doi.org/10.1016/j.conb.2014.02.007

Brainin, M., Tuomilehto, J., Heiss, W.-D., Bornstein, N. M., Bath, P. M. W., Teuschl, Y., Richard, E., Guekht, A., Quinn, T., & Post Stroke Cognition Study Group. (2015). Post-stroke cognitive decline: An update and perspectives for clinical research. *European Journal of Neurology*, *22*(2), 229-238, e13-16. https://doi.org/10.1111/ene.12626

Brancato, S. K., & Albina, J. E. (2011). Wound macrophages as key regulators of repair: Origin, phenotype, and function. *The American Journal of Pathology*, *178*(1), 19-25. https://doi.org/10.1016/j.ajpath.2010.08.003

Breunig, J. J., Sarkisian, M. R., Arellano, J. I., Morozov, Y. M., Ayoub, A. E., Sojitra, S., Wang, B., Flavell, R. A., Rakic, P., & Town, T. (2008). Primary cilia regulate hippocampal neurogenesis by mediating sonic hedgehog signaling. *Proceedings of the National Academy of Sciences of the United States of America*, *105*(35), 13127-13132. https://doi.org/10.1073/pnas.0804558105

Brezun, J. M., & Daszuta, A. (1999). Depletion in serotonin decreases neurogenesis in the dentate gyrus and the subventricular zone of adult rats. *Neuroscience*, *89*(4), 999-1002. https://doi.org/10.1016/s0306-4522(98)00693-9

Brill, M. S., Ninkovic, J., Winpenny, E., Hodge, R. D., Ozen, I., Yang, R., Lepier, A., Gascón, S., Erdelyi, F., Szabo, G., Parras, C., Guillemot, F., Frotscher, M., Berninger, B., Hevner, R. F., Raineteau, O., & Götz, M. (2009). Adult generation of glutamatergic olfactory bulb interneurons. *Nature Neuroscience*, *12*(12), 1524-1533. https://doi.org/10.1038/nn.2416

Brody, M. J., Schips, T. G., Vanhoutte, D., Kanisicak, O., Karch, J., Maliken, B. D., Blair, N. S., Sargent, M. A., Prasad, V., & Molkentin, J. D. (2016). Dissection of Thrombospondin-4 Domains Involved in Intracellular Adaptive Endoplasmic Reticulum Stress-Responsive Signaling. *Molecular and Cellular Biology*, *36*(1), 2-12. https://doi.org/10.1128/MCB.00607-15

Broughton, B. R. S., Reutens, D. C., & Sobey, C. G. (2009). Apoptotic mechanisms after cerebral ischemia. *Stroke*, *40*(5), e331-339. https://doi.org/10.1161/STROKEAHA.108.531632

Brown, A. M. (2004). Brain glycogen re-awakened. *Journal of Neurochemistry*, *89*(3), 537-552. https://doi.org/10.1111/j.1471-4159.2004.02421.x

Buffo, A., Rolando, C., & Ceruti, S. (2010). Astrocytes in the damaged brain: Molecular and cellular insights into their reactive response and healing potential. *Biochemical Pharmacology*, *79*(2), 77-89. https://doi.org/10.1016/j.bcp.2009.09.014

Buffo, A., Vosko, M. R., Ertürk, D., Hamann, G. F., Jucker, M., Rowitch, D., & Götz, M. (2005). Expression pattern of the transcription factor Olig2 in response to brain injuries: Implications for neuronal repair. *Proceedings of the National Academy of Sciences of the United States of America*, *102*(50), 18183-18188. https://doi.org/10.1073/pnas.0506535102

Burda, J. E., & Sofroniew, M. V. (2014). Reactive gliosis and the multicellular response to CNS damage and disease. *Neuron*, *81*(2), 229-248. https://doi.org/10.1016/j.neuron.2013.12.034

Busch, S. A., & Silver, J. (2007). The role of extracellular matrix in CNS regeneration. *Current Opinion in Neurobiology*, *17*(1), 120-127. https://doi.org/10.1016/j.conb.2006.09.004

Bush, T. G., Puvanachandra, N., Horner, C. H., Polito, A., Ostenfeld, T., Svendsen, C. N., Mucke, L., Johnson, M. H., & Sofroniew, M. V. (1999). Leukocyte infiltration, neuronal degeneration, and neurite outgrowth after ablation of scar-forming, reactive astrocytes in adult transgenic mice. *Neuron*, *23*(2), 297-308. https://doi.org/10.1016/s0896-6273(00)80781-3

Butovsky, O., Ziv, Y., Schwartz, A., Landa, G., Talpalar, A. E., Pluchino, S., Martino, G., & Schwartz, M. (2006). Microglia activated by IL-4 or IFN-gamma differentially induce neurogenesis and oligodendrogenesis from adult stem/progenitor cells. *Molecular and Cellular Neurosciences*, *31*(1), 149-160. https://doi.org/10.1016/j.mcn.2005.10.006

Butti, E., Cusimano, M., Bacigaluppi, M., & Martino, G. (2014). Neurogenic and non-neurogenic functions of endogenous neural stem cells. *Frontiers in Neuroscience*, *8*, 92. https://doi.org/10.3389/fnins.2014.00092

References

Campbell, B. C. V., De Silva, D. A., Macleod, M. R., Coutts, S. B., Schwamm, L. H., Davis, S. M., & Donnan, G. A. (2019). Ischaemic stroke. *Nature Reviews. Disease Primers*, *5*(1), 70. https://doi.org/10.1038/s41572-019-0118-8

Candelario-Jalil, E., Yang, Y., & Rosenberg, G. A. (2009). Diverse roles of matrix metalloproteinases and tissue inhibitors of metalloproteinases in neuroinflammation and cerebral ischemia. *Neuroscience*, *158*(3), 983-994. https://doi.org/10.1016/j.neuroscience.2008.06.025

Cao, L., Jiao, X., Zuzga, D. S., Liu, Y., Fong, D. M., Young, D., & During, M. J. (2004). VEGF links hippocampal activity with neurogenesis, learning and memory. *Nature Genetics*, *36*(8), 827-835. https://doi.org/10.1038/ng1395

Cao, X., Li, L.-P., Qin, X.-H., Li, S.-J., Zhang, M., Wang, Q., Hu, H.-H., Fang, Y.-Y., Gao, Y.-B., Li, X.-W., Sun, L.-R., Xiong, W.-C., Gao, T.-M., & Zhu, X.-H. (2013). Astrocytic adenosine 5'-triphosphate release regulates the proliferation of neural stem cells in the adult hippocampus. *Stem Cells (Dayton, Ohio)*, *31*(8), 1633-1643. https://doi.org/10.1002/stem.1408

Capilla-Gonzalez, V., Bonsu, J. M., Redmond, K. J., Garcia-Verdugo, J. M., & Quiñones-Hinojosa, A. (2016). Implications of irradiating the subventricular zone stem cell niche. *Stem Cell Research*, *16*(2), 387-396. https://doi.org/10.1016/j.scr.2016.02.031

Capilla-Gonzalez, V., Cebrian-Silla, A., Guerrero-Cazares, H., Garcia-Verdugo, J. M., & Quiñones-Hinojosa, A. (2014). Age-related changes in astrocytic and ependymal cells of the subventricular zone. *Glia*, *62*(5), 790-803. https://doi.org/10.1002/glia.22642

Carlén, M., Meletis, K., Göritz, C., Darsalia, V., Evergren, E., Tanigaki, K., Amendola, M., Barnabé-Heider, F., Yeung, M. S. Y., Naldini, L., Honjo, T., Kokaia, Z., Shupliakov, O., Cassidy, R. M., Lindvall, O., & Frisén, J. (2009). Forebrain ependymal cells are Notch-dependent and generate neuroblasts and astrocytes after stroke. *Nature Neuroscience*, *12*(3), 259-267. https://doi.org/10.1038/nn.2268

Carpentier, P. A., & Palmer, T. D. (2009). Immune influence on adult neural stem cell regulation and function. *Neuron*, *64*(1), 79-92. https://doi.org/10.1016/j.neuron.2009.08.038

Carulli, D., Pizzorusso, T., Kwok, J. C. F., Putignano, E., Poli, A., Forostyak, S., Andrews, M. R., Deepa, S. S., Glant, T. T., & Fawcett, J. W. (2010). Animals lacking link protein have attenuated perineuronal nets and persistent plasticity. *Brain: A Journal of Neurology*, *133*(Pt 8), 2331-2347. https://doi.org/10.1093/brain/awq145

Carulli, D., Rhodes, K. E., Brown, D. J., Bonnert, T. P., Pollack, S. J., Oliver, K., Strata, P., & Fawcett, J. W. (2006). Composition of perineuronal nets in the adult rat cerebellum and the cellular origin of their components. *The Journal of Comparative Neurology*, *494*(4), 559-577. https://doi.org/10.1002/cne.20822

Cavaliere, F., Urra, O., Alberdi, E., & Matute, C. (2012). Oligodendrocyte differentiation from adult multipotent stem cells is modulated by glutamate. *Cell Death & Disease*, *3*, e268. https://doi.org/10.1038/cddis.2011.144

Cebrian-Silla, A., Nascimento, M. A., Redmond, S. A., Mansky, B., Wu, D., Obernier, K., Romero Rodriguez, R., Gonzalez-Granero, S., García-Verdugo, J. M., Lim, D. A., & Álvarez-Buylla, A. (2021). Single-cell analysis of the ventricular-subventricular zone reveals signatures of dorsal and ventral adult neurogenesis. *eLife*, *10*, e67436. https://doi.org/10.7554/eLife.67436

Chaker, Z., Aïd, S., Berry, H., & Holzenberger, M. (2015). Suppression of IGF-I signals in neural stem cells enhances neurogenesis and olfactory function during aging. *Aging Cell*, *14*(5), 847-856. https://doi.org/10.1111/acel.12365

Chaker, Z., Codega, P., & Doetsch, F. (2016). A mosaic world: Puzzles revealed by adult neural stem cell heterogeneity. *WIREs Developmental Biology*, *5*(6), 640-658. https://doi.org/10.1002/wdev.248

Challacombe, J. F., Snow, D. M., & Letourneau, P. C. (1997). Dynamic microtubule ends are required for growth cone turning to avoid an inhibitory guidance cue. *The Journal of Neuroscience: The Official Journal of the Society for Neuroscience*, *17*(9), 3085-3095.

Chamorro, Á., Meisel, A., Planas, A. M., Urra, X., van de Beek, D., & Veltkamp, R. (2012). The immunology of acute stroke. *Nature Reviews. Neurology*, *8*(7), 401-410. https://doi.org/10.1038/nrneurol.2012.98

Chen, Y., Ma, N., Pei, Z., Wu, Z., Do-Monte, F. H., Huang, P., Yellin, E., Chen, M., Yin, J., Lee, G., Minier-Toribio, A., Hu, Y., Bai, Y., Lee, K., Quirk, G. J., & Chen, G. (2018). *Functional repair after ischemic injury through high efficiency in situ astrocyte-to-neuron conversion* (p. 294967). https://doi.org/10.1101/294967

Chia, N. H., Leyden, J. M., Newbury, J., Jannes, J., & Kleinig, T. J. (2016). Determining the Number of Ischemic Strokes Potentially Eligible for Endovascular Thrombectomy: A Population-Based Study. *Stroke*, *47*(5), 1377-1380. https://doi.org/10.1161/STROKEAHA.116.013165

Chistyakov, D. V., Astakhova, A. A., Azbukina, N. V., Goriainov, S. V., Chistyakov, V. V., & Sergeeva, M. G. (2019). High and Low Molecular Weight Hyaluronic Acid Differentially Influences Oxylipins Synthesis in Course of Neuroinflammation. *International Journal of Molecular Sciences*, *20*(16), E3894. https://doi.org/10.3390/ijms20163894

Chiu, A. Y., Matthew, W. D., & Patterson, P. H. (1986). A monoclonal antibody that blocks the activity of a neurite regeneration-promoting factor: Studies on the binding site and its localization *in vivo*. *The Journal of Cell Biology*, *103*(4), 1383-1398. https://doi.org/10.1083/jcb.103.4.1383

Chou, C.-H., & Modo, M. (2016). Human neural stem cell-induced endothelial morphogenesis requires autocrine/paracrine and juxtacrine signaling. *Scientific Reports*, *6*, 29029. https://doi.org/10.1038/srep29029

Chou, K.-Y., Chang, A.-C., Ho, C.-Y., Tsai, T.-F., Chen, H.-E., Chen, P.-C., & Hwang, T. I.-S. (2021). Thrombospondin-4 promotes bladder cancer cell migration and invasion via MMP2 production. *Journal of Cellular and Molecular Medicine*. https://doi.org/10.1111/jcmm.16463

Christopherson, K. S., Ullian, E. M., Stokes, C. C. A., Mullowney, C. E., Hell, J. W., Agah, A., Lawler, J., Mosher, D. F., Bornstein, P., & Barres, B. A. (2005). Thrombospondins are astrocyte-secreted proteins that promote CNS synaptogenesis. *Cell*, *120*(3), 421-433. https://doi.org/10.1016/j.cell.2004.12.020

Codega, P., Silva-Vargas, V., Paul, A., Maldonado-Soto, A. R., DeLeo, A. M., Pastrana, E., & Doetsch, F. (2014). Prospective Identification and Purification of Quiescent Adult Neural Stem Cells from Their *In Vivo* Niche. *Neuron*, *82*(3), 545-559. https://doi.org/10.1016/j.neuron.2014.02.039

Colak, D., Mori, T., Brill, M. S., Pfeifer, A., Falk, S., Deng, C., Monteiro, R., Mummery, C., Sommer, L., & Götz, M. (2008). Adult neurogenesis requires Smad4-mediated bone morphogenic protein signaling in stem cells. *The Journal of Neuroscience: The Official Journal of the Society for Neuroscience*, *28*(2), 434-446. https://doi.org/10.1523/JNEUROSCI.4374-07.2008

Corbit, K. C., Aanstad, P., Singla, V., Norman, A. R., Stainier, D. Y. R., & Reiter, J. F. (2005). Vertebrate Smoothened functions at the primary cilium. *Nature*, *437*(7061), 1018-1021. https://doi.org/10.1038/nature04117

Coskun, V., Wu, H., Blanchi, B., Tsao, S., Kim, K., Zhao, J., Biancotti, J. C., Hutnick, L., Krueger, R. C., Fan, G., Vellis, J. de, & Sun, Y. E. (2008). CD133+ neural stem cells in the ependyma of mammalian postnatal forebrain. *Proceedings of the National Academy of Sciences*, *105*(3), 1026-1031. https://doi.org/10.1073/pnas.0710000105

Curtis, M. A., Eriksson, P. S., & Faull, R. L. M. (2007). Progenitor cells and adult neurogenesis in neurodegenerative diseases and injuries of the basal ganglia. *Clinical and Experimental Pharmacology & Physiology*, *34*(5-6), 528-532. https://doi.org/10.1111/j.1440-1681.2007.04609.x

Curtis, M. A., Penney, E. B., Pearson, A. G., van Roon-Mom, W. M. C., Butterworth, N. J., Dragunow, M., Connor, B., & Faull, R. L. M. (2003). Increased cell proliferation and neurogenesis in the adult human Huntington's disease brain. *Proceedings of the National Academy of Sciences of the United States of America*, *100*(15), 9023-9027. https://doi.org/10.1073/pnas.1532244100

Danbolt, N. C. (2001). Glutamate uptake. *Progress in Neurobiology*, *65*(1), 1-105. https://doi.org/10.1016/s0301-0082(00)00067-8

de Chevigny, A., Coré, N., Follert, P., Gaudin, M., Barbry, P., Béclin, C., & Cremer, H. (2012). MiR-7a regulation of Pax6 controls spatial origin of forebrain dopaminergic neurons. *Nature Neuroscience*, *15*(8), 1120-1126. https://doi.org/10.1038/nn.3142

Deb, P., Sharma, S., & Hassan, K. M. (2010). Pathophysiologic mechanisms of acute ischemic stroke: An overview with emphasis on therapeutic significance beyond thrombolysis. *Pathophysiology: The Official Journal of the International Society for Pathophysiology*, *17*(3), 197-218. https://doi.org/10.1016/j.pathophys.2009.12.001

Deepa, S. S., Carulli, D., Galtrey, C., Rhodes, K., Fukuda, J., Mikami, T., Sugahara, K., & Fawcett, J. W. (2006). Composition of perineuronal net extracellular matrix in rat brain: A different disaccharide composition for the net-associated proteoglycans. *The Journal of Biological Chemistry*, *281*(26), 17789-17800. https://doi.org/10.1074/jbc.M600544200

Delgado, A. C., Ferrón, S. R., Vicente, D., Porlan, E., Perez-Villalba, A., Trujillo, C. M., D'Ocón, P., & Fariñas, I. (2014). Endothelial NT-3 delivered by vasculature and CSF promotes quiescence of subependymal neural stem cells through nitric oxide induction. *Neuron*, *83*(3), 572-585. https://doi.org/10.1016/j.neuron.2014.06.015

Delgado, A. C., Maldonado-Soto, A. R., Silva-Vargas, V., Mizrak, D., von Känel, T., Tan, K. R., Paul, A., Madar, A., Cuervo, H., Kitajewski, J., Lin, C.-S., & Doetsch, F. (2021). Release of stem cells from quiescence reveals gliogenic domains in the adult mouse brain. *Science (New York, N.Y.)*, *372*(6547), 1205-1209. https://doi.org/10.1126/science.abg8467

References

Delgado, R. N., & Lim, D. A. (2015). Embryonic Nkx2.1-expressing neural precursor cells contribute to the regional heterogeneity of adult V-SVZ neural stem cells. *Developmental Biology*, *407*(2), 265-274. https://doi.org/10.1016/j.ydbio.2015.09.008

Deneen, B., Ho, R., Lukaszewicz, A., Hochstim, C. J., Gronostajski, R. M., & Anderson, D. J. (2006). The transcription factor NFIA controls the onset of gliogenesis in the developing spinal cord. *Neuron*, *52*(6), 953-968. https://doi.org/10.1016/j.neuron.2006.11.019

Dewar, D., Underhill, S. M., & Goldberg, M. P. (2003). Oligodendrocytes and ischemic brain injury. *Journal of Cerebral Blood Flow and Metabolism: Official Journal of the International Society of Cerebral Blood Flow and Metabolism*, *23*(3), 263-274. https://doi.org/10.1097/01.WCB.0000053472.41007.F9

Dias, J. M., Alekseenko, Z., Applequist, J. M., & Ericson, J. (2014). Tgfβ signaling regulates temporal neurogenesis and potency of neural stem cells in the CNS. *Neuron*, *84*(5), 927-939. https://doi.org/10.1016/j.neuron.2014.10.033

Dirnagl, U., Iadecola, C., & Moskowitz, M. A. (1999). Pathobiology of ischaemic stroke: An integrated view. *Trends in Neurosciences*, *22*(9), 391-397. https://doi.org/10.1016/s0166-2236(99)01401-0

Dirnagl, U., Simon, R. P., & Hallenbeck, J. M. (2003). Ischemic tolerance and endogenous neuroprotection. *Trends in Neurosciences*, *26*(5), 248-254. https://doi.org/10.1016/S0166-2236(03)00071-7

Dodson, R. F., Chu, L. W., Welch, K. M., & Achar, V. S. (1977). Acute tissue response to cerebral ischemia in the gerbil. An ultrastructural study. *Journal of the Neurological Sciences*, *33*(1-2), 161-170. https://doi.org/10.1016/0022-510x(77)90190-3

Doetsch, F., Caillé, I., Lim, D. A., García-Verdugo, J. M., & Alvarez-Buylla, A. (1999). Subventricular zone astrocytes are neural stem cells in the adult mammalian brain. *Cell*, *97*(6), 703-716. https://doi.org/10.1016/s0092-8674(00)80783-7

Doetsch, F., García-Verdugo, J. M., & Alvarez-Buylla, A. (1997). Cellular composition and three-dimensional organization of the subventricular germinal zone in the adult mammalian brain. *The Journal of Neuroscience: The Official Journal of the Society for Neuroscience*, *17*(13), 5046-5061.

Doetsch, F., Petreanu, L., Caille, I., Garcia-Verdugo, J.-M., & Alvarez-Buylla, A. (2002). EGF Converts Transit-Amplifying Neurogenic Precursors in the Adult Brain into Multipotent Stem Cells. *Neuron*, *36*(6), 1021-1034. https://doi.org/10.1016/S0896-6273(02)01133-9

Donega, V., Burm, S. M., van Strien, M. E., van Bodegraven, E. J., Paliukhovich, I., Geut, H., van de Berg, W. D. J., Li, K. W., Smit, A. B., Basak, O., & Hol, E. M. (2019). Transcriptome and proteome profiling of neural stem cells from the human subventricular zone in Parkinson's disease. *Acta Neuropathologica Communications*, *7*(1), 84. https://doi.org/10.1186/s40478-019-0736-0

Dougherty, K. D., Dreyfus, C. F., & Black, I. B. (2000). Brain-derived neurotrophic factor in astrocytes, oligodendrocytes, and microglia/macrophages after spinal cord injury. *Neurobiology of Disease*, *7*(6 Pt B), 574-585. https://doi.org/10.1006/nbdi.2000.0318

Du, Y., & Dreyfus, C. F. (2002). Oligodendrocytes as providers of growth factors. *Journal of Neuroscience Research*, *68*(6), 647-654. https://doi.org/10.1002/jnr.10245

Dzwonek, J., & Wilczynski, G. M. (2015). CD44: Molecular interactions, signaling and functions in the nervous system. *Frontiers in Cellular Neuroscience*, *9*, 175. https://doi.org/10.3389/fncel.2015.00175

ElAli, A., Doeppner, T. R., Zechariah, A., & Hermann, D. M. (2011). Increased blood-brain barrier permeability and brain edema after focal cerebral ischemia induced by hyperlipidemia: Role of lipid peroxidation and calpain-1/2, matrix metalloproteinase-2/9, and RhoA overactivation. *Stroke*, *42*(11), 3238-3244. https://doi.org/10.1161/STROKEAHA.111.615559

Emsley, J. G., & Hagg, T. (2003). Endogenous and exogenous ciliary neurotrophic factor enhances forebrain neurogenesis in adult mice. *Experimental Neurology*, *183*(2), 298-310. https://doi.org/10.1016/s0014-4886(03)00129-8

Eriksson, P. S., Perfilieva, E., Björk-Eriksson, T., Alborn, A. M., Nordborg, C., Peterson, D. A., & Gage, F. H. (1998). Neurogenesis in the adult human hippocampus. *Nature Medicine*, *4*(11), 1313-1317. https://doi.org/10.1038/3305

Ernst, A., Alkass, K., Bernard, S., Salehpour, M., Perl, S., Tisdale, J., Possnert, G., Druid, H., & Frisén, J. (2014). Neurogenesis in the striatum of the adult human brain. *Cell*, *156*(5), 1072-1083. https://doi.org/10.1016/j.cell.2014.01.044

Eulenburg, V., Retiounskaia, M., Papadopoulos, T., Gomeza, J., & Betz, H. (2010). Glial glycine transporter 1 function is essential for early postnatal survival but dispensable in adult mice. *Glia*, *58*(9), 1066-1073. https://doi.org/10.1002/glia.20987

Faissner, A., Pyka, M., Geissler, M., Sobik, T., Frischknecht, R., Gundelfinger, E. D., & Seidenbecher, C. (2010). Contributions of astrocytes to synapse formation and maturation—Potential functions of the perisynaptic extracellular matrix. *Brain Research Reviews*, *63*(1-2), 26-38. https://doi.org/10.1016/j.brainresrev.2010.01.001

Faiz, M., Sachewsky, N., Gascón, S., Bang, K. W. A., Morshead, C. M., & Nagy, A. (2015). Adult Neural Stem Cells from the Subventricular Zone Give Rise to Reactive Astrocytes in the Cortex after Stroke. *Cell Stem Cell*, *17*(5), 624-634. https://doi.org/10.1016/j.stem.2015.08.002

Falcão, A. M., Marques, F., Novais, A., Sousa, N., Palha, J. A., & Sousa, J. C. (2012). The path from the choroid plexus to the subventricular zone: Go with the flow! *Frontiers in Cellular Neuroscience*, *6*, 34. https://doi.org/10.3389/fncel.2012.00034

Faulkner, J. R., Herrmann, J. E., Woo, M. J., Tansey, K. E., Doan, N. B., & Sofroniew, M. V. (2004). Reactive astrocytes protect tissue and preserve function after spinal cord injury. *The Journal of Neuroscience: The Official Journal of the Society for Neuroscience*, *24*(9), 2143-2155. https://doi.org/10.1523/JNEUROSCI.3547-03.2004

Fawcett, J. W., & Asher, R. A. (1999). The glial scar and central nervous system repair. *Brain Research Bulletin*, *49*(6), 377-391. https://doi.org/10.1016/s0361-9230(99)00072-6

Fernando, R. N., Eleuteri, B., Abdelhady, S., Nussenzweig, A., Andäng, M., & Ernfors, P. (2011). Cell cycle restriction by histone H2AX limits proliferation of adult neural stem cells. *Proceedings of the National Academy of Sciences of the United States of America*, *108*(14), 5837-5842. https://doi.org/10.1073/pnas.1014993108

Fields, R. D. (2008). Oligodendrocytes changing the rules: Action potentials in glia and oligodendrocytes controlling action potentials. *The Neuroscientist: A Review Journal Bringing Neurobiology, Neurology and Psychiatry*, *14*(6), 540-543. https://doi.org/10.1177/1073858408320294

Fiorelli, R., Azim, K., Fischer, B., & Raineteau, O. (2015). Adding a spatial dimension to postnatal ventricular-subventricular zone neurogenesis. *Development*, *142*(12), 2109-2120. https://doi.org/10.1242/dev.119966

Fluri, F., Schuhmann, M. K., & Kleinschnitz, C. (2015). Animal models of ischemic stroke and their application in clinical research. *Drug Design, Development and Therapy*, *9*, 3445-3454. https://doi.org/10.2147/DDDT.S56071

Franceschi, C., & Campisi, J. (2014). Chronic inflammation (inflammaging) and its potential contribution to age-associated diseases. *The Journals of Gerontology. Series A, Biological Sciences and Medical Sciences*, *69 Suppl 1*, S4-9. https://doi.org/10.1093/gerona/glu057

Franklin, R. J. M., & Ffrench-Constant, C. (2008). Remyelination in the CNS: From biology to therapy. *Nature Reviews. Neuroscience*, *9*(11), 839-855. https://doi.org/10.1038/nrn2480

Frisén, J. (1997). Determinants of axonal regeneration. *Histology and Histopathology*, *12*(3), 857-868.

Frisén, J. (2016). Neurogenesis and Gliogenesis in Nervous System Plasticity and Repair. *Annual Review of Cell and Developmental Biology*, *32*, 127-141. https://doi.org/10.1146/annurev-cellbio-111315-124953

Frisén, J., Johansson, C. B., Török, C., Risling, M., & Lendahl, U. (1995). Rapid, widespread, and longlasting induction of nestin contributes to the generation of glial scar tissue after CNS injury. *Journal of Cell Biology*, *131*(2), 453-464. https://doi.org/10.1083/jcb.131.2.453

Fuentealba, L. C., Rompani, S. B., Parraguez, J. I., Obernier, K., Romero, R., Cepko, C. L., & Alvarez-Buylla, A. (2015). Embryonic Origin of Postnatal Neural Stem Cells. *Cell*, *161*(7), 1644-1655. https://doi.org/10.1016/j.cell.2015.05.041

Fujimoto, M., Hayashi, H., Takagi, Y., Hayase, M., Marumo, T., Gomi, M., Nishimura, M., Kataoka, H., Takahashi, J., Hashimoto, N., Nozaki, K., & Miyamoto, S. (2012). Transplantation of telencephalic neural progenitors induced from embryonic stem cells into subacute phase of focal cerebral ischemia. *Laboratory Investigation; a Journal of Technical Methods and Pathology*, *92*(4), 522-531. https://doi.org/10.1038/labinvest.2012.1

Fujioka, T., Kaneko, N., Ajioka, I., Nakaguchi, K., Omata, T., Ohba, H., Fässler, R., García-Verdugo, J. M., Sekiguchi, K., Matsukawa, N., & Sawamoto, K. (2017). B1 integrin signaling promotes neuronal migration along vascular scaffolds in the post-stroke brain. *EBioMedicine*, *16*, 195-203. https://doi.org/10.1016/j.ebiom.2017.01.005

Gaiano, N., & Fishell, G. (2002). The role of notch in promoting glial and neural stem cell fates. *Annual Review of Neuroscience*, *25*, 471-490. https://doi.org/10.1146/annurev.neuro.25.030702.130823

García-Alías, G., Barkhuysen, S., Buckle, M., & Fawcett, J. W. (2009). Chondroitinase ABC treatment opens a window of opportunity for task-specific rehabilitation. *Nature Neuroscience*, *12*(9), 1145-1151. https://doi.org/10.1038/nn.2377

References

Garcion, E., Halilagic, A., Faissner, A., & ffrench-Constant, C. (2004). Generation of an environmental niche for neural stem cell development by the extracellular matrix molecule tenascin C. *Development (Cambridge, England)*, *131*(14), 3423-3432. https://doi.org/10.1242/dev.01202

Gattazzo, F., Urciuolo, A., & Bonaldo, P. (2014). Extracellular matrix: A dynamic microenvironment for stem cell niche. *Biochimica Et Biophysica Acta*, *1840*(8), 2506-2519. https://doi.org/10.1016/j.bbagen.2014.01.010

Ge, W.-P., Miyawaki, A., Gage, F. H., Jan, Y. N., & Jan, L. Y. (2012). Local generation of glia is a major astrocyte source in postnatal cortex. *Nature*, *484*(7394), 376-380. https://doi.org/10.1038/nature10959

Gelderblom, M., Leypoldt, F., Steinbach, K., Behrens, D., Choe, C.-U., Siler, D. A., Arumugam, T. V., Orthey, E., Gerloff, C., Tolosa, E., & Magnus, T. (2009). Temporal and spatial dynamics of cerebral immune cell accumulation in stroke. *Stroke*, *40*(5), 1849-1857. https://doi.org/10.1161/STROKEAHA.108.534503

George, P. M., Bliss, T. M., Hua, T., Lee, A., Oh, B., Levinson, A., Mehta, S., Sun, G., & Steinberg, G. K. (2017). Electrical preconditioning of stem cells with a conductive polymer scaffold enhances stroke recovery. *Biomaterials*, *142*, 31-40. https://doi.org/10.1016/j.biomaterials.2017.07.020

Giaume, C., Kirchhoff, F., Matute, C., Reichenbach, A., & Verkhratsky, A. (2007). Glia: The fulcrum of brain diseases. *Cell Death and Differentiation*, *14*(7), 1324-1335. https://doi.org/10.1038/sj.cdd.4402144

Girard, F., Eichenberger, S., & Celio, M. R. (2014). Thrombospondin 4 deficiency in mouse impairs neuronal migration in the early postnatal and adult brain. *Molecular and Cellular Neuroscience*, *61*, 176-186. https://doi.org/10.1016/j.mcn.2014.06.010

Gómez-Gaviro, M. V., Scott, C. E., Sesay, A. K., Matheu, A., Booth, S., Galichet, C., & Lovell-Badge, R. (2012). Betacellulin promotes cell proliferation in the neural stem cell niche and stimulates neurogenesis. *Proceedings of the National Academy of Sciences of the United States of America*, *109*(4), 1317-1322. https://doi.org/10.1073/pnas.1016199109

Gordon, R. J., McGregor, A. L., & Connor, B. (2009). Chemokines direct neural progenitor cell migration following striatal cell loss. *Molecular and Cellular Neurosciences*, *41*(2), 219-232. https://doi.org/10.1016/j.mcn.2009.03.001

Göritz, C., & Frisén, J. (2012). Neural stem cells and neurogenesis in the adult. *Cell Stem Cell*, *10*(6), 657-659. https://doi.org/10.1016/j.stem.2012.04.005

Greenberg, M. S. (2016). *Handbook of Neurosurgery*.

Grégoire, C.-A., Goldenstein, B. L., Floriddia, E. M., Barnabé-Heider, F., & Fernandes, K. J. L. (2015). Endogenous neural stem cell responses to stroke and spinal cord injury. *Glia*, *63*(8), 1469-1482. https://doi.org/10.1002/glia.22851

Guerra-Crespo, M., Gleason, D., Sistos, A., Toosky, T., Solaroglu, I., Zhang, J. H., Bryant, P. J., & Fallon, J. H. (2009). Transforming growth factor-alpha induces neurogenesis and behavioral improvement in a chronic stroke model. *Neuroscience*, *160*(2), 470-483. https://doi.org/10.1016/j.neuroscience.2009.02.029

Guo, H., Fan, Z., Wang, S., Ma, L., Wang, J., Yu, D., Zhang, Z., Wu, L., Peng, Z., Liu, W., Hou, W., & Cai, Y. (2021). Astrocytic A1/A2 paradigm participates in glycogen mobilization mediated neuroprotection on reperfusion injury after ischemic stroke. *Journal of Neuroinflammation*, *18*(1), 230. https://doi.org/10.1186/s12974-021-02284-y

Guo, Z., Zhang, L., Wu, Z., Chen, Y., Wang, F., & Chen, G. (2014). *In vivo* direct reprogramming of reactive glial cells into functional neurons after brain injury and in an Alzheimer's disease model. *Cell Stem Cell*, *14*(2), 188-202. https://doi.org/10.1016/j.stem.2013.12.001

Hack, M. A., Saghatelyan, A., de Chevigny, A., Pfeifer, A., Ashery-Padan, R., Lledo, P.-M., & Götz, M. (2005). Neuronal fate determinants of adult olfactory bulb neurogenesis. *Nature Neuroscience*, *8*(7), 865-872. https://doi.org/10.1038/nn1479

Hanke, M. L., & Kielian, T. (2011). Toll-like receptors in health and disease in the brain: Mechanisms and therapeutic potential. *Clinical Science (London, England: 1979)*, *121*(9), 367-387. https://doi.org/10.1042/CS20110164

Hauwel, M., Furon, E., Canova, C., Griffiths, M., Neal, J., & Gasque, P. (2005). Innate (inherent) control of brain infection, brain inflammation and brain repair: The role of microglia, astrocytes, «protective» glial stem cells and stromal ependymal cells. *Brain Research. Brain Research Reviews*, *48*(2), 220-233. https://doi.org/10.1016/j.brainresrev.2004.12.012

Heinrich, C., Bergami, M., Gascón, S., Lepier, A., Viganò, F., Dimou, L., Sutor, B., Berninger, B., & Götz, M. (2014). Sox2-mediated conversion of NG2 glia into induced neurons in the injured adult cerebral cortex. *Stem Cell Reports*, *3*(6), 1000-1014. https://doi.org/10.1016/j.stemcr.2014.10.007

Heinrich, C., Blum, R., Gascón, S., Masserdotti, G., Tripathi, P., Sánchez, R., Tiedt, S., Schroeder, T., Götz, M., & Berninger, B. (2010). Directing astroglia from the cerebral cortex into subtype specific functional neurons. *PLoS Biology*, *8*(5), e1000373. https://doi.org/10.1371/journal.pbio.1000373

Herculano-Houzel, S. (2014). The glia/neuron ratio: How it varies uniformly across brain structures and species and what that means for brain physiology and evolution. Glia, 62(9), 1377-1391. https://doi.org/10.1002/glia.22683

Herndon, M. E., & Lander, A. D. (1990). A diverse set of developmentally regulated proteoglycans is expressed in the rat central nervous system. *Neuron*, *4*(6), 949-961. https://doi.org/10.1016/0896-6273(90)90148-9

Hicks, C., Stevanato, L., Stroemer, R. P., Tang, E., Richardson, S., & Sinden, J. D. (2013). *In vivo* and *in vitro* characterization of the angiogenic effect of CTX0E03 human neural stem cells. *Cell Transplantation*, *22*(9), 1541-1552. https://doi.org/10.3727/096368912X657936

Höglinger, G. U., Rizk, P., Muriel, M. P., Duyckaerts, C., Oertel, W. H., Caille, I., & Hirsch, E. C. (2004). Dopamine depletion impairs precursor cell proliferation in Parkinson disease. *Nature Neuroscience*, *7*(7), 726-735. https://doi.org/10.1038/nn1265

Hossmann, K. A., Fischer, M., Bockhorst, K., & Hoehn-Berlage, M. (1994). NMR imaging of the apparent diffusion coefficient (ADC) for the evaluation of metabolic suppression and recovery after prolonged cerebral ischemia. *Journal of Cerebral Blood Flow and Metabolism: Official Journal of the International Society of Cerebral Blood Flow and Metabolism*, *14*(5), 723-731. https://doi.org/10.1038/jcbfm.1994.93

Humphries, J. D., Byron, A., & Humphries, M. J. (2006). Integrin ligands at a glance. *Journal of Cell Science*, *119*(Pt 19), 3901-3903. https://doi.org/10.1242/jcs.03098

Hynes, R. O. (1987). Integrins: A family of cell surface receptors. *Cell*, *48*(4), 549-554. https://doi.org/10.1016/0092-8674(87)90233-9

Ichikawa, N., Iwabuchi, K., Kurihara, H., Ishii, K., Kobayashi, T., Sasaki, T., Hattori, N., Mizuno, Y., Hozumi, K., Yamada, Y., & Arikawa-Hirasawa, E. (2009). Binding of laminin-1 to monosialoganglioside GM1 in lipid rafts is crucial for neurite outgrowth. *Journal of Cell Science*, *122*(Pt 2), 289-299. https://doi.org/10.1242/jcs.030338

Ihrie, R. A., Shah, J. K., Harwell, C. C., Levine, J. H., Guinto, C. D., Lezameta, M., Kriegstein, A. R., & Alvarez-Buylla, A. (2011). Persistent sonic hedgehog signaling in adult brain determines neural stem cell positional identity. *Neuron*, *71*(2), 250-262. https://doi.org/10.1016/j.neuron.2011.05.018

Imayoshi, I., Sakamoto, M., Ohtsuka, T., Takao, K., Miyakawa, T., Yamaguchi, M., Mori, K., Ikeda, T., Itohara, S., & Kageyama, R. (2008). Roles of continuous neurogenesis in the structural and functional integrity of the adult forebrain. *Nature Neuroscience*, *11*(10), 1153-1161. https://doi.org/10.1038/nn.2185

Imitola, J., Raddassi, K., Park, K. I., Mueller, F.-J., Nieto, M., Teng, Y. D., Frenkel, D., Li, J., Sidman, R. L., Walsh, C. A., Snyder, E. Y., & Khoury, S. J. (2004). Directed migration of neural stem cells to sites of CNS injury by the stromal cell-derived factor 1alpha/CXC chemokine receptor 4 pathway. *Proceedings of the National Academy of Sciences of the United States of America*, *101*(52), 18117-18122. https://doi.org/10.1073/pnas.0408258102

Itano, N., Sawai, T., Yoshida, M., Lenas, P., Yamada, Y., Imagawa, M., Shinomura, T., Hamaguchi, M., Yoshida, Y., Ohnuki, Y., Miyauchi, S., Spicer, A. P., McDonald, J. A., & Kimata, K. (1999). Three isoforms of mammalian hyaluronan synthases have distinct enzymatic properties. *The Journal of Biological Chemistry*, *274*(35), 25085-25092. https://doi.org/10.1074/jbc.274.35.25085

Ito, K., & Suda, T. (2014). Metabolic requirements for the maintenance of self-renewing stem cells. *Nature Reviews. Molecular Cell Biology*, *15*(4), 243-256. https://doi.org/10.1038/nrm3772

Jagielska, A., Lowe, A. L., Makhija, E., Wroblewska, L., Guck, J., Franklin, R. J. M., Shivashankar, G. V., & Van Vliet, K. J. (2017). Mechanical Strain Promotes Oligodendrocyte Differentiation by Global Changes of Gene Expression. *Frontiers in Cellular Neuroscience*, *11*, 93. https://doi.org/10.3389/fncel.2017.00093

Jin, K., Minami, M., Lan, J. Q., Mao, X. O., Batteur, S., Simon, R. P., & Greenberg, D. A. (2001). Neurogenesis in dentate subgranular zone and rostral subventricular zone after focal cerebral ischemia in the rat. *Proceedings of the National Academy of Sciences of the United States of America*, *98*(8), 4710-4715. https://doi.org/10.1073/pnas.081011098

Jin, K., Sun, Y., Xie, L., Peel, A., Mao, X. O., Batteur, S., & Greenberg, D. A. (2003). Directed migration of neuronal precursors into the ischemic cerebral cortex and striatum. *Molecular and Cellular Neurosciences*, *24*(1), 171-189. https://doi.org/10.1016/s1044-7431(03)00159-3

References

Jin, K., Zhu, Y., Sun, Y., Mao, X. O., Xie, L., & Greenberg, D. A. (2002). Vascular endothelial growth factor (VEGF) stimulates neurogenesis *in vitro* and *in vivo*. *Proceedings of the National Academy of Sciences of the United States of America*, *99*(18), 11946-11950. https://doi.org/10.1073/pnas.182296499

Jin, W.-N., Shi, S. X.-Y., Li, Z., Li, M., Wood, K., Gonzales, R. J., & Liu, Q. (2017). Depletion of microglia exacerbates postischemic inflammation and brain injury. *Journal of Cerebral Blood Flow and Metabolism: Official Journal of the International Society of Cerebral Blood Flow and Metabolism*, *37*(6), 2224-2236. https://doi.org/10.1177/0271678X17694185

Johansson, C. B., Momma, S., Clarke, D. L., Risling, M., Lendahl, U., & Frisén, J. (1999). Identification of a neural stem cell in the adult mammalian central nervous system. *Cell*, *96*(1), 25-34. https://doi.org/10.1016/s0092-8674(00)80956-3

Jokinen, H., Melkas, S., Ylikoski, R., Pohjasvaara, T., Kaste, M., Erkinjuntti, T., & Hietanen, M. (2015). Post-stroke cognitive impairment is common even after successful clinical recovery. *European Journal of Neurology*, *22*(9), 1288-1294. https://doi.org/10.1111/ene.12743

Jurkowski, M. P., Bettio, L., K Woo, E., Patten, A., Yau, S.-Y., & Gil-Mohapel, J. (2020). Beyond the Hippocampus and the SVZ: Adult Neurogenesis Throughout the Brain. *Frontiers in Cellular Neuroscience*, *14*, 576444. https://doi.org/10.3389/fncel.2020.576444

Justicia, C., Panés, J., Solé, S., Cervera, A., Deulofeu, R., Chamorro, A., & Planas, A. M. (2003). Neutrophil infiltration increases matrix metalloproteinase-9 in the ischemic brain after occlusion/reperfusion of the middle cerebral artery in rats. *Journal of Cerebral Blood Flow and Metabolism: Official Journal of the International Society of Cerebral Blood Flow and Metabolism*, *23*(12), 1430-1440. https://doi.org/10.1097/01.WCB.0000090680.07515.C8

Kalogeris, T., Baines, C. P., Krenz, M., & Korthuis, R. J. (2012). Cell biology of ischemia/reperfusion injury. *International Review of Cell and Molecular Biology*, *298*, 229-317. https://doi.org/10.1016/B978-0-12-394309-5.00006-7

Kang, P., Lee, H. K., Glasgow, S. M., Finley, M., Donti, T., Gaber, Z. B., Graham, B. H., Foster, A. E., Novitch, B. G., Gronostajski, R. M., & Deneen, B. (2012). Sox9 and NFIA coordinate a transcriptional regulatory cascade during the initiation of gliogenesis. *Neuron*, *74*(1), 79-94. https://doi.org/10.1016/j.neuron.2012.01.024

Katarzyna Greda, A., & Nowicka, D. (2021). Hyaluronidase inhibition accelerates functional recovery from stroke in the mouse brain. *Journal of Neurochemistry*, *157*(3), 781-801. https://doi.org/10.1111/jnc.15279

Katsimpardi, L., Litterman, N. K., Schein, P. A., Miller, C. M., Loffredo, F. S., Wojtkiewicz, G. R., Chen, J. W., Lee, R. T., Wagers, A. J., & Rubin, L. L. (2014). Vascular and neurogenic rejuvenation of the aging mouse brain by young systemic factors. *Science (New York, N.Y.)*, *344*(6184), 630-634. https://doi.org/10.1126/science.1251141

Kazanis, I., Belhadi, A., Faissner, A., & Ffrench-Constant, C. (2007). The adult mouse subependymal zone regenerates efficiently in the absence of tenascin-C. *The Journal of Neuroscience: The Official Journal of the Society for Neuroscience*, *27*(51), 13991-13996. https://doi.org/10.1523/JNEUROSCI.3279-07.2007

Kazanis, I., Lathia, J. D., Vadakkan, T. J., Raborn, E., Wan, R., Mughal, M. R., Eckley, D. M., Sasaki, T., Patton, B., Mattson, M. P., Hirschi, K. K., Dickinson, M. E., & ffrench-Constant, C. (2010). Quiescence and activation of stem and precursor cell populations in the subependymal zone of the mammalian brain are associated with distinct cellular and extracellular matrix signals. *The Journal of Neuroscience: The Official Journal of the Society for Neuroscience*, *30*(29), 9771-9781. https://doi.org/10.1523/JNEUROSCI.0700-10.2010

Kempermann, G. (2012). New neurons for «survival of the fittest». *Nature Reviews. Neuroscience*, *13*(10), 727-736. https://doi.org/10.1038/nrn3319

Kempermann, G., Gage, F. H., Aigner, L., Song, H., Curtis, M. A., Thuret, S., Kuhn, H. G., Jessberger, S., Frankland, P. W., Cameron, H. A., Gould, E., Hen, R., Abrous, D. N., Toni, N., Schinder, A. F., Zhao, X., Lucassen, P. J., & Frisén, J. (2018). Human Adult Neurogenesis: Evidence and Remaining Questions. *Cell Stem Cell*, *23*(1), 25-30. https://doi.org/10.1016/j.stem.2018.04.004

Kerever, A., Schnack, J., Vellinga, D., Ichikawa, N., Moon, C., Arikawa-Hirasawa, E., Efird, J. T., & Mercier, F. (2007). Novel extracellular matrix structures in the neural stem cell niche capture the neurogenic factor fibroblast growth factor 2 from the extracellular milieu. *Stem Cells (Dayton, Ohio)*, *25*(9), 2146-2157. https://doi.org/10.1634/stemcells.2007-0082

Kerever, A., Yamada, T., Suzuki, Y., Mercier, F., & Arikawa-Hirasawa, E. (2015). Fractone aging in the subventricular zone of the lateral ventricle. *Journal of Chemical Neuroanatomy*, *66-67*, 52-60. https://doi.org/10.1016/j.jchemneu.2015.06.001

Kettenmann, H., Kirchhoff, F., & Verkhratsky, A. (2013). Microglia: New roles for the synaptic stripper. *Neuron*, *77*(1), 10-18. https://doi.org/10.1016/j.neuron.2012.12.023

Khaing, Z. Z., & Seidlits, S. K. (2015). Hyaluronic acid and neural stem cells: Implications for biomaterial design. *Journal of Materials Chemistry. B*, *3*(40), 7850-7866. https://doi.org/10.1039/c5tb00974j

Kim, B.-W., More, S. V., Yun, Y.-S., Ko, H.-M., Kwak, J.-H., Lee, H., Suk, K., Kim, I.-S., & Choi, D.-K. (2016). A novel synthetic compound MCAP suppresses LPS-induced murine microglial activation *in vitro* via inhibiting NF-kB and p38 MAPK pathways. *Acta Pharmacologica Sinica*, *37*(3), 334-343. https://doi.org/10.1038/aps.2015.138

Kim, Y., Wang, W.-Z., Comte, I., Pastrana, E., Tran, P. B., Brown, J., Miller, R. J., Doetsch, F., Molnár, Z., & Szele, F. G. (2010). Dopamine stimulation of postnatal murine subventricular zone neurogenesis via the D3 receptor. *Journal of Neurochemistry*, *114*(3), 750-760. https://doi.org/10.1111/j.1471-4159.2010.06799.x

Kippin, T. E., Kapur, S., & van der Kooy, D. (2005). Dopamine specifically inhibits forebrain neural stem cell proliferation, suggesting a novel effect of antipsychotic drugs. *The Journal of Neuroscience: The Official Journal of the Society for Neuroscience*, *25*(24), 5815-5823. https://doi.org/10.1523/JNEUROSCI.1120-05.2005

Kjell, J., Fischer-Sternjak, J., Thompson, A. J., Friess, C., Sticco, M. J., Salinas, F., Cox, J., Martinelli, D. C., Ninkovic, J., Franze, K., Schiller, H. B., & Götz, M. (2020). Defining the Adult Neural Stem Cell Niche Proteome Identifies Key Regulators of Adult Neurogenesis. *Cell Stem Cell*, *26*(2), 277-293.e8. https://doi.org/10.1016/j.stem.2020.01.002

Knoth, R., Singec, I., Ditter, M., Pantazis, G., Capetian, P., Meyer, R. P., Horvat, V., Volk, B., & Kempermann, G. (2010). Murine features of neurogenesis in the human hippocampus across the lifespan from 0 to 100 years. *PloS One*, *5*(1), e8809. https://doi.org/10.1371/journal.pone.0008809

Koh, T. J., & DiPietro, L. A. (2011). Inflammation and wound healing: The role of the macrophage. *Expert Reviews in Molecular Medicine*, *13*, e23. https://doi.org/10.1017/S1462399411001943

Kohwi, M., Osumi, N., Rubenstein, J. L. R., & Alvarez-Buylla, A. (2005). Pax6 is required for making specific subpopulations of granule and periglomerular neurons in the olfactory bulb. *The Journal of Neuroscience: The Official Journal of the Society for Neuroscience*, *25*(30), 6997-7003. https://doi.org/10.1523/JNEUROSCI.1435-05.2005

Kojima, T., Hirota, Y., Ema, M., Takahashi, S., Miyoshi, I., Okano, H., & Sawamoto, K. (2010). Subventricular zone-derived neural progenitor cells migrate along a blood vessel scaffold toward the post-stroke striatum. *Stem Cells (Dayton, Ohio)*, *28*(3), 545-554. https://doi.org/10.1002/stem.306

Kokovay, E., Goderie, S., Wang, Y., Lotz, S., Lin, G., Sun, Y., Roysam, B., Shen, Q., & Temple, S. (2010). Adult SVZ lineage cells home to and leave the vascular niche via differential responses to SDF1/CXCR4 signaling. *Cell Stem Cell*, *7*(2), 163-173. https://doi.org/10.1016/j.stem.2010.05.019

Kolb, B., Morshead, C., Gonzalez, C., Kim, M., Gregg, C., Shingo, T., & Weiss, S. (2007). Growth factor-stimulated generation of new cortical tissue and functional recovery after stroke damage to the motor cortex of rats. *Journal of Cerebral Blood Flow and Metabolism: Official Journal of the International Society of Cerebral Blood Flow and Metabolism*, *27*(5), 983-997. https://doi.org/10.1038/sj.jcbfm.9600402

Köppe, G., Brückner, G., Härtig, W., Delpech, B., & Bigl, V. (1997). Characterization of proteoglycan-containing perineuronal nets by enzymatic treatments of rat brain sections. *The Histochemical Journal*, *29*(1), 11-20. https://doi.org/10.1023/a:1026408716522

Kwok, J. C. F., Dick, G., Wang, D., & Fawcett, J. W. (2011). Extracellular matrix and perineuronal nets in CNS repair. *Developmental Neurobiology*, *71*(11), 1073-1089. https://doi.org/10.1002/dneu.20974

Lalancette-Hébert, M., Gowing, G., Simard, A., Weng, Y. C., & Kriz, J. (2007). Selective ablation of proliferating microglial cells exacerbates ischemic injury in the brain. *The Journal of Neuroscience: The Official Journal of the Society for Neuroscience*, *27*(10), 2596-2605. https://doi.org/10.1523/JNEUROSCI.5360-06.2007

Laterza, C., Wattananit, S., Uoshima, N., Ge, R., Pekny, R., Tornero, D., Monni, E., Lindvall, O., & Kokaia, Z. (2017). Monocyte depletion early after stroke promotes neurogenesis from endogenous neural stem cells in adult brain. *Experimental Neurology*, *297*, 129-137. https://doi.org/10.1016/j.expneurol.2017.07.012

Lau, L. W., Cua, R., Keough, M. B., Haylock-Jacobs, S., & Yong, V. W. (2013). Pathophysiology of the brain extracellular matrix: A new target for remyelination. Nature Reviews. Neuroscience, 14(10), 722-729. https://doi.org/10.1038/nrn3550

Laug, D., Huang, T.-W., Huerta, N. A. B., Huang, A. Y.-S., Sardar, D., Ortiz-Guzman, J., Carlson, J. C., Arenkiel, B. R., Kuo, C. T., Mohila, C. A., Glasgow, S. M., Lee, H. K., & Deneen, B. (2019). Nuclear factor I-A regulates diverse reactive astrocyte responses after CNS injury. *The Journal of Clinical Investigation*, *129*(10), 4408-4418. https://doi.org/10.1172/JCI127492

References

Lawler, J., McHenry, K., Duquette, M., & Derick, L. (1995). Characterization of human thrombospondin-4. *The Journal of Biological Chemistry*, *270*(6), 2809-2814. https://doi.org/10.1074/jbc.270.6.2809

Le Belle, J. E., Orozco, N. M., Paucar, A. A., Saxe, J. P., Mottahedeh, J., Pyle, A. D., Wu, H., & Kornblum, H. I. (2011). Proliferative neural stem cells have high endogenous ROS levels that regulate self-renewal and neurogenesis in a PI3K/Akt-dependant manner. *Cell Stem Cell*, *8*(1), 59-71. https://doi.org/10.1016/j.stem.2010.11.028

Lee, J. H., Lee, J. E., Kahng, J. Y., Kim, S. H., Park, J. S., Yoon, S. J., Um, J.-Y., Kim, W. K., Lee, J.-K., Park, J., Kim, E. H., Lee, J.-H., Lee, J.-H., Chung, W.-S., Ju, Y. S., Park, S.-H., Chang, J. H., Kang, S.-G., & Lee, J. H. (2018). Human glioblastoma arises from subventricular zone cells with low-level driver mutations. *Nature*, *560*(7717), 243-247. https://doi.org/10.1038/s41586-018-0389-3

Lee, N., Batt, M. K., Cronier, B. A., Jackson, M. C., Bruno Garza, J. L., Trinh, D. S., Mason, C. O., Spearry, R. P., Bhattacharya, S., Robitz, R., Nakafuku, M., & MacLennan, A. J. (2013). Ciliary neurotrophic factor receptor regulation of adult forebrain neurogenesis. *The Journal of Neuroscience: The Official Journal of the Society for Neuroscience*, *33*(3), 1241-1258. https://doi.org/10.1523/JNEUROSCI.3386-12.2013

Lehtinen, M. K., & Walsh, C. A. (2011). Neurogenesis at the brain-cerebrospinal fluid interface. *Annual Review of Cell and Developmental Biology*, *27*, 653-679. https://doi.org/10.1146/annurev-cellbio-092910-154026

Lei, W., Li, W., Ge, L., & Chen, G. (2019). Non-engineered and Engineered Adult Neurogenesis in Mammalian Brains. *Frontiers in Neuroscience*, *13*, 131. https://doi.org/10.3389/fnins.2019.00131

Lennington, J. B., Pope, S., Goodheart, A. E., Drozdowicz, L., Daniels, S. B., Salamone, J. D., & Conover, J. C. (2011). Midbrain dopamine neurons associated with reward processing innervate the neurogenic subventricular zone. *The Journal of Neuroscience: The Official Journal of the Society for Neuroscience*, *31*(37), 13078-13087. https://doi.org/10.1523/JNEUROSCI.1197-11.2011

Leonoudakis, D., Zhao, P., & Beattie, E. C. (2008). Rapid tumor necrosis factor alpha-induced exocytosis of glutamate receptor 2-lacking AMPA receptors to extrasynaptic plasma membrane potentiates excitotoxicity. *The Journal of Neuroscience: The Official Journal of the Society for Neuroscience*, *28*(9), 2119-2130. https://doi.org/10.1523/JNEUROSCI.5159-07.2008

Lewén, A., Matz, P., & Chan, P. H. (2000). Free radical pathways in CNS injury. *Journal of Neurotrauma*, *17*(10), 871-890. https://doi.org/10.1089/neu.2000.17.871

Leys, D., Hénon, H., Mackowiak-Cordoliani, M.-A., & Pasquier, F. (2005). Poststroke dementia. *The Lancet. Neurology*, *4*(11), 752-759. https://doi.org/10.1016/S1474-4422(05)70221-0

Li, H., & Chen, G. (2016). *In Vivo* Reprogramming for CNS Repair: Regenerating Neurons from Endogenous Glial Cells. *Neuron*, *91*(4), 728-738. https://doi.org/10.1016/j.neuron.2016.08.004

Li, L., Candelario, K. M., Thomas, K., Wang, R., Wright, K., Messier, A., & Cunningham, L. A. (2014). Hypoxia Inducible Factor-1α (HIF-1α) Is Required for Neural Stem Cell Maintenance and Vascular Stability in the Adult Mouse SVZ. *The Journal of Neuroscience*, *34*(50), 16713-16719. https://doi.org/10.1523/JNEUROSCI.4590-13.2014

Li, L., Harms, K. M., Ventura, P. B., Lagace, D. C., Eisch, A. J., & Cunningham, L. A. (2010). Focal cerebral ischemia induces a multilineage cytogenic response from adult subventricular zone that is predominantly gliogenic. *Glia*, *58*(13), 1610-1619. https://doi.org/10.1002/glia.21033

Li, Q., Zhang, R., Guo, Y.-L., & Mei, Y.-W. (2009). Effect of neuregulin on apoptosis and expressions of STAT3 and GFAP in rats following cerebral ischemic reperfusion. *Journal of Molecular Neuroscience: MN*, *37*(1), 67-73. https://doi.org/10.1007/s12031-008-9121-3

Li, Y., Chen, J., & Chopp, M. (2002). Cell proliferation and differentiation from ependymal, subependymal and choroid plexus cells in response to stroke in rats. *Journal of the Neurological Sciences*, *193*(2), 137-146. https://doi.org/10.1016/s0022-510x(01)00657-8

Liang, H., Zhao, H., Gleichman, A., Machnicki, M., Telang, S., Tang, S., Rshtouni, M., Ruddell, J., & Carmichael, S. T. (2019). Region-specific and activity-dependent regulation of SVZ neurogenesis and recovery after stroke. *Proceedings of the National Academy of Sciences*, *116*(27), 13621-13630. https://doi.org/10.1073/pnas.1811825116

Liddelow, S. A., Guttenplan, K. A., Clarke, L. E., Bennett, F. C., Bohlen, C. J., Schirmer, L., Bennett, M. L., Münch, A. E., Chung, W.-S., Peterson, T. C., Wilton, D. K., Frouin, A., Napier, B. A., Panicker, N., Kumar, M., Buckwalter, M. S., Rowitch, D. H., Dawson, V. L., Dawson, T. M., … Barres, B. A. (2017). Neurotoxic reactive astrocytes are induced by activated microglia. *Nature*, *541*(7638), 481-487. https://doi.org/10.1038/nature21029

Lie, D.-C., Colamarino, S. A., Song, H.-J., Désiré, L., Mira, H., Consiglio, A., Lein, E. S., Jessberger, S., Lansford, H., Dearie, A. R., & Gage, F. H. (2005). Wnt signalling regulates adult hippocampal neurogenesis. *Nature*, *437*(7063), 1370-1375. https://doi.org/10.1038/nature04108

Lim, D. A., & Alvarez-Buylla, A. (2016). The Adult Ventricular–Subventricular Zone (V-SVZ) and Olfactory Bulb (OB) Neurogenesis. *Cold Spring Harbor Perspectives in Biology*, *8*(5), a018820. https://doi.org/10.1101/cshperspect.a018820

Lim, D. A., Tramontin, A. D., Trevejo, J. M., Herrera, D. G., García-Verdugo, J. M., & Alvarez-Buylla, A. (2000). Noggin antagonizes BMP signaling to create a niche for adult neurogenesis. *Neuron*, *28*(3), 713-726. https://doi.org/10.1016/s0896-6273(00)00148-3

Lin, M. P., & Liebeskind, D. S. (2016). Imaging of Ischemic Stroke. *Continuum (Minneapolis, Minn.)*, *22*(5, Neuroimaging), 1399-1423. https://doi.org/10.1212/CON.0000000000000376

Lindwall, C., Olsson, M., Osman, A. M., Kuhn, H. G., & Curtis, M. A. (2013). Selective expression of hyaluronan and receptor for hyaluronan mediated motility (Rhamm) in the adult mouse subventricular zone and rostral migratory stream and in ischemic cortex. *Brain Research*, *1503*, 62-77. https://doi.org/10.1016/j.brainres.2013.01.045

Litwiniuk, M., Krejner, A., Speyrer, M. S., Gauto, A. R., & Grzela, T. (2016). Hyaluronic Acid in Inflammation and Tissue Regeneration. *Wounds: A Compendium of Clinical Research and Practice*, *28*(3), 78-88.

Liu, Q., Sanai, N., Jin, W.-N., La Cava, A., Van Kaer, L., & Shi, F.-D. (2016). Neural stem cells sustain natural killer cells that dictate recovery from brain inflammation. *Nature Neuroscience*, *19*(2), 243-252. https://doi.org/10.1038/nn.4211

Liu, S.-P., Fu, R.-H., Wu, D.-C., Hsu, C.-Y., Chang, C.-H., Lee, W., Lee, Y.-D., Liu, C. H., Chien, Y.-J., Lin, S.-Z., & Shyu, W.-C. (2014). Mouse-induced pluripotent stem cells generated under hypoxic conditions in the absence of viral infection and oncogenic factors and used for ischemic stroke therapy. *Stem Cells and Development*, *23*(4), 421-433. https://doi.org/10.1089/scd.2013.0182

Liu, X. S., Chopp, M., Zhang, R. L., Tao, T., Wang, X. L., Kassis, H., Hozeska-Solgot, A., Zhang, L., Chen, C., & Zhang, Z. G. (2011). MicroRNA profiling in subventricular zone after stroke: MiR-124a regulates proliferation of neural progenitor cells through Notch signaling pathway. *PloS One*, *6*(8), e23461. https://doi.org/10.1371/journal.pone.0023461

Liu, X. S., Zhang, Z. G., Zhang, R. L., Gregg, S., Morris, D. C., Wang, Y., & Chopp, M. (2007). Stroke induces gene profile changes associated with neurogenesis and angiogenesis in adult subventricular zone progenitor cells. *Journal of Cerebral Blood Flow and Metabolism: Official Journal of the International Society of Cerebral Blood Flow and Metabolism*, *27*(3), 564-574. https://doi.org/10.1038/sj.jcbfm.9600371

Liu, X., Wang, Q., Haydar, T. F., & Bordey, A. (2005). Nonsynaptic GABA signaling in postnatal subventricular zone controls proliferation of GFAP-expressing progenitors. *Nature Neuroscience*, *8*(9), 1179-1187. https://doi.org/10.1038/nn1522

Llorens-Bobadilla, E., Chell, J. M., Merre, P. L., Wu, Y., Zamboni, M., Bergenstråhle, J., Stenudd, M., Sopova, E., Lundeberg, J., Shupliakov, O., Carlén, M., & Frisén, J. (2020). A latent lineage potential in resident neural stem cells enables spinal cord repair. *Science*, *370*(6512), Article 6512. https://doi.org/10.1126/science.abb8795

Llorens-Bobadilla, E., Zhao, S., Baser, A., Saiz-Castro, G., Zwadlo, K., & Martin-Villalba, A. (2015). Single-Cell Transcriptomics Reveals a Population of Dormant Neural Stem Cells that Become Activated upon Brain Injury. *Cell Stem Cell*, *17*(3), 329-340. https://doi.org/10.1016/j.stem.2015.07.002

Lo, E. H. (2008). A new penumbra: Transitioning from injury into repair after stroke. *Nature Medicine*, *14*(5), 497-500. https://doi.org/10.1038/nm1735

López-Juárez, A., Howard, J., Ullom, K., Howard, L., Grande, A., Pardo, A., Waclaw, R., Sun, Y.-Y., Yang, D., Kuan, C.-Y., Campbell, K., & Nakafuku, M. (2013). Gsx2 controls region-specific activation of neural stem cells and injury-induced neurogenesis in the adult subventricular zone. *Genes & Development*, *27*(11), 1272-1287. https://doi.org/10.1101/gad.217539.113

Lu, Z., & Kipnis, J. (2010). Thrombospondin 1—A key astrocyte-derived neurogenic factor. *FASEB Journal: Official Publication of the Federation of American Societies for Experimental Biology*, *24*(6), 1925-1934. https://doi.org/10.1096/fj.09-150573

Luckenbill-Edds, L., & Carrington, J. L. (1988). Effect of hyaluronic acid on the emergence of neural crest cells from the neural tube of the quail, Coturnix coturnix japonica. *Cell and Tissue Research*, *252*(3), 573-579. https://doi.org/10.1007/BF00216644

Luo, J., Daniels, S. B., Lennington, J. B., Notti, R. Q., & Conover, J. C. (2006). The aging neurogenic subventricular zone. *Aging Cell*, *5*(2), 139-152. https://doi.org/10.1111/j.1474-9726.2006.00197.x

References

Luskin, M. B. (1998). Neuroblasts of the postnatal mammalian forebrain: Their phenotype and fate. *Journal of Neurobiology*, *36*(2), 221-233.

Luskin, M. B., & McDermott, K. (1994). Divergent lineages for oligodendrocytes and astrocytes originating in the neonatal forebrain subventricular zone. *Glia*, *11*(3), 211-226. https://doi.org/10.1002/glia.440110302

Lynch, J. M., Maillet, M., Vanhoutte, D., Schloemer, A., Sargent, M. A., Blair, N. S., Lynch, K. A., Okada, T., Aronow, B. J., Osinska, H., Prywes, R., Lorenz, J. N., Mori, K., Lawler, J., Robbins, J., & Molkentin, J. D. (2012). A thrombospondin-dependent pathway for a protective ER stress response. *Cell*, *149*(6), 1257-1268. https://doi.org/10.1016/j.cell.2012.03.050

Ma, Y., Wang, J., Wang, Y., & Yang, G.-Y. (2017). The biphasic function of microglia in ischemic stroke. *Progress in Neurobiology*, *157*, 247-272. https://doi.org/10.1016/j.pneurobio.2016.01.005

Macrae, I. M. (2011). Preclinical stroke research—Advantages and disadvantages of the most common rodent models of focal ischaemia. *British Journal of Pharmacology*, *164*(4), 1062-1078. https://doi.org/10.1111/j.1476-5381.2011.01398.x

Magnusson, J. P., & Frisén, J. (2016). Stars from the darkest night: Unlocking the neurogenic potential of astrocytes in different brain regions. *Development (Cambridge, England)*, *143*(7), 1075-1086. https://doi.org/10.1242/dev.133975

Magnusson, J. P., Göritz, C., Tatarishvili, J., Dias, D. O., Smith, E. M. K., Lindvall, O., Kokaia, Z., & Frisén, J. (2014). A latent neurogenic program in astrocytes regulated by Notch signaling in the mouse. *Science (New York, N.Y.)*, *346*(6206), 237-241. https://doi.org/10.1126/science.346.6206.237

Mandai, K., Matsumoto, M., Kitagawa, K., Matsushita, K., Ohtsuki, T., Mabuchi, T., Colman, D. R., Kamada, T., & Yanagihara, T. (1997). Ischemic damage and subsequent proliferation of oligodendrocytes in focal cerebral ischemia. *Neuroscience*, *77*(3), 849-861.

Marcialis, M. A., Coni, E., Pintus, M. C., Ravarino, A., Fanos, V., Coni, C., & Faa, G. (2016). Introduction to embryonic and adult neural stem cells: From the metabolic circuits of the niches to the metabolome. *Journal of Pediatric and Neonatal Individualized Medicine (JPNIM)*, *5*(2), e050215-e050215. https://doi.org/10.7363/050215

Margolis, R. U., & Margolis, R. K. (1989). Nervous tissue proteoglycans. *Developmental Neuroscience*, *11*(4-5), 276-288. https://doi.org/10.1159/000111906

Marquardt, L., Anders, C., Buggle, F., Palm, F., Hellstern, P., & Grau, A. J. (2009). Leukocyte-platelet aggregates in acute and subacute ischemic stroke. *Cerebrovascular Diseases (Basel, Switzerland)*, *28*(3), 276-282. https://doi.org/10.1159/000228710

Marques, F., Sousa, J. C., Coppola, G., Gao, F., Puga, R., Brentani, H., Geschwind, D. H., Sousa, N., Correia-Neves, M., & Palha, J. A. (2011). Transcriptome signature of the adult mouse choroid plexus. *Fluids and Barriers of the CNS*, *8*(1), 10. https://doi.org/10.1186/2045-8118-8-10

Marthiens, V., Kazanis, I., Moss, L., Long, K., & Ffrench-Constant, C. (2010). Adhesion molecules in the stem cell niche—More than just staying in shape? *Journal of Cell Science*, *123*(Pt 10), 1613-1622. https://doi.org/10.1242/jcs.054312

Martí-Fàbregas, J., Romaguera-Ros, M., Gómez-Pinedo, U., Martínez-Ramírez, S., Jiménez-Xarrié, E., Marín, R., Martí-Vilalta, J.-L., & García-Verdugo, J.-M. (2010). Proliferation in the human ipsilateral subventricular zone after ischemic stroke. *Neurology*, *74*(5), 357-365. https://doi.org/10.1212/WNL.0b013e3181cbccec

Martinez, F. O., & Gordon, S. (2014). The M1 and M2 paradigm of macrophage activation: Time for reassessment. *F1000prime Reports*, *6*, 13. https://doi.org/10.12703/P6-13

Martino, G., Butti, E., & Bacigaluppi, M. (2014). Neurogenesis or non-neurogenesis: That is the question. *The Journal of Clinical Investigation*, *124*(3), 970-973. https://doi.org/10.1172/JCI74419

Maslov, A. Y., Barone, T. A., Plunkett, R. J., & Pruitt, S. C. (2004). Neural stem cell detection, characterization, and age-related changes in the subventricular zone of mice. *The Journal of Neuroscience: The Official Journal of the Society for Neuroscience*, *24*(7), 1726-1733. https://doi.org/10.1523/JNEUROSCI.4608-03.2004

Mathiisen, T. M., Lehre, K. P., Danbolt, N. C., & Ottersen, O. P. (2010). The perivascular astroglial sheath provides a complete covering of the brain microvessels: An electron microscopic 3D reconstruction. *Glia*, *58*(9), 1094-1103. https://doi.org/10.1002/glia.20990

Matsuda, T., Irie, T., Katsurabayashi, S., Hayashi, Y., Nagai, T., Hamazaki, N., Adefuin, A. M. D., Miura, F., Ito, T., Kimura, H., Shirahige, K., Takeda, T., Iwasaki, K., Imamura, T., & Nakashima, K. (2019). Pioneer Factor NeuroD1 Rearranges Transcriptional and Epigenetic Profiles to Execute Microglia-Neuron Conversion. *Neuron*, *101*(3), 472-485.e7. https://doi.org/10.1016/j.neuron.2018.12.010

Mattugini, N., Bocchi, R., Scheuss, V., Russo, G. L., Torper, O., Lao, C. L., & Götz, M. (2019). Inducing Different Neuronal Subtypes from Astrocytes in the Injured Mouse Cerebral Cortex. *Neuron*, *103*(6), 1086-1095.e5. https://doi.org/10.1016/j.neuron.2019.08.009

McTigue, D. M., & Tripathi, R. B. (2008). The life, death, and replacement of oligodendrocytes in the adult CNS. *Journal of Neurochemistry*, *107*(1), 1-19. https://doi.org/10.1111/j.1471-4159.2008.05570.x

Menn, B., Garcia-Verdugo, J. M., Yaschine, C., Gonzalez-Perez, O., Rowitch, D., & Alvarez-Buylla, A. (2006). Origin of oligodendrocytes in the subventricular zone of the adult brain. *The Journal of Neuroscience: The Official Journal of the Society for Neuroscience*, *26*(30), 7907-7918. https://doi.org/10.1523/JNEUROSCI.1299-06.2006

Mercier, F., & Douet, V. (2014). Bone morphogenetic protein-4 inhibits adult neurogenesis and is regulated by fractone-associated heparan sulfates in the subventricular zone. *Journal of Chemical Neuroanatomy*, *57-58*, 54-61. https://doi.org/10.1016/j.jchemneu.2014.03.005

Mercier, F., Kitasako, J. T., & Hatton, G. I. (2002). Anatomy of the brain neurogenic zones revisited: Fractones and the fibroblast/macrophage network. *The Journal of Comparative Neurology*, *451*(2), 170-188. https://doi.org/10.1002/cne.10342

Merkle, F. T., Fuentealba, L. C., Sanders, T. A., Magno, L., Kessaris, N., & Alvarez-Buylla, A. (2014). Adult neural stem cells in distinct microdomains generate previously unknown interneuron types. *Nature Neuroscience*, *17*(2), 207-214. https://doi.org/10.1038/nn.3610

Merkle, F. T., Mirzadeh, Z., & Alvarez-Buylla, A. (2007). Mosaic organization of neural stem cells in the adult brain. *Science (New York, N.Y.)*, *317*(5836), 381-384. https://doi.org/10.1126/science.1144914

Merkle, F. T., Tramontin, A. D., García-Verdugo, J. M., & Alvarez-Buylla, A. (2004). Radial glia give rise to adult neural stem cells in the subventricular zone. *Proceedings of the National Academy of Sciences of the United States of America*, *101*(50), 17528-17532. https://doi.org/10.1073/pnas.0407893101

Ming, G.-L., & Song, H. (2011). Adult neurogenesis in the mammalian brain: Significant answers and significant questions. *Neuron*, *70*(4), 687-702. https://doi.org/10.1016/j.neuron.2011.05.001

Miranda, C. J., Braun, L., Jiang, Y., Hester, M. E., Zhang, L., Riolo, M., Wang, H., Rao, M., Altura, R. A., & Kaspar, B. K. (2012). Aging brain microenvironment decreases hippocampal neurogenesis through Wnt-mediated survivin signaling. *Aging Cell*, *11*(3), 542-552. https://doi.org/10.1111/j.1474-9726.2012.00816.x

Mirzadeh, Z., Doetsch, F., Sawamoto, K., Wichterle, H., & Alvarez-Buylla, A. (2010). The subventricular zone en-face: Wholemount staining and ependymal flow. *Journal of Visualized Experiments: JoVE*, *39*, 1938. https://doi.org/10.3791/1938

Mirzadeh, Z., Merkle, F. T., Soriano-Navarro, M., Garcia-Verdugo, J. M., & Alvarez-Buylla, A. (2008). Neural stem cells confer unique pinwheel architecture to the ventricular surface in neurogenic regions of the adult brain. *Cell Stem Cell*, *3*(3), 265-278. https://doi.org/10.1016/j.stem.2008.07.004

Mizrak, D., Levitin, H. M., Delgado, A. C., Crotet, V., Yuan, J., Chaker, Z., Silva-Vargas, V., Sims, P. A., & Doetsch, F. (2019). Single-Cell Analysis of Regional Differences in Adult V-SVZ Neural Stem Cell Lineages. *Cell Reports*, *26*(2), 394-406.e5. https://doi.org/10.1016/j.celrep.2018.12.044

Montilla, A., Zabala, A., Matute, C., & Domercq, M. (2020). Functional and Metabolic Characterization of Microglia Culture in a Defined Medium. *Frontiers in Cellular Neuroscience*, *14*, 22. https://doi.org/10.3389/fncel.2020.00022

Moon, L. D., Asher, R. A., Rhodes, K. E., & Fawcett, J. W. (2001). Regeneration of CNS axons back to their target following treatment of adult rat brain with chondroitinase ABC. *Nature Neuroscience*, *4*(5), 465-466. https://doi.org/10.1038/87415

Morante-Redolat, J. M., & Porlan, E. (2019). Neural Stem Cell Regulation by Adhesion Molecules Within the Subependymal Niche. *Frontiers in Cell and Developmental Biology*, *7*, 102. https://doi.org/10.3389/fcell.2019.00102

Moreno-Jiménez, E. P., Flor-García, M., Terreros-Roncal, J., Rábano, A., Cafini, F., Pallas-Bazarra, N., Ávila, J., & Llorens-Martín, M. (2019). Adult hippocampal neurogenesis is abundant in neurologically healthy subjects and drops sharply in patients with Alzheimer's disease. Nature Medicine, 25(4), 554-560. https://doi.org/10.1038/s41591-019-0375-9

Morgan, M. R., Humphries, M. J., & Bass, M. D. (2007). Synergistic control of cell adhesion by integrins and syndecans. *Nature Reviews. Molecular Cell Biology*, *8*(12), 957-969. https://doi.org/10.1038/nrm2289

Moshayedi, P., & Carmichael, S. T. (2013). Hyaluronan, neural stem cells and tissue reconstruction after acute ischemic stroke. *Biomatter*, *3*(1), e23863. https://doi.org/10.4161/biom.23863

References

Muppala, S., Xiao, R., Krukovets, I., Verbovetsky, D., Yendamuri, R., Habib, N., Raman, P., Plow, E., & Stenina-Adognravi, O. (2017). Thrombospondin-4 mediates TGF-β-induced angiogenesis. *Oncogene*, *36*(36), 5189-5198. https://doi.org/10.1038/onc.2017.140

Musuka, T. D., Wilton, S. B., Traboulsi, M., & Hill, M. D. (2015). Diagnosis and management of acute ischemic stroke: Speed is critical. *CMAJ: Canadian Medical Association Journal = Journal de l'Association Medicale Canadienne*, *187*(12), 887-893. https://doi.org/10.1503/cmaj.140355

Nait-Oumesmar, B., Picard-Riéra, N., Kerninon, C., & Baron-Van Evercooren, A. (2008). The role of SVZ-derived neural precursors in demyelinating diseases: From animal models to multiple sclerosis. *Journal of the Neurological Sciences*, *265*(1-2), 26-31. https://doi.org/10.1016/j.jns.2007.09.032

Nam, H.-S., & Capecchi, M. R. (2020). Lrig1 expression prospectively identifies stem cells in the ventricular-subventricular zone that are neurogenic throughout adult life. *Neural Development*, *15*(1), 3. https://doi.org/10.1186/s13064-020-00139-5

Neumann, S., Porritt, M. J., Osman, A. M., & Kuhn, H. G. (2020). Cranial irradiation at early postnatal age impairs stroke-induced neural stem/progenitor cell response in the adult brain. *Scientific Reports*, *10*(1), 12369. https://doi.org/10.1038/s41598-020-69266-7

Nicholson, C., & Hrabětová, S. (2017). Brain Extracellular Space: The Final Frontier of Neuroscience. Biophysical Journal, 113(10), 2133-2142. https://doi.org/10.1016/j.bpj.2017.06.052

Niu, W., Zang, T., Zou, Y., Fang, S., Smith, D. K., Bachoo, R., & Zhang, C.-L. (2013). *In vivo* reprogramming of astrocytes to neuroblasts in the adult brain. *Nature Cell Biology*, *15*(10), 1164-1175. https://doi.org/10.1038/ncb2843

Obernier, K., & Alvarez-Buylla, A. (2019). Neural stem cells: Origin, heterogeneity and regulation in the adult mammalian brain. *Development (Cambridge, England)*, *146*(4), dev156059. https://doi.org/10.1242/dev.156059

Obernier, K., Cebrian-Silla, A., Thomson, M., Parraguez, J. I., Anderson, R., Guinto, C., Rodas Rodriguez, J., Garcia-Verdugo, J.-M., & Alvarez-Buylla, A. (2018). Adult Neurogenesis Is Sustained by Symmetric Self-Renewal and Differentiation. *Cell Stem Cell*, *22*(2), 221-234.e8. https://doi.org/10.1016/j.stem.2018.01.003

Oh, J., Lee, Y. D., & Wagers, A. J. (2014). Stem cell aging: Mechanisms, regulators and therapeutic opportunities. *Nature Medicine*, *20*(8), 870-880. https://doi.org/10.1038/nm.3651

Okamoto, M., Inoue, K., Iwamura, H., Terashima, K., Soya, H., Asashima, M., & Kuwabara, T. (2011). Reduction in paracrine Wnt3 factors during aging causes impaired adult neurogenesis. *FASEB Journal: Official Publication of the Federation of American Societies for Experimental Biology*, *25*(10), 3570-3582. https://doi.org/10.1096/fj.11-184697

O'Keeffe, G. C., Barker, R. A., & Caldwell, M. A. (2009). Dopaminergic modulation of neurogenesis in the subventricular zone of the adult brain. *Cell Cycle (Georgetown, Tex.)*, *8*(18), 2888-2894. https://doi.org/10.4161/cc.8.18.9512

Okun, E., Griffioen, K. J., Son, T. G., Lee, J.-H., Roberts, N. J., Mughal, M. R., Hutchison, E., Cheng, A., Arumugam, T. V., Lathia, J. D., van Praag, H., & Mattson, M. P. (2010). TLR2 activation inhibits embryonic neural progenitor cell proliferation. *Journal of Neurochemistry*, *114*(2), 462-474. https://doi.org/10.1111/j.1471-4159.2010.06778.x

Olmos, G., & Lladó, J. (2014). Tumor necrosis factor alpha: A link between neuroinflammation and excitotoxicity. *Mediators of Inflammation*, *2014*, 861231. https://doi.org/10.1155/2014/861231

Onténiente, B., Couriaud, C., Braudeau, J., Benchoua, A., & Guégan, C. (2003). The mechanisms of cell death in focal cerebral ischemia highlight neuroprotective perspectives by anti-caspase therapy. *Biochemical Pharmacology*, *66*(8), 1643-1649. https://doi.org/10.1016/s0006-2952(03)00538-0

Onténiente, B., Rasika, S., Benchoua, A., & Guégan, C. (2003). Molecular pathways in cerebral ischemia: Cues to novel therapeutic strategies. *Molecular Neurobiology*, *27*(1), 33-72. https://doi.org/10.1385/MN:27:1:33

Ortega, F., Gascón, S., Masserdotti, G., Deshpande, A., Simon, C., Fischer, J., Dimou, L., Chichung Lie, D., Schroeder, T., & Berninger, B. (2013). Oligodendrogliogenic and neurogenic adult subependymal zone neural stem cells constitute distinct lineages and exhibit differential responsiveness to Wnt signalling. *Nature Cell Biology*, *15*(6), 602-613. https://doi.org/10.1038/ncb2736

Ottersen, O. P., Laake, J. H., Reichelt, W., Haug, F. M., & Torp, R. (1996). Ischemic disruption of glutamate homeostasis in brain: Quantitative immunocytochemical analyses. *Journal of Chemical Neuroanatomy*, *12*(1), 1-14. https://doi.org/10.1016/s0891-0618(96)00178-0

Ottoboni, L., Merlini, A., & Martino, G. (2017). Neural Stem Cell Plasticity: Advantages in Therapy for the Injured Central Nervous System. *Frontiers in Cell and Developmental Biology*, *5*, 52. https://doi.org/10.3389/fcell.2017.00052

Ottoboni, L., von Wunster, B., & Martino, G. (2020). Therapeutic Plasticity of Neural Stem Cells. *Frontiers in Neurology*, *11*, 148. https://doi.org/10.3389/fneur.2020.00148

Paciaroni, M., Caso, V., & Agnelli, G. (2009). The concept of ischemic penumbra in acute stroke and therapeutic opportunities. *European Neurology*, *61*(6), 321-330. https://doi.org/10.1159/000210544

Paez-Gonzalez, P., Abdi, K., Luciano, D., Liu, Y., Soriano-Navarro, M., Rawlins, E., Bennett, V., Garcia-Verdugo, J. M., & Kuo, C. T. (2011). Ank3-dependent SVZ niche assembly is required for the continued production of new neurons. *Neuron*, *71*(1), 61-75. https://doi.org/10.1016/j.neuron.2011.05.029

Paez-Gonzalez, P., Asrican, B., Rodriguez, E., & Kuo, C. T. (2014). Identification of distinct $ChAT^{+}$ neurons and activity-dependent control of postnatal SVZ neurogenesis. *Nature Neuroscience*, *17*(7), 934-942. https://doi.org/10.1038/nn.3734

Palma-Tortosa, S., García-Culebras, A., Moraga, A., Hurtado, O., Perez-Ruiz, A., Durán-Laforet, V., Parra, J. de la, Cuartero, M. I., Pradillo, J. M., Moro, M. A., & Lizasoain, I. (2017). Specific Features of SVZ Neurogenesis After Cortical Ischemia: A Longitudinal Study. *Scientific Reports*, *7*(1), 16343. https://doi.org/10.1038/s41598-017-16109-7

Parent, J. M., Vexler, Z. S., Gong, C., Derugin, N., & Ferriero, D. M. (2002). Rat forebrain neurogenesis and striatal neuron replacement after focal stroke. *Annals of Neurology*, *52*(6), 802-813. https://doi.org/10.1002/ana.10393

Parkhurst, C. N., Yang, G., Ninan, I., Savas, J. N., Yates, J. R., Lafaille, J. J., Hempstead, B. L., Littman, D. R., & Gan, W.-B. (2013). Microglia promote learning-dependent synapse formation through brain-derived neurotrophic factor. *Cell*, *155*(7), 1596-1609. https://doi.org/10.1016/j.cell.2013.11.030

Paul, A., Chaker, Z., & Doetsch, F. (2017). Hypothalamic regulation of regionally distinct adult neural stem cells and neurogenesis. *Science (New York, N.Y.)*, *356*(6345), 1383-1386. https://doi.org/10.1126/science.aal3839

Pavlica, S., Milosevic, J., Keller, M., Schulze, M., Peinemann, F., Piscioneri, A., De Bartolo, L., Darsow, K., Bartel, S., Lange, H. A., & Bader, A. (2012). Erythropoietin enhances cell proliferation and survival of human fetal neuronal progenitors in normoxia. *Brain Research*, *1452*, 18-28. https://doi.org/10.1016/j.brainres.2012.02.043

Pekny, M., Johansson, C. B., Eliasson, C., Stakeberg, J., Wallén, Å., Perlmann, T., Lendahl, U., Betsholtz, C., Berthold, C.-H., & Frisén, J. (1999). Abnormal Reaction to Central Nervous System Injury in Mice Lacking Glial Fibrillary Acidic Protein and Vimentin. *The Journal of Cell Biology*, *145*(3), 503-514.

Pekny, M., & Nilsson, M. (2005). Astrocyte activation and reactive gliosis. *Glia*, *50*(4), 427-434. https://doi.org/10.1002/glia.20207

Peruzzotti-Jametti, L., Donegá, M., Giusto, E., Mallucci, G., Marchetti, B., & Pluchino, S. (2014). The role of the immune system in central nervous system plasticity after acute injury. *Neuroscience*, *283*, 210-221. https://doi.org/10.1016/j.neuroscience.2014.04.036

Peters, A., & Sherman, L. S. (2020). Diverse Roles for Hyaluronan and Hyaluronan Receptors in the Developing and Adult Nervous System. *International Journal of Molecular Sciences*, *21*(17), E5988. https://doi.org/10.3390/ijms21175988

Petreanu, L., & Alvarez-Buylla, A. (2002). Maturation and death of adult-born olfactory bulb granule neurons: Role of olfaction. *The Journal of Neuroscience: The Official Journal of the Society for Neuroscience*, *22*(14), 6106-6113. https://doi.org/20026588

Petrik, D., Myoga, M. H., Grade, S., Gerkau, N. J., Pusch, M., Rose, C. R., Grothe, B., & Götz, M. (2018). Epithelial Sodium Channel Regulates Adult Neural Stem Cell Proliferation in a Flow-Dependent Manner. *Cell Stem Cell*, *22*(6), 865-878.e8. https://doi.org/10.1016/j.stem.2018.04.016

Phillis, J. W., & O'Regan, M. H. (2004). A potentially critical role of phospholipases in central nervous system ischemic, traumatic, and neurodegenerative disorders. *Brain Research. Brain Research Reviews*, *44*(1), 13-47. https://doi.org/10.1016/j.brainresrev.2003.10.002

Pierre, K., & Pellerin, L. (2005). Monocarboxylate transporters in the central nervous system: Distribution, regulation and function. *Journal of Neurochemistry*, *94*(1), 1-14. https://doi.org/10.1111/j.1471-4159.2005.03168.x

Platel, J.-C., Angelova, A., Bugeon, S., Wallace, J., Ganay, T., Chudotvorova, I., Deloulme, J.-C., Béclin, C., Tiveron, M.-C., Coré, N., Murthy, V. N., & Cremer, H. (2019). Neuronal integration in the adult mouse olfactory bulb is a non-selective addition process. *eLife*, *8*, e44830. https://doi.org/10.7554/eLife.44830

Plenz, D., & Kitai, S. T. (1996). Organotypic cortex-striatum-mesencephalon cultures: The nigrostriatal pathway. *Neuroscience Letters*, *209*(3), 177-180. https://doi.org/10.1016/0304-3940(96)12644-6

References

Pohjasvaara, T., Erkinjuntti, T., Ylikoski, R., Hietanen, M., Vataja, R., & Kaste, M. (1998). Clinical determinants of poststroke dementia. *Stroke*, *29*(1), 75-81. https://doi.org/10.1161/01.str.29.1.75

Ponti, G., Obernier, K., Guinto, C., Jose, L., Bonfanti, L., & Alvarez-Buylla, A. (2013). Cell cycle and lineage progression of neural progenitors in the ventricular-subventricular zones of adult mice. *Proceedings of the National Academy of Sciences of the United States of America*, *110*(11), E1045-1054. https://doi.org/10.1073/pnas.1219563110

Pous, L., Deshpande, S. S., Nath, S., Mezey, S., Malik, S. C., Schildge, S., Bohrer, C., Topp, K., Pfeifer, D., Fernández-Klett, F., Doostkam, S., Galanakis, D. K., Taylor, V., Akassoglou, K., & Schachtrup, C. (2020). Fibrinogen induces neural stem cell differentiation into astrocytes in the subventricular zone via BMP signaling. *Nature Communications*, *11*(1), 630. https://doi.org/10.1038/s41467-020-14466-y

Preston, M., & Sherman, L. S. (2011a). Neural Stem Cell Niches: Critical Roles for the Hyaluronan-Based Extracellular Matrix in Neural Stem Cell Proliferation and Differentiation. *Frontiers in Bioscience (Scholar Edition)*, *3*, 1165-1179.

Preston, M., & Sherman, L. S. (2011b). Neural stem cell niches: Roles for the hyaluronan-based extracellular matrix. *Frontiers in Bioscience (Scholar Edition)*, *3*, 1165-1179. https://doi.org/10.2741/218

Puyal, J., Ginet, V., & Clarke, P. G. H. (2013). Multiple interacting cell death mechanisms in the mediation of excitotoxicity and ischemic brain damage: A challenge for neuroprotection. *Progress in Neurobiology*, *105*, 24-48. https://doi.org/10.1016/j.pneurobio.2013.03.002

Qian, H., Kang, X., Hu, J., Zhang, D., Liang, Z., Meng, F., Zhang, X., Xue, Y., Maimon, R., Dowdy, S. F., Devaraj, N. K., Zhou, Z., Mobley, W. C., Cleveland, D. W., & Fu, X.-D. (2020). Reversing a model of Parkinson's disease with in situ converted nigral neurons. *Nature*, *582*(7813), 550-556. https://doi.org/10.1038/s41586-020-2388-4

Qin, C., Zhou, L.-Q., Ma, X.-T., Hu, Z.-W., Yang, S., Chen, M., Bosco, D. B., Wu, L.-J., & Tian, D.-S. (2019). Dual Functions of Microglia in Ischemic Stroke. *Neuroscience Bulletin*, *35*(5), 921-933. https://doi.org/10.1007/s12264-019-00388-3

Quiñones-Hinojosa, A., & Chaichana, K. (2007). The human subventricular zone: A source of new cells and a potential source of brain tumors. *Experimental Neurology*, *205*(2), 313-324. https://doi.org/10.1016/j.expneurol.2007.03.016

Quiñones-Hinojosa, A., Sanai, N., Soriano-Navarro, M., Gonzalez-Perez, O., Mirzadeh, Z., Gil-Perotin, S., Romero-Rodriguez, R., Berger, M. S., Garcia-Verdugo, J. M., & Alvarez-Buylla, A. (2006). Cellular composition and cytoarchitecture of the adult human subventricular zone: A niche of neural stem cells. *The Journal of Comparative Neurology*, *494*(3), 415-434. https://doi.org/10.1002/cne.20798

Rabie, T., Kunze, R., & Marti, H. H. (2011). Impaired hypoxic response in senescent mouse brain. *International Journal of Developmental Neuroscience: The Official Journal of the International Society for Developmental Neuroscience*, *29*(6), 655-661. https://doi.org/10.1016/j.ijdevneu.2011.06.003

Rahman, M. T., Muppala, S., Wu, J., Krukovets, I., Solovjev, D., Verbovetskiy, D., Obiako, C., Plow, E. F., & Stenina-Adognravi, O. (2020). Effects of thrombospondin-4 on pro-inflammatory phenotype differentiation and apoptosis in macrophages. *Cell Death & Disease*, *11*(1), 1-14. https://doi.org/10.1038/s41419-020-2237-2

Ritter, M. A., Jurk, K., Schriek, C., Nabavi, D. G., Droste, D. W., Kehrel, B. E., & Bernd Ringelstein, E. (2009). Microembolic signals on transcranial Doppler ultrasound are correlated with platelet activation markers, but not with platelet-leukocyte associates: A study in patients with acute stroke and in patients with asymptomatic carotid stenosis. *Neurological Research*, *31*(1), 11-16. https://doi.org/10.1179/174313208X331590

Rivetti di Val Cervo, P., Romanov, R. A., Spigolon, G., Masini, D., Martín-Montañez, E., Toledo, E. M., La Manno, G., Feyder, M., Pifl, C., Ng, Y.-H., Sánchez, S. P., Linnarsson, S., Wernig, M., Harkany, T., Fisone, G., & Arenas, E. (2017). Induction of functional dopamine neurons from human astrocytes *in vitro* and mouse astrocytes in a Parkinson's disease model. *Nature Biotechnology*, *35*(5), 444-452. https://doi.org/10.1038/nbt.3835

Rodriguez-Grande, B., Swana, M., Nguyen, L., Englezou, P., Maysami, S., Allan, S. M., Rothwell, N. J., Garlanda, C., Denes, A., & Pinteaux, E. (2014). The acute-phase protein PTX3 is an essential mediator of glial scar formation and resolution of brain edema after ischemic injury. *Journal of Cerebral Blood Flow and Metabolism: Official Journal of the International Society of Cerebral Blood Flow and Metabolism*, *34*(3), 480-488. https://doi.org/10.1038/jcbfm.2013.224

Rodriguez-Grande, B., Varghese, L., Molina-Holgado, F., Rajkovic, O., Garlanda, C., Denes, A., & Pinteaux, E. (2015). Pentraxin 3 mediates neurogenesis and angiogenesis after cerebral ischaemia. *Journal of Neuroinflammation*, *12*, 15. https://doi.org/10.1186/s12974-014-0227-y

Rohatgi, R., Milenkovic, L., & Scott, M. P. (2007). Patched1 regulates hedgehog signaling at the primary cilium. *Science (New York, N.Y.)*, *317*(5836), 372-376. https://doi.org/10.1126/science.1139740

Roth, T. L., Nayak, D., Atanasijevic, T., Koretsky, A. P., Latour, L. L., & McGavern, D. B. (2014). Transcranial amelioration of inflammation and cell death after brain injury. *Nature*, *505*(7482), 223-228. https://doi.org/10.1038/nature12808

Ruiz de Almodovar, C., Lambrechts, D., Mazzone, M., & Carmeliet, P. (2009). Role and therapeutic potential of VEGF in the nervous system. *Physiological Reviews*, *89*(2), 607-648. https://doi.org/10.1152/physrev.00031.2008

Ruoslahti, E. (1996). Brain extracellular matrix. *Glycobiology*, *6*(5), 489-492. https://doi.org/10.1093/glycob/6.5.489

Rusanen, H., Saarinen, J. T., & Sillanpää, N. (2015). Collateral Circulation Predicts the Size of the Infarct Core and the Proportion of Salvageable Penumbra in Hyperacute Ischemic Stroke Patients Treated with Intravenous Thrombolysis. *Cerebrovascular Diseases (Basel, Switzerland)*, *40*(3-4), 182-190. https://doi.org/10.1159/000439064

Saha, B., Jaber, M., & Gaillard, A. (2012). Potentials of endogenous neural stem cells in cortical repair. *Frontiers in Cellular Neuroscience*, *6*, 14. https://doi.org/10.3389/fncel.2012.00014

Saha, B., Peron, S., Murray, K., Jaber, M., & Gaillard, A. (2013). Cortical lesion stimulates adult subventricular zone neural progenitor cell proliferation and migration to the site of injury. *Stem Cell Research*, *11*(3), 965-977. https://doi.org/10.1016/j.scr.2013.06.006

Sakata, H., Narasimhan, P., Niizuma, K., Maier, C. M., Wakai, T., & Chan, P. H. (2012). Interleukin 6-preconditioned neural stem cells reduce ischaemic injury in stroke mice. *Brain: A Journal of Neurology*, *135*(Pt 11), 3298-3310. https://doi.org/10.1093/brain/aws259

Sanai, N., Nguyen, T., Ihrie, R. A., Mirzadeh, Z., Tsai, H.-H., Wong, M., Gupta, N., Berger, M. S., Huang, E., Garcia-Verdugo, J.-M., Rowitch, D. H., & Alvarez-Buylla, A. (2011). Corridors of migrating neurons in the human brain and their decline during infancy. *Nature*, *478*(7369), 382-386. https://doi.org/10.1038/nature10487

Sanai, N., Tramontin, A. D., Quiñones-Hinojosa, A., Barbaro, N. M., Gupta, N., Kunwar, S., Lawton, M. T., McDermott, M. W., Parsa, A. T., Manuel-García Verdugo, J., Berger, M. S., & Alvarez-Buylla, A. (2004). Unique astrocyte ribbon in adult human brain contains neural stem cells but lacks chain migration. *Nature*, *427*(6976), 740-744. https://doi.org/10.1038/nature02301

Santopolo, G., Magnusson, J. P., Lindvall, O., Kokaia, Z., & Frisén, J. (2020). Blocking Notch-Signaling Increases Neurogenesis in the Striatum after Stroke. *Cells*, *9*(7), E1732. https://doi.org/10.3390/cells9071732

Schaapsmeerders, P., Maaijwee, N. A. M., van Dijk, E. J., Rutten-Jacobs, L. C. A., Arntz, R. M., Schoonderwaldt, H. C., Dorresteijn, L. D. A., Kessels, R. P. C., & de Leeuw, F.-E. (2013). Long-term cognitive impairment after first-ever ischemic stroke in young adults. *Stroke*, *44*(6), 1621-1628. https://doi.org/10.1161/STROKEAHA.111.000792

Schwab, M. E., Kapfhammer, J. P., & Bandtlow, C. E. (1993). Inhibitors of neurite growth. *Annual Review of Neuroscience*, *16*, 565-595. https://doi.org/10.1146/annurev.ne.16.030193.003025

Seib, D. R. M., Corsini, N. S., Ellwanger, K., Plaas, C., Mateos, A., Pitzer, C., Niehrs, C., Celikel, T., & Martin-Villalba, A. (2013). Loss of Dickkopf-1 restores neurogenesis in old age and counteracts cognitive decline. *Cell Stem Cell*, *12*(2), 204-214. https://doi.org/10.1016/j.stem.2012.11.010

SEN, A. (s. f.). *El Atlas del Ictus*. Recuperado 29 de octubre de 2021, de https://www.sen.es/actividades/91-articulos/2617-el-atlas-del-ictus

Shabani, Z., Ghadiri, T., Karimipour, M., Sadigh-Eteghad, S., Mahmoudi, J., Mehrad, H., & Farhoudi, M. (2021). Modulatory properties of extracellular matrix glycosaminoglycans and proteoglycans on neural stem cells behavior: Highlights on regenerative potential and bioactivity. *International Journal of Biological Macromolecules*, *171*, 366-381. https://doi.org/10.1016/j.ijbiomac.2021.01.006

Shen, C.-C., Yang, Y.-C., Chiao, M.-T., Cheng, W.-Y., Tsuei, Y.-S., & Ko, J.-L. (2010). Characterization of endogenous neural progenitor cells after experimental ischemic stroke. *Current Neurovascular Research*, *7*(1), 6-14. https://doi.org/10.2174/156720210790820208

Shen, Q., Goderie, S. K., Jin, L., Karanth, N., Sun, Y., Abramova, N., Vincent, P., Pumiglia, K., & Temple, S. (2004). Endothelial cells stimulate self-renewal and expand neurogenesis of neural stem cells. *Science (New York, N.Y.)*, *304*(5675), 1338-1340. https://doi.org/10.1126/science.1095505

Shi, C., & Pamer, E. G. (2011). Monocyte recruitment during infection and inflammation. *Nature Reviews. Immunology*, *11*(11), 762-774. https://doi.org/10.1038/nri3070

References

Shi, Y., Sun, G., Zhao, C., & Stewart, R. (2008). Neural stem cell self-renewal. *Critical Reviews in Oncology/Hematology*, *65*(1), 43-53. https://doi.org/10.1016/j.critrevonc.2007.06.004

Shi, Y., Sun, L., Zhang, R., Hu, Y., Wu, Y., Dong, X., Dong, D., Chen, C., Geng, Z., Li, E., & Fan, Y. (2021). Thrombospondin 4/integrin α2/HSF1 axis promotes proliferation and cancer stem-like traits of gallbladder cancer by enhancing reciprocal crosstalk between cancer-associated fibroblasts and tumor cells. *Journal of Experimental & Clinical Cancer Research: CR*, *40*(1), 14. https://doi.org/10.1186/s13046-020-01812-7

Shin, J. E., Lee, H., Jung, K., Kim, M., Hwang, K., Han, J., Lim, J., Kim, I.-S., Lim, K.-I., & Park, K. I. (2020). Cellular Response of Ventricular-Subventricular Neural Progenitor/Stem Cells to Neonatal Hypoxic-Ischemic Brain Injury and Their Enhanced Neurogenesis. *Yonsei Medical Journal*, *61*(6), 492-505. https://doi.org/10.3349/ymj.2020.61.6.492

Shingo, T., Gregg, C., Enwere, E., Fujikawa, H., Hassam, R., Geary, C., Cross, J. C., & Weiss, S. (2003). Pregnancy-stimulated neurogenesis in the adult female forebrain mediated by prolactin. *Science (New York, N.Y.)*, *299*(5603), 117-120. https://doi.org/10.1126/science.1076647

Shook, B. A., Manz, D. H., Peters, J. J., Kang, S., & Conover, J. C. (2012). Spatiotemporal changes to the subventricular zone stem cell pool through aging. *The Journal of Neuroscience: The Official Journal of the Society for Neuroscience*, *32*(20), 6947-6956. https://doi.org/10.1523/JNEUROSCI.5987-11.2012

Siegenthaler, J. A., Ashique, A. M., Zarbalis, K., Patterson, K. P., Hecht, J. H., Kane, M. A., Folias, A. E., Choe, Y., May, S. R., Kume, T., Napoli, J. L., Peterson, A. S., & Pleasure, S. J. (2009). Retinoic acid from the meninges regulates cortical neuron generation. *Cell*, *139*(3), 597-609. https://doi.org/10.1016/j.cell.2009.10.004

Sierra, A., Beccari, S., Diaz-Aparicio, I., Encinas, J. M., Comeau, S., & Tremblay, M.-È. (2014). Surveillance, phagocytosis, and inflammation: How never-resting microglia influence adult hippocampal neurogenesis. *Neural Plasticity*, *2014*, 610343. https://doi.org/10.1155/2014/610343

Sierra, A., Encinas, J. M., Deudero, J. J. P., Chancey, J. H., Enikolopov, G., Overstreet-Wadiche, L. S., Tsirka, S. E., & Maletic-Savatic, M. (2010). Microglia shape adult hippocampal neurogenesis through apoptosis-coupled phagocytosis. *Cell Stem Cell*, *7*(4), 483-495. https://doi.org/10.1016/j.stem.2010.08.014

Silverman, I. E., & Rymer, M. M. (2009). *Ischemic Stroke: An Atlas of Investigation and Treatment*. Clinical Publishing.

Sirerol-Piquer, M. S., Belenguer, G., Morante-Redolat, J. M., Duart-Abadia, P., Perez-Villalba, A., & Fariñas, I. (2019). Physiological Interactions between Microglia and Neural Stem Cells in the Adult Subependymal Niche. *Neuroscience*, *405*, 77-91. https://doi.org/10.1016/j.neuroscience.2019.01.009

Sofroniew, M. V. (2009). Molecular dissection of reactive astrogliosis and glial scar formation. *Trends in Neurosciences*, *32*(12), 638-647. https://doi.org/10.1016/j.tins.2009.08.002

Sofroniew, M. V. (2014). Astrogliosis. *Cold Spring Harbor Perspectives in Biology*, *7*(2), a020420. https://doi.org/10.1101/cshperspect.a020420

Sohn, J., Orosco, L., Guo, F., Chung, S.-H., Bannerman, P., Mills Ko, E., Zarbalis, K., Deng, W., & Pleasure, D. (2015). The subventricular zone continues to generate corpus callosum and rostral migratory stream astroglia in normal adult mice. *The Journal of Neuroscience: The Official Journal of the Society for Neuroscience*, *35*(9), 3756-3763. https://doi.org/10.1523/JNEUROSCI.3454-14.2015

Song, M., Yu, S. P., Mohamad, O., Cao, W., Wei, Z. Z., Gu, X., Jiang, M. Q., & Wei, L. (2017). Optogenetic stimulation of glutamatergic neuronal activity in the striatum enhances neurogenesis in the subventricular zone of normal and stroke mice. *Neurobiology of Disease*, *98*, 9-24. https://doi.org/10.1016/j.nbd.2016.11.005

Soria, F. N., Paviolo, C., Doudnikoff, E., Arotcarena, M.-L., Lee, A., Danné, N., Mandal, A. K., Gosset, P., Dehay, B., Groc, L., Cognet, L., & Bezard, E. (2020). Synucleinopathy alters nanoscale organization and diffusion in the brain extracellular space through hyaluronan remodeling. *Nature Communications*, *11*(1), 3440. https://doi.org/10.1038/s41467-020-17328-9

Sorrells, S. F., Paredes, M. F., Cebrian-Silla, A., Sandoval, K., Qi, D., Kelley, K. W., James, D., Mayer, S., Chang, J., Auguste, K. I., Chang, E. F., Gutierrez, A. J., Kriegstein, A. R., Mathern, G. W., Oldham, M. C., Huang, E. J., Garcia-Verdugo, J. M., Yang, Z., & Alvarez-Buylla, A. (2018). Human hippocampal neurogenesis drops sharply in children to undetectable levels in adults. *Nature*, *555*(7696), 377-381. https://doi.org/10.1038/nature25975

Spalding, K. L., Bergmann, O., Alkass, K., Bernard, S., Salehpour, M., Huttner, H. B., Boström, E., Westerlund, I., Vial, C., Buchholz, B. A., Possnert, G., Mash, D. C., Druid, H., & Frisén, J. (2013). Dynamics of hippocampal neurogenesis in adult humans. *Cell*, *153*(6), 1219-1227. https://doi.org/10.1016/j.cell.2013.05.002

Spassky, N., Merkle, F. T., Flames, N., Tramontin, A. D., García-Verdugo, J. M., & Alvarez-Buylla, A. (2005). Adult ependymal cells are postmitotic and are derived from radial glial cells during embryogenesis. *The Journal of Neuroscience: The Official Journal of the Society for Neuroscience*, *25*(1), 10-18. https://doi.org/10.1523/JNEUROSCI.1108-04.2005

Stenina-Adognravi, O., & Plow, E. F. (2019). Thrombospondin-4 in tissue remodeling. *Matrix Biology: Journal of the International Society for Matrix Biology*, *75-76*, 300-313. https://doi.org/10.1016/j.matbio.2017.11.006

Storini, C., Bergamaschini, L., Gesuete, R., Rossi, E., Maiocchi, D., & De Simoni, M. G. (2006). Selective inhibition of plasma kallikrein protects brain from reperfusion injury. *The Journal of Pharmacology and Experimental Therapeutics*, *318*(2), 849-854. https://doi.org/10.1124/jpet.106.105064

Su, W., Foster, S. C., Xing, R., Feistel, K., Olsen, R. H. J., Acevedo, S. F., Raber, J., & Sherman, L. S. (2017). CD44 Transmembrane Receptor and Hyaluronan Regulate Adult Hippocampal Neural Stem Cell Quiescence and Differentiation. *The Journal of Biological Chemistry*, *292*(11), 4434-4445. https://doi.org/10.1074/jbc.M116.774109

Sultan, S., Li, L., Moss, J., Petrelli, F., Cassé, F., Gebara, E., Lopatar, J., Pfrieger, F. W., Bezzi, P., Bischofberger, J., & Toni, N. (2015). Synaptic Integration of Adult-Born Hippocampal Neurons Is Locally Controlled by Astrocytes. *Neuron*, *88*(5), 957-972. https://doi.org/10.1016/j.neuron.2015.10.037

Sun, A. X., Yuan, Q., Tan, S., Xiao, Y., Wang, D., Khoo, A. T. T., Sani, L., Tran, H.-D., Kim, P., Chiew, Y. S., Lee, K. J., Yen, Y.-C., Ng, H. H., Lim, B., & Je, H. S. (2016). Direct Induction and Functional Maturation of Forebrain GABAergic Neurons from Human Pluripotent Stem Cells. *Cell Reports*, *16*(7), 1942-1953. https://doi.org/10.1016/j.celrep.2016.07.035

Suzuki, S. O., & Goldman, J. E. (2003). Multiple cell populations in the early postnatal subventricular zone take distinct migratory pathways: A dynamic study of glial and neuronal progenitor migration. *The Journal of Neuroscience: The Official Journal of the Society for Neuroscience*, *23*(10), 4240-4250.

Swanson, R. A., Ying, W., & Kauppinen, T. M. (2004). Astrocyte influences on ischemic neuronal death. *Current Molecular Medicine*, *4*(2), 193-205. https://doi.org/10.2174/1566524043479185

Takeuchi, O., & Akira, S. (2010). Pattern recognition receptors and inflammation. *Cell*, *140*(6), 805-820. https://doi.org/10.1016/j.cell.2010.01.022

Tan, L. A., Al Chawaf, A., Vaccarino, F. J., Boutros, P. C., & Lovejoy, D. A. (2011). Teneurin C-terminal associated peptide (TCAP)-1 modulates dendritic morphology in hippocampal neurons and decreases anxiety-like behaviors in rats. *Physiology & Behavior*, *104*(2), 199-204. https://doi.org/10.1016/j.physbeh.2011.03.015

Tan, X.-D., Liu, B., Jiang, Y., Yu, H.-J., & Li, C.-Q. (2021). Gadd45b mediates environmental enrichment-induced neurogenesis in the SVZ of rats following ischemia stroke via BDNF. *Neuroscience Letters*, *745*, 135616. https://doi.org/10.1016/j.neulet.2020.135616

Tanaka, K., Nogawa, S., Suzuki, S., Dembo, T., & Kosakai, A. (2003). Upregulation of oligodendrocyte progenitor cells associated with restoration of mature oligodendrocytes and myelination in peri-infarct area in the rat brain. *Brain Research*, *989*(2), 172-179. https://doi.org/10.1016/s0006-8993(03)03317-1

Tatebayashi, K., Tanaka, Y., Nakano-Doi, A., Sakuma, R., Kamachi, S., Shirakawa, M., Uchida, K., Kageyama, H., Takagi, T., Yoshimura, S., Matsuyama, T., & Nakagomi, T. (2017). Identification of Multipotent Stem Cells in Human Brain Tissue Following Stroke. *Stem Cells and Development*, *26*(11), 787-797. https://doi.org/10.1089/scd.2016.0334

Taverna, E., Götz, M., & Huttner, W. B. (2014). The cell biology of neurogenesis: Toward an understanding of the development and evolution of the neocortex. *Annual Review of Cell and Developmental Biology*, *30*, 465-502. https://doi.org/10.1146/annurev-cellbio-101011-155801

Tepavčević, V., Lazarini, F., Alfaro-Cervello, C., Kerninon, C., Yoshikawa, K., Garcia-Verdugo, J. M., Lledo, P.-M., Nait-Oumesmar, B., & Baron-Van Evercooren, A. (2011). Inflammation-induced subventricular zone dysfunction leads to olfactory deficits in a targeted mouse model of multiple sclerosis. *The Journal of Clinical Investigation*, *121*(12), 4722-4734. https://doi.org/10.1172/JCI59145

Thomsen, G. M., Le Belle, J. E., Harnisch, J. A., Mc Donald, W. S., Hovda, D. A., Sofroniew, M. V., Kornblum, H. I., & Harris, N. G. (2014). Traumatic brain injury reveals novel cell lineage relationships within the subventricular zone. *Stem Cell Research*, *13*(1), 48-60. https://doi.org/10.1016/j.scr.2014.04.013

References

Thored, P., Wood, J., Arvidsson, A., Cammenga, J., Kokaia, Z., & Lindvall, O. (2007). Long-Term Neuroblast Migration Along Blood Vessels in an Area With Transient Angiogenesis and Increased Vascularization After Stroke. *Stroke*, *38*(11), 3032-3039. https://doi.org/10.1161/STROKEAHA.107.488445

Tian, X., Azpurua, J., Hine, C., Vaidya, A., Myakishev-Rempel, M., Ablaeva, J., Mao, Z., Nevo, E., Gorbunova, V., & Seluanov, A. (2013). High-molecular-mass hyaluronan mediates the cancer resistance of the naked mole rat. *Nature*, *499*(7458), 346-349. https://doi.org/10.1038/nature12234

Tonchev, A. B., Yamashima, T., Sawamoto, K., & Okano, H. (2005). Enhanced proliferation of progenitor cells in the subventricular zone and limited neuronal production in the striatum and neocortex of adult macaque monkeys after global cerebral ischemia. *Journal of Neuroscience Research*, *81*(6), 776-788. https://doi.org/10.1002/jnr.20604

Tong, C. K., Chen, J., Cebrián-Silla, A., Mirzadeh, Z., Obernier, K., Guinto, C. D., Tecott, L. H., García-Verdugo, J. M., Kriegstein, A., & Alvarez-Buylla, A. (2014). Axonal control of the adult neural stem cell niche. *Cell Stem Cell*, *14*(4), 500-511. https://doi.org/10.1016/j.stem.2014.01.014

Torper, O., Pfisterer, U., Wolf, D. A., Pereira, M., Lau, S., Jakobsson, J., Björklund, A., Grealish, S., & Parmar, M. (2013). Generation of induced neurons via direct conversion *in vivo*. *Proceedings of the National Academy of Sciences of the United States of America*, *110*(17), 7038-7043. https://doi.org/10.1073/pnas.1303829110

Tramontin, A. D., García-Verdugo, J. M., Lim, D. A., & Alvarez-Buylla, A. (2003). Postnatal development of radial glia and the ventricular zone (VZ): A continuum of the neural stem cell compartment. *Cerebral Cortex (New York, N.Y.: 1991)*, *13*(6), 580-587. https://doi.org/10.1093/cercor/13.6.580

Tremblay, M.-È., Stevens, B., Sierra, A., Wake, H., Bessis, A., & Nimmerjahn, A. (2011). The role of microglia in the healthy brain. *The Journal of Neuroscience: The Official Journal of the Society for Neuroscience*, *31*(45), 16064-16069. https://doi.org/10.1523/JNEUROSCI.4158-11.2011

Tropepe, V., Craig, C. G., Morshead, C. M., & van der Kooy, D. (1997). Transforming growth factor-alpha null and senescent mice show decreased neural progenitor cell proliferation in the forebrain subependyma. *The Journal of Neuroscience: The Official Journal of the Society for Neuroscience*, *17*(20), 7850-7859.

Udo, H., Yoshida, Y., Kino, T., Ohnuki, K., Mizunoya, W., Mukuda, T., & Sugiyama, H. (2008). Enhanced adult neurogenesis and angiogenesis and altered affective behaviors in mice overexpressing vascular endothelial growth factor 120. *The Journal of Neuroscience: The Official Journal of the Society for Neuroscience*, *28*(53), 14522-14536. https://doi.org/10.1523/JNEUROSCI.3673-08.2008

Ueki, T., Tanaka, M., Yamashita, K., Mikawa, S., Qiu, Z., Maragakis, N. J., Hevner, R. F., Miura, N., Sugimura, H., & Sato, K. (2003). A novel secretory factor, Neurogenesin-1, provides neurogenic environmental cues for neural stem cells in the adult hippocampus. *The Journal of Neuroscience: The Official Journal of the Society for Neuroscience*, *23*(37), 11732-11740.

van den Berge, S. A., van Strien, M. E., Korecka, J. A., Dijkstra, A. A., Sluijs, J. A., Kooijman, L., Eggers, R., De Filippis, L., Vescovi, A. L., Verhaagen, J., van de Berg, W. D. J., & Hol, E. M. (2011). The proliferative capacity of the subventricular zone is maintained in the parkinsonian brain. *Brain: A Journal of Neurology*, *134*(Pt 11), 3249-3263. https://doi.org/10.1093/brain/awr256

Van Harreveld, A., Crowell, J., & Malhotra, S. K. (1965). A STUDY OF EXTRACELLULAR SPACE IN CENTRAL NERVOUS TISSUE BY FREEZE-SUBSTITUTION. *The Journal of Cell Biology*, *25*(1), 117-137.

Vanhoutte, D., Schips, T. G., Kwong, J. Q., Davis, J., Tjondrokoesoemo, A., Brody, M. J., Sargent, M. A., Kanisicak, O., Yi, H., Gao, Q. Q., Rabinowitz, J. E., Volk, T., McNally, E. M., & Molkentin, J. D. (2016). Thrombospondin expression in myofibers stabilizes muscle membranes. *ELife*, *5*, e17589. https://doi.org/10.7554/eLife.17589

Vecino, E., Heller, J. P., Veiga-Crespo, P., Martin, K. R., & Fawcett, J. W. (2015). Influence of extracellular matrix components on the expression of integrins and regeneration of adult retinal ganglion cells. *PloS One*, *10*(5), e0125250. https://doi.org/10.1371/journal.pone.0125250

Ventura, R. E., & Goldman, J. E. (2007). Dorsal radial glia generate olfactory bulb interneurons in the postnatal murine brain. *The Journal of Neuroscience: The Official Journal of the Society for Neuroscience*, *27*(16), 4297-4302. https://doi.org/10.1523/JNEUROSCI.0399-07.2007

Verkhratsky, A., Parpura, V., Pekna, M., Pekny, M., & Sofroniew, M. (2014). Glia in the pathogenesis of neurodegenerative diseases. *Biochemical Society Transactions*, *42*(5), 1291-1301. https://doi.org/10.1042/BST20140107

Victor, M. B., Richner, M., Hermanstyne, T. O., Ransdell, J. L., Sobieski, C., Deng, P.-Y., Klyachko, V. A., Nerbonne, J. M., & Yoo, A. S. (2014). Generation of human striatal neurons by microRNA-dependent direct conversion of fibroblasts. *Neuron*, *84*(2), 311-323. https://doi.org/10.1016/j.neuron.2014.10.016

Vidale, S., & Agostoni, E. (2014). Thrombolysis in acute ischaemic stroke. *Brain: A Journal of Neurology*, *137*(Pt 6), e281. https://doi.org/10.1093/brain/awu065

Villeda, S. A., Luo, J., Mosher, K. I., Zou, B., Britschgi, M., Bieri, G., Stan, T. M., Fainberg, N., Ding, Z., Eggel, A., Lucin, K. M., Czirr, E., Park, J.-S., Couillard-Després, S., Aigner, L., Li, G., Peskind, E. R., Kaye, J. A., Quinn, J. F., … Wyss-Coray, T. (2011). The ageing systemic milieu negatively regulates neurogenesis and cognitive function. *Nature*, *477*(7362), 90-94. https://doi.org/10.1038/nature10357

Wakade, C. G., Mahadik, S. P., Waller, J. L., & Chiu, F.-C. (2002). Atypical neuroleptics stimulate neurogenesis in adult rat brain. *Journal of Neuroscience Research*, *69*(1), 72-79. https://doi.org/10.1002/jnr.10281

Wake, H., Moorhouse, A. J., Jinno, S., Kohsaka, S., & Nabekura, J. (2009). Resting microglia directly monitor the functional state of synapses *in vivo* and determine the fate of ischemic terminals. *The Journal of Neuroscience: The Official Journal of the Society for Neuroscience*, *29*(13), 3974-3980. https://doi.org/10.1523/JNEUROSCI.4363-08.2009

Wang, D., & Fawcett, J. (2012). The perineuronal net and the control of CNS plasticity. *Cell and Tissue Research*, *349*(1), 147-160. https://doi.org/10.1007/s00441-012-1375-y

Wang, Y.-Q., Guo, X., Qiu, M.-H., Feng, X.-Y., & Sun, F.-Y. (2007). VEGF overexpression enhances striatal neurogenesis in brain of adult rat after a transient middle cerebral artery occlusion. *Journal of Neuroscience Research*, *85*(1), 73-82. https://doi.org/10.1002/jnr.21091

Wang, Y.-Z., Yamagami, T., Gan, Q., Wang, Y., Zhao, T., Hamad, S., Lott, P., Schnittke, N., Schwob, J. E., & Zhou, C. J. (2011). Canonical Wnt signaling promotes the proliferation and neurogenesis of peripheral olfactory stem cells during postnatal development and adult regeneration. *Journal of Cell Science*, *124*(Pt 9), 1553-1563. https://doi.org/10.1242/jcs.080580

Wanner, I. B., Anderson, M. A., Song, B., Levine, J., Fernandez, A., Gray-Thompson, Z., Ao, Y., & Sofroniew, M. V. (2013). Glial scar borders are formed by newly proliferated, elongated astrocytes that interact to corral inflammatory and fibrotic cells via STAT3-dependent mechanisms after spinal cord injury. *The Journal of Neuroscience: The Official Journal of the Society for Neuroscience*, *33*(31), 12870-12886. https://doi.org/10.1523/JNEUROSCI.2121-13.2013

Wardlaw, J. M., Murray, V., Berge, E., & del Zoppo, G. J. (2014). Thrombolysis for acute ischaemic stroke. *The Cochrane Database of Systematic Reviews*, *7*, CD000213. https://doi.org/10.1002/14651858.CD000213.pub3

Wei, Z. Z., Zhang, J. Y., Taylor, T. M., Gu, X., Zhao, Y., & Wei, L. (2018). Neuroprotective and regenerative roles of intranasal Wnt-3a administration after focal ischemic stroke in mice. *Journal of Cerebral Blood Flow and Metabolism: Official Journal of the International Society of Cerebral Blood Flow and Metabolism*, *38*(3), 404-421. https://doi.org/10.1177/0271678X17702669

Wey, H.-Y., Desai, V. R., & Duong, T. Q. (2013). A review of current imaging methods used in stroke research. *Neurological Research*, *35*(10), 1092-1102. https://doi.org/10.1179/1743132813Y.0000000250

Wieloch, T., & Nikolich, K. (2006). Mechanisms of neural plasticity following brain injury. *Current Opinion in Neurobiology*, *16*(3), 258-264. https://doi.org/10.1016/j.conb.2006.05.011

Williams, A., Piaton, G., & Lubetzki, C. (2007). Astrocytes—Friends or foes in multiple sclerosis? *Glia*, *55*(13), 1300-1312. https://doi.org/10.1002/glia.20546

Williamson, M. R., Fuertes, C. J. A., Dunn, A. K., Drew, M. R., & Jones, T. A. (2021). Reactive astrocytes facilitate vascular repair and remodeling after stroke. *Cell Reports*, *35*(4), 109048. https://doi.org/10.1016/j.celrep.2021.109048

Winpenny, E., Lebel-Potter, M., Fernandez, M. E., Brill, M. S., Götz, M., Guillemot, F., & Raineteau, O. (2011). Sequential generation of olfactory bulb glutamatergic neurons by Neurog2-expressing precursor cells. *Neural Development*, *6*, 12. https://doi.org/10.1186/1749-8104-6-12

Wojcinski, A., Lawton, A. K., Bayin, N. S., Lao, Z., Stephen, D. N., & Joyner, A. L. (2017). Cerebellar granule cell replenishment postinjury by adaptive reprogramming of Nestin+ progenitors. *Nature Neuroscience*, *20*(10), 1361-1370. https://doi.org/10.1038/nn.4621

Writing Group Members, Mozaffarian, D., Benjamin, E. J., Go, A. S., Arnett, D. K., Blaha, M. J., Cushman, M., Das, S. R., de Ferranti, S., Després, J.-P., Fullerton, H. J., Howard, V. J., Huffman, M. D., Isasi, C. R., Jiménez, M. C., Judd, S. E., Kissela, B. M., Lichtman,

References

J. H., Lisabeth, L. D., … Stroke Statistics Subcommittee. (2016). Heart Disease and Stroke Statistics-2016 Update: A Report From the American Heart Association. *Circulation*, *133*(4), e38-360. https://doi.org/10.1161/CIR.0000000000000350

Wu, Y., Wu, J., Ju, R., Chen, Z., & Xu, Q. (2015). Comparison of intracerebral transplantation effects of different stem cells on rodent stroke models. *Cell Biochemistry and Function*, *33*(4), 174-182. https://doi.org/10.1002/cbf.3083

Wyss-Coray, T. (2016). Ageing, neurodegeneration and brain rejuvenation. *Nature*, *539*(7628), 180-186. https://doi.org/10.1038/nature20411

Yamashita, T., Ninomiya, M., Hernández Acosta, P., García-Verdugo, J. M., Sunabori, T., Sakaguchi, M., Adachi, K., Kojima, T., Hirota, Y., Kawase, T., Araki, N., Abe, K., Okano, H., & Sawamoto, K. (2006). Subventricular zone-derived neuroblasts migrate and differentiate into mature neurons in the post-stroke adult striatum. *The Journal of Neuroscience: The Official Journal of the Society for Neuroscience*, *26*(24), 6627-6636. https://doi.org/10.1523/JNEUROSCI.0149-06.2006

Yamazaki, Y., Hozumi, Y., Kaneko, K., Fujii, S., Goto, K., & Kato, H. (2010). Oligodendrocytes: Facilitating axonal conduction by more than myelination. *The Neuroscientist: A Review Journal Bringing Neurobiology, Neurology and Psychiatry*, *16*(1), 11-18. https://doi.org/10.1177/1073858409334425

Yao, H., Gao, M., Ma, J., Zhang, M., Li, S., Wu, B., Nie, X., Jiao, J., Zhao, H., Wang, S., Yang, Y., Zhang, Y., Sun, Y., Wicha, M. S., Chang, A. E., Gao, S., Li, Q., & Xu, R. (2015). Transdifferentiation-Induced Neural Stem Cells Promote Recovery of Middle Cerebral Artery Stroke Rats. *PloS One*, *10*(9), e0137211. https://doi.org/10.1371/journal.pone.0137211

Yao, H., Takasawa, R., Fukuda, K., Shiokawa, D., Sadanaga-Akiyoshi, F., Ibayashi, S., Tanuma, S., & Uchimura, H. (2001). DNA fragmentation in ischemic core and penumbra in focal cerebral ischemia in rats. *Brain Research. Molecular Brain Research*, *91*(1-2), 112-118. https://doi.org/10.1016/s0169-328x(01)00135-8

Yenari, M. A., & Han, H. S. (2012). Neuroprotective mechanisms of hypothermia in brain ischaemia. *Nature Reviews. Neuroscience*, *13*(4), 267-278. https://doi.org/10.1038/nrn3174

Yin, Y., Henzl, M. T., Lorber, B., Nakazawa, T., Thomas, T. T., Jiang, F., Langer, R., & Benowitz, L. I. (2006). Oncomodulin is a macrophage-derived signal for axon regeneration in retinal ganglion cells. *Nature Neuroscience*, *9*(6), 843-852. https://doi.org/10.1038/nn1701

Young, K. M., Fogarty, M., Kessaris, N., & Richardson, W. D. (2007). Subventricular zone stem cells are heterogeneous with respect to their embryonic origins and neurogenic fates in the adult olfactory bulb. *The Journal of Neuroscience: The Official Journal of the Society for Neuroscience*, *27*(31), 8286-8296. https://doi.org/10.1523/JNEUROSCI.0476-07.2007

Young, S. Z., Taylor, M. M., Wu, S., Ikeda-Matsuo, Y., Kubera, C., & Bordey, A. (2012). NKCC1 knockdown decreases neuron production through GABA(A)-regulated neural progenitor proliferation and delays dendrite development. *The Journal of Neuroscience: The Official Journal of the Society for Neuroscience*, *32*(39), 13630-13638. https://doi.org/10.1523/JNEUROSCI.2864-12.2012

Zamanian, J. L., Xu, L., Foo, L. C., Nouri, N., Zhou, L., Giffard, R. G., & Barres, B. A. (2012). Genomic analysis of reactive astrogliosis. *The Journal of Neuroscience: The Official Journal of the Society for Neuroscience*, *32*(18), 6391-6410. https://doi.org/10.1523/JNEUROSCI.6221-11.2012

Zamboni, M., Llorens-Bobadilla, E., Magnusson, J. P., & Frisén, J. (2020). A Widespread Neurogenic Potential of Neocortical Astrocytes Is Induced by Injury. *Cell Stem Cell*, *27*(4), 605-617.e5. https://doi.org/10.1016/j.stem.2020.07.006

Zatorre, R. J., Fields, R. D., & Johansen-Berg, H. (2012). Plasticity in gray and white: Neuroimaging changes in brain structure during learning. *Nature Neuroscience*, *15*(4), 528-536. https://doi.org/10.1038/nn.3045

Zhang, L., Marsboom, G., Glick, D., Zhang, Y., Toth, P. T., Jones, N., Malik, A. B., & Rehman, J. (2014). Bioenergetic shifts during transitions between stem cell states (2013 Grover Conference series). *Pulmonary Circulation*, *4*(3), 387-394. https://doi.org/10.1086/677353

Zhang, L., Yin, J.-C., Yeh, H., Ma, N.-X., Lee, G., Chen, X. A., Wang, Y., Lin, L., Chen, L., Jin, P., Wu, G.-Y., & Chen, G. (2015). Small Molecules Efficiently Reprogram Human Astroglial Cells into Functional Neurons. *Cell Stem Cell*, *17*(6), 735-747. https://doi.org/10.1016/j.stem.2015.09.012

Zhang, R., Chopp, M., & Zhang, Z. G. (2013). Oligodendrogenesis after cerebral ischemia. *Frontiers in Cellular Neuroscience*, *7*, 201. https://doi.org/10.3389/fncel.2013.00201

Zhang, R. L., Chopp, M., Roberts, C., Liu, X., Wei, M., Nejad-Davarani, S. P., Wang, X., & Zhang, Z. G. (2014). Stroke increases neural stem cells and angiogenesis in the neurogenic niche of the adult mouse. *PloS One*, *9*(12), e113972. https://doi.org/10.1371/journal.pone.0113972

Zhang, R. L., LeTourneau, Y., Gregg, S. R., Wang, Y., Toh, Y., Robin, A. M., Zhang, Z. G., & Chopp, M. (2007). Neuroblast division during migration toward the ischemic striatum: A study of dynamic migratory and proliferative characteristics of neuroblasts from the subventricular zone. *The Journal of Neuroscience: The Official Journal of the Society for Neuroscience*, *27*(12), 3157-3162. https://doi.org/10.1523/JNEUROSCI.4969-06.2007

Zhang, R. L., Zhang, Z. G., Zhang, L., & Chopp, M. (2001). Proliferation and differentiation of progenitor cells in the cortex and the subventricular zone in the adult rat after focal cerebral ischemia. *Neuroscience*, *105*(1), 33-41. https://doi.org/10.1016/s0306-4522(01)00117-8

Zhang, R., Zhang, Z., Wang, L., Wang, Y., Gousev, A., Zhang, L., Ho, K.-L., Morshead, C., & Chopp, M. (2004). Activated neural stem cells contribute to stroke-induced neurogenesis and neuroblast migration toward the infarct boundary in adult rats. *Journal of Cerebral Blood Flow and Metabolism: Official Journal of the International Society of Cerebral Blood Flow and Metabolism*, *24*(4), 441-448. https://doi.org/10.1097/00004647-200404000-00009

Zhang, Y., Sloan, S. A., Clarke, L. E., Caneda, C., Plaza, C. A., Blumenthal, P. D., Vogel, H., Steinberg, G. K., Edwards, M. S. B., Li, G., Duncan, J. A., Cheshier, S. H., Shuer, L. M., Chang, E. F., Grant, G. A., Gephart, M. G. H., & Barres, B. A. (2016). Purification and Characterization of Progenitor and Mature Human Astrocytes Reveals Transcriptional and Functional Differences with Mouse. *Neuron*, *89*(1), 37-53. https://doi.org/10.1016/j.neuron.2015.11.013

Zhang, Y., Xu, D., Qi, H., Yuan, Y., Liu, H., Yao, S., Yuan, S., & Zhang, J. (2018). Enriched environment promotes post-stroke neurogenesis through NF-κB-mediated secretion of IL-17A from astrocytes. *Brain Research*, *1687*, 20-31. https://doi.org/10.1016/j.brainres.2018.02.030

Zhang, Z. G., & Chopp, M. (2009). Neurorestorative therapies for stroke: Underlying mechanisms and translation to the clinic. *The Lancet. Neurology*, *8*(5), 491-500. https://doi.org/10.1016/S1474-4422(09)70061-4

Zhao, B.-Q., Wang, S., Kim, H.-Y., Storrie, H., Rosen, B. R., Mooney, D. J., Wang, X., & Lo, E. H. (2006). Role of matrix metalloproteinases in delayed cortical responses after stroke. *Nature Medicine*, *12*(4), 441-445. https://doi.org/10.1038/nm1387

Zhao, L.-R., & Willing, A. (2018). Enhancing endogenous capacity to repair a stroke-damaged brain: An evolving field for stroke research. *Progress in Neurobiology*, *163-164*, 5-26. https://doi.org/10.1016/j.pneurobio.2018.01.004

Zhao, T., Wang, Z., Zhu, T., Xie, R., & Zhu, J. (2020). Downregulation of Thbs4 caused by neurogenic niche changes promotes neuronal regeneration after traumatic brain injury. *Neurological Research*, *42*(8), 703-711. https://doi.org/10.1080/01616412.2020.1795590

Zheng, S., Eacker, S. M., Hong, S. J., Gronostajski, R. M., Dawson, T. M., & Dawson, V. L. (2010). NMDA-induced neuronal survival is mediated through nuclear factor I-A in mice. *The Journal of Clinical Investigation*, *120*(7), 2446-2456. https://doi.org/10.1172/JCI33144

Zheng, X., Boyer, L., Jin, M., Mertens, J., Kim, Y., Ma, L., Ma, L., Hamm, M., Gage, F. H., & Hunter, T. (2016). Metabolic reprogramming during neuronal differentiation from aerobic glycolysis to neuronal oxidative phosphorylation. *ELife*, *5*, e13374. https://doi.org/10.7554/eLife.13374

Zhou, Y., & Danbolt, N. C. (2013). GABA and Glutamate Transporters in Brain. *Frontiers in Endocrinology*, *4*, 165. https://doi.org/10.3389/fendo.2013.00165

Zimmermann, D. R., & Dours-Zimmermann, M. T. (2008). Extracellular matrix of the central nervous system: From neglect to challenge. *Histochemistry and Cell Biology*, *130*(4), 635-653. https://doi.org/10.1007/s00418-008-0485-9

Zywitza, V., Misios, A., Bunatyan, L., Willnow, T. E., & Rajewsky, N. (2018). Single-Cell Transcriptomics Characterizes Cell Types in the Subventricular Zone and Uncovers Molecular Defects Impairing Adult Neurogenesis. *Cell Reports*, *25*(9), 2457-2469.e8. https://doi.org/10.1016/j.celrep.2018.11.00